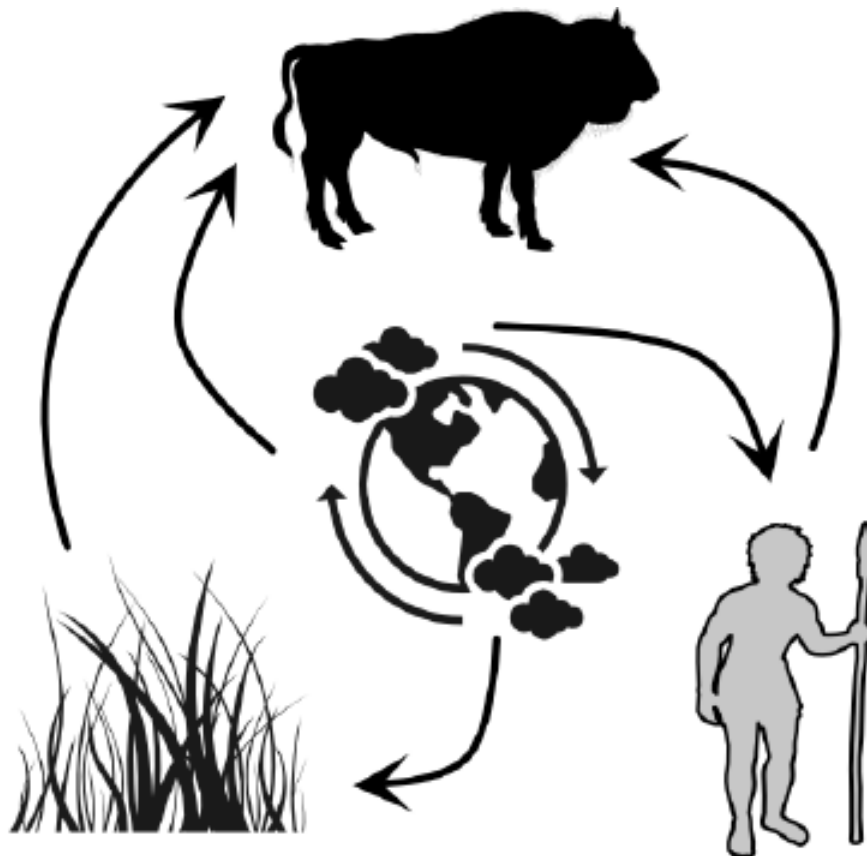**PhD in Biology**

Revealing ecological processes of range dynamics through space and time

Julia Aaron Pilowsky

Supervised by Carsten Rahbek and Damien Fordham

December 2022

Julia Aaron Pilowsky
Revealing ecological processes of range dynamics through space and time
PhD in Biology, December 2022
Supervisors: Carsten Rahbek and Damien Fordham
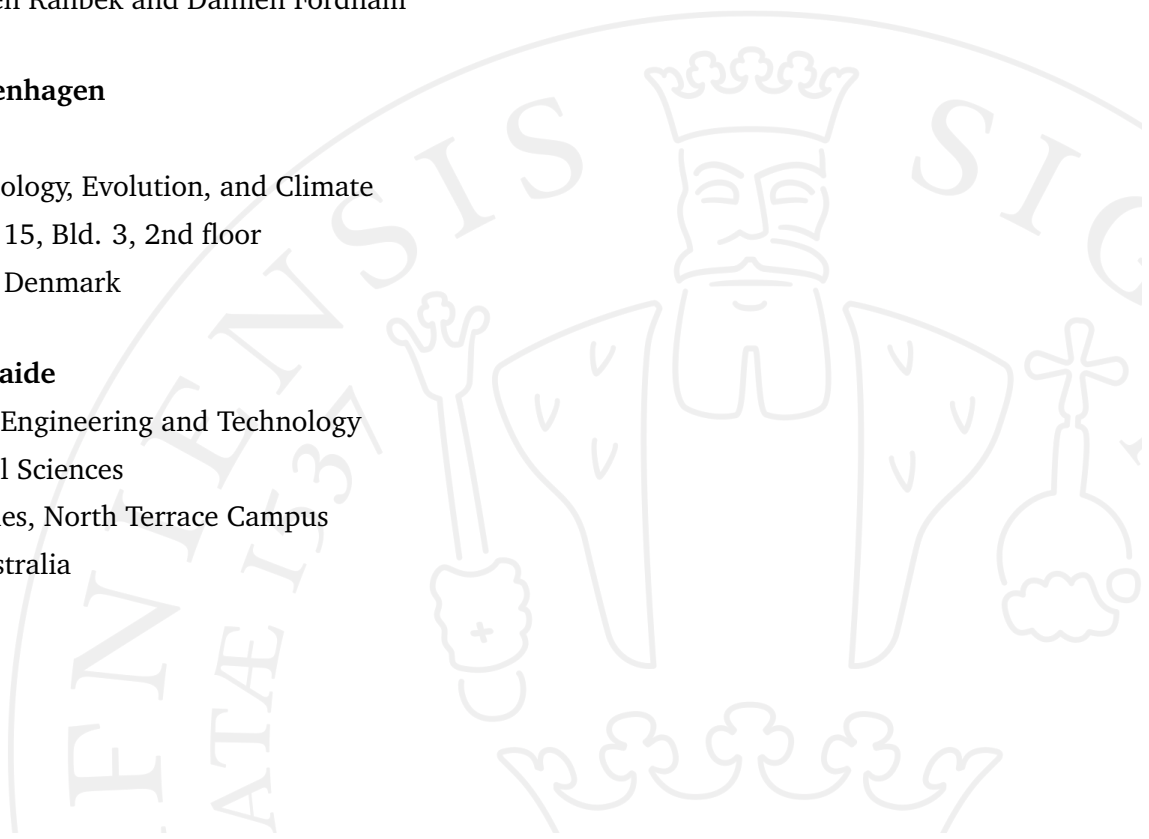
TABLE OF CONTENTS

ABSTRACT

In ecology, process-explicit models represent the dynamics of ecological systems as explicit functions of the mechanisms and drivers that produced them. Process-explicit models are therefore able to link observed ecological patterns, such as species spatial abundance patterns, directly to their causes, such as climate and environmental change. In this PhD thesis, I show how process-explicit models can be used to establish determinants of range collapses and extinction by unpacking complex interactions between ecological lifestyles, biological traits, climate change, and human-driven threats. By providing a more complete understanding of the ecological mechanisms that regulate species' responses to climate and environmental change, my PhD research provides information needed to better predict vulnerability to future climate and environmental change.

In **Chapter I**, I reviewed and interpreted the techniques used to unlock ecological and evolutionary mechanisms responsible for spatial and temporal patterns of biodiversity ranging from the gene to the ecosystem. By revealing how models can codify the generalisable mechanisms responsible for the distributions of life on Earth, this review will help to enable important advances in macroecology, evolutionary biogeography and conservation biology, strengthening both basic and applied science.

Chapter II is a sensitivity analysis of the Climate Informed Spatial Genetic Model (CISGeM), a process-explicit model of human migration out of Africa. While it is well-known that correlative models of species ranges, such as environmental niche models, are highly sensitive to the climate dataset used for parameterisation, the sensitivity of process-explicit models of human migration to climate data and other model parameters has never been tested. I found that the outputs of CISGeM are robust to the choice of palaeoclimate simulation data, but sensitive to the values for key demographic processes.

In **Chapter III**, I used process-explicit models to reconstruct the late Quaternary range dynamics of the steppe bison (*Bison priscus*) using a new R package, paleopop, that I co-developed. The approach linked spatially explicit population models with inferences of demographic change from fossils and ancient DNA to continuously simulate 45,000 years of steppe bison extinction dynamics. The models included dispersal and demographic processes responding to human

harvesting and rapid deglacial warming. I found that deglacial warming interacted with hunting pressure from humans to cause the range of the steppe bison to contract to refugial highland populations, which became extinct in the early Holocene.

Chapter IV used a related approach to reconstruct the range dynamics of the European bison (*Bison bonasus*) from the last ice age to the year 1500. The European bison became extinct in the wild in 1927 and has been bred back from captive animals. It is a goal of European Union policy to reintroduce the bison more broadly, but there is a debate about the optimal locations and habitats for reintroduction. I inform this debate by showing where bison became extinct due to hunting, land use change, and climate change.

General findings from my PhD will help macroecologists to better model and understand species range and extinction dynamics, providing important theoretical and applied insights for conserving vulnerable species in the Anthropocene.

RESUMÉ

I økologi er de økologiske systemers dynamikker repræsenterede ved processpecifikke modeller i form af specifikke funktioner af de mekanismer og drivkræfter som står bag disse dynamikker. Derfor er processpecifikke modeller i stand til at kæde observerede økologiske mønstre, som f.eks. arters rummelige hyppighed, direkte sammen med deres årsager som f.eks. klima- og miljøforandringer mv. I denne ph.d.-afhandling viser jeg, hvordan processpecifikke modeller kan anvendes til at fastslå de bestemmende indvirkninger på udbredelseskollaps og en arts udryddelse ved at udrede indviklede vekselvirkninger mellem økologiske livstile, biologiske træk, klimaforandringer, og menneskedrevne trusler. Ved at fremsætte en større forståelse for de økologiske mekanismer som regulerer en arts reaktioner til klima- og miljøforandringer, indeholder min ph.d.-forskning oplysninger som er nødvendige for bedre at forudse en arts sårbarhed ved fremtidige klima- og miljøforandringer.

I **Kapitel 1** gennemgår og analyserer jeg de teknikker som anvendes til at afdække de økologiske og evolutionære mekanismer som er ansvarlige for rummelige og tidsmæssige biodiversitetsmønstre, som spænder fra genet til økosystemet. Ved at afdække hvordan modeller kan kodificere de generaliserbare mekanismer som er ansvarlige for udbredelserne af liv på jorden, vil denne gennemgang hjælpe med at muliggøre vigtige fremskridt i makroøkologi, evolutionær biogeografi og fredningsbiologi, og derved styrke både grundforskning og anvendt forskning inden for disse emner.

Kapitel 2 består af en følsomhedsanalyse af Climate Informed Spatial Genetic Model (CISGeM), som er en processpecifik model af menneskevandring fra Afrika. Mens det er velkendt at indbyrdes relaterede modeller af en arts udbredelsesområder, som f.eks. miljømæssige niche modeller, er meget følsomme over for det klimadatasæt som anvendes til at bestemme parametrene, er følsomheden af processpecifikke modeller for menneskevandring overfor klimadata og andre modelparametre aldrig blevet afprøvet. Jeg fandt at resultaterne fra CISGeM er robuste ift. valget af paleoklima simulationsdata, men følsomme ift. værdierne for nøgle demografiske processer.

I **Kapitel 3** anvender jeg procesbestemte modeller til at rekonstruere de sene Kvartærtidens udbredelsesdynamikker hos steppebisonen (*Bison priscus*) ved at anvende en ny R pakke, paleopop,

som jeg er medudvikler af. Denne tilgang kæder rummeligspecifikke bestandsmodeller med følgeslutninger baseret på demografiske forandringer som er baseret på fossiler og forhistorisk DNA samt løbende simulering af 45.000 års udryddelsesdynamikker ift. steppebisonen. Modellerne indeholder både spredningsprocesser og demografiske processer som reaktion på menneskets høst af afgrøder og i øvrigt den hurtige smeltning af gletsjere, forårsaget af klimaforandringer, som førte til, at steppebisonens udbredelsesområde skrumpede ind til tilflugtssteder med højlandsbestande som uddøde i den tidlige Holocæn.

Kapitel 4 anvender en lignende tilgang til at rekonstruere den europæiske bisons (*Bison bonasus*) udbredelsesområdedynamik fra den sidste istid til året 1500 e.Kr. Den europæiske bison uddøde i naturen i 1927, og er blevet genavlet fra dyr i fangeskab. Det er et af den Europæiske Unions mål at genindføre den europæiske bison mere bredt, men der er debat om, hvor de mest velegnede områder og habitater til genindføringen er. Jeg præger denne debat ved at vise, hvor bisonen blev udryddet pga. jagt, ændringer i brugen af naturarealer, og klimaforandringer.

De mere brede resultater fra mit ph.d.-studie vil kunne hjælpe makroøkologer til bedre at modellere og forstå arters udbredelsesområder og udryddelsesdynamikker, og derved bidrage med væsentlige teoretiske og anvendte indsigter i beskyttelse af sårbare arter i Antropocenen.

DECLARATION

I certify that this work contains no material which has been accepted for the award of any other degree or diploma in my name in any university or other tertiary institution and, to the best of my knowledge and belief, contains no material previously published or written by another person, except where due reference has been made in the text. In addition, I certify that no part of this work will, in the future, be used in a submission in my name for any other degree or diploma in any university or other tertiary institution without the prior approval of the University of Adelaide and where applicable, any partner institution responsible for the joint award of this degree. The author acknowledges that copyright of published works contained within this thesis resides with the copyright holder(s) of those works.

I give permission for the digital version of my thesis to be made available on the web, via the University's digital research repository, the Library Search and also through web search engines, unless permission has been granted by the University to restrict access for a period of time.

ACKNOWLEDGMENTS

LIST OF MANUSCRIPTS

I. Pilowsky, J. A., Colwell, R. K., Rahbek, C., & Fordham, D. A. (2022). Process-explicit models reveal the structure and dynamics of biodiversity patterns. *Science Advances*, *8*(31), eabj2271. DOI: 10.1126/sciadv.abj2271

II. Pilowsky, J. A., Haythorne, S., Brown, S. C., Krapp, M., Armstrong, E., Brook, B. W., Rahbek, C., & Fordham, D. A. (2022). Range and extinction dynamics of the steppe bison in Siberia: A pattern-oriented modelling approach. *Global Ecology and Biogeography*. DOI: 10.1111/geb.13601

III. Pilowsky, J. A., Manica, A., Brown, S. C., Rahbek, C., & Fordham, D. A. (2022). Simulations of human migration into North America are more sensitive to demography than choice of palaeoclimate model. *Ecological Modelling*. DOI: 10.1016/j.ecolmodel.2022.110115

IV. Pilowsky, J. A., Llamas, B., Kowalczyk, R., Hofman-Kamińska, E., Rahbek, C., Fordham, D.A. Causes of range collapse and extinction in the wild of European bison. *Unsubmitted work written in manuscript style.*

INTRODUCTION

Macroecology is the study of interactions among organisms and the environment on large spatial and temporal scales (J. H. Brown & Maurer, 1989). Macroecology describes and explains the distribution of life on our planet: how it came to be the way it is now, and how it will respond to global change drivers such as anthropogenic climate change. Because macroecology can be very difficult to study using experimental methods due to its scale, ecological modelling is crucial to the discipline (Fordham et al., 2020).

Process-explicit models

In ecology, process-explicit models represent the dynamics of an ecological system as explicit functions of the processes that drive change in that system (Connolly, Keith, Colwell, & Rahbek, 2017). They are able to causally link ecological patterns to the processes, drivers, and interactions that generated them. By contrast, correlative models represent the dynamics of an ecological system as a set of statistical relationships between ecologically relevant variables. Here, ecological processes are *implicit* in the relationships between the variables. Correlative models are more often used in ecology than process-explicit models because they require fewer data and are more appropriate for study systems that are still poorly understood. However, when they can be implemented, process-explicit models have key advantages over correlative models.

Process-explicit models are better able to *describe* the dynamics of an ecological system, as well as *predict* its future dynamics, than correlative models. Process-explicit models are more descriptive of ecological systems because they can make inferences about causal drivers of ecological dynamics, e.g., the minimum human population density and hunting rate required to cause megafaunal extinction in North America (Alroy, 2001). Process-explicit models can also make better predictions about ecological systems (Fordham, Bertelsmeier, et al., 2018) because they can make predictions under novel future conditions, while correlative models are limited by the conditions that produced past data and the correlations among them (Fordham et al., 2020).

However, process-explicit models are limited in their applications by data availability and the problem of equifinality. Process-explicit models are often data-intensive because each ecological

process and driver must be parameterised, while correlative models require only, at minimum, a response variable and a predictor variable. Process-explicit models also face the problem of equifinality (Beven, 2006), whereby multiple combinations of processes and drivers can produce the same empirically observed pattern, making it difficult to determine which one accurately describes the ecological system.

Process-explicit models hold great promise for the field of macroecology because they enable virtual experiments over spatial extents and timescales that are not possible in the lab or the field and make inferences about the processes that produce large-scale ecological patterns. In **Chapter I**, my co-authors and I review the applications of process-explicit models for conserving biodiversity and indicate promising avenues of research.
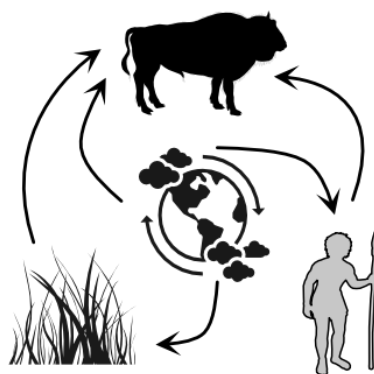
Process-explicit models of species range dynamics for conservation

Chapter I: Review of process-explicit models
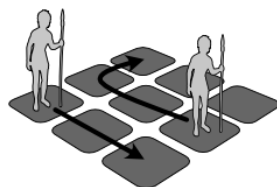
Chapter II: Key parameters in human migration models
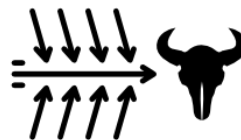
Chapter III: Drivers of extinction in the steppe bison

Chapter IV: Drivers of extinction in the European bison

Modelling the past to understand range dynamics

Many of the classic ecological studies on extinction, establishing proximate mechanisms of extinction such as demographic stochasticity, inbreeding depression, and genetic drift that occur in small populations; however, extinction processes such as habitat fragmentation and loss of mutualistic partners often begin long before the population has become small. These two paradigms of extinction are known as the *small* and *declining* population paradigms (Caughley,

2

1994). The small population paradigm can be developed in real time studies of rapid population collapses. The declining population paradigm, however, requires a longer timescale. Studies must begin well before the proximate mechanisms of extinction begin.

Another important reason to model biodiversity in the past is that there are regions where past climates resemble our predictions of future climates (Fordham et al., 2020). By modelling biodiversity under past conditions, we can learn about the biodiversity changes that can be expected under future climates, on a larger scale than is possible with temperature manipulations in laboratory experiments.

During the deglaciation period from the last ice age, 20,000 to 10,000 years before present (BP), there were regions, mostly in the Northern Hemisphere, where warming was as rapid as it is projected to become under the most extreme forecasts of future warming (Fordham et al., 2020). During this period, the loss of many Arctic megaherbivores drove a shift from the "mammoth steppe" biome in the Northern Hemisphere to a tundra-taiga ecotone (Zimov et al., 1995). Modelling biodiversity changes in the transition from the last ice age to the warmer Holocene is our best analogue from the past for the magnitude of change we can expect under future climate scenarios. Further, the last deglaciation is well within the window for accurate radiocarbon dating, which makes this time period tractable to study.

In **Chapters II**, **III**, and **IV**, I present three process-explicit modelling studies examining changes in biodiversity over the last deglaciation in the Northern Hemisphere. My co-authors and I model the range dynamics of steppe bison, humans, and European bison, respectively.

Modelling the future for conservation biogeography

One of the oldest and most established techniques for modelling species extinction risk is population viability analysis (PVA), which projects time to quasi-extinction and minimum viable population for long-term survival using deterministic functions or stochastic probability draws (Boyce, 1992). However, PVA is limited because it does not include climate data or spatial dynamics. Environmental niche models (ENMs) address these shortfalls: they are spatially explicit and account for changes in climate in their forecasts of species ranges. However, as noted above,

correlative models like ENMs struggle to make accurate predictions under novel conditions that were not present in the data used to train the model, and under anthropogenic global change, novel conditions are very likely to occur.

In **Chapter IV**, my co-authors and I address the shortfalls of PVA and ENMs as forecasting tools for threatened species by forecasting the potential range of the European bison using spatially explicit population models (SEPMs) and pattern-oriented validation (POV). SEPMs are spatially explicit, process-explicit models of populations on an interconnected lattice of possible habitats. POV is a validation procedure that optimises parameters in a process-explicit model by converging summary metrics from these models toward multiple observed patterns. By combining SEPMs with POV, the demographic and ecological parameters in a SEPM can be optimised to accurately reconstruct real-world patterns of population dynamics. These optimised parameters can be used to make forecasts under future conditions, including novel ecological conditions.

Spatially explicit population models optimised with POV can do more than simply predict the future range of a species. They can explicitly link changes in the range to their causes, such as human harvesting or land-use change. They can predict abundance and population growth across the range, indicating which populations may persist or become extinct. From a conservation policy perspective, forecasts from SEPMs and POV can be used to propose reintroduction sites as well as stocking rates needed to ensure a viable population at the proposed sites.

Objectives and aims

My objective in this PhD dissertation is to show how process-explicit models can be used to better understand the range dynamics of species under threat from human harvesting and land use change as well as rapid climatic change. First, I review the use of process-explicit models in ecology to conserve biodiversity, identifying key types of process-explicit models and indicating promising future avenues of research (**Chapter I**). I then apply spatially explicit population models to reconstruct the range dynamics of three species in the late Pleistocene and Holocene periods: humans (**Chapter II**), steppe bison (**Chapter III**), and European bison (**Chapter IV**).

Reconstructions of prehistoric human migration patterns are important to studies of human-driven biodiversity change over long timescales. It is well-established that correlative models of species distribution are highly sensitive to the choice of climate data used (L. J. Beaumont, Pitman, Poulsen, & Hughes, 2007; Tuck, Glendining, Smith, House, & Wattenbach, 2006), but process-explicit models of human migration have not yet been tested for their sensitivity to climate dataset and other model parameters. **Chapter II** is a sensitivity analysis of a process-explicit model of human migration, to determine which parameters in these models have the greatest impact on the accuracy of their reconstructions.

My study of the steppe bison (*Bison priscus*), once a widespread species, provides important insight into the declining species paradigm. The steppe bison had a vast circumpolar distribution in the Northern Hemisphere, until it disappeared from Europe, Asia, and finally North America. In **Chapter III** I use SEPMs and POV to reconstruct the extinction of the steppe bison in Siberia from 50,000 years BP to 5,000 years BP, demonstrating the utility of these techniques for simulating range collapses that match observed fossil evidence.

The European bison (*Bison bonasus*) is a closely related species to the steppe bison which was once widespread in Eurasia, then became extinct in the wild in 1927. Since then, an extensive conservation effort has brought back the species from captive populations, but it is still threatened. In **Chapter IV**, I use SEPMs and POV to uncover the role of environmental change, land use transformation, and human hunting in the extinction of the bison in space and time, clarifying the regions and time periods where humans and climate have had the greatest impact on the species' decline.

In this thesis, I show concrete ways that process-explicit models can identify causes of extinction in action well before the extinction occurs, as well as inform policy for the conservation of threatened species into the future.

CHAPTER I: PROCESS-EXPLICIT MODELS REVEAL THE STRUCTURE AND DYNAMICS OF BIODIVERSITY PATTERNS
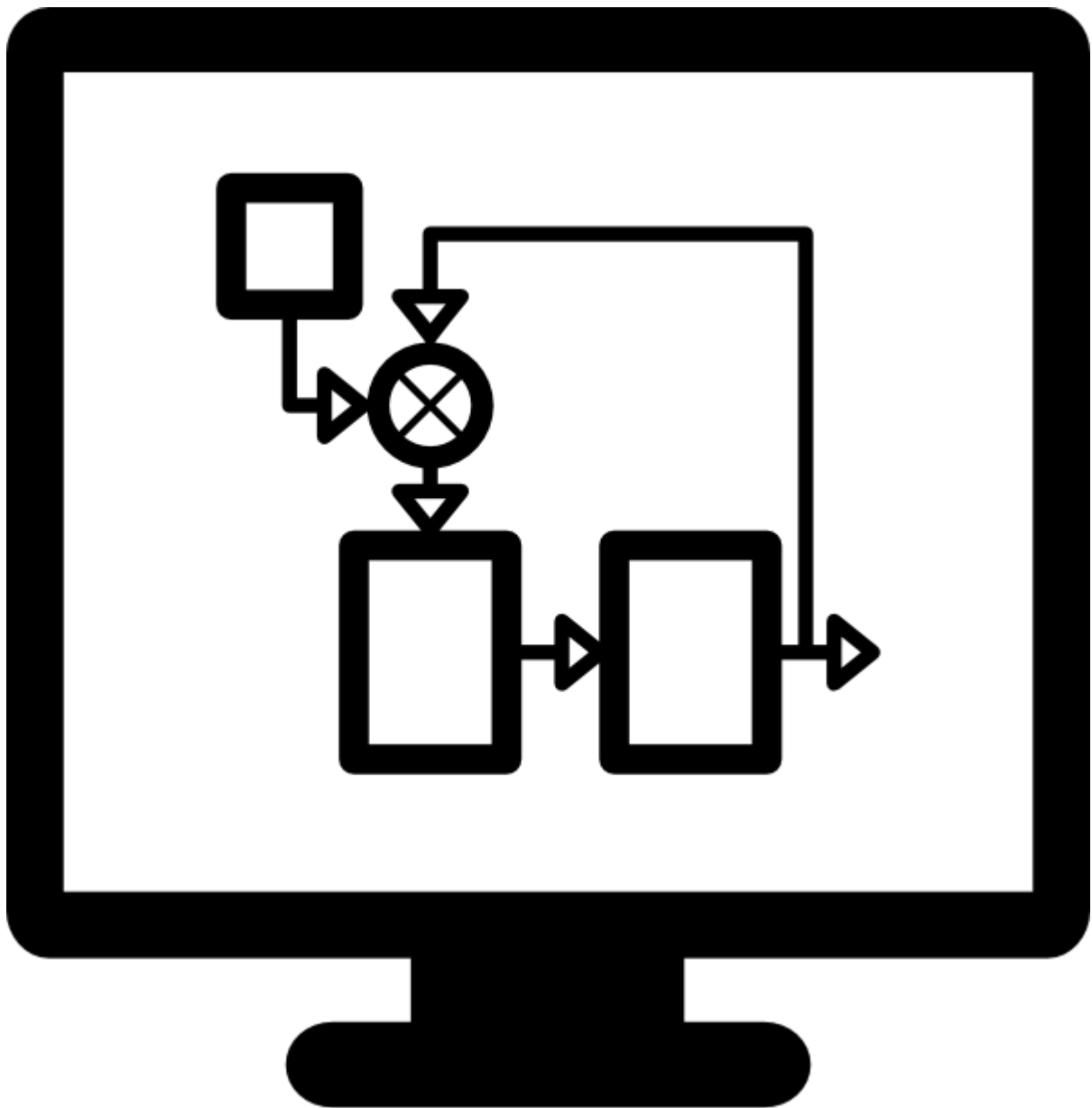
Statement of Authorship

Title of Paper	Process-explicit models reveal the structure and dynamics of biodiversity patterns
Publication Status	Published
Publication Details	Journal: Science Advances Authors: Julia Pilowsky, Robert Colwell, Carsten Rahbek, Damien Fordham

Principal Author

Name of Principal Author (Candidate)	Julia Pilowsky
Contribution to the Paper	The candidate conceptualised the study, did the literature review, analysis, and wrote the paper with contributions from co-authors.
Overall percentage (%)	75%
Certification:	This paper reports on original research I conducted during the period of my Higher Degree by Research candidature and is not subject to any obligations or contractual agreements with a third party that would constrain its inclusion in this thesis. I am the primary author of this paper.

Signature		ate	22 November 2022

Principal Author

Co-Author Contributions

By signing the Statement of Authorship, each author certifies that:

i.   the candidate's stated contribution to the publication is accurate (as detailed above);

ii.   permission is granted for the candidate in include the publication in the thesis; and

iii.   the sum of all co-author contributions is equal to 100% less the candidate's stated contribution.

Name of Co-Author	Prof. Robert Colwell
Contribution to the Paper	Contributed to writing and design of the paper.
Signature	17 November 2022

Name of Co-Author	Prof. Carsten Rahbek
Contribution to the Paper	Helped conceptualise the study, design, and write the paper.
Signature	Date	5 Dec 2022

Name of Co-Author	A/Prof. Damien Fordham

Contribution to the Paper	Helped conceptualise the study, design, and write the paper.		
Signature		Date	18/11/2022

Title Page

Process-explicit models reveal the structure and dynamics of biodiversity patterns

Short Title

Deciphering biodiversity with process-explicit models

Authors

Julia A. Pilowsky[1,2], Robert K. Colwell[2,3,4,5], Carsten Rahbek[2,6,7,8], Damien A. Fordham[1]

Affiliations

[1]The Environment Institute, School of Biological Sciences, University of Adelaide, Australia

[2]Center for Macroecology, Evolution, and Climate, Globe Institute, University of Copenhagen, Denmark

[3]University of Colorado Museum of Natural History, USA

[4]Department of Ecology and Evolutionary Biology, University of Connecticut, USA

[5]Departmento de Ecología, Universidade Federal de Goiás, Brazil

[6]Center for Global Mountain Biodiversity, Globe Institute, University of Copenhagen, Denmark

[7]Institute of Ecology, Peking University, China

[8]Danish Institute for Advanced Study, University of Southern Denmark, Denmark

Funding

Abstract

With ever-growing data availability and computational power at our disposal, we now have the capacity to use process-explicit models more widely to reveal the ecological and evolutionary mechanisms responsible for spatiotemporal patterns of biodiversity. Most research questions focused on the distribution of diversity cannot be answered experimentally, because many important environmental drivers and biological constraints operate at large spatiotemporal scales. However, we can encode proposed mechanisms into models, observe the patterns they produce in virtual environments, and validate these patterns against real-world data or theoretical expectations. This approach can advance understanding of generalisable mechanisms responsible for the distributions of organisms, communities, and ecosystems in space and time, advancing basic and applied science. We review recent developments in process-explicit models and how they have improved knowledge of the distribution and dynamics of life on Earth, enabling biodiversity to be better understood and managed through a deeper recognition of the processes that shape genetic, species, and ecosystem diversity.

Teaser

Process-explicit models can help explain the distribution of life on Earth.

Introduction

The patterns of biodiversity we observe at different temporal and spatial scales result from the key evolutionary and ecological processes of speciation, ecological interaction, adaptation, movement, and extinction, acting separately or in concert (Holt, 2003). These processes can be stochastic, or forced by natural drivers of environmental change (e.g., plate tectonics, palaeoclimate change) or by human drivers, such as invasive species, land use, pollution, and harvesting (Brook, Sodhi, & Bradshaw, 2008). However, the interplay among these processes and their drivers is complex (Davidson, Hamilton, Boyer, Brown, & Ceballos, 2009), and different sets of circumstances can produce similar patterns. This ambiguity has made it difficult to discern which ecological and evolutionary processes and drivers have shaped current-day patterns of biodiversity based on empirical data alone (Beven, 2006). Fortunately, key advances in process-explicit models over the last 50 years are now enabling the processes and drivers responsible for contemporary patterns of biodiversity to be disentangled in space and time. Here we show how these advances in biodiversity modelling are revealing the generalisable mechanisms responsible for the distributions, abundances, and diversity of life on Earth; and how they are strengthening basic and applied science, resulting in improved guidelines for the management of nature.

Process-explicit models in ecology and evolution represent the dynamics of a biological system as explicit functions of the events that drive change in that system (Connolly et al., 2017). By causally linking current patterns to the past events that produced them (Figure 1), process-explicit models help achieve a deeper understanding of the chain of causality leading to current-day spatial patterns of biodiversity, including human diversity (Eriksson et al., 2012). These models allow contested ecological and evolutionary theories to be assessed, enabling biodiversity to be understood and managed more effectively through a deeper recognition of the processes of genetic-, species- and ecosystem-level endangerment and collapse (Fordham et al., 2020).

Models that are process-explicit provide platforms for directly integrating ecological and evolutionary theory into conservation and environmental science (Fordham et al., 2016), enhancing knowledge of the effects of biodiversity and its drivers on the functioning of species and ecosystems (Bonan, 2008), and strengthening projections of biodiversity in a changing world

(Briscoe et al., 2019), resulting in improvements to conservation management and policy (Ferrier, Ninan, Leadley, & Alkemade, 2016). For example, process-explicit models derived from the neutral theory of biodiversity (Hubbell, 2001) were some of the first models to show that rare species are less frequent in island communities than in adjacent mainland communities (Mangel, 2002), providing important new information to conservation policy makers regarding vulnerability to human-driven environmental change (Halley & Iwasa, 2011). Process-explicit models of the neutral theory of molecular evolution, which simulate rates of genetic drift as products of effective population size and generation length (Kimura, 1979), enabled conservation geneticists to study the behaviour of neutral alleles to better understand why extinction risk increases for species with small population sizes (Yoder, Poelstra, Tiley, & Williams, 2018). A stronger integration of ecological and evolutionary theory in conservation science using process-explicit modelling promises to further link the evolution of species traits at the individual level to the dynamics of communities and the overall functioning of ecosystems (Loreau, 2010). Together, these advances are improving knowledge of how climatic and environmental changes have shaped species assemblages in the past, strengthening confidence in projections of biodiversity's future (Fordham et al., 2020).

Recent reviews have established important benefits of process-explicit modelling approaches in macroecology (Cabral, Valente, & Hartig, 2017; Connolly et al., 2017), ecosystem ecology (Loreau, 2010), conservation science (Briscoe et al., 2019), and related disciplines. These studies highlight a need to use process-explicit models for managing ecosystems (Loreau, 2010), improving theory (Cabral et al., 2017; Connolly et al., 2017), and predicting species' range shifts under ongoing and future climate change (Briscoe et al., 2019). However, there has been no synthesis of the broader uses of process-explicit models for unravelling the biological mechanisms responsible for shaping patterns of biodiversity in space and time in response to Earth system drivers of environmental change. Here we identify key properties of the structure and dynamics of biodiversity first uncovered by process-explicit models, many of which are now guiding the future management of biodiversity.

The application of process-explicit models of spatiotemporal diversity in ecology and evolution can be traced back to MacArthur and Wilson's model of island biogeography (Figure 1), which linked

patterns of biodiversity on islands to processes of movement (colonisation) and local extinction (MacArthur & Wilson, 1967). Early process-explicit models include metapopulation models (Levins, 1969), which are used frequently today for conservation planning (Hanski, Pakkala, Kuussaari, & Lei, 1995) and for informing species' extinction risk (Pearson et al., 2014). These models, which were initially limited to interactions and movements of subpopulations of a species, have now been expanded to include demographic and environmental stochasticity (Hanski, 1989), species interactions, and community-level dynamics (Wilson, 1992), allowing interlinked patches with different community compositions to be simulated and their dynamics understood. The first individual-based models followed shortly after the development of metapopulation models, permitting the inclusion of individual variation in dispersal behaviour, genotype, competitive ability, and life history traits in simulations of population change (DeAngelis & Mooij, 2005). Today, individual-based models are used frequently not only for the management of specific populations, including fisheries stocks (Rice et al., 2003), but also to answer paradigmatic questions about community assembly, food web ecology, and zoonotic disease (DeAngelis & Grimm, 2014).

In the 1980s, development of coalescent models of simulated genealogies (Kingman, 1982) enabled the diversification of lineages to be studied in space and time (Avise, 2000), giving rise to the field of phylogeography. These early models showed how lineages can diverge without geographic isolation, illustrating potential mechanisms of sympatric speciation. More recently, they have been used to show how pathogens can rapidly evolve as they spread through a network of hosts (Knowles, 2009), enriching fundamental understanding of past, current, and future disease dynamics (Prohaska et al., 2019). The latest generation of coalescent models can reconstruct genomic erosion in endangered species (Díez-del-Molino, Sánchez-Barreiro, Barnes, Gilbert, & Dalén, 2018) and rapid directional selection (Bi et al., 2019) in response to sub-centennial periods of environmental change.

The 1990s saw the advent of dynamic global vegetation models (DGVMs): process-explicit models that replicate global patterns of vegetation by simulating the growth and mortality of plant functional groups under different climatic conditions (Foley et al., 1996). This development enabled predictions of the capacity of the biosphere to store carbon (A. White, Cannell, & Friend,

14

2000) and produce crops (Boit et al., 2019) under future climate conditions. Today DGVMs are being used to inform regional-to-global policies on food security, greenhouse gas emission scenarios and the maintenance of ecosystem services (Kim et al., 2018). They can account for the effects of herbivory on vegetation structure and fire regimes (Zhu et al., 2018), allowing the impacts of competing land management strategies to be compared (Contreras et al., 2019; Ferrier et al., 2016).

In the early 2000s, models began to be developed that integrate the evolutionary processes of speciation and adaptation with the ecological processes of movement, extinction, and interaction. By providing a mechanistic understanding of the physical and biological processes that shape Earth's biodiversity, these models have aimed to illuminate the origins of biodiversity through direct tests of competing scenarios (May, Wiegand, Lehmann, & Huth, 2016). Many of these theories, established long ago by early naturalists (Brenner, 1921; Humboldt, 1877; Wallace, 1863), could not be directly tested with simpler process-explicit models or phenomenological approaches. Today, eco-evolutionary simulators provide opportunities to achieve new levels of realism in projections of assemblage dynamics under past and future global change (Hagen et al., 2021).

The most recent developments in process-explicit modelling, which simulate multiple processes and patterns of biodiversity using complex mathematical components and logical algorithms, have resulted from a rapid rise in computational power following the turn of the 21st century (Hagen et al., 2021; Rangel, Diniz-Filho, & Colwell, 2007; Rangel et al., 2018). This advance, coupled with wider access to large ecological, genomics, and satellite-based remote sensing datasets, has enabled the generation and increasingly frequent application of a broad variety of process-explicit models in ecological and evolutionary studies, parameterised or validated with more data and based on more-realistic assumptions than previously possible. Despite this accelerated expansion, the development and application of process-explicit models has followed an opportunistic path, with little strategy or coordination (M. C. Urban et al., 2016).

To address this current shortfall, we provide here a much-needed review of recent developments in process-explicit models, outlining considerations for researchers who contemplate building process-explicit models to evaluate the mechanisms that govern the structure and dynamics of past,

present, and future biodiversity. We scrutinise the processes of codifying theory into models, identify key scientific advances from simulation outputs, and illustrate with examples how process-explicit models can safeguard future biodiversity.

Process versus pattern

Narrative accounts (Wallace, 1863), correlative studies (R. D. Guthrie, 2006), and experiments (Yoshida, Jones, Ellner, Fussmann, & Hairston, 2003) lead to hypotheses about the underlying causes of biodiversity change, and theoretical models demonstrate possible mechanisms (Doebeli & Dieckmann, 2003). In comparison, spatiotemporal process-explicit models can directly assess and disentangle competing theories for drivers of biodiversity, helping to elucidate interactions among underlying ecological and evolutionary mechanisms and drivers (Connolly et al., 2017). An example of competing theories for biodiversity dynamics and resultant patterns is the contrast between niche (Chase & Leibold, 2003) and neutral theory (Hubbell, 2001). The former focuses on the role of environmental determinism, while the latter focuses on contingent and stochastic determinants of biodiversity dynamics.

Process-explicit models differ from pattern-based models by generating predictions based on explicit causal relationships between environmental drivers and ecological and evolutionary responses, rather than inferring implicit causal relationships based on correlations between observed and modelled patterns (Gotelli et al., 2009). A physiological model, for example, is process-explicit if it characterises the occurrence of a tree species in a landscape based on where the tree can minimise water stress. In contrast, a model is phenomenological (or correlative) if it maps the tree's occurrence based on the statistical relationship between annual precipitation and observations of occurrence, because no processes linking precipitation and fitness are specified. The process-explicit model allows patterns (e.g., a contraction of the tree species' range) to be connected to processes that cause them (e.g., an increase in seedling mortality in a drought), while the phenomenological model cannot explicitly link a changing pattern to a causative agent (Kearney & Porter, 2009). Similarly, a phenomenological model that hindcasts plant functional types on the landscape based on correlations between climate and pollen records cannot link

pattern and process in the same way as a DGVM that hindcasts plant nutrient cycling and competition over the same period (Gritti et al., 2010).

Phenomenological models and experimental observations sometimes find strong or unexpected correlations that can suggest the mechanisms that produce them. Proposed mechanisms can be used to build process-explicit models that can then be tested against observed patterns (Fordham et al., 2020). Studies of the effect of biodiversity on ecosystem function offer an example of this ontology (Figure 2). Effects of depauperate plant richness on ecosystem function were first observed empirically in experimental chambers and plots, which led to the proposed mechanism of niche complementarity, which in turn became the basis for mechanistic models of ecosystem function (Naeem, 2002). In this way, phenomenological and experimental analysis can provide important insights into the workings of nature that can be tested using process-explicit models.

Revealing structure and dynamics

Process-explicit models can operate at diverse levels of biological organisation, ranging from the gene to the ecosystem (Figure 3). The level of biological organisation that is simulated—genetic, species, or ecosystem diversity—has, to date, dictated the number and combination of possible biotic processes that are modelled (Fordham et al., 2020). The five primary processes responsible for the origin, structure, and dynamics of biodiversity are speciation, ecological interaction, adaptation, movement, and extinction (including population extirpation). In this context, ecological interactions encompass both interspecific species interactions (competition, predation, herbivory, parasitism, and mutualism), and ecosystem processes (nutrient cycling, photosynthesis, stability, etc.).

Ecosystem- and population-level models were the earliest process-explicit models. They generally include ecological interaction and local- to range-wide extinction processes (Figure 3), but not movement, speciation or adaptation. In contrast, more recently developed community level models simulate all five primary biotic processes (Rangel et al., 2018). These and individual-based models are becoming more frequently used to unravel biological mechanisms that underpin

spatiotemporal patterns of biodiversity (Figure 3). These advances promise to lead to a greater awareness of the importance of eco-evolutionary processes in shaping biodiversity (Gotelli et al., 2009).

Genetic diversity

Although coalescent models have simulated genetic diversity—trait inheritance within species—for 40 years (Kingman, 1982), early approaches did not model differences in DNA among individuals in space and time. This advance was not made until the beginning of the 21st century (Figure 3) with the advent of a spatially explicit simulation framework for population genetics: the serial-genetic simulator SPLATCHE (SPatial and Temporal Coalescent in a Heterogeneous Environment). The first studies to use SPLATCHE found that range expansions in heterogeneous environments produce genetic diversity patterns contingent on the geographical origin of the expansion, allowing spatially explicit genetic models to trace back the origin points of range expansions (Ray, Currat, Berthier, & Excoffier, 2005). Subsequently, coalescent-based process-explicit models have been frequently used to infer the effects of species' range expansions, contractions, and shifts on patterns of genetic diversity, using ancient and modern DNA. They have revealed that genetic diversity declines toward the leading edge of a species range more steeply than predicted by neutral theory (T. A. White, Perkins, Heckel, & Searle, 2013) and that rapid range contractions conserve more genetic diversity in refugial populations than slow range contractions (Arenas, Ray, Currat, & Excoffier, 2012). These models have also shown that present-day isolation of a population is a poor indicator of the past diversity of the lineage and historical barriers to gene flow (J. L. Brown & Knowles, 2012), and that rapid warming events can reconfigure species assemblages (Bemmels, Knowles, & Dick, 2019). Together, these reconstructions of past patterns of genetic diversity using process-explicit models are helping to improve projections of future patterns of genetic diversity by parameterising known responses to environmental shifts (J. L. Brown et al., 2016).

Virtual genomes can be simulated to test and refine theories of genetic diversity. These genomes are simulated with mutation, migration, and divergence on computer-generated landscapes using *a priori* mutation rates and dispersal patterns. This approach has been used to simulate species' range

expansions, revealing that introgression (transfer of genetic information from one species to another as a result of hybridisation (E. Anderson & Hubricht, 1938)) is likely to occur from the resident population to the invading population, regardless of the relative densities of the resident and invader populations (Currat, Ruedi, Petit, & Excoffier, 2008). Simulations of virtual genomes have also shown that new mutations near the leading edge of an expanding range have a higher frequency and wider spatial distribution than in a stationary population (Klopfstein, Currat, & Excoffier, 2006). This result suggests that spatially expanding populations have an increased rate of evolution at their frontier (Klopfstein et al., 2006), with important implications for the management of invasive populations and range-shifting native species.

Species Diversity

Process-explicit models used to decipher patterns of species diversity can focus on the individual, species, or community level of biological organisation, and findings about the operation of biological processes at different levels of species diversity can reinforce or amplify one another. For example, an individual-level model can elucidate the evolution of optimal dispersal strategies within a single habitat island (Dytham, 2009), a population-level model can reveal species diversity patterns across a chain of islands shaped by different dispersal strategies (Hovestadt & Poethke, 2005), and a community-level model can infer dispersal strategies in different functional groups, based on diversity across an entire region (Sukumaran, Economo, & Knowles, 2016). In this way, process-explicit models at these three levels of organisation allow us to investigate and potentially to integrate the impact of movement on species diversity patterns at multiple biological scales.

Processes can be modelled at the level of the individual organism with agent-based models (Welch, Kwan, & Sajeev, 2014) and physiological approaches (Yue Wang et al., 2018). The former can potentially capture any of the five fundamental biotic processes responsible for biodiversity and can generate complex population- and community-level phenomena that arise from ecological interactions among individuals (Grimm et al., 2005). For example, individual-based models of initial colonisation in a range expansion or shift have shown that the interaction of local adaptation with timing (Mark C. Urban & De Meester, 2009) and speed (Phillips, 2012) of colonisation can alter the expected distribution of a species along an environmental gradient.

However, models built at the individual level can be computationally intensive, particularly if they simulate complex eco-evolutionary processes for many populations of individuals. Moreover, they can be difficult to parameterise and validate (Figure 4), because data on biotic processes like movement and other attributes are often unavailable at the level of the individual. The computational demands of these models have led some researchers to use machine learning techniques (as emulators) to generalise process-explicit model behaviour post-hoc at small scales and apply those generalisations to larger scales (Vahdati, Weissmann, Timmermann, Ponce de León, & Zollikofer, 2019). Others have used virtual landscapes to simulate and explore the population-level effects of different movement strategies, requiring neither biotic nor environmental data for parameterisation (Mark C. Urban & De Meester, 2009). This approach, which allows for the simulation of data-poor processes at the individual level, has shown that range shifts can be accelerated by the evolution of greater dispersal ability in marginal habitats (Dytham, 2009).

Physiological models, such as NicheMapper (United States Patent No. US7155377B2, 2006), and forest gap models, such as ForClim (Risch, Heiri, & Bugmann, 2005) and PHENOFIT (Chuine & Beaubien, 2001), simulate only local- to range-wide extinction in animals and trees, respectively, making them computationally less intensive than individual-level models at large spatial scales. These approaches assume that if environmental conditions are suitable given an organism's physiological traits, it will persist; otherwise, it will die. These models are built on physiology and thermal tolerances, which are used to predict where individuals can survive. Physiological models can refine projections from phenomenological models of species distribution by identifying locales where heat stress will cause local extinction, informing conservation management (Kearney & Porter, 2009; Mathewson et al., 2017).

Individual-level models are, nevertheless, often constrained to ecological and evolutionary processes at local extents, often failing to account for potentially important coarser-scale processes that can affect species diversity. Population models, which find their roots in simple logistic growth equations or matrix population models (Caswell, 2001), can simulate movement and mortality in a network of populations extending across a species range (Fordham et al., 2022, 2013). They can simulate trait values and genes, thus incorporating adaptation or speciation

20

among populations over time, uncovering interactive effects of adaptation and dispersal on distributions of phenotypes (Cheptou & Massol, 2009). Although these models usually feature one or a few focal species, they can be used to simulate many populations of interacting species, capturing ecological interactions and community dynamics (Hovestadt & Poethke, 2005). For example, a model of competing and evolving populations has shown that certain syndromes of life history traits (mating system and dispersal ability) outcompete others—a mechanistic prediction that fits with empirical observations in plants (Cheptou & Massol, 2009).

Pathways to extinction are difficult to detect and disentangle phenomenologically (Cardillo & Bromham, 2001) because they are complex, often starting long before the extinction event, resulting from biological responses to natural and human-induced factors that operate at multiple spatiotemporal scales (Fordham et al., 2022). Linking population models to correlative species distribution models to address well-recognised limitations of pattern-based approaches (Fordham, Bertelsmeier, et al., 2018) is allowing the processes of movement, extinction, and—most recently— adaptation to be simulated over multiple millennia (Diniz-Filho et al., 2019). This approach is revealing how ecological strategies, and demographic and evolutionary traits, interact dynamically with past environmental change and human-driven factors to cause the decline and eventual extinction of species (Fordham et al., 2022).

Biodiversity loss can be modelled for groups of interacting species using community-level models. Process-explicit models at the community level simulate biogeographical dynamics with species as functional units within the simulation (Gotelli et al., 2009). Unlike population models, which typically have species or population distributions as their outputs, or ecosystem models, which generally produce maps of ecosystem function or plant functional guilds (see below), these community-level biogeographical models usually generate species richness maps and range size frequencies (Rangel et al., 2018).

Most community-level process-explicit models encompass all of the five biotic processes that drive biodiversity, making them aptly suited for testing differing hypotheses about the underlying causes of patterns of biodiversity, including how lineages diversify over space and time. For example, community-level process-explicit models have been used to determine if neutral theory can explain

empirical patterns of reef community dynamics, finding support for the theoretical expectation that range size should increase with dispersal ability (Alzate, Janzen, Bonte, Rosindell, & Etienne, 2019). However, models of community-level processes are not only used to answer theoretical questions about biodiversity—they can also be applied directly to real-world ecological systems to understand patterns of species richness (Leprieur et al., 2016), community assembly (Stegen, Lin, Fredrickson, & Konopka, 2015), and diversity loss (Halley, Sgardeli, & Triantis, 2014) in a changing world. Diversification models with simple parameterisation have applications in conservation biology, including identifying the effects of environmental change on biodiversity hotspots (Descombes et al., 2018) and predicting the loss of species in a community after habitat destruction (Halley et al., 2014). Despite their complexity, these process-explicit models of biogeographical dynamics can be validated (Figure 4) using targets of current-day range size frequency distributions (Rangel et al., 2007).

Ecosystem Diversity

Ecosystem diversity models simulate the structure of functional groups of terrestrial and marine organisms. The coexistence and interactions of these groups are used to map the distribution of ecosystems (Kutzbach et al., 1998). Interactions among terrestrial autotrophs and the abiotic environment are modelled with DGVMs (Foley et al., 1996), while fisheries management models (Collie et al., 2016) and general ecosystem models (GEMs) (Harfoot et al., 2014) also include primary and secondary consumer dynamics, enabling simulation of energy transfer through food webs. These ecosystem diversity models are being used to forecast and manage ecosystem services, including carbon storage (Bondeau et al., 2007), clean water supply (Rieb et al., 2017), and food security (Fulton et al., 2011) in a changing world. They have shown that freshwater supply will be reduced under future warming to the detriment of terrestrial ecosystem functioning (Cramer et al., 2001), that increased hurricane frequency threatens the structure and productivity of reef-fish communities (Mumby, 2006), and that habitat fragmentation affects the trophic structure of ecosystems (Bartlett, Newbold, Purves, Tittensor, & Harfoot, 2016). Furthermore, process-explicit ecosystem models have shown that forest function is more resilient to warming events in high than in low diversity forests (Sakschewski et al., 2016), illustrating causative mechanisms for experimental observations (Naeem, 2002).

DGVMs simulate the distribution of plant functional types as well as their fluxes of carbon, water, and nutrients through the environment (Foley et al., 1996), enabling them to simulate dynamic feedbacks between the biosphere and the climate when coupled to climate models (Houghton et al., 2001). This coupling of models has uncovered important interactions between climate, CO_2, and ecosystem function, including evidence that a positive interaction between plant productivity and elevated levels of CO_2 can potentially offset the negative effects that climate change and, more specifically, increased aridification can have on productivity (Sitch et al., 2008). Moreover, by hindcasting ecosystem diversity dynamics over glacial-interglacial cycles, DGVMs have disentangled many of the effects of climate on ecosystem structure (Kaplan et al., 2003). For example, modelling the interaction between deglacial warming and megaherbivore die-off following the last glacial maximum reveals how high-latitude mammoth steppe—the earth's most extensive biome at the time—was converted to a taiga-tundra ecotone (Zhu et al., 2018).

While GEMs can simulate the entire ecosphere, from phyto- and zooplankton to apex carnivores, capturing complex food web dynamics, they do not as yet include two-way interactions with climate (Bartlett et al., 2016; Harfoot et al., 2014). Consequently, they are frequently used to test theories regarding ecosystem structure, including relationships between heterotroph biomass and net primary productivity (Harfoot et al., 2014), and to determine the impact of recent land-use change on ecosystem function (Bartlett et al., 2016). The application of ecosystem-level models in fisheries management has uncovered the crucial ecosystem services provided by coral reefs, including calcium carbonate deposition and coastal protection, showing how overfishing disrupts these services to nature and people (McClanahan, 1995).

Relationship to data and theory

Process-explicit models have a variety of relationships with data and theory (Figure S1). Some process-explicit models are *theory-driven*: their purpose is to explore the implications or applications of an ecological theory, such as the neutral theory of biodiversity (Hubbell, 2001), the species-area relationship (Connor & McCoy, 1979) or the general dynamic theory of island biogeography (Whittaker, Triantis, & Ladle, 2008). Others are *theory-scaffolded*: their purpose is to

understand an ecological system empirically, and to use theory as a scaffold by which to structure the model and interpret its outputs (Sitch et al., 2008).

While process-explicit models are diverse in structure (Bemmels et al., 2019; Diniz-Filho et al., 2019), they exist on two distinct continua, based on (i) their use of empirical data for parameterisation and (ii) how they are verified and/or validated (Figure 4). Empirical data are not necessary to build and run a process-explicit model. Indeed, many theory-driven models use arbitrary values for parameters and explore the interactions and patterns that result from the model (Stegen et al., 2015). These models are at one end of a parameterisation continuum. Further along the continuum are models that use either biotic data (such as genetic sequences or species occurrence) or environmental data (such as spatiotemporal climatic fluctuations or bathymetry change) to parameterise models, but not both (Rangel et al., 2018). The next category of models includes those that use biotic and static environmental data (Alroy, 2001), followed by models that use biotic and dynamic environmental data (Foley et al., 1996). In the last two cases, biotic data represent a single level of biological organisation: gene, individual, population, community, or ecosystem (Fordham et al., 2020). At the most extreme end of the parameterisation continuum lie models that use dynamic environmental data and biotic data to simulate processes across multiple levels of biological organisation: for example, simulating individual-level movement (based on seed dispersal by wind) as well as population-level mortality (based on survival across individuals) (Snell, 2014).

A second, distinct gradient specifies how data are used for verification and validation in process-explicit models (Figure 4). *Verification* is a check to ensure that the implemented model meets the primary theoretical assumptions it has been built to represent. In contrast, *validation* evaluates the level of correspondence between the implemented model and the study system (Rykiel, 1996). At one end of the verification and validation continuum, model outputs are not verified or validated at all. Moving up the continuum, output patterns can be verified for congruence with theory by comparing model outputs with well-established theoretical relationships, such as the mid-domain effect (Keith & Connolly, 2013). Models can be validated through visual inspection of patterns based on observational data, using non-statistical procedures (Bonan, Levis, Sitch, Vertenstein, &

Oleson, 2003). Statistical validation allows model outputs to be evaluated with patterns of empirical data, by means of measures such as coefficient of determination (r^2), root mean square error, or true skill statistic (Kaplan et al., 2003). At the most data-heavy end of the verification and validation continuum lies multivariate statistical validation (J. L. Brown & Knowles, 2012), in which models are evaluated based on their ability to simultaneously demonstrate goodness of fit to multiple empirical patterns. This demanding level of validation is now being applied to pattern-oriented modelling (an emerging and powerful technique in data science), in which mechanisms governing the structure and dynamics of biodiversity are identified by converging model simulations to independent multivariate validation targets (Fordham et al., 2022; Rangel et al., 2007).

Figure 4 shows how process-explicit models with diverse relationships to data can be used to decipher the mechanisms underlying the structure of biodiversity. Models that use little or no empirical data can be used to test ecological and evolutionary theories, such as modes of speciation (Skeels & Cardillo, 2019). These primarily theory-driven models are useful even when biological data are not available for validation; for example, data-free process-explicit models can test the sensitivity of model outputs to underlying processes (Skeels & Cardillo, 2019), distinguishing metapopulation dynamics from neutral dynamics or random community assemblage (N. A. Urban & Matter, 2018). Theory-scaffolded models with complex parameterisation often have greater explanatory power, particularly if they use more than one level of biotic data for parameterisation and validation, and if they simulate dynamic drivers of global change affecting the spatial structure of biodiversity. These additional data inputs can allow otherwise necessary model assumptions to be relaxed, such as an assumption of unlimited movement (Snell, 2014) or static human land use (Contreras et al., 2019), while multivariate validation targets (despite being, so far, rarely used) provide more stringent tests of model simulations.

Safeguarding biodiversity

Sustainable management of biodiversity has been recognised as a policy goal for 30 years ("Text of Convention Treaties and Agreements," 1992); however, progress in halting the decline and degradation of biodiversity has been limited (Mace et al., 2018). Reasons for failing to reduce

biodiversity loss are complex, reflecting long-lasting knowledge gaps on biodiversity dynamics (M. C. Urban et al., 2016), as well as insufficient integration of biodiversity science in policy making (Young et al., 2014) and lack of motivation to deliver the required biodiversity changes (Díaz et al., 2020). An incomplete understanding of the mechanisms that govern the structure and dynamics of biodiversity, and a tendency to use correlative rather than process-explicit approaches to forecast the future of biodiversity in a changing world (Briscoe et al., 2019), have constrained capabilities to set productive biodiversity targets, develop cross-cutting solutions for restoring nature, and obtain national commitments to biodiversity conservation.

Process-explicit models have a diverse range of applications, including formulating and assessing potential solutions for mitigating future genetic-, species-, and ecosystem-level collapse. Currently, for example, the palaeorecord is being used to identify biological mechanisms that mediate responses to climate- and human-driven change using process-explicit models (Nogués-Bravo et al., 2018). These palaeo-models can disentangle past determinants of genetic diversity, range shifts, species richness, and ecosystem structure and function. By specifying the causal processes that underpin biodiversity change, they can provide the context needed to improve confidence in predictions of biodiversity's future (Fordham et al., 2020), leading to improved computational platforms for setting biodiversity targets and better solutions for mitigating adverse changes to biodiversity (Fordham et al., 2016).

The genetic signatures of demographic responses of species to environmental changes can be decoded using genetic simulation models (Eriksson et al., 2012) to better manage future biodiversity (Fordham, Brook, Moritz, & Nogués-Bravo, 2014). For example, process-explicit models of gene fixation, which allow demographic trends and gene flow to be reconstructed (Yoder et al., 2018), are establishing the importance of intraspecific genetic diversity for resilience to accelerated climatic change (Frankham, 2010). There is now a push to use this technique more widely to improve knowledge of how rapid climatic change affects patterns of genetic diversity (J. L. Brown et al., 2016). In the absence of ample genetic samples, process-explicit models can still be used to test theories central to conservation genetics using virtual genetic sequences and landscapes

(Erm & Phillips, 2019) to deliver valuable information for conserving future genetic diversity (Theodoridis et al., 2020).

Historical context is crucial for understanding the threat of future declines in species distributions. Process-explicit models constructed at the individual and population level can be used to identify demographic processes that cause range shifts for a species or suites of species in response to climatic and environmental drivers, improving species threat assessments (Mathewson et al., 2017). Because individual-based models often operate at a level of detail that is not necessary for simulating range dynamics across large extents, process-explicit population-level models are more commonly used to project past and future range dynamics. These population-level models can be used to identify ecological traits that cause species to be differentially prone to regional and range-wide extinction (Pereira, Daily, & Roughgarden, 2004) and to evaluate the efficacy of current methods for identifying threatened species (Stanton, Shoemaker, Pearson, & Akçakaya, 2015). Population-level models that incorporate adaptation as a process have been influential and instructive in revealing the role of gene flow along ecological selection gradients, and its inhibiting effect on local adaptation to environmental change (Kirkpatrick & Barton, 1997).

Hotspots of biodiversity are of particular conservation concern because they support high concentrations of species, particularly endemics (Mittermeier, Turner, Larsen, Brooks, & Gascon, 2011). Process-explicit models built and validated at the community level to simulate geographical patterns of species richness and endemism can identify mechanisms central to the maintenance of past and contemporary hotspots of biodiversity (S. C. Brown, Wigley, Otto-Bliesner, Rahbek, & Fordham, 2020), providing a framework for assessing vulnerability to future climate and environmental change (Figure 5). If simulations can capture community-level responses to realistic tempos and magnitudes of future global change, these new predictive approaches will benefit 21st century environmental management and conservation (Fordham et al., 2020).

To illustrate the state of the art in broad-scale modelling of biodiversity and its potential application for biodiversity conservation, we offer an example of a community-level, process-explicit model that incorporates all five biological processes that govern the structure and dynamics of biodiversity in a temporally dynamic environment (Rangel et al., 2018). The model was

designed to simulate the geographic distributions and patterns of overlap of species ranges in response to the past 800,000 years of climate change in South America (Figure 5). In this model, evolutionary niche dynamics drive range expansion and fragmentation (leading to speciation), adaptation to climatic conditions, and extinction. Combinations of parameter settings (dispersal distance, evolutionary rate, time for speciation, and intensity of competition) for virtual species were chosen *a priori*, producing many different potentially plausible range maps. Although not directed by any empirical validation targets, the emerging maps closely resembled contemporary species richness of major South American taxa. Combinations of parameters that closely reproduced the current-day biodiversity of South American avifauna (including hotspots of species richness and endemism) showed that low rates of adaptation to past climatic change were required to reconstruct observed patterns of species richness. In the future such community-level simulation models (built to simulate the past and validated in the present; Figure 5) could be parameterised with climate forecasts to predict strongholds of species richness under future climates. The subsequent results could be used to guide the protection and future management of biodiversity.

By identifying the biological mechanisms, drivers, and their interactions that mediate changes in ecosystem structure and function, process-explicit models can help safeguard the services ecosystems provide to nature and people. Early ecosystem models were used to investigate the effects of increased atmospheric carbon on vegetation communities (Cramer et al., 2001). More recent models have incorporated complex interactions between multiple drivers of global change and ecosystem-level processes, including the effects of agriculture and land-use change (Bondeau et al., 2007). This research has strengthened knowledge of the drivers and responses that underpin change in ecosystem structure and function (Boit et al., 2019; Bondeau et al., 2007), improving projections (Leadley, 2010) and informing protocols for assessing ecosystem threat status (IUCN-CEM, 2016). For example, DGVMs have shown mechanistically how 20th century agriculture caused a 24% reduction in global vegetation and a 10% reduction in global soil carbon (Bondeau et al., 2007). A better understanding of processes of ecosystem change enables the simulation of the effects of current and future climatic and environmental change (including altered fire regimes) on

important ecosystem services, such as agricultural productivity, freshwater availability, and timber production (Boit et al., 2019; Contreras et al., 2019).

Climate projections are currently made using models characterised by complex system dynamics, including interactions and feedbacks between the atmosphere, ocean, land and society (O'Neill et al., 2016). While analogous models for projecting biodiversity change have typically been simpler than approaches used in climate science, mechanistic general ecosystem models (Harfoot et al., 2014) and process-based community assemblage models (Hagen et al., 2021) offer new and more robust methods for projecting the future distribution of life on Earth. These next generation biodiversity models, which explicitly capture the structure and dynamics of biodiversity, will strengthen our capacity to set achievable biodiversity targets that promote engagement and investment where change is needed.

Looking forward

Although phenomenological models are a crucial first step towards understanding the potential determinants of current and past spatial patterns of biodiversity, process-explicit models are needed to identify causal processes that govern the structure and dynamics of biodiversity, and to exclude those that do not. Increased open access to curated georeferenced occurrence records, dated fossils, libraries of genetic sequences, and climate simulations will continue to provide innovative opportunities to apply process-explicit models, especially to connect inferences of past responses of biodiversity to different rates and magnitudes of contemporary climate and environmental change (Nogués-Bravo et al., 2018). These opportunities include testing key assumptions of existing biodiversity models—such as the common assumption that processes driving changes in biodiversity are scale invariant (J. H. Brown et al., 2002)—and competing theories for large scale biodiversity patterns, including geographical gradients in species richness (Hagen et al., 2021).

Continuous simulations of the transient late Quaternary climate are needed, ideally at fine spatial resolutions, to determine population-, species-, community-, and ecosystem-level responses to abrupt (as well as gradual) climatic change using process-explicit models (Fordham, Saltré, Brown, Mellin, & Wigley, 2018). The TRaCE21ka experiment based on the Community Climate System Model version 3 (Z. Liu et al., 2009) has bridged this gap, but it spans only the last 21,000 years.

Higher spatiotemporal resolution palaeoclimate simulations from Earth systems models prior to 21,000 years ago that include solar flux, ice sheet extent, and sea level changes will provide a more thorough understanding of the mechanisms responsible for spatiotemporal patterns of biodiversity at evolutionary time scales (Fordham et al., 2020). Statistical emulators of climatic change will be useful in filling this data and knowledge gap (Holden et al., 2019), particularly in the Southern Hemisphere, for which there is a paucity of high-resolution simulated data before the last glacial maximum (Neukom & Gergis, 2012). Including better reconstructions of solar variability, volcanic eruptions, and land use during the Holocene in transient simulations of the earth's climate will provide a more complete picture of more recent temporal change in regional climates and the biodiversity they support.

Integrating palaeoecological and neoecological perspectives into process-explicit models is key to contextualising the present and anticipating and visualising ecological responses to future global change (Nogués-Bravo et al., 2018). Emerging genomic techniques are allowing genetic diversity and effective population size to be estimated over short periods (<100 years) of environmental change, providing inferences of eco-evolutionary change to recent and/or punctuated disturbance events (Bi et al., 2019; Díez-del-Molino et al., 2018; Roycroft et al., 2021) that can feed directly into process-explicit models of range collapse and population declines. Importantly, projections of recent climate, vegetation, and land-use change have been harmonised with ancient projections, allowing their effects on biodiversity to be characterised continuously in process-explicit models that run from as far back as 21,000 years ago to the present day (Hurtt et al., 2020) and, in some cases, into the future (S. C. Brown, Wigley, Otto-Bliesner, & Fordham, 2020).

Adaptation was first incorporated into spatial process-explicit models in the early 2000s (Heino & Hanski, 2001) and has become more common in ecological and evolutionary models since. However, it remains the most infrequently modelled biological process. A more regular integration of adaptation into process-explicit models of climate change responses will benefit from taxonomically diverse datasets of historic DNA that are readily available today (Benson et al., 2012) and from technological advances that allow ancient DNA to be used to reconstruct shifts in genetic diversity and adaptations to large-magnitude and abrupt climatic change (van der Valk et

al., 2021). Adding community dynamics to population models and demography to community models will also strengthen projections of biodiversity change. Metacommunity models with simplified food webs can bridge this gap by modelling demographic interactions between populations of multiple species in a spatiotemporally explicit manner (Leibold et al., 2004). Community-level models can integrate a higher level of biological organisation by combining ecosystem-level drivers such as fire with processes of plant community assembly (Scheiter, Langan, & Higgins, 2013).

Achieving more detailed mechanistic understandings of patterns of biodiversity—from the gene to the ecosystem level—will require a greater focus on rigorous statistical validation of process-explicit models using independent multivariate data that are spatiotemporally explicit. In systems where theory is not yet well-developed, empirical data for model parameterisation are needed to simulate realistic outputs. However, as the mechanisms underpinning a system's biodiversity become better understood, model outputs will be simulated using theory alone. Realistic predictions generated from a strong theoretical framework are the pinnacle that ecologists and evolutionary biologists should be aiming for when wielding process-explicit models.

Process-explicit models have been instrumental in improving knowledge of the distribution of life on Earth, revealing complex causal processes for contemporary patterns of biodiversity that could not be discerned from experimental approaches or phenomenological models. A deeper recognition of the structure and dynamics of organisms, communities, and ecosystems in process-explicit models is helping to protect and restore biodiversity by formulating remedies to existing problems and countering undesirable future changes.

Figures
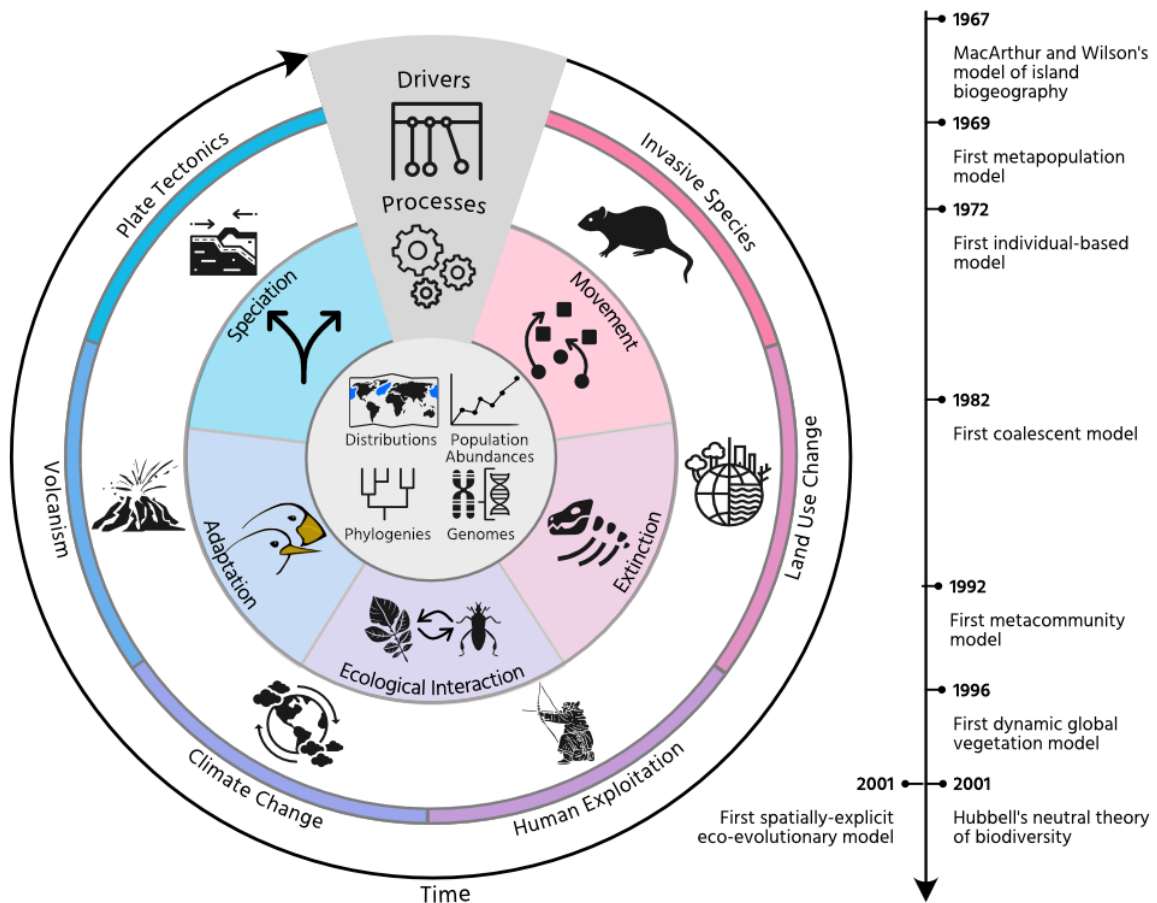
Figure 1: Modelling the mechanisms that govern the structure and dynamics of biodiversity. Process-explicit models can simulate changes in species distributions, population abundance, phylogenies, and genomes based on evolutionary and ecological processes (movement, extinction, ecological interaction, adaptation, and speciation) and drivers of environmental change (invasive species, land use change, human exploitation, climate change, volcanism, and plate tectonics.) Processes and drivers are ordered clockwise according to the temporal scale at which they operate. The timeline shows breakthrough developments in process-explicit models of biodiversity up to 2001.
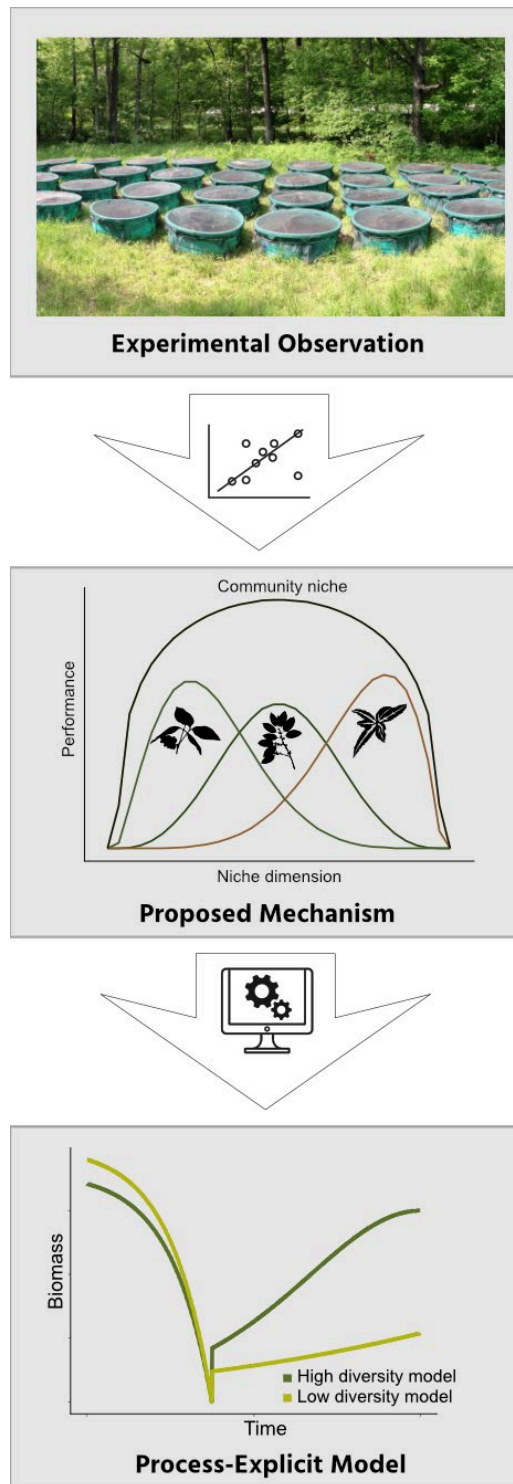
Figure 2: Pipeline from empirical observations to process-explicit models. The relationship between biodiversity and ecosystem functioning can be observed experimentally in mesocosms. Statistical analysis of experimental data can lead to proposed mechanisms of biodiversity functioning, such as niche complementarity (Naeem, 2002). This mechanism can be integrated into process-explicit models to simulate interactions between community structure and function.
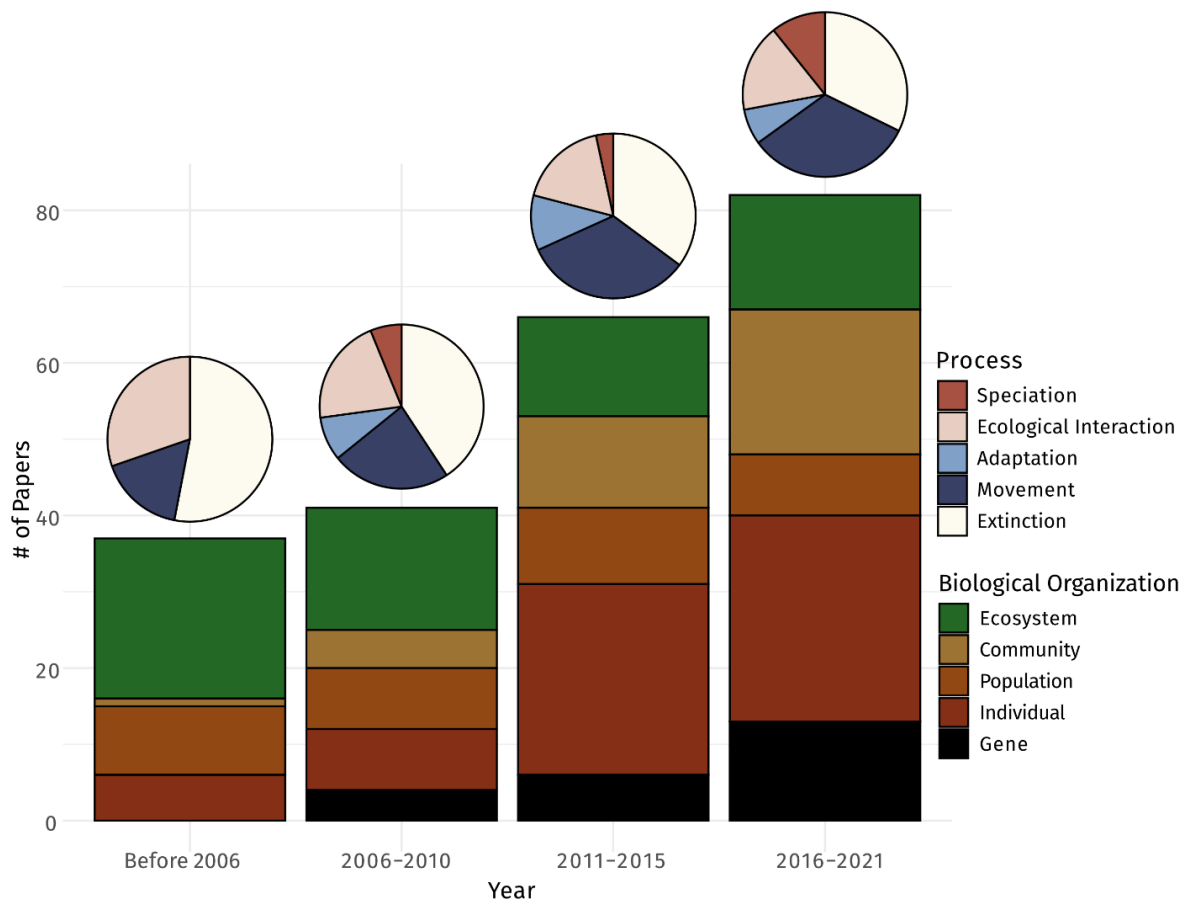
Figure 3: Processes and levels of biological organisation. Bars show the number (#) of studies using process-explicit models published before 2006 and in the five-year periods from 2006 to 2016, and from 2016 to 2021, color-coded to indicate the unit of biological organisation simulated. Pie charts show the biotic processes (speciation, ecological interaction, adaptation, movement, and extinction) modelled as fractions of the total number of processes modelled across all studies for each time bin.
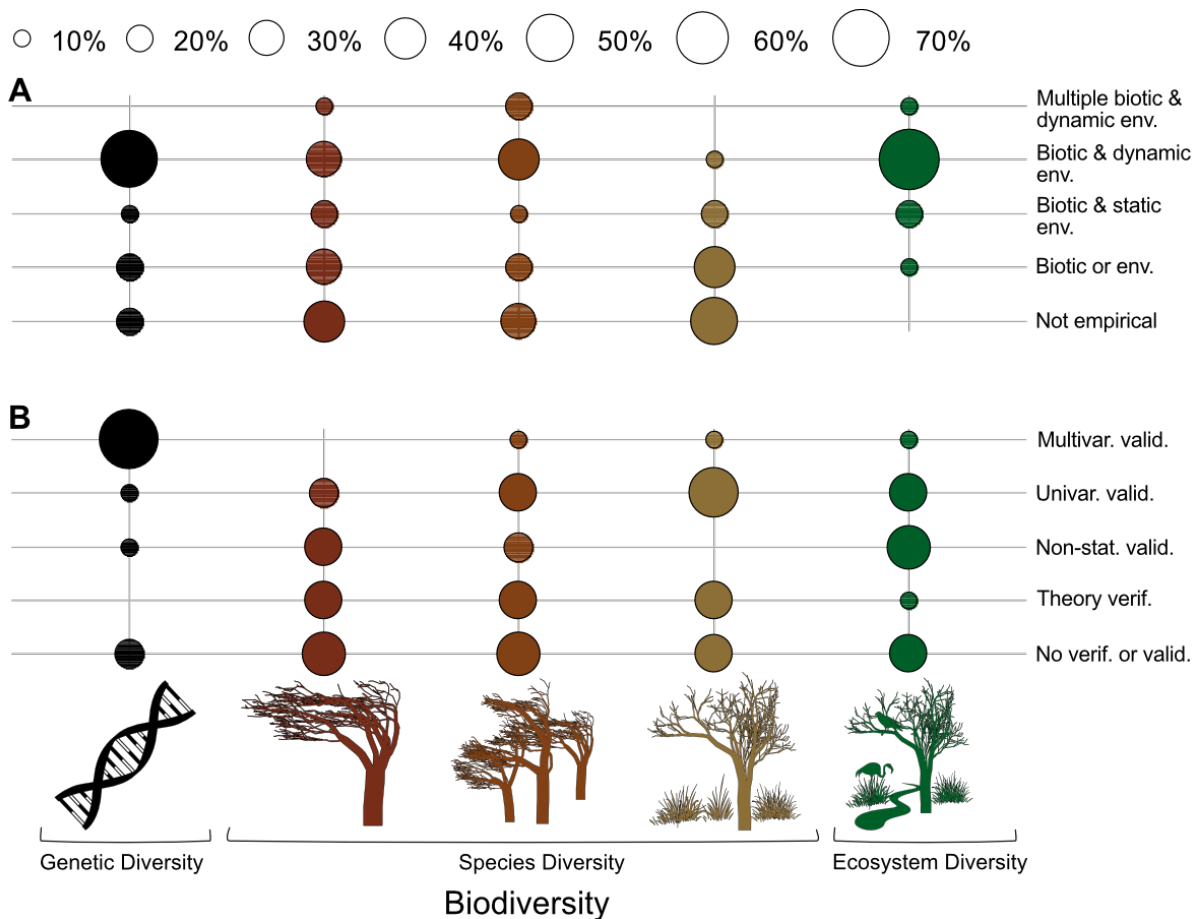
Figure 4: Model structure and assessment. A shows model structure (Parameterisation) and **B** shows model assessment (Verification & Validation) for five levels of biological organisation: gene, individual, population, community, and ecosystem (from left to right). Data categories in A for model parameterisation are: multiple biotic and dynamic environmental (env.), biotic and dynamic env., biotic and static env., biotic or env., and not empirical. Validation categories in B are: multivariate (multivar.) validation (valid.), univariate (univar.) valid., non-statistical (non-stat.) valid., theory verification (verif.), no verif. or valid. The categories of model parameterisation and validation are described in detail in "Relationship to data and theory" and Supplementary Methods. Size of circles indicates the relative number of studies reviewed (total = 225).
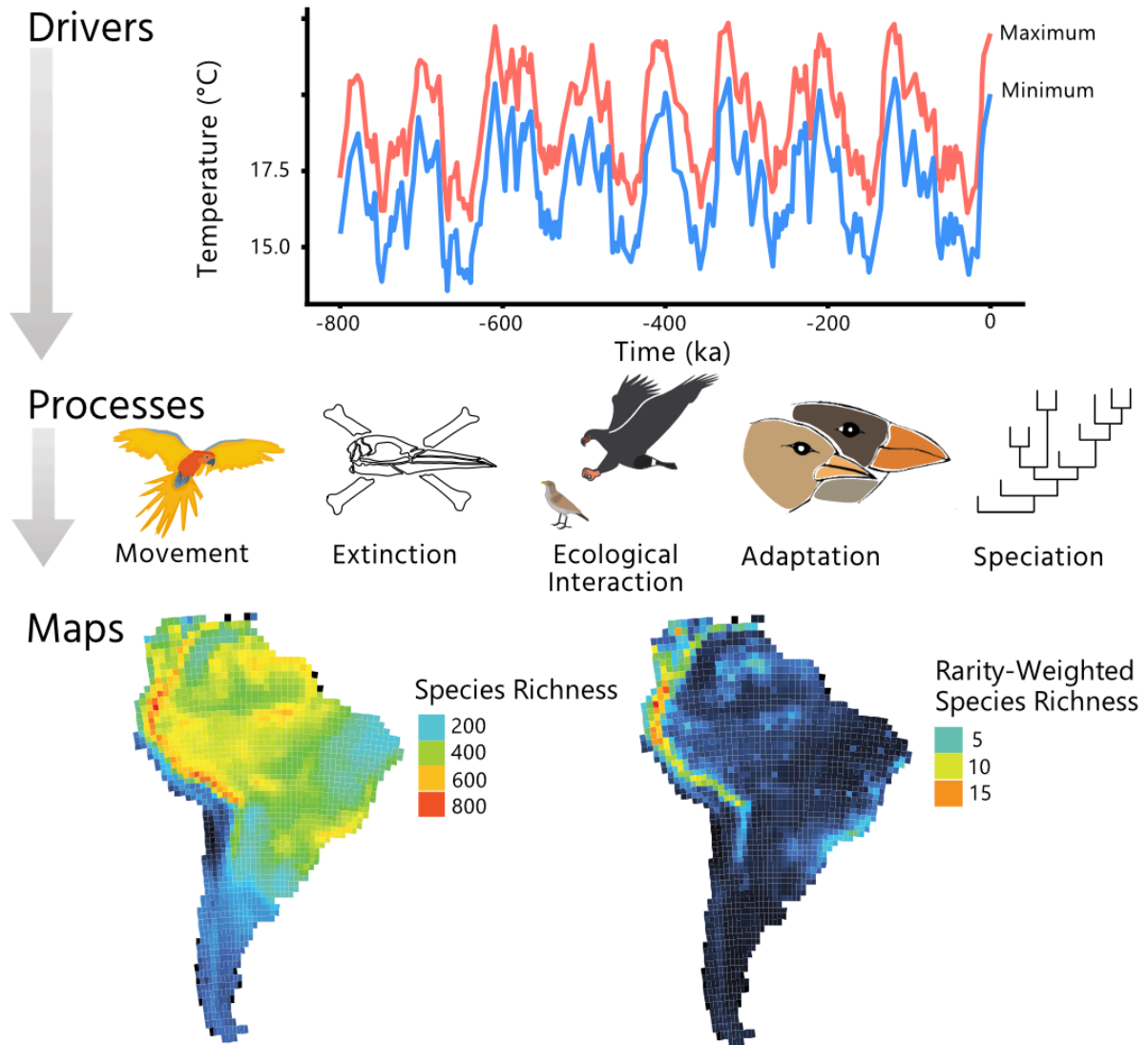
Figure 5: Models for predicting continental species richness. Community-level biogeographical models (Rangel et al., 2018), driven by interactions between climate and biological processes, can incorporate all five biological processes that govern biodiversity: movement, extinction, ecological interaction, adaptation, and speciation. Model outputs can simulate maps of current-day and future species richness and endemism (rarity-weighted species richness).

Supplementary Material

Supplementary Methods

Literature Search

To identify process-explicit models that simulate the structure and dynamics of biodiversity in space and time, we did a literature search on Web of Science on 30 Aug. 2021. We searched the title, abstract, and the keywords of papers using the following search:

(mechanism OR process* OR "range dynamics" OR "population dynamics" OR dispersal OR diversification OR speciation OR extinction OR movement) AND

(macroecology* OR paleoecolog* OR biogeograph* OR phylogeograph* OR "evolutionary ecology" or "ancient DNA") AND

("simulation model*" OR "mechanistic model*" OR "vegetation model*" OR "evolutionary model*" OR "metapopulation model*" OR "approximate bayesian computation" OR "demographic model*" OR "metacommunity model*" OR "evolutionary model*" OR "movement model*" OR "agent-based model*" OR "individual-based model*")

We did an additional and equivalent search on Scopus to ensure that we did not miss any papers in the Web of Science search. We only considered papers published 2020 or earlier in our literature review.

The first term in our literature search was used to identify studies that analysed key processes that govern biodiversity across space and time. The second term limited the literature search to papers in the scientific fields of biogeography (including phylogeography), evolutionary biology, and macroecology—fields that are pioneering the use of process-explicit models in understanding mechanisms governing spatiotemporal patterns of biodiversity (Connolly et al., 2017). The third term ensured that the literature review captured studies directly using process-explicit models— models that simulate the dynamics of a system as explicit functions of events that drive change in that system.

The literature searches returned 734 papers from Web of Science and 662 papers from Scopus. We retained papers that met three primary criteria: (i) models had to be process- and spatially explicit; (ii) models had to simulate at least one component of biodiversity: genetic, species, or ecosystem; and (iii) models had to explore the biological processes and drivers responsible for biological diversity across space and time. These filters reduced the number of papers to 225.

Data extraction

From these papers we first collected data on the biological processes and drivers of global change. To do so, we identified classes of biological processes: speciation, ecological interaction, adaptation, movement, and extinction (see Main Text and Table S1). Global change drivers modelled included climate, environmental and land-use change, geology (e.g., ocean bathymetry and island formation), human harvesting, and environmental variability.

We extracted the focal unit of biological organisation (Fordham et al., 2020) from each study (gene, individual, population, community, ecosystem) using a string of keywords (Table S2). We also considered the spatial extent being modelled as four classes: local, regional, continental, and global. We defined a study as local if it was at the site level, covering a region of < 200 km^2, or if it used a virtual landscape focused on the patch/population level. Regional studies were larger than the local scale but did not span an entire continent (Fordham et al., 2020).

We assessed process-explicit models along a parameterisation continuum (Table S3), based on the way studies used data for parameterisation (0-4). We categorised a model as:

0. if *a priori* or arbitrary settings were used for the model, or if the data were generated procedurally;
1. if the model was parameterised with biotic data or environmental data, but not both;
2. if the model was parameterised with biotic data at one scale of biological organisation, as well as environmental data from one timepoint;
3. if the model was parameterised with biotic data at one scale of biological organisation as well as environmental data over multiple timepoints; and

4. if the model was parameterised with dynamic environmental data as well as biotic data at multiple scales of biological organisation.

We placed models along a verification and validation continuum (Table S4). This continuum was based on the way studies used data for verification and validation. We define verification as a check that the logic of the model accurately formalises a theory, and validation as a check that the model mimics the real world well enough for its intended purpose, after Rykiel (Rykiel, 1996). We categorised a paper as:

0. if the model was not verified or validated against an external pattern;
1. if the model was checked for conceptual consistency with a well-established theoretical expectation such as the latitudinal species richness gradient;
2. if the model was validated with a non-statistical comparison to empirical data;
3. if the model was validated by statistical comparison to empirical data one variable at a time; and
4. if the model was validated by statistical congruence with multiple variables simultaneously.

In addition to extracting information on biological processes, global change drivers, and levels of biological and spatial organisation, we developed new heuristics to categorise process-explicit models by their relationship to theory (theory-driven or theory-scaffolded). Models were classified as theory-driven if their primary purpose was to explore an ecological theory, such as the mid-domain effect. Models were classified as theory-scaffolded if their primary purpose was to empirically explore an ecological system using theory as a scaffold—for example, using metapopulation theory to study whether a particular species might become locally extinct.

To help researchers conceptualise and build process-explicit models aimed at understanding the mechanisms responsible for spatiotemporal patterns of biodiversity, we developed a dichotomous key based on data requirements for different types of process-explicit models. The key includes examples of models and studies for different data types and modelling aims (Pilowsky, Colwell, Rahbek, & Fordham, 2022a).

Process	Example keywords
Speciation	Diversification, allopatry, sympatry, simulated phylogeny, speciation
Ecological interaction	Carbon flux, water flux, predation, competition, facilitation, mutualism, ecological interaction
Adaptation	Mutation, niche evolution, trait evolution, adaptation
Movement	Dispersal, range shift, colonisation, expansion, contraction, migration, movement
Extinction	Mortality, life history, extirpation, demography, recruitment, extinction

Table S1: **Words used to identify primary biological processes simulated in process-explicit models**. Note that the keywords used to identify the processes being simulated were not limited to the examples above. Papers could include anywhere from one to five of these processes.

Biological Organisation	Example keywords
Ecosystem	Dynamic vegetation model, functional group, biomass, carbon cycling, ecosystem
Community	Diversity pattern, species richness, assemblage, biodiversity, range size frequency distribution, community
Population	Species range, demography, extinction pattern, species distribution, regional/local extinction, population
Individual	Agent, organism, gap model, individual
Gene	Coalescent, diversity, differentiation, divergence, lineage, gene

Table S2: Words used to identify the focal unit of biological organisation simulated. Some models incorporated data from multiple levels of biological organisation, but in all cases, a single focal level of biodiversity was modelled. Note that the keywords used to identify the focal unit being modelled were not limited to the examples above.

Parameterisation	Example
0	Random draws from a Gaussian distribution (Stegen et al., 2015)
1	Temperature and precipitation from a palaeoclimate emulator (Rangel et al., 2018)
2	Species distribution data from megafauna fossils in North America and a static map of net primary productivity (Alroy, 2001)
3	Dynamic climate data and data on physiological tolerances of plant functional types (Bonan et al., 2003)
4	Dynamic climate data, data on physiological tolerances of plant functional types, individual-level data on seed dispersal (Snell, 2014)

Table S3: Types of data used for parameterisation of process-explicit models. Examples are shown for different classes of parameterisation along a continuum, arranged from least data-intensive to most data-intensive.

Verification/Validation	Example
0	Results are not compared to any external pattern (Pereira et al., 2004)
1	Verified by comparison to the species-area relationship (Pereira & Daily, 2006)
2	Validated by visual comparison between simulated and observed maps of biome distributions (Bonan et al., 2003)
3	Validated by statistical comparison of output species richness with empirical fossil diversity at different timepoints (Leprieur et al., 2016)
4	Validated by statistical convergence of simulated demography toward multiple genetic distances among populations (J. L. Brown & Knowles, 2012)

Table S4: Types of data used for verification or validation of process-explicit models.
Examples are shown for different classes of verification/validation along a continuum, arranged from least data-intensive to most data-intensive.
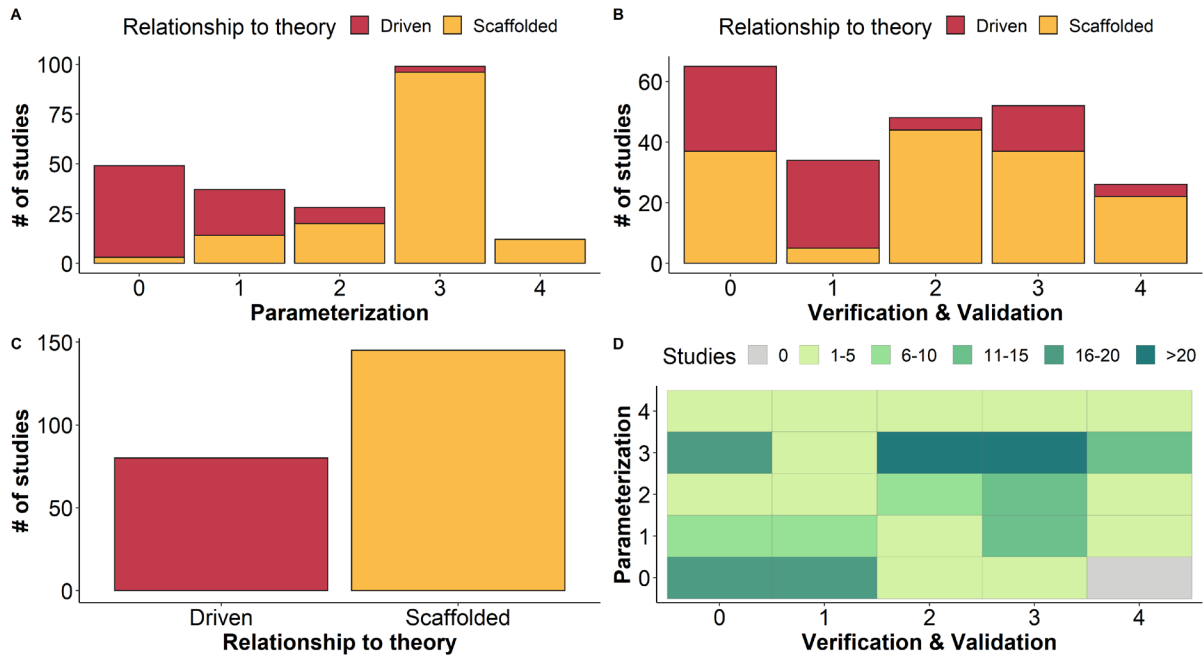
Figure S1: Diverse relationships to theory and data. Literature (225 papers) sorted along gradients of (**A**) parameterisation and (**B**) verification and validation for (**C**) theory-driven and theory-scaffolded models. **A** shows number (#) of studies in which model was parameterised using no empirical data [Parameterisation category (p) = 0]; environmental or biotic data, but not both (p = 1); biotic data and static environmental data (p = 2); biotic and dynamic environmental data (p = 3); and dynamic environmental data and biotic data at multiple scales of biological organisation (p = 4). **B** shows the number of studies in which models were not verified or validated [Verification & Validation (v) = 0]; verified by comparison to a well-established theoretical relationship (v = 1); validated by non-statistical comparison to empirical data (v = 2); validated by statistical comparison to empirical data using univariate (v = 3); and multivariate approaches (v = 4). **C** shows studies that explored or tested an ecological theory (Driven) and those that explored an ecological system empirically using theory as a scaffold (Scaffolded). **D** shows the number of studies that fall in each possible intersection of the parameterisation and the verification and validation continua. Categories in A-C are described in the text.

CHAPTER II: SIMULATIONS OF HUMAN MIGRATION INTO NORTH AMERICA ARE MORE SENSITIVE TO DEMOGRAPHY THAN PALAEOCLIMATE
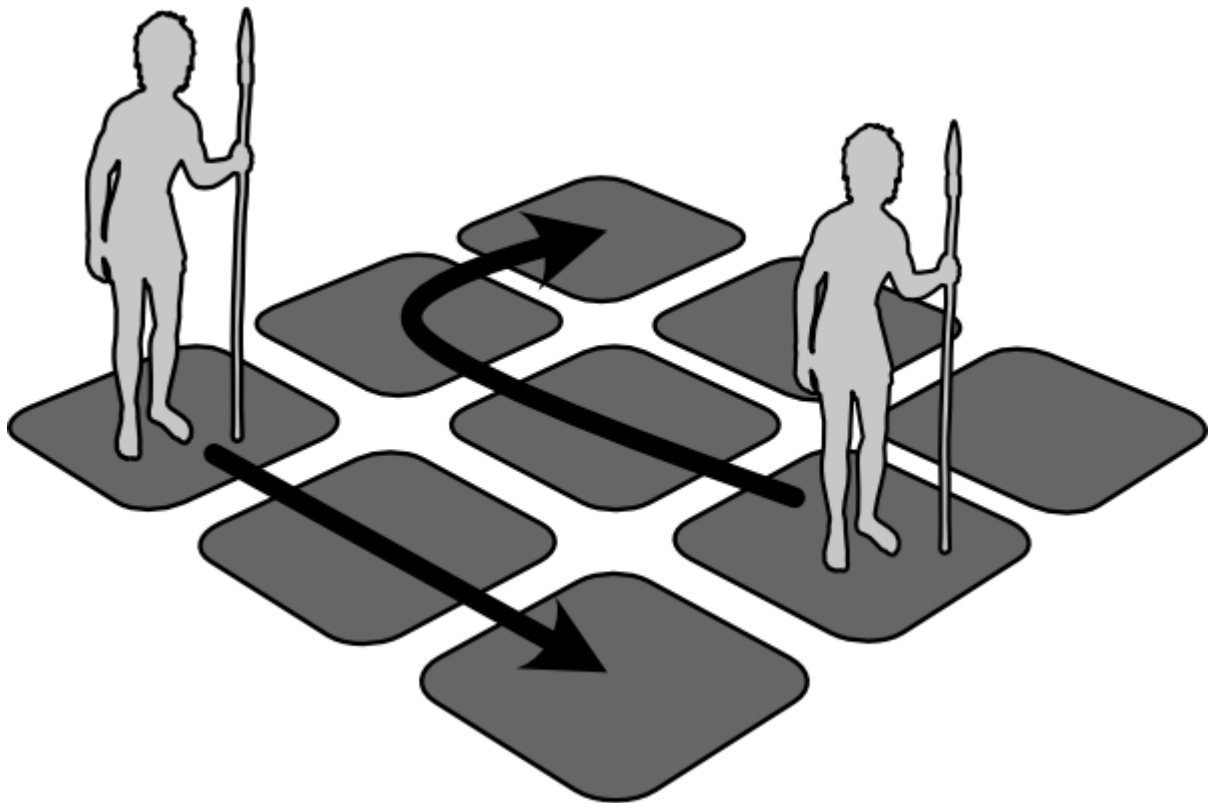
Statement of Authorship

Title of Paper	Simulations of human migration into North America are more sensitive to demography than choice of palaeoclimate model
Publication Status	Published
Publication Details	Journal: Ecological Modelling. Authors: Julia Pilowsky, Andrea Manica, Stuart Brown, Carsten Rahbek, Damien Fordham

Principal Author

Name of Principal Author (Candidate)	Julia Pilowsky
Contribution to the Paper	Conceived the idea for the manuscript with advisors Prof. Rahbek and A/Prof. Fordham. I ran the simulations, analysed the results, and wrote the manuscript, with contributions from co-authors.
Overall percentage (%)	80 %
Certification:	This paper reports on original research I conducted during the period of my Higher Degree by Research candidature and is not subject to any obligations or contractual agreements with a third party that would constrain its inclusion in this thesis. I am the primary author of this paper.

Signature		Date	18/11/2022

Co-Author Contributions

By signing the Statement of Authorship, each author certifies that:

i.   the candidate's stated contribution to the publication is accurate (as detailed above);

ii.   permission is granted for the candidate in include the publication in the thesis; and

iii. the sum of all co-author contributions is equal to 100% less the candidate's stated contribution.

Name of Co-Author	Prof. Andrea Manica		
Contribution to the Paper	Assisted in running the simulations and writing the paper.		
Signature		Date	3/8/2022

Name of Co-Author	Dr. Stuart Brown		
Contribution to the Paper	Assisted with the statistical analysis of results and writing the paper.		
Signature		Date	24/11/2022

Name of Co-Author	A.Prof. Damien Fordham

Contribution to the Paper	Helped to conceptualise the study, analyse results, and write the paper.		
Signature		Date	6/12/2022

Name of Co-Author	Prof. Carsten Rahbek		
Contribution to the Paper	Helped to conceptualise the study and write the paper.		
Signature		Date	5 Dec 2022

Title Page

Simulations of human migration into North America are more sensitive to demography than palaeoclimate

Julia A. Pilowsky*[1,2], Andrea Manica[3], Stuart Brown[1,4], Carsten Rahbek[2,5,6,7], Damien A. Fordham*[1]

[1]The Environment Institute and School of Biological Sciences, University of Adelaide, South Australia 5005, Australia.

[2]Center for Macroecology, Evolution, and Climate, Globe Institute, University of Copenhagen, Copenhagen Ø 2100, Denmark.

[3]Department of Zoology, University of Cambridge, Cambridge, England

[4]Section for Evolutionary Genomics, Globe Institute, University of Copenhagen, Copenhagen K 1350, Denmark.

[5] Centre for Global Mountain Biodiversity, Globe Institute, University of Copenhagen, Denmark

[6]Danish Institute for Advanced Study, University of Southern Denmark, Odense 5230, Denmark.

[7]Institute of Ecology, Peking University, Beijing 100871, China.

Abstract

Reconstructions of the spatiotemporal dynamics of human dispersal away from evolutionary origins in Africa are important for determining the ecological consequences of the arrival of anatomically modern humans in naïve landscapes and interpreting inferences from ancient genomes on indigenous population history. While efforts have been made to independently validate these projections against the archaeological record and contemporary measures of genetic diversity, there has been no comprehensive assessment of how parameter values and choice of palaeoclimate model affect projections of early human migration. We simulated human migration into North America with a process-explicit migration model using data from two different palaeoclimate simulations and did a sensitivity analysis on the outputs using a machine learning algorithm. We found that simulated human migration was more sensitive to uncertainty in demographic parameters than choice of palaeoclimate model. Our findings indicate that the accuracy of process-explicit human migration models will be improved with further research on the population dynamics of ancient humans, and that uncertainties in model parameters must be considered in estimates of the timing and rate of human colonisation and their consequence on biodiversity.

Keywords

Introduction

Early human migration has been reconstructed indirectly (R. M. Beyer, Krapp, Eriksson, & Manica, 2021), correlatively (Giampoudakis et al., 2017), and process-explicitly (Timmermann & Friedrich, 2016), allowing pathways for the expansion of modern humans to be identified by inferring or modelling relationships between climatic conditions, occupancy and population growth (Eriksson et al., 2012; Steele, Adams, & Sluckin, 1998). Process-explicit models have advantages over correlative reconstructions and inferences based on climate metrics because they explicitly capture demographic responses to changing climatic and environmental conditions in model simulations (Pilowsky, Colwell, Rahbek, & Fordham, 2022b). However, they are generally data intensive, with complex model structures, often resulting in high variability among simulations of early human migration owing to large uncertainties in underlying demographic parameters (Timmermann & Friedrich, 2016). Furthermore, most models are fitted to a single set of simulated climatic reconstructions. However, it is unclear how different assumptions and biases in palaeoclimate simulations (Solomon et al., 2007) affect model projections, and how important these effects are relative to uncertainties in demographic parameters. Sensitivity analyses can help improve projections of human expansion from process-explicit macroecology models by identifying parameters that contribute the most to model output, those that are insignificant and can be potentially omitted from the model and those that need refining to improve model accuracy (Hamby, 1994).

The Climate-Informed Spatial Genetic Model (CISGeM) is one example of a process-explicit model of human dispersal out of Africa, which has been validated using genetic distances between contemporary human populations (Eriksson et al., 2012). Its outputs include human arrival times on non-African continents and islands, as well as spatial maps of effective population size (a proxy for relative abundance; Fordham et al. 2022) from 120 kilo-years before present (ka BP). The simulated outputs of CISGeM have been used to parameterise and inform other models of phenomena including megafaunal extinctions (Fordham et al., 2022) and species range dynamics (Canteri et al., 2022; Pilowsky, Haythorne, Brown, et al., 2022c). However, CISGeM has never been subjected to a sensitivity analysis, meaning there is no knowledge of the importance of

demographic parameters and climatic conditions on model projections. Here we simulate human migration into North America in the Pleistocene using CISGeM parameterised with two widely used atmosphere-ocean general circulation models (AOGCMs): the Hadley Centre Coupled Model, version 3 (HadCM3) (Singarayer & Valdes, 2010) and the Transient Climate Evolution (TraCE-21ka) simulation (Z. Liu et al., 2009). We do a sensitivity analysis to determine whether well-established differences in these palaeoclimate models (E. Armstrong, Hopcroft, & Valdes, 2019) strongly influence projections of human colonisation of North America when uncertainties in key demographic parameters are also considered.

Material and Methods

1. Human Expansion Model

We modelled the peopling of North America using CISGeM (Climate-Informed Spatial Genetic Model), which is a process- and spatially-explicit population model of global human migration during the late Pleistocene and Holocene (Eriksson et al., 2012). The model is driven by demographic processes responding to glacial-interglacial ice-land-sea dynamics, and spatiotemporal variation in net primary productivity (NPP) that affects carrying capacities. The latter has been shown to be an important driver of population density for hunter-gatherers (Tallavaara, Eronen, & Luoto, 2018; Zhu et al., 2018). Previous model testing has shown that CISGeM accurately reconstructs global genetic diversity and human arrival times on the non-African continents (Eriksson et al., 2012; Raghavan et al., 2015). See Supplementary Information for more details on the model structure of CISGeM.

Model parameters in CISGeM have been optimised using pattern-oriented modelling methods (Grimm et al., 2005) and Approximate Bayesian Computation (Csilléry, Blum, Gaggiotti, & François, 2010). In this study, we used the posterior ranges of optimised model parameters to generate 4,950 plausible CISGeM models, each with different parameter values. We used Latin hypercube sampling to generate a stratified random subset of parameter input values for simulations by specifying the posterior range for each parameter and sampling all portions of the distributions (Stein, 1987). We then ran each of these models using palaeoclimate data from two

AOGCMs, and did a global sensitivity analysis (Antoniadis, Lambert-Lacroix, & Poggi, 2021) to determine the influence of demographic parameters and climate model parameterisation on CISGeM projections of human colonisation of North America (Figure S2).

2. Climate Data

Plausible models (n = 4,950) were simulated using palaeoclimate AOGCM data from the HadCM3 model (Singarayer & Valdes, 2010) and the TraCE-21ka palaeoclimate model (Z. Liu et al., 2009). While projections from the HadCM3 have been shown to be congruent with those from the TraCE-21ka model in some regions and for some climatic parameters, key differences remain (E. Armstrong et al., 2019).

Unlike the TraCE-21ka simulation, the HadCM3 is not a fully transient climate model, meaning that outputs from HadCM3 are climate snapshots rather than continuous projections. Climate snapshots from the HadCM3 outputs (separated by ≥ 1 ka) were temporally downscaled to 25 year timesteps to match the timestep of CISGeM simulations using a stochastic weather generator, which draws random values from empirical distributions adjusted to fit the temperature and precipitation intervals found in the climate data (Semenov & Barrow, 2002). The grid cell resolution of HadCM3 data is 3.75° longitude × 2.5° latitude. Forcings include orbitally forced insolation changes, changes in long-lived greenhouse gases, and meltwater from evolving ice sheets. These are the same forcings used in TraCE-21ka, with a key difference that HadCM3 does not account for vegetation-air-ocean interactions (Collins et al., 2006).

The TraCE-21ka simulation (Z. Liu et al., 2009) uses the Community Climate System Model version 3 (CCSM3; Yeager et al. 2006) to reconstruct daily global climate conditions at a spatial resolution of 3.75° longitude × 3.75 latitude (over land and sea) for the last 21,000 years. It accurately reproduces major climatic features associated with the most recent deglaciation event, and predicts present-day climate patterns with verified hindcast skill (Fordham et al., 2017). Importantly, both HadCM3 and TRaCE-21ka model ice sheet dynamics using the ICE-5G reconstruction (Peltier, 2004), meaning that ice sheet barriers to human dispersal in CISGeM models were identical in simulations regardless of palaeoclimate model (Movie S1). We spatially

downscaled data from both models to the equal-area resolution of CISGeM (100 km width). See Supplementary Information for details.

3. Simulations

We ran a single replicate of CISGeM for each combination of plausible parameters and recorded the simulated effective population size at each hex cell and time point. Previously, it has been shown that running a single simulation iteration per parameter sample is optimal for sensitivity analysis if the parameter space is extensively sampled (Prowse et al., 2016). All simulations were global, began at the same starting location in East Africa at 120 ka BP, and proceeded until present (0 BP, 1950 C.E.) at 25-year time steps (Eriksson et al., 2012).

We identified, *a priori*, time of movement out of Alaska and rate of expansion through North America as being sensitive to changes in demographic parameters and variation in climate model projections of NPP, because simulated population density depends on NPP as well as demographic parameters (Eriksson et al., 2012). We calculated time of movement out of Alaska (after 19 ka BP) and rate of expansion through North America (14.7 to 11 ka BP) for each projection. Movement out of Alaska was calculated as the time when the population-weighted centroid of the leading edge of the human range (Watts, Fordham, Akçakaya, Aiello-Lammens, & Brook, 2013) crossed 130°W or 51°N. Rate of expansion through North America was calculated as the rate of movement, in kilometres per year, of the population-weighted centroid of the leading edge of the human range. See Supplementary Information for more details on how these variables were calculated. CISGeM projections of time of movement out of Alaska were independently validated using inferences of the timing of arrival of Clovis culture in North America (13,250 to 12,800 years BP; Waters and Stafford 2007).

4. Sensitivity Analysis

To determine which parameters contribute most to model projections of human expansion in North America, we did a global sensitivity analysis using our summary metrics of time of movement out of Alaska and rate of expansion through North America (Antoniadis et al., 2021). Sensitivity analyses were done in two ways: (i) using only CISGeM models simulated using

HadCM3 climate data; (ii) using models simulated with both HadCM3 and CCSM3 TRaCE-21ka climate data. This two-step approach was done because CISGeM were originally optimised using HadCM3 climate data (Eriksson et al., 2012). We determined the sensitivity of timing of movement out of Alaska and expansion rate using random forest learning methods (Antoniadis et al., 2021) following techniques established for process-explicit macroecology models (Pearson et al., 2014). We assessed variable importance using unscaled permutation importance (Strobl, Boulesteix, Zeileis, & Hothorn, 2007). See Supplementary Information for details.

Results

While human range size in North America varied according to palaeoclimate model (Figure 1), time of movement out of Alaska and rate of human migration were most sensitive to uncertainty in key demographic parameters (Figure 2). The sensitivity analysis done on only HadCM3 model-based simulations revealed: i) time of movement out of Alaska was most sensitive to colonisation rate, upper net primary productivity (NPP) threshold of the carrying capacity and population growth rate; while ii) population-weighted rate of expansion was most sensitive to population growth rate and colonisation rate (Figure 2). This order of relative importance remained unchanged when the sensitivity analysis was done on simulations from the two palaeoclimate models combined, indicating relatively low sensitivity of model projections to model-based differences in palaeoclimate conditions when compared to uncertainties in demographic model parameters.

Independent tests of CISGeM projections of time of movement out from Alaska showed that simulations of land migration from CISGeM parametrized with TraCE21-ka climate data gave a median exit date from Alaska that was closer to the estimated Clovis arrival (median: 14,375 years BP, MAD: 482) compared to simulations parametrized with HadCM3 data (median: 15,000 years BP, MAD: 111). The difference for TraCE-21ka and HadCM3 was 1,144 years (95% confidence interval [CI] = 1,138 - 1,150 years) and 1,682 years (CI = 1,663 - 1,700 years), respectively. Model projections of migration patterns into North America and relative N_e for both models can be accessed on Figshare (Pilowsky, Manica, Brown, Rahbek, & Fordham, 2022d).

Conclusions

Projections of the peopling of North America from process-explicit models vary in response to palaeoclimate model; however, uncertainties in key demographic parameters have a disproportionately larger influence on simulations of time of movement out of Alaska and rate of expansion through North America. Therefore, it is important to consider the uncertainty of demographic parameters in process-explicit projections of timing, rate and mechanisms of initial human expansion across continents (Raghavan et al., 2015), and the broader ecological consequences of human colonisation on biodiversity (Canteri et al., 2022; Fordham et al., 2022).

While arrival times of humans in different regions have been established archaeologically with reasonable certainty (Goebel, Waters, & O'Rourke, 2008; Groucutt et al., 2015), and dispersal rates have been inferred from genomic analysis of aDNA (Rasmussen et al., 2011), the pattern of human growth and expansion has been more difficult to reconstruct at fine spatiotemporal scales. Consequently, projections of early human migration across continents are still uncertain (H. Liu, Prugnolle, Manica, & Balloux, 2006), owing partly to overly simplistic parametrisation of the relationship between NPP and population growth (Zhu, Galbraith, Reyes-García, & Ciais, 2021) and large uncertainties in other demographic parameters, including population growth and dispersal (French, Riris, Fernandéz-López de Pablo, Lozano, & Silva, 2021)

Resolving these issues should be a priority, particularly given how sensitive the rate of human movement in North America is to rates of population growth and colonisation. Promising avenues of research that could reduce uncertainty in early human demography include Bayesian analysis of spatiotemporal distributions of radiocarbon dates (Price et al., 2020); phylogenetic analysis of the human palaeoproteome, which is more resistant to degradation over long timescales compared to the palaeogenome (Welker, 2018); and sampling of environmental DNA, which can detect arrival and movement of small populations better than the archaeological or fossil record (Yucheng Wang et al., 2021).

Our finding that uncertainty in projections of human migration from process-explicit models is only weakly sensitive to the choice of climate model is in stark contrast to findings for correlative

models of species distributions (L. J. Beaumont et al., 2007; Tuck et al., 2006), which model demographic processes implicitly, not explicitly (Pilowsky, Colwell, Rahbek, et al., 2022b). When interpreting the generality of this result, it is important to recognise that CISGeM simulates pathways for the global expansion of modern humans. Therefore, in other regions and time periods, the parametrisation of palaeoclimate could have a larger effect on human migration. Nevertheless, our results highlight the importance of realistically capturing demographic mechanisms in process-explicit human migration models.

Figures
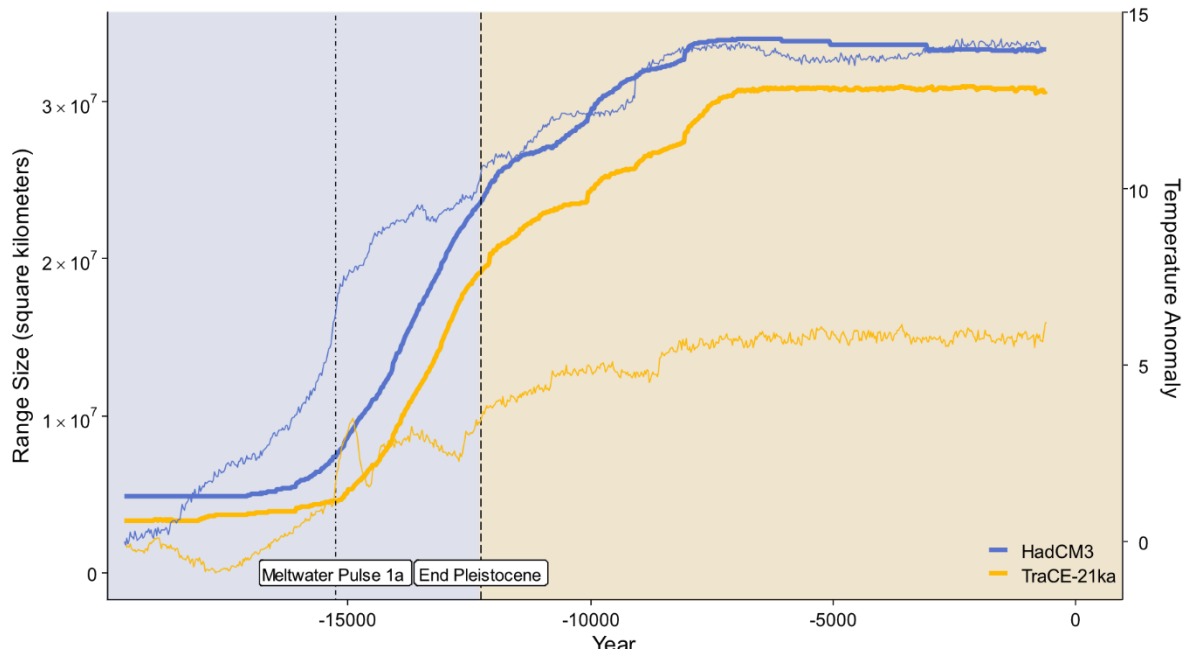
Figure 1: Human range expansion in North America. Range size for humans in North America from 19,000 years ago to present according to simulations with the HadCM3 (blue) and TraCE-21ka (yellow) AOGCMs (thick lines). Thin lines show mean annual temperature anomaly for the two AOGCMs.
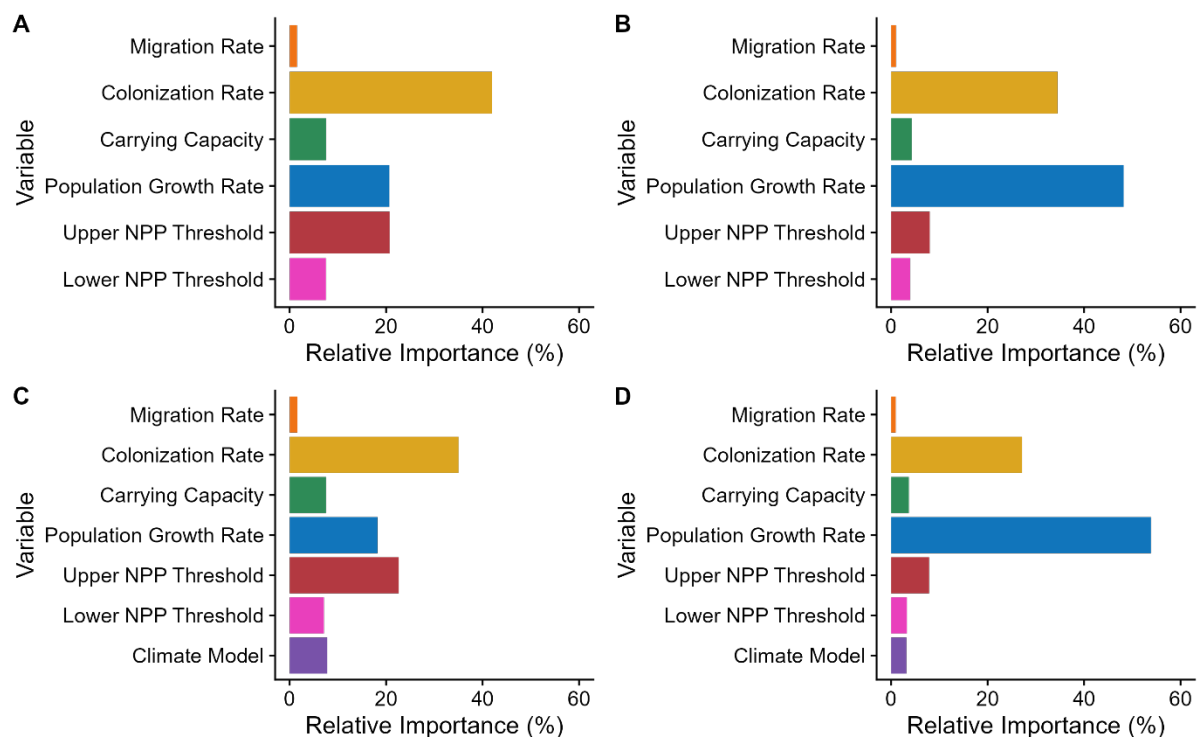
Figure 2: Sensitivity analysis of human migration model parameters. Sensitivity of simulations of timing of human migration out of Alaska (A, C) and rate of southward expansion through North America (B, D). A and B are only for simulations run on HadCM3 climate data, while C and D are for both HadCM3- and TraCE-21ka-based simulations. Relative importance scores from random forest models in B and C are shown for demographic parameters: migration rate, colonisation rate, carrying capacity, population growth rate, upper and lower net primary productivity (NPP) thresholds for occupancy. For C and D, relative importance scores also have choice of climate model (HadCM3 or TraCE-21ka).

Supplementary Material

1. Human Expansion Model

In CISGeM, population growth and movement of anatomically modern humans are simulated from 120 ka BP (thousand years before present) to 0 years BP at 25-year timesteps, which is approximately the generation length of female hunter-gatherers (Fenner, 2005). The world is represented as a hexagonal grid with 100 km wide hexagons, enabling equidirectional dispersal

distances. The carrying capacity of each hexagon is a piecewise linear function of NPP, with a temporal land-sea-ice mask which designates entire cells as occupiable or unoccupiable.

The model simulation starts with a single human population in East Africa (11°7′ S, 34°21′ E) which increases at the population growth rate r until it reaches its carrying capacity K (defined by a lower NPP threshold [$x1$] and upper NPP threshold [$x2$]). Occupied cells may exchange migrants at migration rate m at any population size, while cells at carrying capacity can send out emigrants at colonisation rate c to neighbouring unoccupied cells (Figure S1). All population abundances are simulated as effective population size. See Eriksson et al. (2012) for more details.

The model was originally developed and run using simulated palaeoclimate data from the Hadley Centre Coupled Model, version 3 (HadCM3) coupled atmosphere-ocean-sea ice-land general circulation model (AOGCM) (Singarayer & Valdes, 2010). Outputs were validated and parameters optimised using molecular information and pattern-oriented modelling methods, a technique for optimising model parameters by converging model outputs toward independent validation targets (Grimm et al., 2005) using Approximate Bayesian Computation (Sisson, Fan, & Beaumont, 2018).

The summary targets for model calibration were pairwise genetic distances for modern human populations between continents (Eriksson et al., 2012). Simulated genealogies were generated from each CISGeM simulation, and model parameters were selected that generated the best congruence between simulated and true genetic distances among populations within and across continents. In this way, the demography was calibrated to produce realistic global genetic differentiation patterns. The optimised parameter values are shown in Table S1.

2. Climate Data

Calculating net primary productivity

For both AOGCMs, we estimated net primary productivity at the grid cell level through time using the Miami vegetation model (Lieth, 1975). In this model, NPP is estimated independently as an empirical function of temperature and precipitation, and the minimum of the two values is the predicted NPP. While the model does not account for carbon cycling, humidity, insolation, and

vegetation structure, it robustly estimates NPP (Figure S3), having been used elsewhere in studies of biodiversity patterns (Currie, 1991).

Downscaling and harmonisation

We spatially downscaled both sets of climate data from their native resolutions to the 100 km wide hexagonal grid used by CISGeM using first-order conservative remapping (Jones, 1999). This is a procedure that remaps fields between different grids, regardless of their shape or coordinate system. The interpolation from one grid to another is weighted based on the ratio of overlap between the source grid cells and the destination grid cells.

Because CISGeM requires palaeoclimate data from 120 ka BP and TRaCE-21ka begins at 22 ka BP, we harmonised the HadCM3 and TRaCE-21ka data following Fordham et al. (2022). We did this using the delta method, ensuring a smooth transition between the two AOGCMs at 21 ka BP (R. Beyer, Krapp, & Manica, 2020). We used an additive correction for temperature and multiplicative correction for precipitation. This approach is identical to bias-correcting projections for differences between modelled and observed climate, making the fundamental assumption that even if there are differences in the absolute estimates of the models, changes produced by the models are correct (Fordham et al., 2017).

3. Simulations

We used Latin hypercube sampling to generate a stratified random subset of CISGeM parameter input values for simulations by specifying the posterior range for each parameter and sampling all portions of the distributions (Stein, 1987). We then ran each of these models using palaeoclimate data from two AOGCMs, running a single replicate of CISGeM for each combination of plausible parameters (Prowse et al., 2016). All simulations were global, began at the same starting location in East Africa at 120 ka BP, and proceeded until present (0 BP, 1950 C.E.) at 25-year time steps (Eriksson et al., 2012). The period of the simulation prior to 19 ka BP was treated as a burn-in period, ensuring model stability prior to the first extensive land colonisation of North America by humans. We removed all simulations with parameter combinations that did not result in human

colonisation of North America (n = 430 HadCM3, n = 1,699 TraCE-21ka). Figure S4 shows ranges of parameter values for models that were retained for this study.

Projections of effective population size from the retained models were spatially cropped to North America (178.5 to 49.5°W, 6.5 to 83.5°N), temporally cropped to 19 ka BP to the present, and converted from the hexagonal grid of CISGeM to a 1° x 1° latitude-longitude grid using first-order conservative remapping (Jones, 1999). Focusing on the most recent period of deglaciation (19 ka – 11 ka BP) and the Holocene allowed us to disentangle the influence of uncertainties in key CISGeM demographic and climate parameters on human migration dynamics in North America.

4. Sensitivity Analysis

To determine which parameters contribute most to model projections of human expansion in North America, we did a global sensitivity analysis (Antoniadis et al., 2021) on the response variables of i) time of movement out of Alaska (after 19 ka BP) and ii) rate of expansion through North America (14.7 to 11 ka BP).

We calculated time of movement out of Alaska, and later expansion rate through North America, by calculating the population-weighted centroid of the leading edge of the range of humans (Fordham et al., 2022). Since overland dispersal out of Alaska proceeded in a south-easterly direction (Waters & Stafford, 2007), we calculated the frontier of human expansion through time (at 25-year time steps) as the south-eastern 90th percentile of the North American range, based on effective population size through time (Movie S2). We calculated time out of Alaska as the timepoint when the frontier of human expansion crossed 130°W or 51°N. If the south-eastern 90th percentile had already crossed one of these lines by 19 ka BP, the time out of Alaska was set to 19 ka BP.

We calculated expansion rate through North America for the time period 14.7 to 11 ka BP because the Bølling-Allerød warm period from Meltwater Pulse 1a (14.7 ka BP) to the end of the Pleistocene epoch (11.7 ka BP) was when the bulk of freshwater melted from ice sheets during the most recent deglaciation (Weaver, Saenko, Clark, & Mitrovica, 2003). We calculated the great circle distance in kilometres between the frontier of human expansion (as described above) at each

timestep and the one preceding it and divided by 25 years to obtain a rate of south-easterly expansion in kilometres per year, then calculated the mean expansion rate during the Bølling-Allerød warm period.

We determined the sensitivity of timing of movement out of Alaska and expansion rate using random forest learning methods (Antoniadis et al., 2021) following techniques established for process-explicit macroecology models (Pearson et al., 2014). We used the R package randomForest v4.6 (Liaw & Wiener, 2002) for all analysis, including tuning the number of variables sampled at each split and the minimum node size by optimising the out-of-bag error and growing 1000 regression trees (Oliveira, Oehler, San-Miguel-Ayanz, Camia, & Pereira, 2012). We assessed variable importance using unscaled permutation importance (Strobl et al., 2007).

Parameter	Function	Optimised Values
x1	Minimum NPP value needed to support human occupancy	0.024 (0 – 0.040)
x2	NPP value at which the carrying capacity comes into effect	0.493 (0.013 – 1.000)
K	Carrying capacity	3002 (100 – 9997)
r	Intrinsic growth rate of populations	0.317 (0.157 – 0.500)
m	Migration rate from occupied cells to other occupied cells	0.045 (0.001 – 0.167)
c	Colonisation rate from occupied cells to unoccupied cells	0.055 (0.0002 – 0.166)

Table S1: CISGeM parameters for simulating early human migration. Parameters with notations used in CISGeM, a description of their function, and their optimised values based on Eriksson et al. (2012). Mean values are shown with minimum and maximum in brackets. *x1* and *x2* are expressed as a proportion of maximum NPP, *K* and *K0* are expressed as effective population size and the rates of *r*, *m*, and *c* are given on the natural scale.
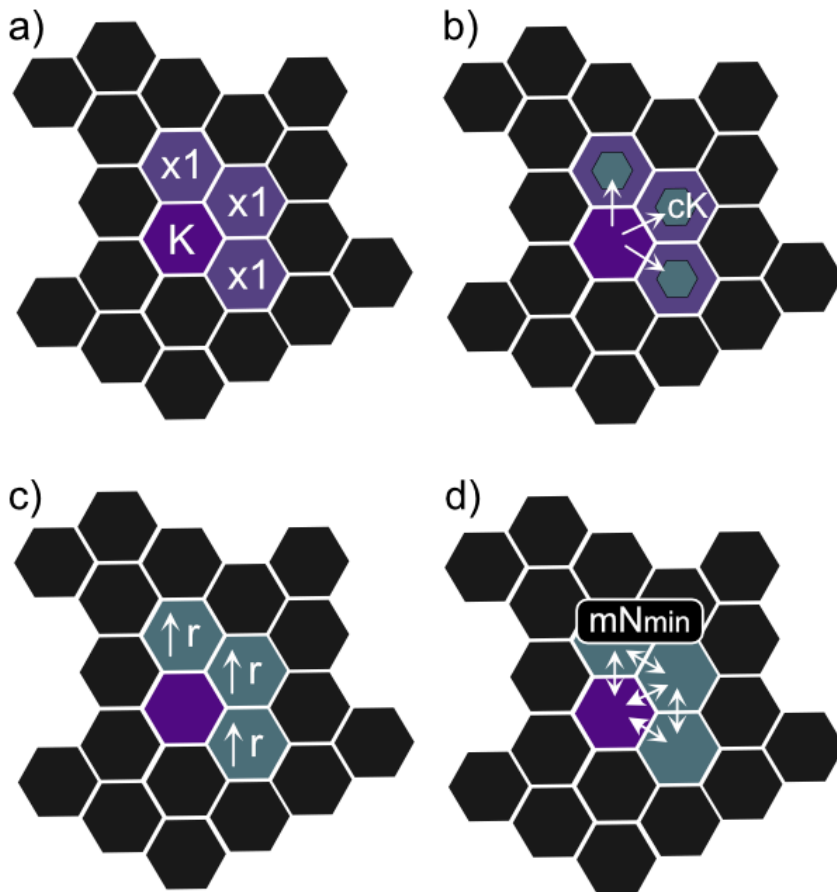
Figure S1: Conceptual representation of CISGeM demography. a) At the upper NPP threshold x2, the human population stabilises at the carrying capacity K. Meanwhile, cells become habitable when the NPP reaches the lower threshold x1. b) Cells at carrying capacity can send out colonists to neighbouring unoccupied habitable cells at colonisation rate c multiplied by K. c) Occupied cells grow at population growth rate r until they reach the carrying capacity. d) Occupied neighbouring cells exchange migrants at migration rate m multiplied by the smaller population size of the two neighbouring cells.
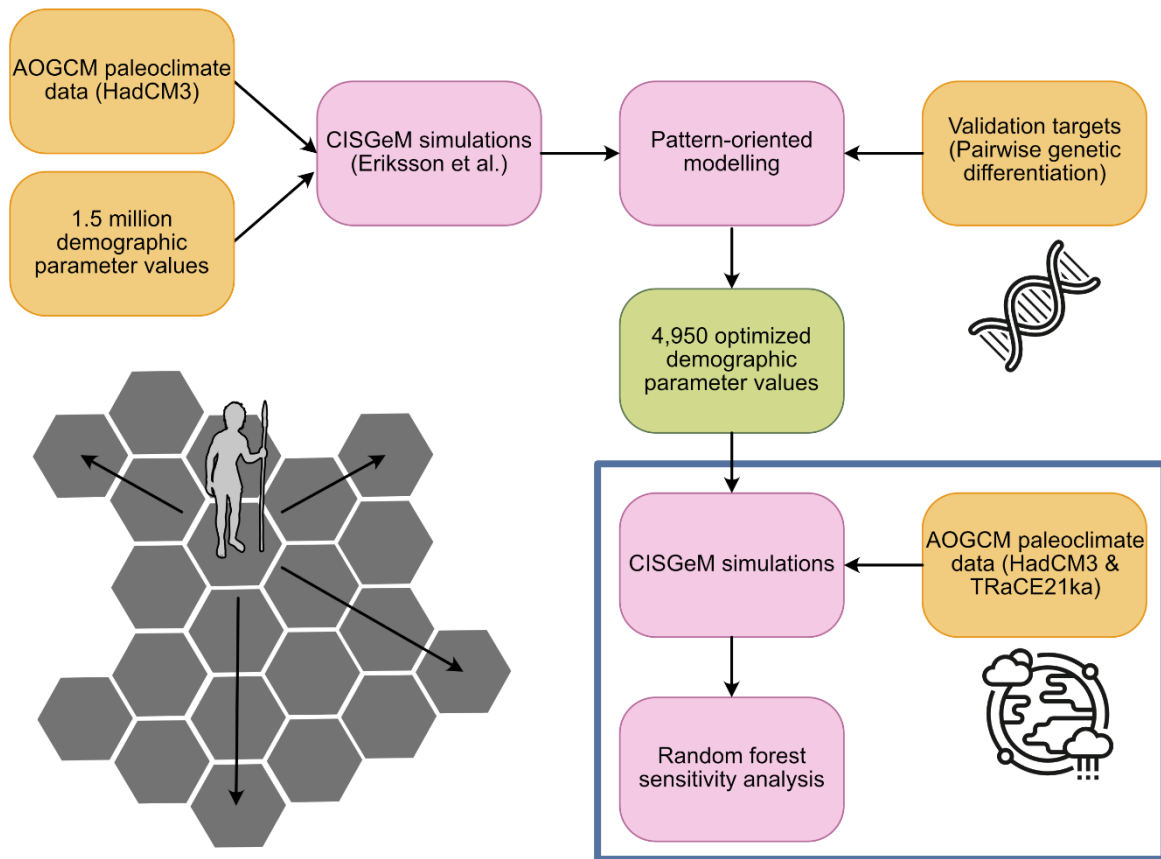
Figure S2: Workflow of the analysis. The top row of the flow chart shows the previous work on CISGeM by Eriksson et al. (2012), and how the outputs were used in our study of the sensitivity of CISGeM. The blue box indicates the part of the workflow done in this study.
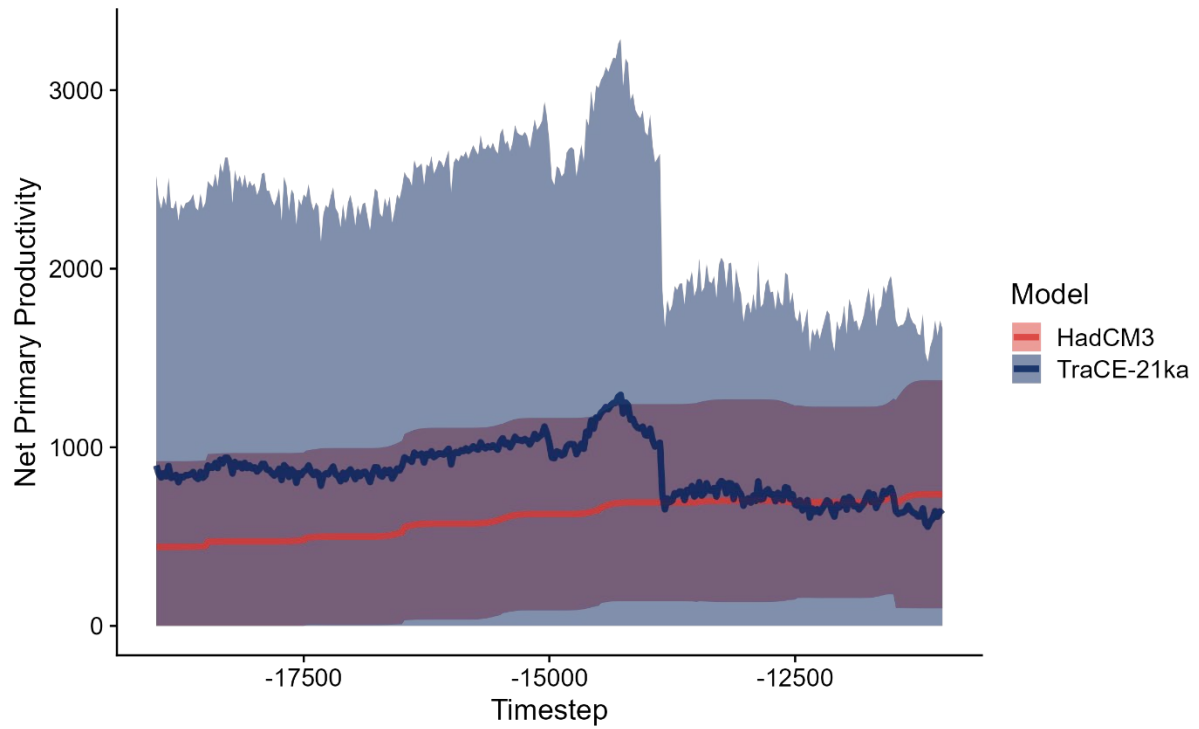
Figure S3: Comparison of net primary productivity during the deglaciation period. Mean net primary productivity (NPP) in Alaska for the HadCM3 and TraCE-21ka palaeoclimate simulations from 19,000 years BP to 11,000 years BP, with spatial variation shown as +/- 1 SD.
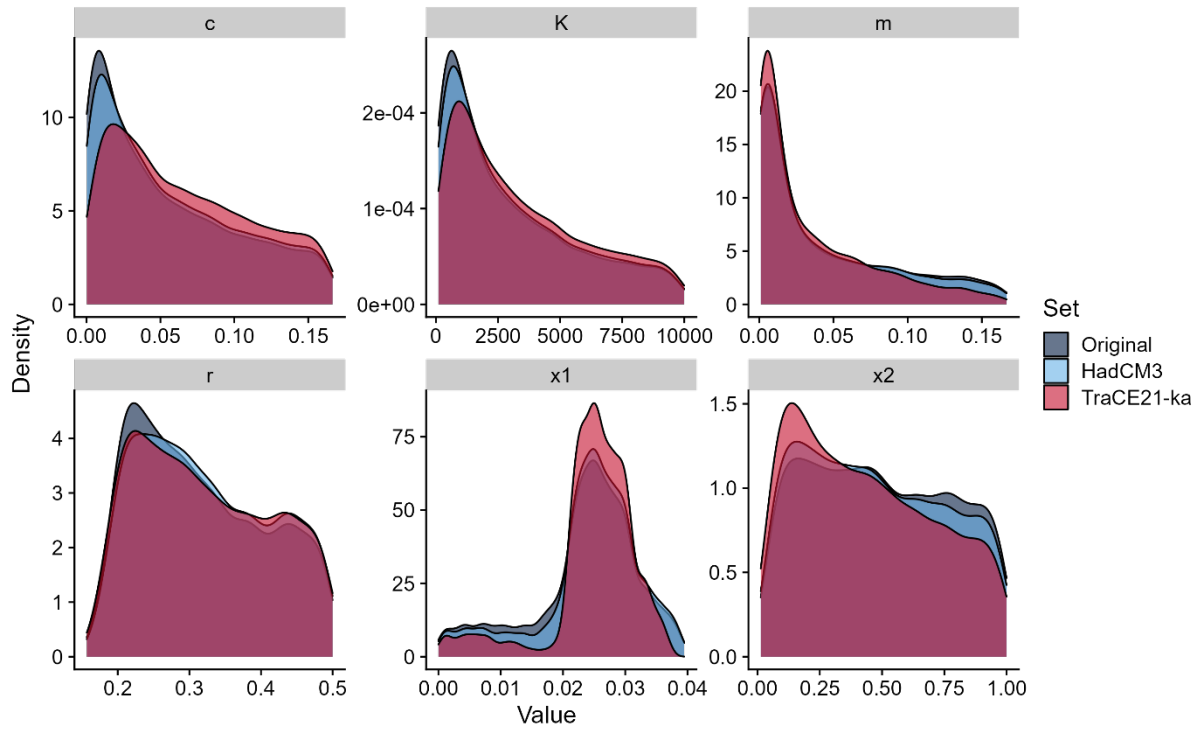
Figure S4: Parameter values used in the sensitivity analysis after filtering. Distribution of parameter values for colonisation rate (c), carrying capacity (K), migration rate (m), growth rate (r), lower net primary productivity threshold (x1), and upper net primary productivity threshold (x2) for the 4,950 plausible models (original); and after filtering these simulations for arrival in North America using the HadCM3 and TraCE-21ka palaeoclimate simulations.

Box.com link to Movie S1

Movie S1: Ice sheet reconstructions used in HadCM3 and CCSM3 palaeoclimate data inputs. Both the HadCM3 and CCSM3 palaeoclimate data we used to parameterise CISGeM models of human migration in North America used the ICE-5G reconstruction (Peltier, 2004); the dynamics of the melting ice sheets in the deglaciation period 19 – 11 ka BP are shown. Ice sheets are white, ocean is light grey, coastline is dark grey, and present-day coastline is medium grey.

Box.com link to Movie S2

Movie S2: Effective population-weighted leading-edge centroid of human migration in North America. We calculated time of movement out of Alaska and colonisation rate of humans in North America using leading-edge centroids of the expanding human range, weighted by the effective population size outputs from the human migration model CISGeM. The centroid (red) indicates the leading 10th percentile of the expanding human population.

CHAPTER III: SIMULATING THE RANGE DYNAMICS OF THE STEPPE BISON ACROSS MULTIPLE MILLENNIA USING PROCESS-EXPLICIT AND PATTERN-ORIENTED MODELS
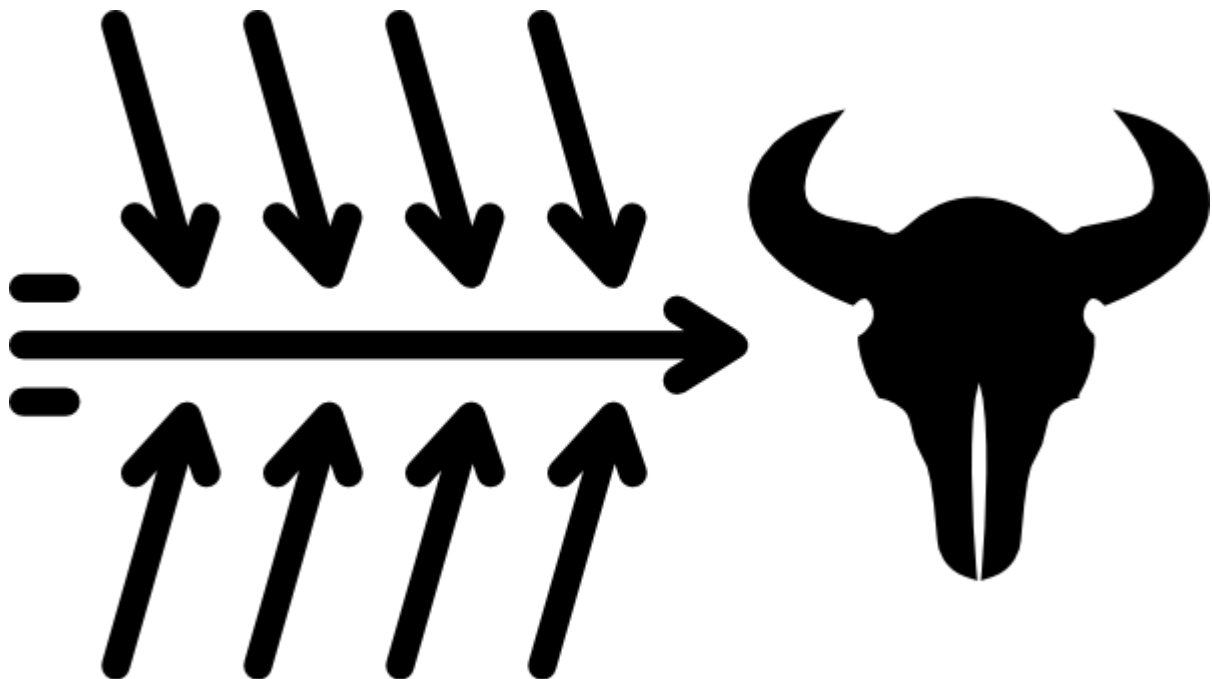
Statement of Authorship

Title of Paper	Simulating the range dynamics of the steppe bison across multiple millennia using process-explicit and pattern-oriented models
Publication Status	Published
Publication Details	Journal: Global Ecology and Biogeography Authors: Julia Pilowsky, Sean Haythorne, Stuart Brown, Mario Krapp, Edward Armstrong, Barry Brook, Carsten Rahbek, Damien Fordham

Principal Author

Name of Principal Author (Candidate)	Julia Aaron Pilowsky		
Contribution to the Paper	The candidate conceptualised the study, ran simulations, analysed results, and wrote the paper, with contributions from co-authors.		
Overall percentage (%)	80%		
Certification:	This paper reports on original research I conducted during the period of my Higher Degree by Research candidature and is not subject to any obligations or contractual agreements with a third party that would constrain its inclusion in this thesis. I am the primary author of this paper.		
Signature		Date	18/11/2022

Co-Author Contributions

By signing the Statement of Authorship, each author certifies that:

i. the candidate's stated contribution to the publication is accurate (as detailed above);

ii. permission is granted for the candidate in include the publication in the thesis; and

iii. the sum of all co-author contributions is equal to 100% less the candidate's stated contribution.

Name of Co-Author	Dr. Sean Haythorne		
Contribution to the Paper	Wrote the simulation software and assisted with running simulations.		
Signature		Date	18/11/2022

Name of Co-Author	Dr. Stuart Brown		
Contribution to the Paper	Assisted with running simulations and writing the paper.		
Signature		Date	24/11/2022

Name of Co-Author	Dr. Mario Krapp
Contribution to the Paper	Assisted with running simulations and writing the paper.

Signature		Date	23/11/22

Name of Co-Author	Dr. Edward Armstrong		
Contribution to the Paper	Provided climate data and assisted with writing the paper.		
Signature		Date	23/11/22

Name of Co-Author	Prof. Barry Brook		
Contribution to the Paper	Contributed to writing the paper.		
Signature		Date	18/11/2022

Name of Co-Author	Prof. Carsten Rahbek		
Contribution to the Paper	Helped conceptualise the study and write the paper.		
Signature		Date	5 Dec 2022

Name of Co-Author	A/Prof. Damien Fordham

Contribution to the Paper	Helped conceptualise the study, develop the simulation, and write the paper.		
Signature		Date	18/11/2022

Title Page

Simulating species' range dynamics across multiple millennia using process-explicit and pattern-oriented models

Authors

Julia A. Pilowsky[1,2], Sean Haythorne[1,3], Stuart C. Brown[1,4], Mario Krapp[5,6], Edward Armstrong[7], Barry W. Brook[7], Carsten Rahbek[2,9,10,11], Damien A. Fordham[1,11]

Affiliations

[1]The Environment Institute and School of Biological Sciences, University of Adelaide, South Australia 5005, Australia.

[2]Center for Macroecology, Evolution, and Climate, Globe Institute, University of Copenhagen, Copenhagen Ø 2100, Denmark.

[3]School of BioSciences, University of Melbourne, Victoria 3010, Australia.

[4]Section for Evolutionary Genomics, Globe Institute, University of Copenhagen, Copenhagen K 1350, Denmark.

[5]Antarctic Science Platform National Modelling Hub, Victoria University of Wellington, Wellington 6140, New Zealand.

[6]GNS Science, Lower Hutt, New Zealand

[7]Department of Geosciences and Geography, University of Helsinki, Helsinki 00014, Finland.

[8]School of Biological Sciences and Australian Research Council Centre of Excellence for Australian Biodiversity and Heritage, University of Tasmania, Hobart, Tasmania 7001, Australia.

[9]Danish Institute for Advanced Study, University of Southern Denmark, Odense 5230, Denmark.

[10]Institute of Ecology, Peking University, Beijing 100871, China.

74

[11]Center for Mountain Biodiversity, Globe Institute, University of Copenhagen, Copenhagen Ø, Denmark

Abstract

Aim: To determine the ecological processes and drivers of range collapse, population decline, and eventual extinction of the steppe bison in Eurasia.

Location: Siberia

Time period: Pleistocene and Holocene

Major taxa studied: Steppe bison (*Bison priscus*)

Methods: We configured 110,000 spatially explicit population models (SEPMs) of climate-human-steppe bison interactions in Siberia, which we ran at generational timesteps from 50,000 years before present. We used fossil-based inferences of distribution and demographic change and pattern-oriented modelling (POM) methods to identify which SEPMs adequately simulated important interactions between ecological processes and biological threats. These 'best models' were then used to disentangle the mechanisms that were integral in the population decline and later extinction of steppe bison in its last stronghold in Eurasia.

Results: Our continuous reconstructions of the range and extinction dynamics of steppe bison were able to reconcile inferences of spatiotemporal occurrence and timing and location of extinction for steppe bison in Siberia based on hundreds of radiocarbon-dated fossils. We show that simulating the ecological pathway to extinction for steppe bison in Siberia in the early Holocene required very specific ecological niche constraints, demographic processes, and a constrained synergy of climate and human hunting dynamics during the Pleistocene-Holocene transition.

Main conclusions: Ecological processes and drivers that caused ancient population declines of species can be reconstructed at high spatiotemporal resolutions using SEPMs and POM. Using this approach, we found that climatic change and hunting by humans are likely to have interacted with key ecological processes to cause the extinction of steppe bison in its last refuge in Eurasia.

Keywords:

climate change, distribution, extinction dynamics, mechanistic model, metapopulation,

palaeoclimate, range shift, spatially explicit population model, steppe bison, synergistic threats

Introduction

Several hypotheses have been proposed for how extinctions manifest in space and time (Davidson et al., 2009; Owens & Bennett, 2000), but generalities across landscapes and time periods have been difficult to formulate (Laliberte & Ripple, 2004). Theories of range shifts, population declines, and extinctions are now being directly tested using historic and palaeo reconstructions (Fordham et al., 2022; Fordham, Haythorne, Brown, Buettel, & Brook, 2021), permitting inferences of how biodiversity is likely to respond to future environmental change (Fordham et al., 2020). However, reconstructing past demographic changes at landscape scales poses unique modelling challenges, including reliance on indirect proxies to make inferences about range collapses and timing and location of extinction (Dietl et al., 2015); uncertainty in reconstructions of past climates (Rutherford et al., 2005) and human-driven environmental threats (Ellis et al., 2021; Pilowsky, Manica, Brown, Rahbek, & Fordham, 2022e); and a lack of information on the ecological lifestyles and traits of many species (Fordham et al., 2016).

Some of these issues can be addressed, at least in part, using process-explicit models, particularly if they are combined with pattern-oriented modelling (POM) techniques (Box 1). Process-explicit models simulate ecological and evolutionary mechanisms responsible for spatiotemporal patterns of biodiversity (Pilowsky, Colwell, Rahbek, et al., 2022b). These mechanisms include extirpation, movement, ecological interactions, adaptation, and speciation. Unlike correlative approaches, such as species distribution models, process-explicit models establish causal links between process and pattern (M. C. Urban et al., 2016). However, high data demand and model complexity have meant that, to date, they have been used less frequently in studies of the structure and dynamics of patterns of biodiversity. This is steadily changing, owing to increased data availability, computational power (Pilowsky, Colwell, Rahbek, et al., 2022b), and a growing need for stronger inferences about the causes of contemporary and ancient changes in biodiversity (Fordham et al., 2020; Pontarp et al., 2019; Rangel et al., 2018).

POM methods (Grimm & Railsback, 2012) can directly address some of the problems of data availability, and subsequent parameter uncertainty, in process-explicit models of species distributions and community dynamics (Canteri et al., 2022; Fordham et al., 2022; Rangel et al.,

2018). While POM was first used in ecology and evolution to optimise uncertain parameters in individual- and agent-based models (Thulke et al., 1999), it has since been used to simulate demographic change using spatially explicit population models (Canteri et al., 2022; Fordham et al., 2022), genetic diversification in lineages of species (Knowles & Alvarado-Serrano, 2010), changes in community structure (Colwell & Rangel, 2010), and evolutionary shifts in populations (Barnes & Clark, 2017). It uses optimisation routines to determine model parameter values based on observed (or inferred, if operating across palaeo timeframes) empirical patterns (Grimm & Railsback, 2012), increasing the likelihood of capturing key biological processes in model simulations. This strategy assumes that observed patterns are fingerprints of underlying ecological and evolutionary processes, enabling models to be initially parameterised using uncertain but plausible information on these processes (Gallagher et al., 2021).

Despite offering new opportunities to better understand the mechanisms that regulate biodiversity under past climate and environmental change, POM methods are only now being used in conjunction with spatially explicit population models (SEPMs) to reconstruct species' range and extinction dynamics over palaeo timescales (but see Fordham et al., 2022, Canteri et al. 2022). SEPMs simulate movement, mortality, and reproduction in networks of populations over time (B. J. Anderson et al., 2009; Hanski, 1998), allowing the identification of ecological mechanisms and threats that caused ancient extinctions and range collapses (Canteri et al., 2022). POM optimisation is done using patterns inferred from the fossil record and ancient DNA (Fordham et al., 2022). Here, we show the utility of combining POM methods with SEPMs to reconstruct and disentangle the extinction dynamics of the steppe bison (*Bison priscus*) in Eurasia. The approach uses multiple rounds of SEPM optimisation to continuously reconstruct interactions between the ecological lifestyle and demography of steppe bison and drivers of global change (climatic change and human activities) over a period going back 50,000 years. We do this using the R package 'paleopop' v2.1.0 (Haythorne, Pilowsky, Brown, & Fordham, 2021) that we developed as an e-xtension to 'poems' (Fordham et al., 2021), adding important new functionality for modelling species' range dynamics over multi-millennial timescales.

The steppe bison was one of the many large herbivores that dominated the "mammoth steppe" biome of the Ice Age (R. Dale Guthrie, 1989), all of which declined in range size as the mammoth steppe was replaced by a taiga-tundra ecotone during the Pleistocene-Holocene transition (Lorenzen et al., 2011; Markova et al., 2015). The relative abundance of steppe bison (based on reconstructions of effective population size) peaked during the late Pleistocene (Shapiro et al., 2004), when the mammoth steppe was maximally distributed (P. M. Anderson & Lozhkin, 2001), going regionally extinct in Eurasia at ~8.7 kilo-years before present (kyr BP) (Boeskorov et al., 2016) and globally extinct in North America some 6 to 8 kyr later (Shapiro et al., 2004). In Eurasia, isotopic analysis of late Pleistocene fossils shows that the steppe bison was a strict grazer that did not migrate seasonally (Julien et al., 2012). Here they competed with the European bison (*Bison bonasus*) for ecological dominance until climate-induced vegetation change following the Last Glacial Maximum (LGM; a period from 26.5 to 19 kyr BP (P. U. Clark et al., 2009)) restricted the less ecologically flexible steppe bison to Siberia (Soubrier et al., 2016).

The processes leading to the megafaunal extinctions of the mammoth steppe during the late Pleistocene and early Holocene are uncertain, with intense debate regarding timing, location, and the roles of human hunting and climatic change (Mann, Groves, Gaglioti, & Shapiro, 2019; Stuart, 2015; Yucheng Wang et al., 2021). Here we configure 110,000 SEPMs of climate-human-steppe bison interactions in Siberia, which we test against inferences of demographic change and range collapse inferred from fossils using POM methods. Our continuous reconstructions of the range and extinction dynamics of steppe bison from 50 kyr BP reveal the ecological processes and threats that led to the demise of the steppe bison in its last stronghold in Eurasia at approximately 9 kyr BP.

Material and Methods

The steppe bison is an extinct species of bison which was once widespread in the steppe of the Northern Hemisphere (Markova et al., 2015). Its relative abundance (based on reconstructions of effective population size) peaked during the late Pleistocene (Shapiro et al., 2004), when the mammoth steppe biome was maximally distributed (P. M. Anderson & Lozhkin, 2001) becoming

regionally extinct in Eurasia approximately 8.7 kyr BP (Boeskorov et al., 2016). We simulated the ecological pathway to extinction for the steppe bison in Siberia (Shapiro et al., 2004).

1. paleopop

'paleopop' is an object-oriented R package (Haythorne et al., 2021) which we developed to simulate range and extinction dynamics of species over multiple millennia, enabling causal insights into likely past driver-state relationships. 'paleopop' uses a lattice-grid population model to simulate ecological processes (demography and ecological requirements) and their interactions across long temporal scales. 'paleopop' is an extension to the R package 'poems' v1.0.1 (Fordham et al., 2021), which implements process-explicit models and pattern-oriented methods to identify ecological processes of range shifts and extinctions (Figure 1). 'paleopop' adds three major features to 'poems': 1) the capacity to simulate long term processes of landscape change (sea level rise; movement of glacial ice sheets) occurring over glacial inter-glacial cycles, 2) a palaeo-population simulator optimised for simulating demographic change resulting from metapopulation and dispersal dynamics over multiple millennia, and 3) a palaeo-results object suitable for storing the data-heavy output from the palaeo-population simulator.

2. Steppe bison niche

2a. Fossil data

We gathered radiocarbon-dated data on steppe bison fossils from the palaeontological literature (see Appendix S1 in the Supplementary Information for details). We regularised inconsistent and outdated species names, discarding any records where the species was ambiguous (e.g., "bison" without clear indicators whether it was the steppe bison or another bison species.) In cases where a site name was available, but latitude and longitude were not, we compared maps from the source literature against OpenStreetMap and Google Earth to geocode locations manually. The quality of all radiocarbon dates was assessed based on stratigraphy, association, and the material dated. We retained 378 records rated as "reliable" (Barnosky & Lindsey, 2010). We calibrated these radiocarbon dates using the OxCal v4.4 tool (Ramsey, 2017) and the IntCal13 curve (Reimer et al.,

2013), which returned calibrated age and standard deviation (SD) estimates. The fossil record can be accessed from Figshare (Pilowsky et al., 2021).

2b. Climate data

Palaeoclimate simulations of precipitation, temperature, and latent heat flux used to model the ecological niche of the steppe bison (see below) are from the HadCM3B coupled ocean-ice-atmosphere model (Valdes et al., 2017). These palaeoclimate simulations incorporate monthly and interannual climate variability (directly from model output) and millennial scale variability (by assimilating model and Greenland ice core data), and have been downscaled to 0.5° x 0.5° spatial resolution (E. Armstrong et al., 2019). We extracted monthly data for the study region of Siberia (Figure S1.1) from 50 kyr BP to 5 kyr BP and generated 30-year averages at a 12-year (generational; see description of the process-explicit model below) time step for: 1) total annual precipitation, 2) mean boreal winter (DJF) temperature, and 3) total evapotranspiration during boreal spring and summer (MAMJJA). Evapotranspiration was calculated by dividing the average monthly latent heat flux by the latent heat of vaporisation based on average monthly temperatures:

$$\text{ET (mm/month)} = \left(\frac{\text{heat flux}}{(2.501 - 0.00237 \times \text{temp}) \times 1e6} \right) \times 86400 \times 30 \qquad \text{Eq. 1}$$

where *heat flux* and *temp* are the modelled monthly heat flux (W m²) and temperature (°C) for each month.

Mean temperature of the coldest month, mean temperature of the warmest month, and annual precipitation have been used previously to model the ecological niche and distribution of high-latitude herbivores, including the steppe bison (Lorenzen et al., 2011) and the American bison (*Bison bison*) (Metcalf et al., 2014). This is because these variables likely capture the upper and lower thermal limits of the species, while precipitation drives demographic rates in extant bison species (Koons et al., 2012). Because spring and summer evapotranspiration was correlated with the temperature of the warmest month ($\tau = 0.548$), we chose to model only spring and summer evapotranspiration because it better captures the structure of vegetation available as forage in the warmer months (R. D. Guthrie, 2006). We used average temperature across all boreal winter

months (DJF) instead of only the coldest month, because it better captures the stressors and limitations created by winter conditions (DelGiudice, Moen, Singer, & Riggs, 2001; DelGiudice, Singer, Seal, & Bowser, 1994). None of the three variables were correlated with each other by more than $\tau = 0.51$.

2c. Niche model

We generated continuous habitat suitability maps (based on probability of occurrence) for the steppe bison in Siberia from 50 kyr BP to 5 kyr BP using ecological niche models (Nogués-Bravo, 2009). To do this, we paired fossil occurrences with our three selected climate variables, accounting for dating uncertainty (Fordham et al., 2022). Climate data were paired spatially as determined by the grid cell where the fossil occurred, and temporally as determined by the band of uncertainty (±2 SD, which is commonly used for calibrated radiocarbon date distributions [Blaauw, 2010]) around the calibrated radiocarbon date. We removed any duplicate climate data created by two fossil occurrences falling within identical or overlapping spatiotemporal bins (Canteri et al., 2022). We used this climate dataset to create a full (multi-temporal) Gaussian hypervolume, optimised for appropriate bandwidth (Blonder et al., 2018), which provided an estimate of the fundamental niche of steppe bison (Nogués-Bravo, 2009)

Because the realised climatic niche of steppe bison is likely to be a subset of its fundamental niche (Soberón & Nakamura, 2009), we thoroughly subsampled the full hypervolume of potentially liveable climatic conditions (Figure S1.2), and determined the realised niche using SEPMs and POM (see below). We did this by cutting the full hypervolume into smaller hypervolumes (n = 1000) of different volumes and marginalities (climatic specialisation) using Outlying Mean Index analysis (Dolédec, Chessel, & Gimaret-Carpentier, 2000). We projected the hypervolumes back into geographic space, creating time series of maps of habitat suitability based on the probability density of the climate hypervolume at the set of environmental conditions in each grid cell (77.8 km by 71.0 km grid cell resolution) from 50 kyr BP to 5 kyr BP. We scaled the suitability scores of each projection to a 0 – 1 interval based on the 95th percentile of maximum habitat suitability values in grid cells across time and space.

3. Palaeolithic humans

The expansion of Palaeolithic humans into northern Eurasia was modelled using a process-explicit climate-informed spatial genetic model ('CISGeM') that has been shown to accurately reconstruct the dispersal of *Homo sapiens* out of Africa (Eriksson et al., 2012). 'CISGeM' simulates local effective population size (N_e) based on a cellular demographic model with carrying capacity modulated by net primary productivity. We ran 'CISGeM' from 120 kyr BP to present using the HadCM3B ocean-ice-atmosphere model (Valdes et al., 2017) and 4,950 parameter combinations that had previously been shown to robustly reconstruct patterns of human migration and growth (Eriksson et al., 2012). We calculated the mean and variance of the 4,950 simulation results (Figure S1.3) and scaled the projections of N_e between 0 and 1 (using an approach identical to the scaling of steppe bison habitat suitability projections). We then resampled the outputs from the timestep of 'CISGeM' (25 years) to the timestep of the bison simulations (12 years). To parameterise human hunting in our demographic models, we generated 50,000 potential trajectories of relative human density (using relative N_e as a proxy) in Siberia by sampling a lognormal distribution of relative effective population size (based on the mean and variance of the 4,950 simulations), accounting for spatially autocorrelated stochasticity (see Appendix S1 in the Supplementary Information for an extended version of the methods).

4. Process-explicit model

We generated a SEPM in 'paleopop' that simulated the ecological processes of movement and demographic change (extinction), responding to shifting climates, sea levels, ice sheets, and human hunting. Key ecological processes we modelled for the steppe bison included density dependent population growth, dispersal, and source and sink dynamics. These processes were simulated at generational time steps (12 years) using a spatially explicit scalar-type population model Habitat suitability from the potential realised niche models were used to structure the metapopulation by providing estimates of relative upper abundance in space and time (Fordham et al., 2022), assuming no adaptation to climatic or environmental change over the course of the simulation. Simulations were run at 12-year time steps from 50 kyr BP to 5 kyr BP. To ensure stable metapopulation dynamics at the beginning of the simulation (Fordham, Bertelsmeier, et al., 2018),

all simulations were preceded by a burn-in period of 100 generations, whereby grid cell upper abundance were held at 50 kyr BP values for the burn-in period.

4a. Demography

Demographic rates for congeneric species (*B. bison* and *B. bonasus*) were used as surrogates for the steppe bison (Fordham et al., 2016). We estimated maximum annual growth rate and its variance using time series data for *B. bison* and *B. bonasus* (see Appendix S1 for details). We scaled these growth rates to a generational time step based on the 12-year generation length of *B. bison* (Pacifici et al., 2013). After testing the stability of population dynamics with different density dependence functions, we modelled population growth with Ricker logistic density dependence (Ricker, 1954), with the carrying capacity dependent on the habitat suitability in a given grid cell. At a habitat suitability of 1, the carrying capacity was equal to the maximum density (Table 1), reducing with lower suitability scores. We modelled a negative Allee effect, using a quasi-extinction threshold below which populations immediately dropped to zero (Fordham, Bertelsmeier, et al., 2018).

We simulated natal dispersal based on empirical estimates for *B. bison* (Jung, 2017). Between 5 and 25% of the population dispersed per generation, with a maximum dispersal distance of 100 – 500 km (Table 1). A dispersal friction landscape (Adriaensen et al., 2003) based on ice sheet reconstructions was used to ensure that bison dispersed only through ice-free grid cells. Human hunting was simulated based on relative abundance (see above). The harvest z parameter shaped the hunting function from a type II ($z = 1$) to type III ($z = 2$) functional response (Brook & Bowman, 2002) with the maximum harvest set from 0 to 35% (Fordham et al., 2022). All demographic parameters are described in more detail in Appendix S1.

4b. Model simulations

To address parameter uncertainty, which is inevitably high for extinct species (Brook & Bowman, 2004), we created 50,000 unique SEPM parameterisations using Latin hypercube sampling (Stein, 1987), drawing samples from uniform prior distributions for 11 model parameters (Table 1). This stratified sampling of the priors allowed us to generate a large suite of SEPMs, covering the

parameter space of demographic processes, ecological requirements (based on realised niche breadth and specialty), and hunting pressure. We selected realised niches to generate the carrying capacity landscapes in each simulation. Each sampled combination of parameters, including niche estimates, were integrated into an SEPM and simulated for a single replicate (Fordham et al., 2022). 50,000 simulations took 214 hours in parallel on an eight-core Windows machine with a 3.6 GHz processor.

5. Pattern-oriented modelling

5a. Validation targets

Pattern-oriented modelling (Grimm et al., 2005) was used to evaluate different SEPM parameterisations. Simulations were validated using POM methods, by comparing simulated estimates of spatiotemporal occurrences in Siberia, and timing and location of extinction, with fossil-based inferences (Appendix S1). We estimated the timing of extinction in Siberia from the fossil record to be 8,734 cal yr BP (95% CI: 8,810 – 8,657 cal yr BP) using a Gaussian-resampled, inverse-weighted method (Bradshaw, Cooper, Turney, & Brook, 2012) that accounts for the Signor-Lipps effect (Signor, Lipps, Silver, & Schultz, 1982). We estimated the extinction location to be in the Lena River basin based on the youngest fossil (Pilowsky et al., 2021). To calculate spatiotemporal occurrence, we set a spatiotemporal window of uncertainty around each steppe bison fossil in our study region (n = 31) and then quantified the agreement between simulated and inferred occurrence. The spatial window was based on the grid cell and its eight nearest neighbours, while the temporal band of uncertainty was based on ±2 × the error (SD) of the calibrated date. The same temporal band of uncertainty was used to quantify climatic conditions for the multi-temporal niche. A simulated presence of bison within the inferred window of occurrence was treated as a correctly simulated occurrence.

5b. Statistical procedure

Pattern-oriented modelling was done in the R package 'abc' v2.1 (Csillery, Lemaire, Francois, & Blum, 2015) using Approximate Bayesian Computation with the rejection algorithm to select the 100 best models. All summary metrics for analysis were scaled based on their standard deviations

(van der Vaart, Beaumont, Johnston, & Sibly, 2015). The pattern-oriented modelling procedure was repeated using informed priors from previous model runs. This was done until Bayes factors indicated that the posteriors had converged (Figure S2.1). The procedure involved running four additional rounds of 10,000 simulations each, selecting the best 100 models each time and using the posterior distributions as the priors for the subsequent round. Posterior predictive checks were done to determine whether the posterior distributions result in good resemblance between simulated and observed data (Gelman, Hwang, & Vehtari, 2014).

6. Counterfactual scenarios

Counterfactual scenarios create possible alternatives to what historically occurred (Mondal & Southworth, 2010). We used counterfactual analysis to determine the consequences of rates of past climatic change and hunting by humans on the decline and extinction of steppe bison in Siberia (Fordham et al., 2022). We created an optimised ensemble based on the 100 best models selected from the final round of simulations, which served as a "baseline scenario" (non-counterfactual) of what is historically likely to have occurred in Siberia based on our POM approach. We used this optimised ensemble of models to simulate two counterfactual scenarios: *no harvest*, which modelled no hunting of steppe bison by humans from 50 kyr BP (i.e., steppe bison responding only to climate change); and *constant climate*, which held climatic suitability for steppe bison in Siberia at Last Glacial Maximum values from 21 kyr BP to the end of the simulation. For the *constant climate* scenario, the density of humans remained dynamic. Demographic and ecological parameters for the counterfactual scenarios were generated using random draws from the posterior distributions of the optimised ensemble model, using the Latin hypercube sampling approach described above. The counterfactual and baseline scenarios were compared using 10,000 simulations per scenario.

Results

Our validated simulations show that the range of the steppe bison in Siberia contracted in a north-easterly direction, until 33 kyr BP, when the range fragmented into smaller populations (Figure 2). This fragmentation continued through the Pleistocene-Holocene transition, resulting in only

refugial populations in north-eastern Siberia from 11 kyr BP (Supplementary Movie). Time of extinction in Siberia was simulated to occur at 7.4 kyr BP (± 1.5 kyr BP) based on the ABC-weighted average of the best 100 process-explicit models. The oldest end of the window of uncertainty in our simulated estimate of time of extinction overlaps with the time of extinction based on the fossil record (8.81 – 8.66 kyr BP; see Methods). The youngest end overlaps with independent environmental DNA evidence of prolonged persistence of steppe bison in north-eastern Siberia, with the youngest inference of occurrence being at 6.4 ± 0.6 kyr BP (Yucheng Wang et al., 2021). This ensemble of 'best models' projected the last surviving population to be in the east Siberian highlands, occurring ~500 km from the last known fossil, located at Batagaika in the Lena River valley (Murton et al., 2017).

The capacity of SEPMs to simulate fossil-based inferences of timing and location of extinction was high after improving through five iterations of POM (Figure 3). Bayes factors showed convergence in prior and posterior distributions after five iterations of pattern-oriented modelling (all Bayes factors < 1; Figure S2.1). Posterior predictive checks showed that these posterior parameter distributions result in reasonable resemblance between simulated and observed data for extinction location and extinction time (p > 0.01) (Table S2.1). However, there was a poorer fit between the simulated spatiotemporal occurrence of bison at fossil sites and the observed fossil-based inference of spatiotemporal occurrence (p < 0.01).

Posterior distributions of model parameters

Comparison of posterior and prior parameters show that accurately reconstructing inferences of range contraction and timing and location of extinction from the fossil record required specific demographic and niche constraints, and hunting pressure (Figure 4). Posterior distributions show that specific niche requirements were needed to reconstruct the range and extinction dynamics of steppe bison. The posterior distributions for niche volume and outlying mean index (Table 1) indicate that steppe bison in Siberia fulfilled a subset of core climatic conditions available to the species across its entire multi-temporal range. This is shown by a small-to-medium niche volume (60% of the full multi-temporal niche volume) and small outlying mean index. Among demographic processes, the posterior distributions show that a high variance in growth rate, a

medium-sized Allee effect, high maximum density, and high dispersal (both in terms of maximum dispersal distance and dispersing fraction) are important for reconstructing range and extinction dynamics of the steppe bison in Siberia (Table 1). Furthermore, hitting validation targets requires high human densities and high rates of harvest (Table 1).

Counterfactual scenarios

In a *no hunting* scenario, the total population size of steppe bison in Siberia was higher throughout the simulation compared to the baseline (with hunting) and they did not go extinct before the end of the simulation at 5 kyr BP (Figure 5). Prior to 30 kyr BP in the *no hunting* scenario, the range of the steppe bison extended further south and west, fragmenting into smaller subpopulations only in the final 5000 years of the simulation (Supplementary Movie). In a *constant climate* scenario, where the climate was unvarying from 21 kyr BP, total population size stabilized at 19 kyr BP (Figure 5), while the range contracted to two large subpopulations that were linked by dispersal, both of which persisted to the end of the simulation (Supplementary Movie).

Neither of the counterfactual scenarios did as well as the baseline model at predicting timing and location of extinction (Figure S2.2). Models without human hunting (*no hunting* scenario) were generally better able to simulate spatiotemporal occurrence than the *constant climate* and *baseline* scenarios. This is because the absence of hunting by humans resulted in larger areas of occupied habitat in Siberia through time (Supplementary Movie).

Discussion

We were able to reconcile inferences of spatiotemporal occurrence and timing and location of extinction for steppe bison in Siberia based on hundreds of radiocarbon-dated fossils. Our ensemble of 'best models' projected extinction to have occurred in the east Siberian highlands at 7.4 kyr BP, occurring on average 1,300 years after the fossil estimate. This is consistent with fossil-based estimates of extinction often being hundreds to thousands of years earlier than the likely timing of the actual extinction event (Haile et al., 2009; Yucheng Wang et al., 2021), because they represent the last time that a species was abundant (Mann et al., 2019). We show that simulating the ecological pathway to extinction for steppe bison in its last refuge in Eurasia required very

specific ecological niche constraints, demographic processes, and hunting dynamics. It also required these processes to respond to climatic change, human abundance, and their interaction to regulate these ecological processes during the Pleistocene-Holocene transition. Counterfactual scenarios confirmed that human hunting and climatic change were both pivotal long-term drivers of regional extinction for the steppe bison in Siberia, and most likely Eurasia more generally. These results demonstrate how spatially explicit population models (SEPMs) and pattern-oriented modelling (POM) methods can be used in macroecology and palaeoecology to disentangle mechanisms that were integral in the decline and later extinction of species.

The processes leading to the megafauna extinctions of the late Pleistocene and early Holocene are uncertain, with intense debate on the roles of human hunting and climatic change (Mann et al., 2019; Stuart, 2015). The steppe bison was an iconic herbivore that dominated the "mammoth steppe" of the Ice Age Arctic (R. Dale Guthrie, 1989). While the timing, location, and causes of megafaunal extinctions in this biome are contested (Cooper et al., 2015; Koch & Barnosky, 2006; Stuart, 2015), our process-explicit models show that a synergy of climatic change and exploitation by humans most likely drove the steppe bison, and perhaps other herbivores of the mammoth steppe, extinct during the late Pleistocene and early Holocene.

Pattern-oriented modelling revealed the ecological processes that regulated the extinction dynamics of steppe bison. Reconstructing fossil-based evidence of spatiotemporal occurrence and extinction in the northern Lena River valley requires steppe bison to have an ecological niche volume of 59 - 74% of the size of the full multi-temporal niche (Nogués-Bravo, 2009). This reduced niche volume has low marginality (Dolédec et al., 2000), meaning that the ecological niche for steppe bison in Siberia represented the core climatic preferences of steppe bison more generally. Among demographic processes, dispersal and the effect of small population size on extirpation are likely to have influenced the range and extinction dynamics of steppe bison. Hitting our multivariate validation target required a pronounced Allee effect and the capacity for high dispersal, among other demographic constraints. Evidence for an Allee effect at low population densities has been found in natural populations of other temperate and polar ungulates: bighorn sheep (*Ovis canadensis*), chamois (*Rupicapra rupicapra*), elk (*Cervus elaphus*), pronghorn (*Antilocapra*

americana), and woodland caribou (*Rangifer tarandus*) (Kramer, Dennis, Liebhold, & Drake, 2009). This has been attributed largely to cooperative defence and predator satiation reducing mortality at high densities, although mate selection at low density could also be a factor (Kramer et al., 2009). A high capacity for movement, including long distance dispersal, was also needed to reconstruct inferences of demographic change from the fossil record. Research on American bison has shown that they migrate seasonally in response to forage availability in winter (Gates & Larter, 1990). They will also disperse toward unoccupied habitat when population densities become high (Plumb, White, Coughenour, & Wallen, 2009).

Reconciling inferences of range collapse and extinction from the palaeo-record required hunting by humans. More specifically, humans needed to be found in medium-to-high regional densities (based on projections for Siberia) with high harvest offtake. Holding the hunting of bison constant to zero exploitation and then analysing the effect of this constraint on dynamic processes and emergent patterns revealed that human hunting was a crucial and chronic driver of extinction of steppe bison in Siberia. Without hunting by humans, steppe bison maintained a wider distribution and larger population size and did not go extinct by 5 kyr BP (the end of the simulation). Rather, bison persisted in two small subpopulations in the far north of Siberia with suitable climatic conditions. This finding aligns with archaeological evidence showing that human hunters in Siberia relied heavily on bison prey during the Pleistocene-Holocene transition (Vasil'ev, 2003), and that bison were disproportionately selected by hunters (Pushkina & Raia, 2008).

Keeping climatic conditions constant for steppe bison (but not humans) since the Last Glacial Maximum in the *constant climate* counterfactual scenario showed that hunting alone could not have driven the steppe bison to extinction. Without deglacial warming negatively affecting range and abundance, steppe bison were projected to be at large abundances at 5 kyr BP despite hunting by humans. Taken together, our counterfactual hypotheses of the drivers of range collapse and extinction of steppe bison show that human hunting and climatic change were important determinants of the ecological pathway to extinction for steppe bison in Siberia. This association is likely to have been synergistic, with humans accelerating the range collapse of steppe bison during the Pleistocene-Holocene transition, hastening the extirpation of populations that had become

fragmented due to deglacial warming and associated shifts in vegetation. A similar mechanistic explanation has been proposed for the extinction of the woolly mammoth (Fordham et al., 2022).

While we have shown that the application of POM methods to process-explicit modelling provides a powerful approach for continuously reconstructing range dynamics over thousands of years, the approach is only as accurate as the validation targets being used. Our validation targets were independent from the data used to parameterise the model, they captured a hierarchy of demographic responses (Gallagher et al., 2021), and they were estimated robustly using statistical techniques applied to fossil data (Bradshaw et al., 2012). Therefore, we have confidence in our POM and results, including the posterior distributions for model parameters and their multi-model averaged projections of range and extinction dynamics (Grimm & Railsback, 2012). However, for many other species, an abundant and spatially representative fossil record will not be available to optimise SEPMs of species' range dynamics using POM. Here, other types of palaeo validation data could be considered, including ancient DNA estimates of past population change (Fordham et al., 2014) and inferences of spatiotemporal occurrence from environmental DNA in sediments and ice cores (Yucheng Wang et al., 2021). For threatened species, or species that went extinct recently (such as the thylacine in Australia), historic sightings can provide important sources of validation data (Fordham et al., 2021).

Posterior predictive checks of our process-explicit model showed that the posterior ranges of model parameters reconstruct extinction time and location reasonably well (Gelman et al., 2014). However, it was more difficult to reconcile fossil evidence of spatiotemporal occurrence. Indeed, this target was easier to reconstruct in simulations without human hunting, because in the *no hunting* scenario, steppe bison maintained larger ranges through time. Larger ranges resulted in occurrence not only being higher at fossil sites, but also in areas which were unlikely to have been habitable by steppe bison during periods in the past. It is possible that the difficulty with correctly simulating spatiotemporal occurrence at fossil sites could stem from the hunting dynamics in our process-explicit model. This was relatively simple, not accounting for technological developments which are likely to have occurred during the timeframe of the simulation (Goebel, 2002). The wide posterior range for the functional response of human hunting of steppe bison, extends from the

selected best models having a diverse range of hunting strategies — suggesting that a variety of parameter values can give a close fit to inferences of extinction dynamics from the fossil record. Also, the model we used to simulate the peopling of Siberia (and Eurasia more generally in 'CISGeM') does not account for topography, which could have caused barriers to movement, particularly in the Siberian highlands (Eriksson et al., 2012), affecting spatiotemporal harvest rates.

Our process-explicit modelling shows that climatic change and hunting by humans in Siberia during the late Pleistocene and early Holocene is likely to have interacted with key ecological requirements and demographic processes of steppe bison to cause its extinction in Eurasia during the early Holocene. Moreover, it shows that process-explicit models validated with pattern-oriented modelling methods can continuously simulate the ecological processes and drivers that cause the population declines of species over many millennia, as well as the final extinction event. While synthesis of the declining and small population paradigms (Caughley, 1994) remains rare, the integrated computational framework used here provides new opportunities to better establish ecological pathways to extinction over long time periods. If applied to a diverse range of species, generalities in ecological processes of extinction could be identified.

Acknowledgments

Figures, Boxes & Tables

Tables

Parameter	Mean Prior	Mean Posterior
Ecological niche		
Niche volume	0.5 (0 – 1)	0.438 (0.332 – 0.775)
Niche outlier marginality index (OMI)	0.5 (0 – 1)	0.197 (0.166 – 0.237)
Human harvesting		
Maximum harvest (percent)	17.5 (0 – 35)	25.3 (9.5 – 34.1)
Harvest function (z)	1.5 (1 – 2)	1.46 (1.04 – 1.89)
Human density (p)	0.5 (0 – 1)	0.782 (0.585 – 0.984)
Dispersal		
Dispersing fraction	0.15 (0.05 – 0.25)	0.212 (0.121 – 0.249)
Maximum dispersal distance (km)	300 (100 – 500)	419 (285 – 495)
Population model		
Maximum growth rate (r)	2.07 (1.31 – 2.84)	2.066 (1.566 – 2.816)
Variance of growth rate	0.123 (0 – 0.245)	0.172 (0.095 – 0.228)
Allee effect (abundance threshold)	250 (0 – 500)	212 (126 – 298)
Maximum density (bison per grid cell)	1875 (500 – 3250)	2542 (1840 – 3203)

Table 1: Parameter distributions. The prior and posterior means, minima, and maxima are shown for parameters in the process-explicit model of steppe bison range and extinction dynamics. All priors are uniformly distributed. See Methods for details.

Boxes

Approximate Bayesian Computation (ABC): A statistical technique that uses Bayesian statistics to estimate the distributions of model parameters by comparing simulated probability distributions of summary statistics against the observed distribution (M. A. Beaumont, Zhang, & Balding, 2002).

Correlative models: Models that statistically relate environmental variables to observation data in order to infer biological patterns (Pilowsky, Colwell, Rahbek, et al., 2022b).

Pattern-oriented modeling (POM): An approach for optimising model parameters using independent validation targets (Grimm et al., 2005).

Process-explicit models: Models that represent the dynamics of an ecological system as explicit functions of the processes that drive change in that system. Also known as process-based and mechanistic models (Connolly et al., 2017).

Spatially explicit population models (SEPMs): Process-explicit models that simulate mortality, reproduction, and movement in a network of populations on a landscape map (Dunning et al., 1995).

Box 1: Biodiversity modelling terms.

Figures

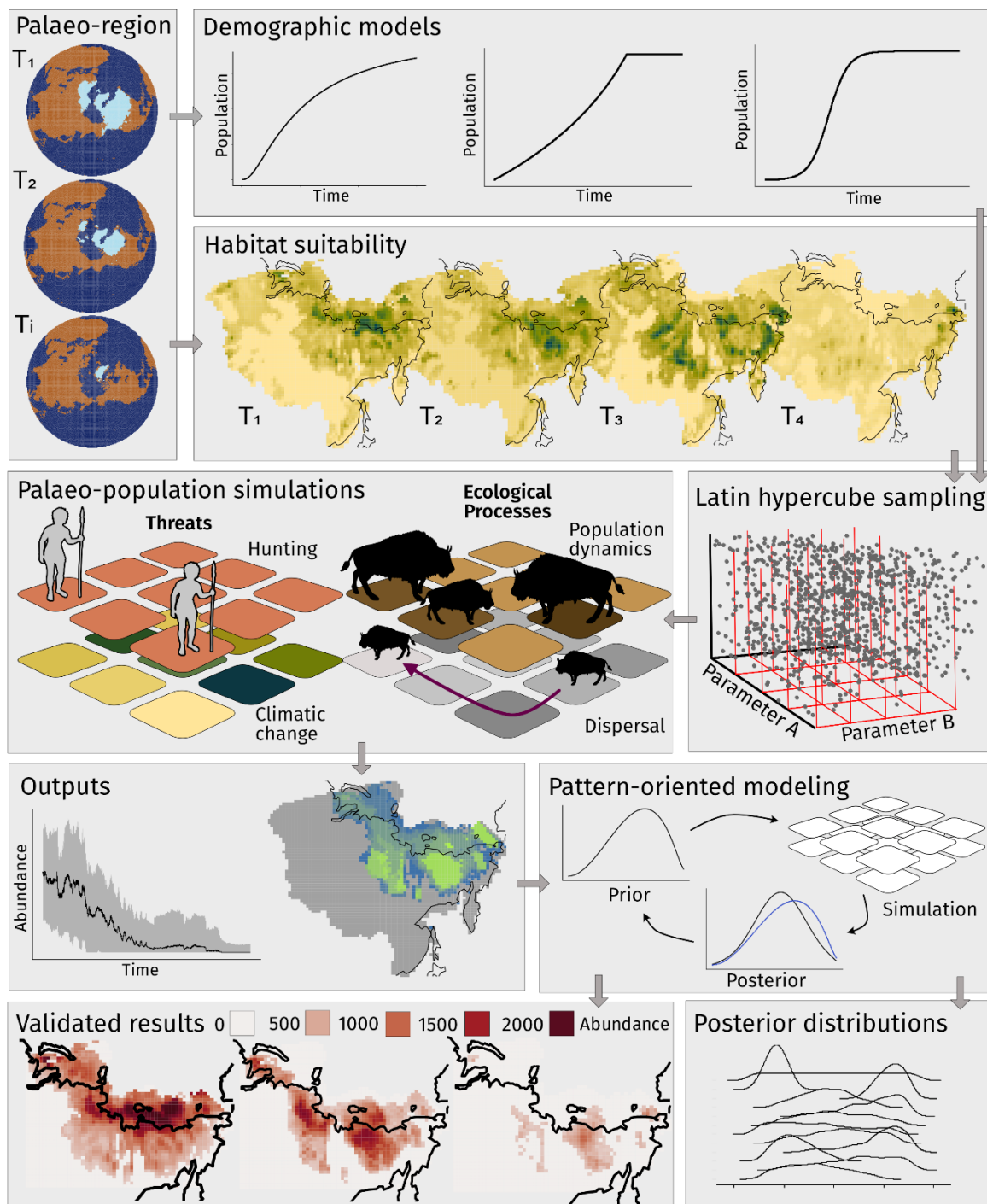**Figure 1: Modelling species' range dynamics over palaeo timescales.** The modelled dynamic *palaeo-region* changes temporally due to climatic change and associated rising sea levels and melting ice sheets. Spatially explicit population models (SEPMs) are built by coupling a *demographic model* with a grid-lattice-type spatial structure of *habitat suitability*. *Latin hypercube sampling* is used to

exhaustively sample SEPM parameter space, resulting in tens of thousands of parameter combinations, each of which is used to parameterise a SEPM. The *palaeo-population simulations* include ecological processes (including dispersal and extinction) responding to key threats of human hunting and climatic change. These simulations reconstruct *outputs* of past population size and abundance maps. *Pattern-oriented modelling* (POM) is used to identify models that reconcile patterns of demographic change inferred from palaeo-archives. This involves optimising values of SEPM parameters by comparing the distributions of posterior and prior parameter ranges (*posterior distributions*) for successive iterations of model building and testing. Models that do best at simulating inferred patterns of range and extinction dynamics are used to generate *validated projections*.
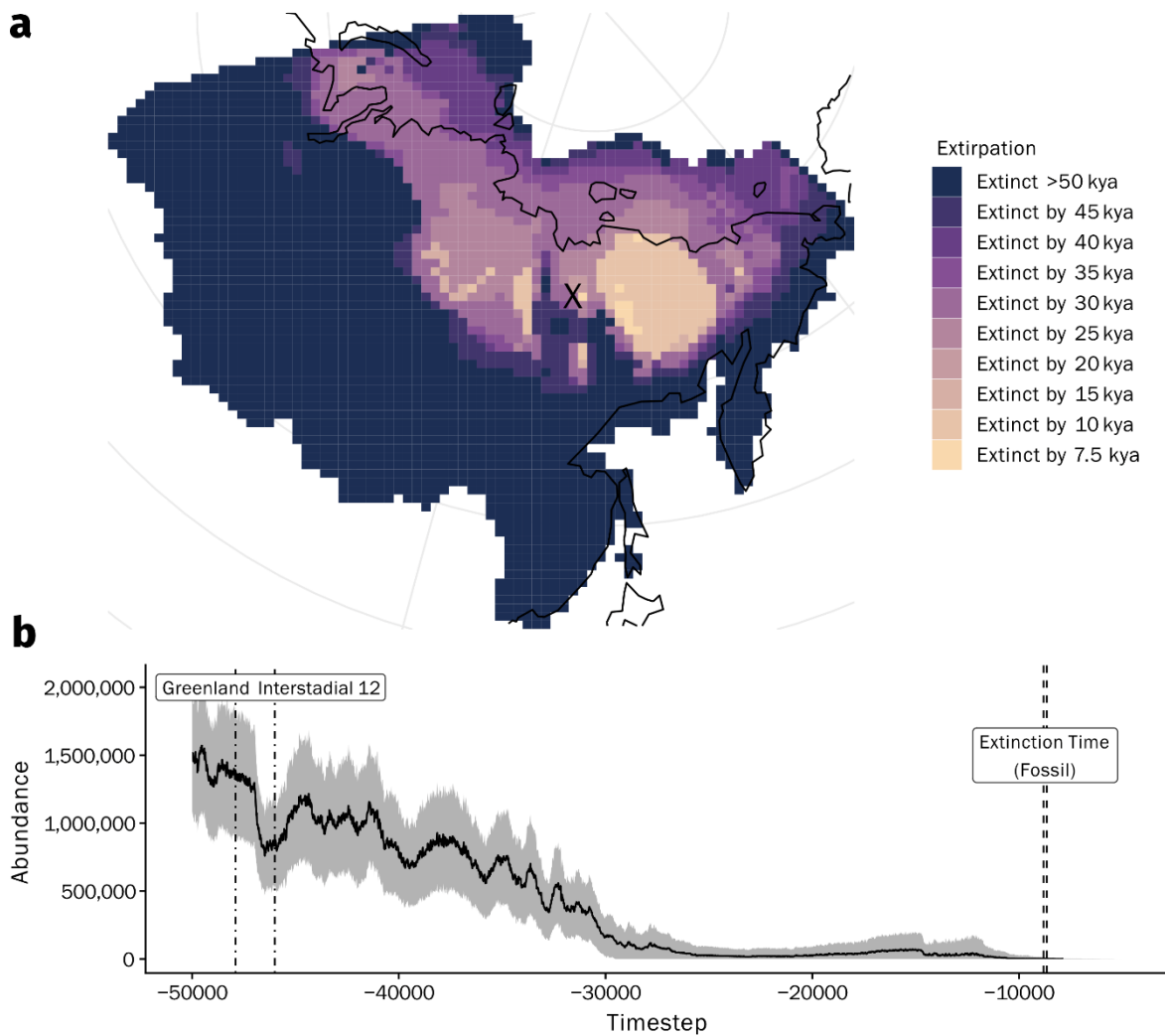
Figure 2: Validated reconstruction of the extinction of the steppe bison in Siberia. The map (a) shows the multi-model average estimate of time of extirpation for the best models according to pattern-oriented modelling. The location of the site of extinction based on fossil data is marked with a cross. The time series (b) shows simulated total population size for steppe bison in Siberia. Vertical lines show extinction time as estimated from the fossil record and Greenland Interstadial 12, a period of climatic warming between 47.9 and 46.0 kyr BP.
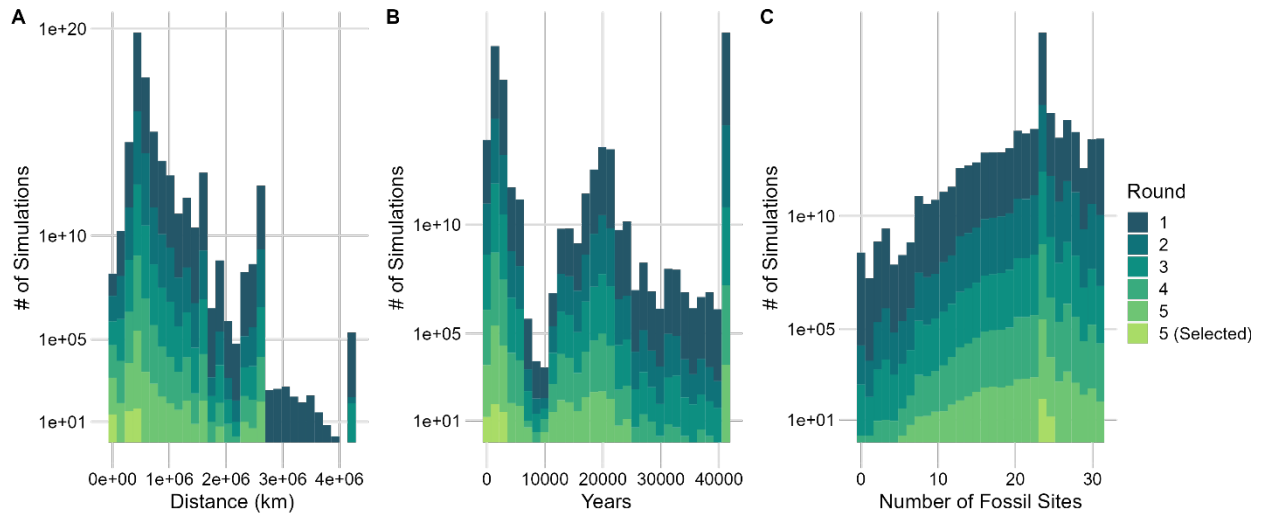
Figure 3: Reconstructions of validation targets using pattern-oriented modelling.

Validation targets for pattern-oriented modelling (POM) are A) Extinction location, evaluated by difference in kms between simulated extinction location and the location based on the youngest fossil; B) Extinction time, evaluated by difference in years between simulated and inferred time of extinction based on the fossil record; and C) fossil-based occurrence, evaluated by the number of sites where spatiotemporal occurrence is simulated correctly. For A) and B) the target for POM was 0 (no difference between simulated and target). For C) the target was 31, which is equal to the total number of fossil occurrence sites. Different colours show five successive iterations of pattern-oriented modelling. See Methods for further details.
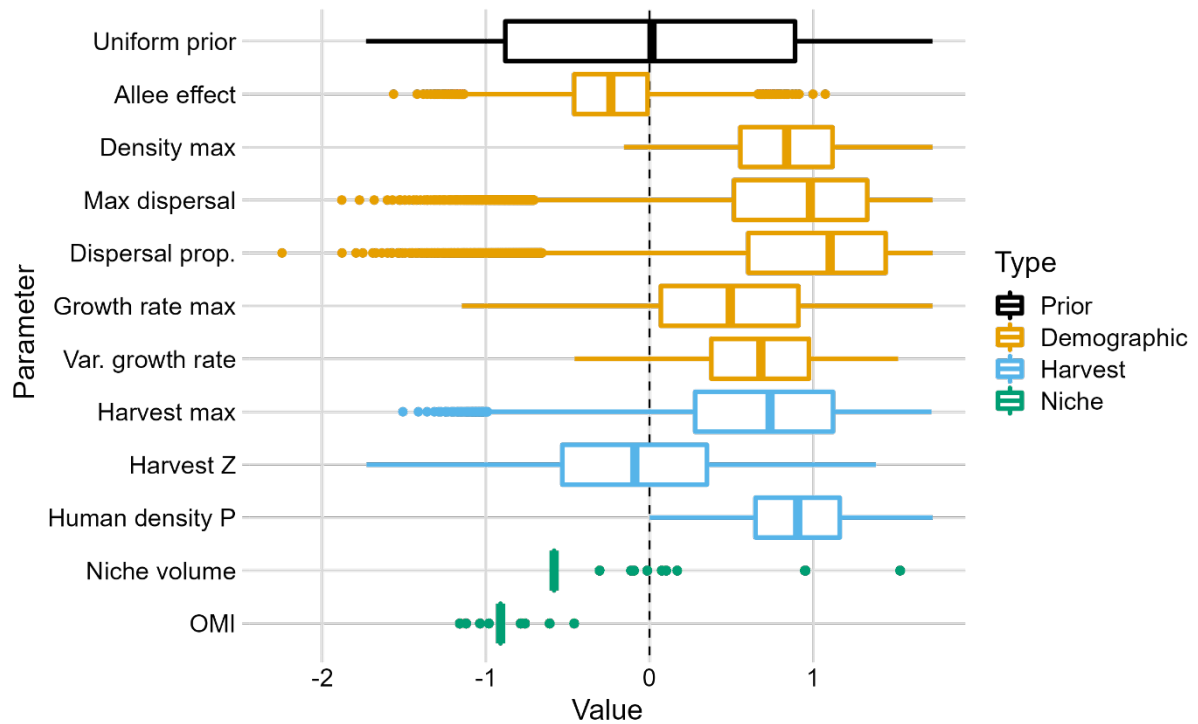
Figure 4: Regression-adjusted posterior distributions for parameters. Maximum dispersal distance and the fraction of bison that dispersed in each generation (Dispersing fraction) simulate dispersal. Maximum density of bison in each grid cell, Allee effect, variance (Var.) and maximum growth rate, all interact to simulate population growth. Human density (relative human density), harvest z (shape of the harvest function), and maximum (Max.) harvest (maximum proportion of bison hunted) determine the hunting rate. Volume and Outlying Mean Index (OMI) are measures of climatic niche space (the size of the climatic niche and the marginality of climatic preferences, respectively). All prior distributions were uniform (black.) Parameters are described in more detail in the Methods. Unscaled parameter ranges are provided in Table 1.
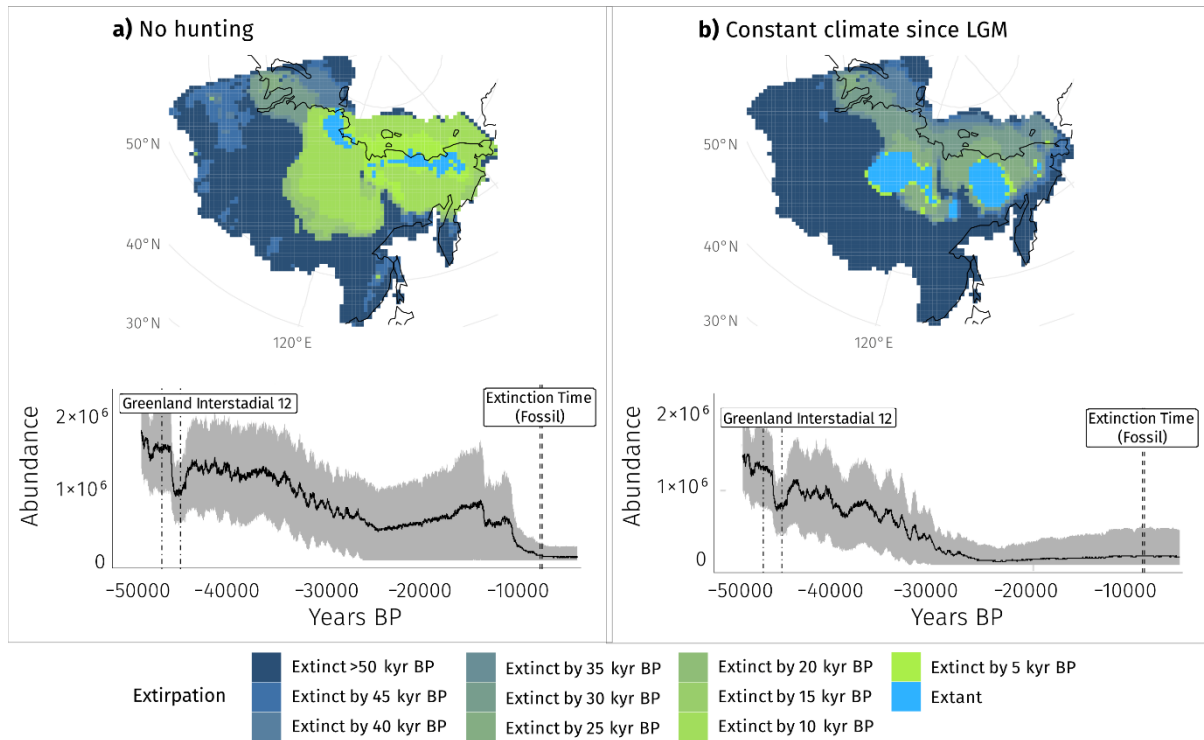
Figure 5: Alternative scenarios of extirpation and population decline. Counterfactual scenarios simulate a) climate change but no human harvesting of bison (*No hunting*) and b) no climate change from 21 kyr BP but harvesting of bison before and after that time (*Constant climate since LGM*). Maps show when populations in each grid cell went locally extinct. Populations that survived to the end of the simulation are shown in bright blue (Extant). Line graphs show the simulated trajectories of total abundance in Siberia (± 1 SD). They include timing of Greenland Interstadial 12 and timing of extinction in Siberia inferred from fossils. See Figure 2 for details.

Supplementary Material

1. paleopop

'paleopop' is an object-oriented R package for building spatially explicit population models (SEPMs) that can simulate species' range and extinction dynamics across multiple millennia with pattern-oriented validation (Haythorne et al., 2021). 'paleopop' is an extension to the package 'poems' (Fordham et al., 2021). It consists of a collection of interoperable R6 (Chang, 2019) object classes. The package allows multiple SEPMs with different combinations of model parameters to be built by drawing parameters from an n-dimensional plausible space using Latin Hypercube

sampling (Fordham et al., 2021). 'paleopop' adds functionality for modelling populations over large temporal scales: a dynamic palaeo-region that incorporates sea-level and other changes in study extent, a palaeo-population simulator optimised for modelling populations over multi-millennial time scales, and a palaeo-results object for storing the output of the simulator.

At the core of the 'poems'/' paleopop' framework are manager components for managing the parallel processing of multiple simulations and extracting their results. The simulation manager object is responsible for initiating simulation runs and storing the simulation results. For each combination of model parameters, the simulation manager builds and runs a SEPM. The simulation manager stores the results of each simulation to disk. The results manager object is responsible for processing the stored simulation results to produce summary metrics for each model (i.e., with a unique sample of the parameter space). For each simulation result, the results manager generates summary metrics via user-defined functions that calculate metrics using the saved simulation results, as well as several useful dynamically generated results, such as extinction locations and abundance trends.

The approach allows parameter uncertainty to propagate through to model simulations of range and extinction dynamics. Their effects can be evaluated using Approximate Bayesian Computation (ABC) (Csilléry et al., 2010), a statistical procedure for pattern-oriented modelling (Grimm et al., 2005). This validation method identifies models with the structure and parameterisation needed to simulate the effects of past changes in climate, environment and human activities on species' distributional shifts and extinction risk (Fordham et al., 2021). The validator object utilises the sampled model parameters, their corresponding summary metrics, and observed target values for each metric. The simulation models with the best congruence between summary metrics and observed targets are selected. Pattern-oriented modelling weights, which are calculated by the ABC algorithm and are indicative of model congruence with target patterns, can be used to generate weighted multi-model average estimates of spatiotemporal abundance, extinction risk, and other metrics (Fordham et al., 2022).

The five minimum parameters required to run 'paleopop' are number of timesteps, number of populations, initial abundance, carrying capacity, and transition rate between generations. For our simulations, we added five static parameters and eleven dynamic parameters (Table 1).

2. Steppe bison niche

2a. Fossil data

Fossil data came from publicly available databases and from the published literature. We regularised inconsistent and outdated species names, discarding any records where the species identity was ambiguous (e.g., "bison" without clear indicators whether it was the steppe bison or another bison species.) In cases where a site name was available, but latitude and longitude were not, we geocoded locations manually using OpenStreetMap and Google Earth. Because our models were in a Lambert equal area projection with 77.8 km by 71.0 km resolution, we did not require a high degree of precision in geolocations. We assessed the quality of the radiocarbon dates using the approach advocated by Barnosky and Lindsey (Barnosky & Lindsey, 2010) which rates the quality of radiocarbon dates based on stratigraphy, association, and the material dated. We retained all records rated as "reliable" (score > 10) and calibrated their radiocarbon dates using the OxCal tool (Ramsey, 2017) and the IntCal13 curve (Reimer et al., 2013). We later recalibrated the radiocarbon dates with the IntCal20 curve (Reimer et al., 2020) and found that there was a mean difference between the IntCal13- and IntCal20-calibrated dates of 0.3%, which led us to conclude that a re-evaluation of the fossil dates for the analysis was not necessary. The fossil data are available online (Pilowsky et al., 2021).

2b. Climate data

We accessed palaeoclimate reconstructions from 50 kiloyears before present (kyr BP) to 5 kyr BP from the HadCM3B coupled ocean-ice-atmosphere model (Valdes et al., 2017), provided by Armstrong et al. (E. Armstrong et al., 2019). These palaeoclimate simulations incorporate monthly and interannual climate variability (directly from model output) and millennial scale variability (by assimilating model and climate proxies), and have been downscaled to 0.5° x 0.5° spatial resolution (E. Armstrong et al., 2019). We extracted monthly data for precipitation, temperature, and latent

heat flux for the study region of Siberia, defined using the present-day political boundaries of the Siberian provinces in Russia, with a northern buffer to account for sea level changes. From these, we calculated three focal climate variables: winter temperature, spring & summer evapotranspiration, and annual precipitation (Figure S1). The rationale for choosing these variables is explained in detail in the main paper.

2c. Niche model

We generated climate suitability for the steppe bison (*Bison priscus*) in Siberia from 50 kyr BP to 5 kyr BP using ecological niche models, and more specifically an n-dimensional hypervolume approach (Blonder & Harris, 2019). To do this, we first paired fossil occurrences with our three selected climate variables by sampling the simulated palaeoclimate in a spatiotemporal bin around each fossil occurrence. This bin was defined spatially by the grid cell where the fossil occurred and temporally by a band of ±2 calibrated SD around the calibrated radiocarbon date (Fordham et al., 2022). We removed any duplicate climate data created by two fossil occurrences falling within identical or overlapping spatiotemporal bins. We used this climate dataset to create a full Gaussian hypervolume, optimising for appropriate bandwidth (Figure S2) (Blonder et al., 2018). This approach is analogous to modelling the fundamental niche (Nogués-Bravo, 2009).

We identified thousands of possible realised niches by sectioning the full hypervolume of potentially liveable climatic conditions (Figure S2). We did this by cutting the full hypervolume into smaller hypervolumes (n = 1000) of different volumes and marginalities (climatic specialisation) using Outlying Mean Index analysis (Dolédec et al., 2000). When sectioning the full hypervolume we ensured uniform distributions for volume and marginality.

We calculated niche samples using sampling windows of different volumes, from 70% to 95% of the breadth of the full hypervolume, some overlapping and some non-overlapping (Fordham et al., 2022). We created a uniform distribution of volume and marginality for the hypervolumes and sampled evenly across the distribution, resulting in 772 plausible realised niches once duplicates and edge cases with very few data points had been removed. In this way, we were able to randomly sample realised niches for the simulations while maintaining uniform priors for volume and

marginality. All the hypervolumes were centred and scaled to the same scale as the full hypervolume and projected into geographic space. We tuned these projections using different functions of Gaussian decay, selecting the weighted function that produced a wide distribution of suitability scores while still clearly differentiating cells with zero suitability (Blonder et al., 2018). We scaled the suitability scores of each projection to a 0 – 1 interval, using the 95th percentile for the upper bound to remove outliers.

3. Palaeolithic humans

The expansion of Palaeolithic humans into northern Eurasia was modelled using a process-explicit climate-informed spatial genetic model (CISGeM) that has been shown to accurately reconstruct the dispersal of humans out of Africa (Eriksson et al., 2012). CISGeM simulates local effective population size (N_e) based on a cellular demographic model with carrying capacity modulated by net primary productivity (NPP). The cellular model is on a 100 km hexagonal grid, which allows for equidistant dispersal in all directions. The model has been validated using pattern-oriented modelling and shown to have the structure and parameterisation needed to reconstruct spatiotemporal genetic validation targets (Eriksson et al., 2012).

We parameterised the model using net primary productivity calculated from the HadCM3-based climate simulations generated by Eriksson et al. (Eriksson et al., 2012) in the original CISGeM study, averaged at 30-year intervals on generational time steps for humans (25 years). More specifically, simulations of temperature and precipitation were converted to net primary productivity via the Miami vegetation model (Lieth, 1975). The relationship between carrying capacity and NPP, as well as demographic parameters (including colonisation rate, maximum growth rate, and NPP extinction threshold) were treated as variable parameters. We used 4,950 parameter combinations based on the posterior ranges of validated models (Eriksson et al., 2012).

We ran CISGeM from 120 kya to present to produce 4,950 continuous simulations of human migration out of Africa and growth and spread across the world. We converted estimates of N_e to a latitude-longitude grid, calculated the mean and variance of N_e for each grid cell at each time step (Fordham et al., 2022), and resampled the outputs to the 12-year timestep of the bison simulations

(Figure S3). N_e was scaled between 0 and 1 and used as a proxy of relative abundance of humans in the bison simulation model (Fordham et al., 2022).

4. Process-explicit model

The potential range dynamics of *Bison priscus* were simulated at generational time steps from 50 kyr BP to 5 kyr BP using a scalar lattice-grid type SEPM configured in 'paleopop'. Life-history traits from congeneric species (*B. bison* and *B. bonasus*) were used as surrogates for *B. priscus* in our model (Fordham et al., 2016). These are described below and in the main paper.

Bioclimatic envelope models of climate suitability and CISGeM estimates of human abundance were coupled with stochastic population models that capture extinction as well as colonisation dynamics by simulating landscape-level population processes, including dispersal with source-sink dynamics. Each grid cell was modelled with a scalar-type stochastic model, which simulates the finite rate of population increase "R", its variance and the population carrying capacity (Dunham, Akçakaya, & Bridges, 2006). The approach has been shown to be superior at reconstructing the historical range dynamics of species compared to bioclimatic envelope models alone (Fordham, Saltré, et al., 2018). The model was run at generational time steps (12 years, see below).

4a. Demography

Carrying capacity

The carrying capacity of each grid cell was based on the climate suitability (VanDerWal et al., 2009). We converted habitat suitability to carrying capacity by multiplying the habitat suitability score (on a 0 – 1 scale) by the maximum density, which was one of the varying demographic parameters in the model. We estimated plausible bounds for maximum density using estimates from American bison (*Bison bison*) and European bison (*Bison bonasus*) (Fuller, Garrott, & White, 2007; Mysterud et al., 2007). Based on the assumption that a maximum of one-quarter of each grid cell could be suitable habitat for the steppe bison (Fordham et al., 2013), we scaled the maximum density values to one-quarter of each equal-area projection grid cell, resulting in a range of 500 to 3250 bison per grid cell.

Generation length and population growth

Maximum annual growth rate and its variance were estimated using time series data on reintroduced bison populations in and outside reserves (Gates & Larter, 1990; Mysterud et al., 2007; Samojlik, Fedotova, Borowik, & Kowalczyk, 2019). If the time series contained gaps, we estimated growth rates across the gaps by fitting splines (Petzoldt, 2019). Where possible, maximum annual growth rate was calculated using time series data for founding populations growing exponentially (Fordham et al., 2022). This provided a mean estimate of 0.179 at an annual time scale. To measure the annual variation in growth rate, we used time series data for stable populations fluctuating around the carrying capacity (Fordham et al., 2022). This provided a mean estimate of 0.091 at an annual time scale.

To convert estimates of maximum growth rate and variation in growth rate to generational rates, we exponentiated the lower and upper bound of maximum annual growth rate to the generation length of the steppe bison, which is 12 years, based on its closest living relative the American bison (Pacifici et al., 2013), resulting in a R0 of 1.31 – 2.84 (0.27 – 1.04 on the natural scale). We calculated the variance in population growth rate at a generational time step by running 1000 simulations of an annual model for 100 years and calculating the standard deviation of population growth rate at a generational time step (Fordham et al., 2022). The mean estimate of variance on the generational time scale for the highest value of annual variation was 0.06. Density dependence was modelled as a Ricker logistic density dependent response (Ricker, 1954), which has been shown to be an appropriate model for species with slow life histories like the steppe bison, especially when environmental variation is high (Koetke, Duarte, & Weckerly, 2020).

Dispersal

We used movement data from a radio-collar study of reintroduced American bison (Jung, 2017) to simulate natal dispersal. We modelled a mean dispersal rate of 15% of the population moving per generation at an average maximum distance of 300 km. We set upper and lower bounds on these estimates of 5 – 25% and 100 – 500 km, respectively. We did this by parameterising the following dispersal equation:

$$m_{ij} = \begin{cases} a^{\left(\frac{-D_{ij}}{b}\right)}, & D < D_{max} \\ 0, & D \geq D_{max} \end{cases}$$

where movement (m) between cells i and j is a function of D_{max} (the maximum dispersal distance), a, and b. The parameter a is half the total proportion of dispersers that leave a cell at each time step. The parameter b comes from fitting an exponential function of dispersal distance in which D_{max} is the 95th percentile of the distribution of distances. The lambda parameter of the fitted exponential function is the estimate of b.

The dispersal function was modulated by the dispersing fraction parameter, which set a ceiling on how many bison dispersed out of a grid cell. This approach prevents excessively large dispersal rates between closely neighbouring grid cells (Fordham et al., 2022).

Human hunting

We modelled human hunting as a function of human density (see above) and prey density in a given grid cell. The maximum harvest for the harvest function varied from 0 - 35% of the bison in a grid cell (Fordham et al., 2022). The proportion of bison harvested in a grid cell is given by the following equation:

$$H` = \frac{\left(\frac{N \times F \times P^z}{G + P^z}\right)}{P}$$

where N is the relative abundance of humans scaled between $0 - 1$, F is the maximum harvest, P is the prey density, G is a constant equal to the prey density at which harvest is half-maximal (Alroy, 2001; Brook & Bowman, 2004) and z shapes the harvest function from a type II to a type III functional response, where $z = 1$ corresponds to a type II response and $z = 2$ corresponds to a type III response. At $z = 1$, hunting is purely a function of prey density and predator satiation, resulting in higher hunting rates at low prey densities and lower hunting rates at high prey densities. At $z = 2$, hunting rates are lower at low densities and high densities, reaching their peak at an inflection point, due to prey adaptation and/or prey switching at low prey densities. We did not model any changes in the density of humans in response to predation, as the archaeological literature suggests

that Eurasian hunter-gatherer populations changed largely in response to climate, and relied on a diverse array of food resources (Bevan et al., 2017).

At each time step, the simulator performs four basic steps: 1) the carrying capacity and human density landscapes update, 2) the population growth in each grid cell adjusts according to stochastic variation, carrying capacity and population density (if density dependence is switched on), 3) bison are harvested in each grid cell according to the bison density and human density (if human hunting is switched on), and 4) bison disperse between grid cells according to the carrying capacity of target cells, distance between origin cell and target cell, and dispersal barriers on the landscape (i.e., ice sheets).

4b. Model simulations

We used Latin hypercube sampling to thoroughly explore the parameter space of the 11 dynamic model parameters (Table 1). Latin hypercube sampling is stratified by sectioning distributions into subsets of equal probability density (Stein, 1987). We sampled variable parameters using uniform distributions. Using this procedure, we initially generated 50,000 plausible combinations of parameter values. We also had 5 static parameters that were the same across all simulations: the palaeo-region, years per timestep (12), logistic density dependence, minimum carrying capacity for a cell to attract dispersers (10), and minimum number of populations required for all populations to persist (1). We ran each one of these combinations of parameters for a single replicate (Fordham et al., 2022).

5. Pattern-oriented modelling

5a. Validation targets

To validate the model, we used pattern-oriented techniques, using timing and location of regional extinction, and fossil-based occurrence as model targets. We estimated the timing of extinction in Siberia from the fossil record to be 8,734 BP (95% CI: 8,810 BP – 8,657 BP) using a Gaussian-resampled, inverse-weighted method (Bradshaw et al., 2012). The approach accounts for biases in estimating time of extinctions caused by the Signor-Lipps effect, which arises from the inability of an incomplete fossil record to accurately measure extinction time (Signor et al., 1982).

For each model simulation, we assigned a penalty. If the simulation of regional extinction time fell within the interval of uncertainty in the fossil-based estimate, the penalty was zero. The penalty increased in a linear fashion both forward and backward from the estimated extinction interval.

Using the fossil record, we estimated the extinction location to be at Batagaika in the Lena River valley. For each model, we assigned a penalty of zero if extinction occurred in the 77.8 km by 71.0 km grid cell of the last known steppe bison fossil in Siberia or its eight nearest neighbour grid cells. If the extinction location was outside this area, a linear increasing penalty with distance was applied. If the bison went extinct in multiple cells simultaneously, a population-weighted centroid of these last populations was used to calculate extinction location (B. J. Anderson et al., 2009). If the bison survived to the end of the simulation, the population-weighted centroid of the surviving population was used instead of the extinction location. We did this in order to more heavily weight those simulations in which the steppe bison persisted with refugial populations in the correct location for the last known fossil.

We also used the spatiotemporal occurrence from the fossil record in our study region and time scale (n = 31) as a validation target. We added a spatiotemporal envelope around each fossil corresponding to the 77.8 km by 71.0 km grid cell and its eight nearest neighbours, and ±2 × the error of the calibrated date. Our pattern-oriented validation selected for models that were able to simulate 31 inferences of fossil occurrence.

5b. Statistical procedure

For the first round of pattern-oriented modelling, we ran 50,000 simulations based on uniform priors for all 11 parameters. We calculated the summary metrics detailed above, scaled them by their standard deviations, then did pattern-oriented modelling using the ABC rejection algorithm. We fitted appropriate statistical distributions (uniform, Poisson, negative binomial, beta, or truncated normal) to the validated posteriors, used these as informed priors for a second round of 10,000 simulations, and again selected the best 100 models using ABC. We continued through three more rounds of 10,000 simulations, until the Bayes factors indicated that the posterior distributions had stabilised relative to the priors.

6b. Posterior predictive checks

After the final round of pattern-oriented validation, we simulated 10,000 draws from the validated posteriors, calculated summary metrics, and evaluated model performance using posterior predictive checks (Crespi & Boscardin, 2009). The posterior predictive check compares the distance among the simulated summary metrics against the distance between the simulated and observed metrics. The model passes the posterior predictive check if there is high overlap (small difference in means) between the two sets of distances.

[Box.com link to view supplementary movie](#)

Supplementary Movie: Spatiotemporal abundances of steppe bison in the baseline, no hunting, and constant climate scenarios.

Target	Estimate	t-value	p value
Spatiotemporal occurrence	0.985435	31.1378	< 0.01
Extinction time	0.056049	1.769989	> 0.01
Extinction location	-0.31638	-9.99192	> 0.05

Table S1: Posterior predictive checks for the three validation targets. The validation targets are detailed in Fig S5. Posterior predictive checks are based on 10,000 draws from posterior distributions of parameters (Table 1), showing the Estimate (the estimated difference between distances among simulated targets and distances to observed targets), t-value and p value. A model is considered to have good performance on a validation metric when there is little difference between the distances among simulated targets and the distances to observed targets.
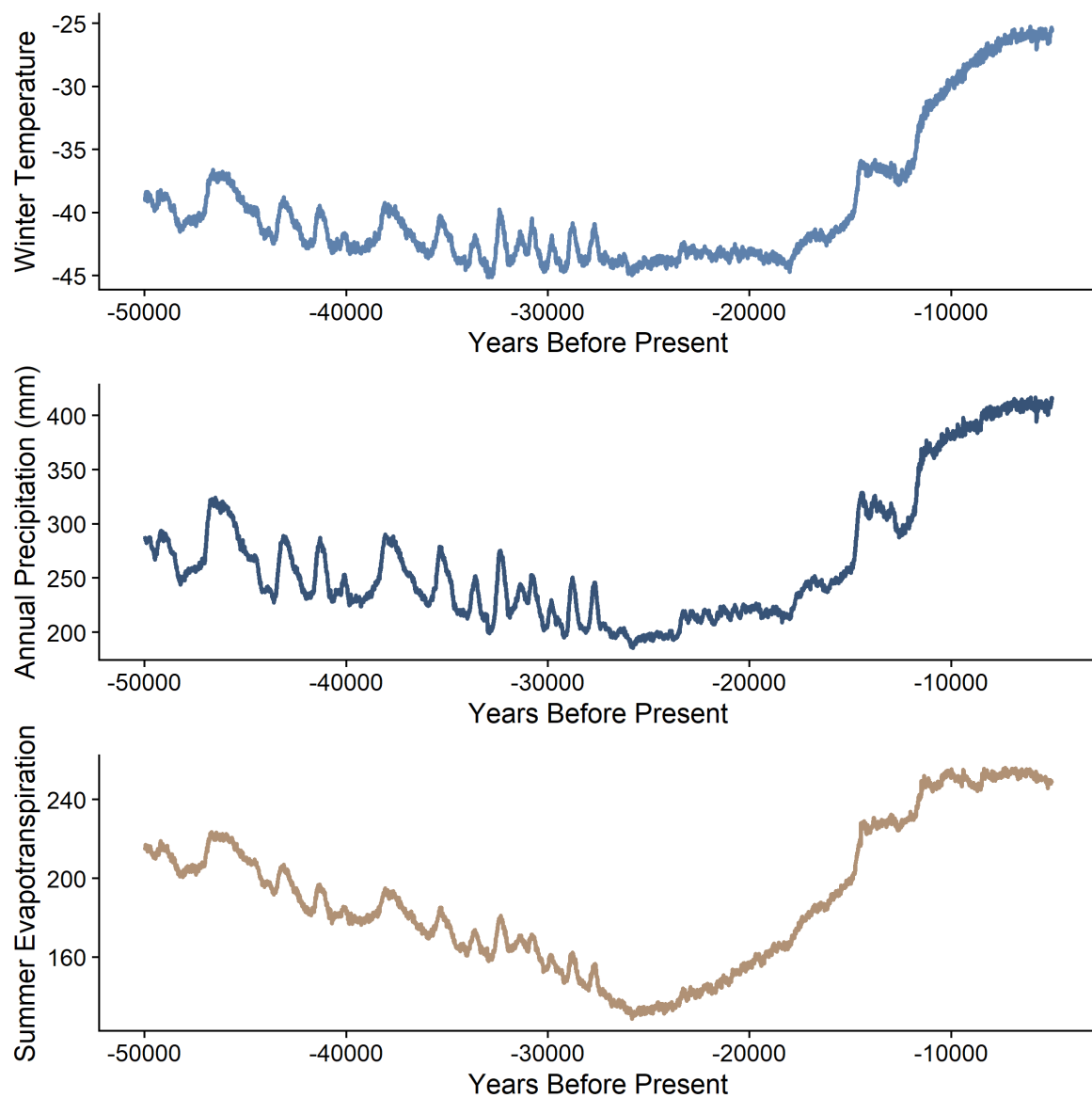
Figure S1: Time series of climate variables in the steppe bison climatic niche. The time series show the HadCM3B-based data (see above) used to model the climatic niche of the steppe bison, in the study region of Siberia, for the duration of the simulation (50 kyr BP to 5 kyr BP).
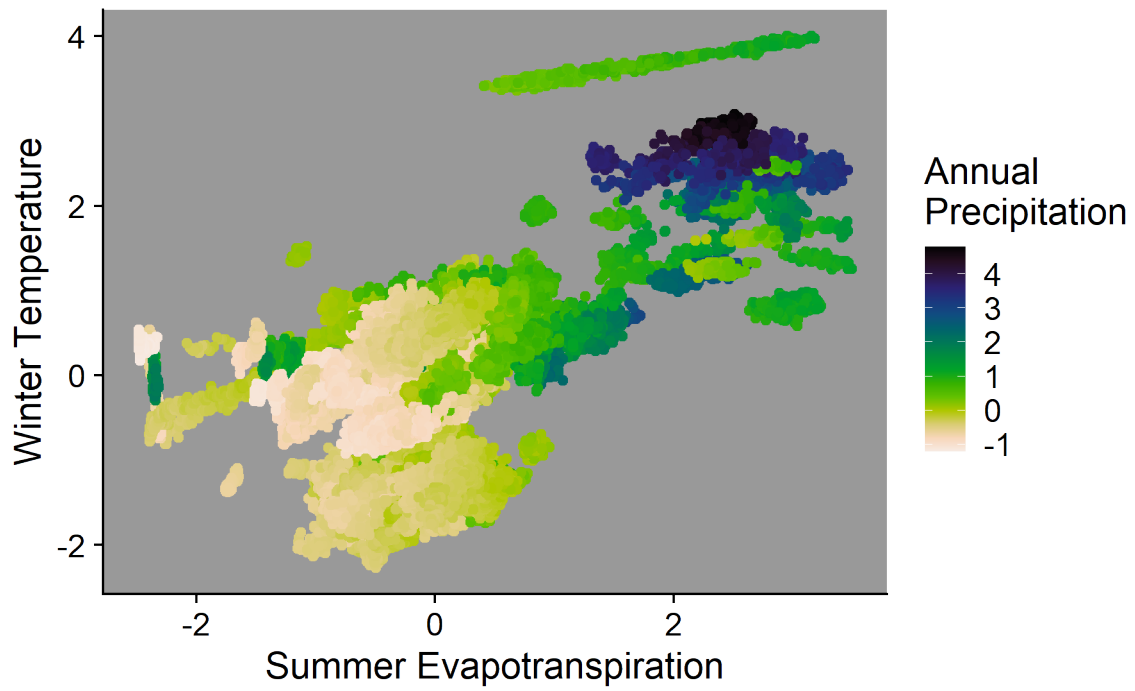
Figure S2: Full multi-temporal climate hypervolume. The hypervolume is estimated by the R package `hypervolume` based on the steppe bison fossil record in North America, Beringia, and Siberia. All climate values are centred and scaled.
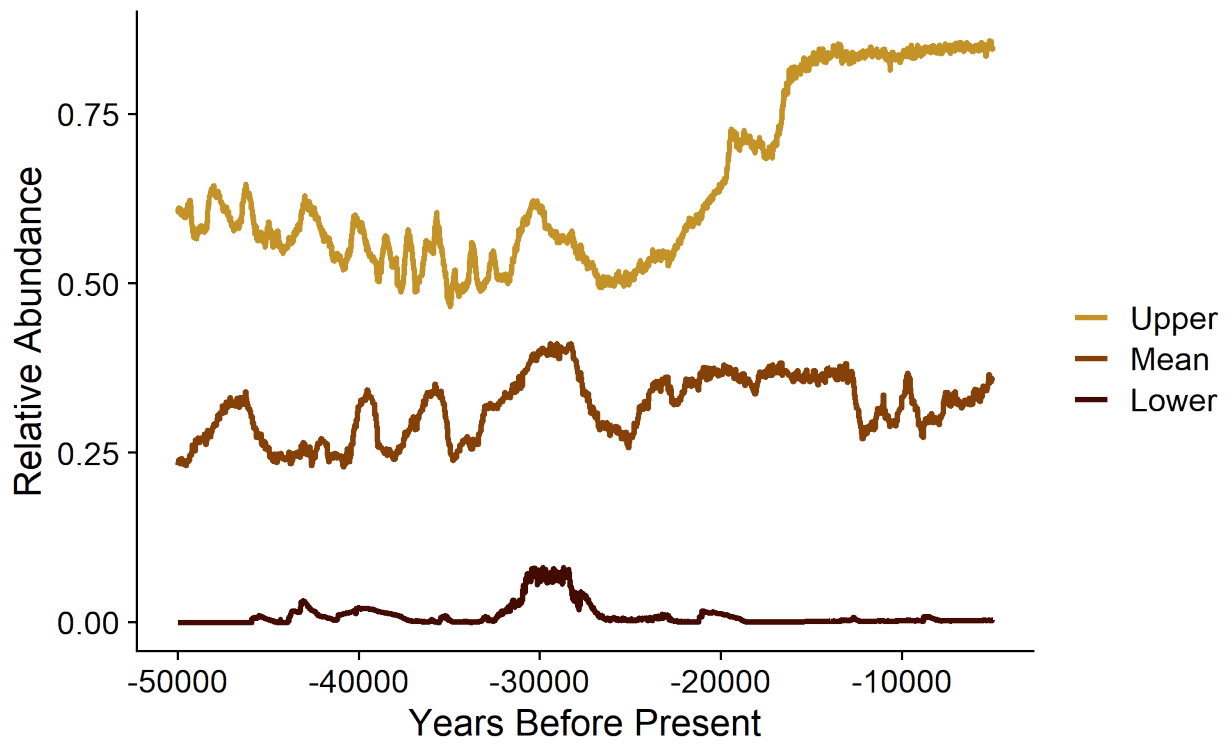
Figure S3: Relative abundance of humans in Siberia. Relative abundance is scaled to a 0 – 1

interval from effective population size. Upper and lower bounds are +/- 1 SD.
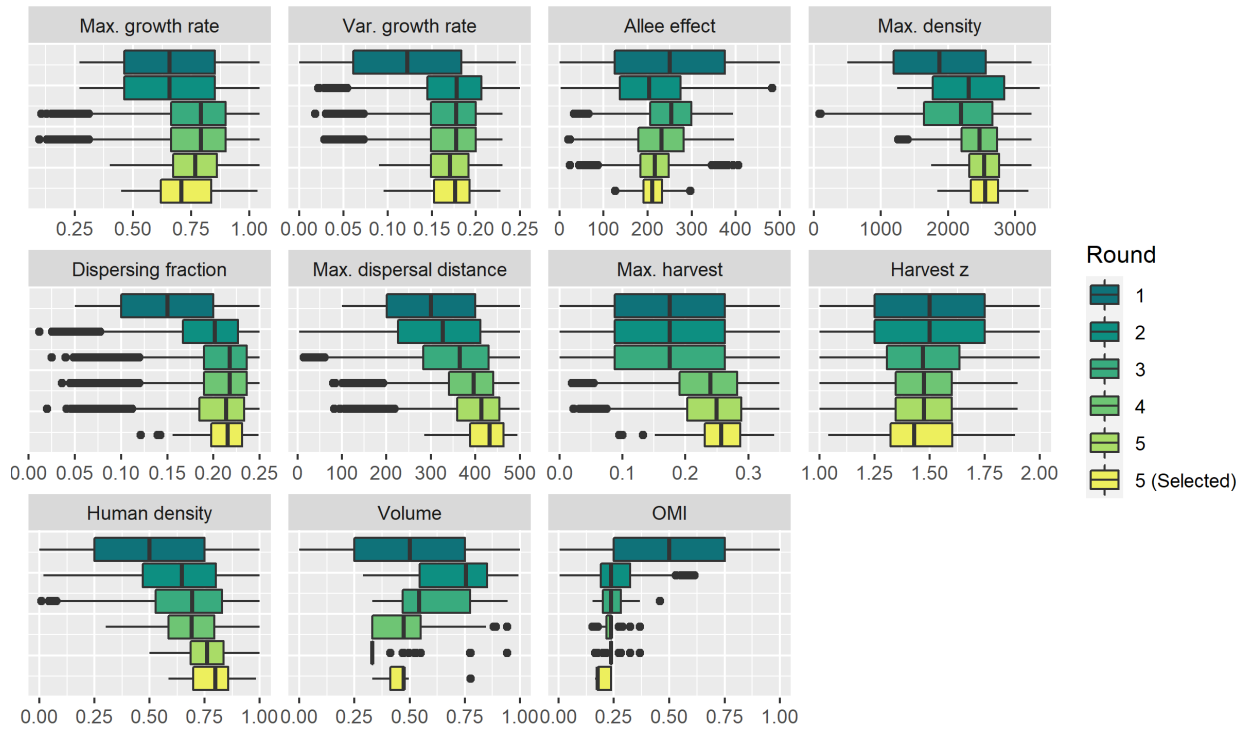
Figure S4: Convergence of informed priors. Boxplots show priors for consecutive rounds of pattern-oriented modelling (POM), as well as the final set of posteriors used in the final optimised model. The first round of POM was based on 50,000 simulations and uniform priors, while subsequent rounds of 10,000 simulations were based on informed priors that came from the posteriors selected by ABC in the previous round of POM. In each round of simulations, we selected the best 100 models.
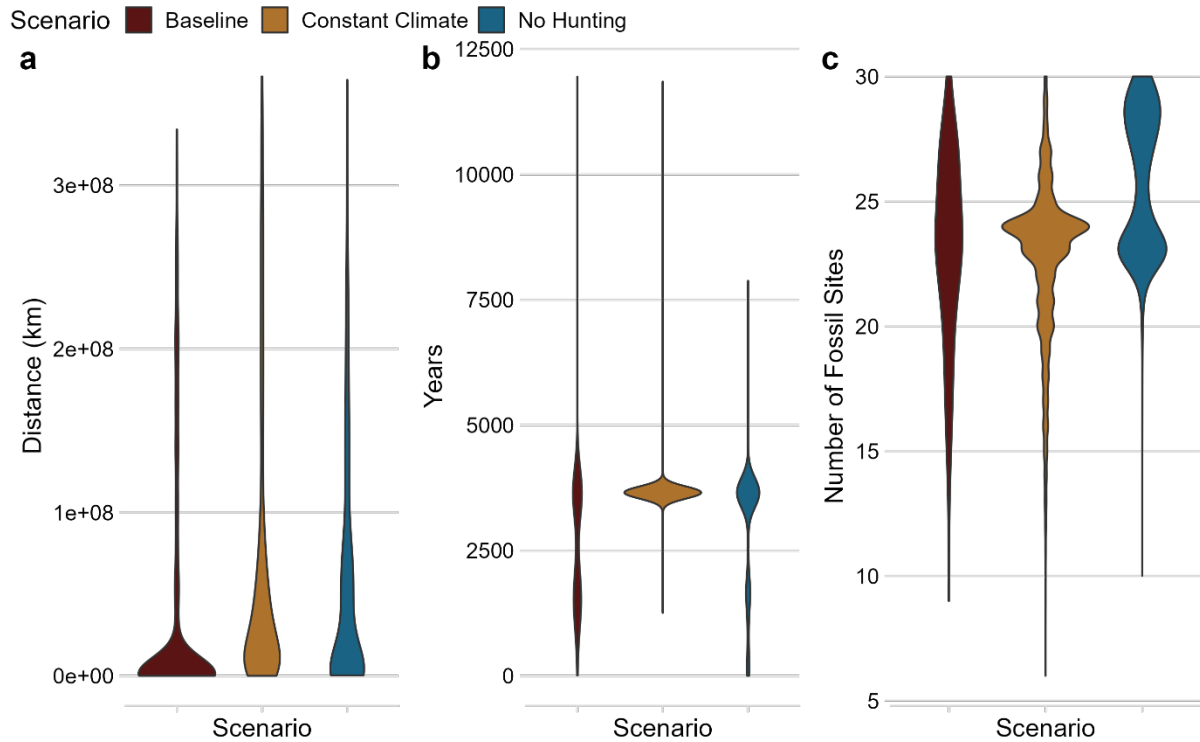
Figure S5: Comparison of reconstructions of validation targets for the baseline and two counterfactual models. Validation targets are (a) Extinction location: distance in km between simulated extinction location and the location based on the youngest fossil; (b) Extinction time: years between simulated and inferred time of extinction based on the fossil record; and (c) Fossil-based occurrence: number of fossil sites out of 31 where spatiotemporal occurrence is simulated. Density of simulations at different distances from validation targets are shown, with outliers (> 90% quantile of target distances) removed. Different colours show the optimised *baseline* model and two competing counterfactual scenarios: climate change but no human harvesting of bison (*no hunting*); and (b) no climate change from 21 kyr BP but harvesting of bison before and after that time (*constant climate*).

CHAPTER IV: CAUSES OF RANGE COLLAPSE AND EXTINCTION IN THE WILD OF EUROPEAN BISON

Statement of Authorship

Title of Paper	Causes of range collapse and extinction in the wild of European bison
Publication Status	Unpublished and Unsubmitted work written in manuscript style
Publication Details	Journal: Authors: Julia Pilowsky, Stuart C. Brown, Bastien Llamas, Rafał Kowalczyk, Emilia Hofman-Kamińska, Carsten Rahbek, Damien Fordham

Principal Author

Name of Principal Author (Candidate)	Julia Pilowsky
Contribution to the Paper	The candidate conceptualized the study, collected the data, developed the models, led the analysis and writing of the paper, with contributions from co-authors.
Overall percentage (%)	80%
Certification:	This paper reports on original research I conducted during the period of my Higher Degree by Research candidature and is not subject to any obligations or contractual agreements with a third party that would constrain its inclusion in this thesis. I am the primary author of this paper.

Signature		Date	1 Dec 2022

Co-Author Contributions

By signing the Statement of Authorship, each author certifies that:

i.   the candidate's stated contribution to the publication is accurate (as detailed above);

ii.   permission is granted for the candidate in include the publication in the thesis; and

iii.   the sum of all co-author contributions is equal to 100% less the candidate's stated contribution.

Name of Co-Author	Bastien Llamas		
Contribution to the Paper	Contributed expertise on ancient genetic structure and dynamics.		
Signature		Date	05 Dec 2022

Name of Co-Author	Stuart C. Brown		
Contribution to the Paper	Provided statistical guidance and support.		
Signature		Date	5 Dec 2022

Name of Co-Author	Emilia Hofman-Kamińska

Contribution to the Paper	Contributed fossil data on the European bison and expertise working with the species.		
Signature		Date	5/12/2022

Name of Co-Author	Rafał Kowalczyk		
Contribution to the Paper	Contributed his expertise on the European bison and long-term demographic data on the species.		
Signature		Date	5/12/2022

Name of Co-Author	Carsten Rahbek		
Contribution to the Paper	Helped conceptualise the study and interpret results in the broader context of the field.		
Signature		Date	5 Dec 2022

Name of Co-Author	Damien Fordham		
Contribution to the Paper	Helped conceptualise the study and provided modelling, analysis and writing support.		

Signature		Date	5/12/2022

Title Page

Causes of range collapse and extinction in the wild of European bison

Authors

Julia A. Pilowsky*[1,2], Stuart C. Brown[1,3], Bastien Llamas[1,4,5], Rafał Kowalczyk[6], Emilia Hofman-Kamińska[6], Carsten Rahbek[2,7,8,9], Damien A. Fordham[1,2,9]

Affiliations

[1]The Environment Institute and School of Biological Sciences, University of Adelaide, South Australia 5005, Australia.

[2]Center for Macroecology, Evolution and Climate, Globe Institute, University of Copenhagen, Copenhagen Ø 2100, Denmark.

[3]Section for Evolutionary Genomics, Globe Institute, University of Copenhagen, Copenhagen K 1350, Denmark.

[4]Indigenous Genomics Research Group, Telethon Kids Institute, Adelaide, SA 5001, Australia.

[5]National Centre for Indigenous Genomics, Australian National University, Canberra, ACT 2601, Australia.

[6]Mammal Research Institute, Polish Academy of Sciences, Białowieża, Poland.

[7]Danish Institute for Advanced Study, University of Southern Denmark, Odense, Denmark.

[8]Institute of Ecology, Peking University, Beijing, China.

[9]Center for Mountain Biodiversity, Globe Institute, University of Copenhagen, Copenhagen Ø, Denmark.

Abstract

European bison (*Bison bonasus*) were widespread throughout Eurasia during the late Pleistocene. However, the contributions of environmental change and humans on their near extinction have never been resolved. We reconstructed the contraction and population decline of the European bison at high spatiotemporal resolution using process-explicit models, fossils, and ancient DNA. We reveal important ecological and demographic attributes of European bison, showing that while a combination of climatic warming and human pressures drove population declines and regional extinctions of European bison, these drivers varied spatiotemporally. The population size of European bison declined abruptly at the termination of the Pleistocene in response to rapid warming, hunting by humans and their interaction. Human activities prevented populations of European bison from rebounding in the Holocene, despite improved environmental conditions. During the Holocene, hunting caused range loss in the north and east of its distribution, while land use change was responsible for losses in the west and south. From 1500 CE, advances in hunting technologies, resulting in a 30% increase in offtake, explain population estimates in 1870. While our findings show that humans were an important driver of the extinction of the European bison in the wild, vast areas of its range vanished during the Pleistocene-Holocene transition because of deglacial warming. These areas have been climatically unsuitable for millennia and should not be considered in translocation and reintroduction efforts.

Keywords

Extinction dynamics, European bison, mechanistic model, spatially explicit population model, climate change, metapopulation, megafauna, range dynamics, conservation biogeography

Introduction

The European bison (*Bison bonasus*) is a large grazer that was widely distributed in Eurasia during the Pleistocene (Soubrier et al., 2016), where it was hunted for food and skins (Pucek, Belousova, Krasinska, Krasinski, & Olech, 2004). Following the late Pleistocene, the range of European bison collapsed (Pucek et al., 2004), with the species going extinct in the wild in 1927 (Krasińska & Krasiński, 2013). Since its near extinction, enormous effort and resources have been directed toward restoring healthy wild populations of European bison (Krasińska & Krasiński, 2013). These conservation measures have been incredibly effective, resulting in a progressive downgrading of the threat status of European bison, from extinct in the wild to near threatened in a 93 year period (Plumb, Kowalczyk, & Hernandez-Blanco, 2020). However, as European bison increase in number and size (Plumb et al., 2020), their long-term persistence relies on knowing how and why it nearly went extinct in the first place. This is because there is much speculation as to whether the pathway to near extinction for the European bison was a recent and abrupt event, or a long and drawn-out process due to past climatic change, human activities and their interaction (Caughley, 1994; Kerley, Cromsigt, & Kowalczyk, 2020).

It has been suggested that the cause of the European bison's near extinction was habitat loss due to deforestation. This is because the European bison is considered a forest specialist (Pucek et al., 2004). However, this idea has been criticised because of its reliance on a relatively short temporal perspective, focusing on evidence from the Holocene, when Europe was already mostly forested (Kerley et al., 2020). A competing hypothesis is that the European bison are primarily grazers, adapted to mosaic rather than strictly forest habitats. This is supported by stable isotope data from modern and ancient European bison bone collagen, which shows a shift in diet from grazing to browsing in the early to late Holocene (Bocherens, Hofman-Kamińska, Drucker, Schmölcke, & Kowalczyk, 2015; Hofman-Kamińska et al., 2019). Accordingly, the species became trapped in suboptimal forest habitat as Eurasia emerged from the last ice age, causing a northward contraction of steppe vegetation and its replacement with forest (Zimov et al., 1995). Human hunting in open areas during the Holocene is theorised to have driven European bison into forested habitats (Kerley, Kowalczyk, & Cromsigt, 2012). Another view is that humans, not climate, were the

primary cause of the range collapse and population decline of the European bison (Faurby & Svenning, 2015; Sales et al., 2022). What is clear is that the contributions of environmental change and humans on the near extinction of European bison have never been resolved.

Currently, there are approximately 2,750 free-ranging European bison in the European Union (Kajetan Perzanowski, Klich, & Olech, 2022). Efforts to re-establish and conserve the species in the wild are far-reaching. This is because the European bison is an ecosystem engineer with important roles in maintaining landscapes and facilitating biodiversity (Cromsigt, Kemp, Rodriguez, & Kivit, 2018). By stripping bark from trees, the European bison can restore grasslands and prevent forest encroachment (Bakker et al., 2016; Macias-Fauria, Jepson, Zimov, & Malhi, 2020). However, the rewilding of landscapes with European bison has been done without a rigorously informed and coordinated strategy based on a strong understanding of habitats and regions where European bison once thrived (Kerley et al., 2020; Kajetan Perzanowski et al., 2022). This has meant that European bison have been released at sites as disparate as the coastal dunes of the Netherlands (Cromsigt et al., 2018) and the mountains of the French Alps (Ramos, Petit, Longour, Pasquaretta, & Sueur, 2016), with mixed success (Plumb et al., 2020). Continued efforts to reintroduce the European bison to prevent its extinction and restore grasslands will benefit from a more thorough understanding of its past range dynamics and the causes for range collapse and population decline.

While correlative approaches, such as ecological niche models (ENMs), have provided reasonable first approximations of the range of the European bison in the Holocene (Kuemmerle, Hickler, Olofsson, Schurgers, & Radeloff, 2012), their range in the Pleistocene, when the steppe biome was widespread, is less clear. Furthermore, these same approaches have been unable to directly disentangle the relative roles of climatic change, human hunting, and deforestation on the decline and near extinction of the European bison. Recent developments in process-explicit macroecological modelling are revealing how effects of human hunting and climate change on large mammal decline can vary over space and time (Canteri et al., 2022; Fordham et al., 2022). This is made possible because these approaches simulate species range and extinction dynamics as

explicit functions of global change, ecological processes and their interactions (Pilowsky, Colwell, Rahbek, et al., 2022b).

A powerful technique for modelling species range dynamics with a high degree of biological realism is spatially explicit population models (SEPMs) (B. J. Anderson et al., 2009) combined with pattern-oriented validation (Grimm et al., 2005). SEPMs are process-explicit macroecological models of population networks that can be used to model species range dynamics over thousands of years, reconstructing the spatial dynamics of extinction (Fordham et al., 2022) and identifying suitable areas for reintroduction (Canteri et al., 2022). Outputs from these models, such as minimum population densities required for persistence, can be used to directly inform conservation policy (Tomlinson et al., 2022). Pattern-oriented validation is an optimisation technique for reducing uncertainty in model parameters based on the assumption that observed ecological patterns are fingerprints of the underlying processes that produced them (Gallagher et al., 2021). Empirical patterns are used as validation targets, and model outputs are evaluated against these targets to determine which combinations of parameter values produce the most accurate results (Grimm et al., 2005).

Here we investigate the causes of the near extinction of the European bison across space and time, using 55,000 SEPMs to reconstruct the range and population dynamics of the European bison at high spatiotemporal resolution from 21,000 years before present (21 ka BP) to 0.45 ka BP (or 1500 CE), establishing the timing and magnitude of the range and population collapse of European bison and their most likely causes. Using models validated on inferences of demographic change from fossils, historical accounts, and ancient DNA, we identify areas where the European bison would be distributed today if hunting and land use change had not occurred. In doing so, we identify suitable areas for reintroduction.

Materials and Methods

We built process-explicit macroecological models of European bison that simulate interactions between metapopulation dynamics, environmental variability, human hunting, and land use change. We used these models to continuously reconstruct 21,000 years of range dynamics across

Eurasia. We validated model projections of spatiotemporal abundance and refined model parameters using pattern-oriented modelling (POM) methods (Grimm et al., 2005) and inferences of demographic change from the historical record and 120 radiocarbon-dated fossils. The approach is described in detail in the Supplementary Methods, and the fossil record (Pilowsky, Brown, Llamas, et al., 2022b) and R code for running the models (Pilowsky, Brown, & Fordham, 2022) are in public repositories.

1. Ecological niche

To reconstruct the ecological niche of the European bison, we intersected radiocarbon (^{14}C) dated and georeferenced fossils with simulated climate and land use projections. To do this, we first compiled a database of ^{14}C dated European bison fossils using published and unpublished sources (Pilowsky, Brown, Llamas, et al., 2022b). Dated fossils without geolocations were geocoded manually using the name of the fossil site and OpenStreetMap and Google Earth. The quality and reliability of all radiocarbon dates was assessed based on dating method, stratigraphy, association and material dated (Barnosky & Lindsey, 2010). Only fossils with an age quality score >10 were used (Pilowsky, Haythorne, Brown, et al., 2022c). This resulted in 120 high-quality ^{14}C dates. The ^{14}C ages of these fossils were calibrated using the OxCal tool (Ramsey, 2017) and the IntCal13 curve (Reimer et al., 2013).

Occurrence records from fossils were intersected with monthly palaeoclimate data from the HadCM3 general circulation model (GCM). The HadCM3 GCM has a native resolution of 3.75° × 2.75° that incorporates monthly, interannual and millennial scale variability in climate in the ocean and atmosphere (Valdes et al., 2017). It has previously been shown to accurately represent land and sea surface temperatures, precipitation and ocean circulation (Valdes et al., 2017). The data have been bilinearly downscaled to 0.5° x 0.5° spatial resolution and bias-corrected to current-day conditions (E. Armstrong et al., 2019).

We extracted monthly data for annual precipitation, winter temperature and spring and summer evapotranspiration (Figure S1). These three climatic variables have been used previously to model the range dynamics of large vertebrates in Eurasia, including during the Pleistocene-Holocene

transition (Canteri et al., 2022; Lorenzen et al., 2011; Pilowsky, Haythorne, Brown, et al., 2022c). European bison are strongly limited by forage availability in winter and the desiccation of grass in summer (Krasińska & Krasiński, 2013), and these three variables capture climatic controls on these food sources.

We temporally upscaled the climate data to a 10-year average (the generation length of the European bison; see below) using a 30-year sliding window (Fordham et al., 2022). We projected the climate data to an Albers Equal Area projection centred on a reference latitude of 57.5°N and a reference longitude of 25°E with a resolution of 86.6 by 75.6 km.

To determine habitat and resource availability for European bison, we reconstructed the biomass of boreal trees, boreal shrubs, and temperate trees and shrubs using output from a dynamic vegetation model (LPJ-GUESS) coupled to HadCM3 palaeoclimate data (Allen et al., 2020). These were the plant functional types present at fossil sites when the fossil was deposited. We adjusted the spatiotemporal estimates of biomass of these vegetation types according to land use transformation data from the Hyde 3.2 dataset (Klein Goldewijk, Beusen, Doelman, & Stehfest, 2017), providing us with a measure of human-driven vegetation change specific to European bison. To do this we converted the land use change data to the same projection and spatial scale as the LPJ-GUESS data—a temporal resolution of 1000 years and a 0.5° x 0.5° grid-cell resolution—using linear interpolation. For each grid cell, we calculated the proportion of that cell that had been converted to unusable land use types for bison (urban, pastoral, and agricultural.) We multiplied the combined plant biomass in the grid cell by the proportion of land that had been converted to unusable types to produce a measure of land use adjusted biomass. We then converted adjusted biomass to the same Lambert Azimuthal Equal Area projection as the climate data and temporally downscaled it to a decadal timestep using linear interpolation. See Supplementary Methods for details.

To model the ecological preferences of European bison through space and time, we built a 4-dimensional multi-temporal ENM (Nogués-Bravo, 2009). This allowed us to generate a biologically relevant representation of the climatic and environmental conditions over which the European bison occurred at fossil sites. To do this we paired fossil occurrences with the three

climate variables and adjusted biomass by intersecting these climate and environmental data in a spatiotemporal bin: the spatial location of the fossil, the timing of its presence at that site (calibrated ^{14}C date) and its associated uncertainty (±2 SD) (Blaauw, 2010). We removed any duplicate data created by two fossil occurrences falling within identical or overlapping spatiotemporal bins (Fordham et al., 2022). We used this dataset to create a gaussian hypervolume of ecological suitability, a technique for niche estimation that does not require absence data (Blonder & Harris, 2019). We tuned the kernel density estimation bandwidth by optimising the mean square error using cross-validation (Blonder et al., 2018).

The resulting hypervolume, which approximates the fundamental niche of the European bison (Nogués-Bravo, 2009), was exhaustively subsampled to generate thousands of potential realised niches (Fordham et al., 2022). To do this, we subsampled the full multi-temporal estimate of the ecological niche using Outlying Mean Index (OMI) analysis (Dolédec et al., 2000) and plausible bounds for climatic specialisation and niche volume (Fordham et al., 2022). For each niche subsample (n = 549) we generated projections of habitat suitability into geographic space from 21 ka BP to 1850 CE, creating suitability maps. We scaled the suitability scores of each projection between zero and one based on the 95th percentile of habitat suitability from all projections (Fordham et al., 2022). See Supplementary Methods for more details.

2. Human density

The population growth and expansion of Palaeolithic humans following the last glacial maximum (LGM, a period from 26.5 to 19 ka BP (P. U. Clark et al., 2009)) was modelled using a process-explicit climate-informed spatial genetic model (CISGeM) that accurately reconstructs global genetic patterns and arrival times of anatomically modern humans (Pilowsky, Manica, Brown, et al., 2022e). This model has previously been used to disentangle the impact of humans on megafauna over palaeo timescales (Canteri et al., 2022; Pilowsky, Haythorne, Brown, et al., 2022c). CISGeM simulates effective population size (N_e) using a cellular demographic model in which local N_e is a function of sea level, net primary productivity, and local demography (Eriksson et al., 2012). We ran CISGeM from 120 ka BP to present using climate data from the HadCM3 GCM (Valdes et al., 2017). To account for parameter uncertainty in projections of N_e, we used published

upper and lower confidence bounds for CISGeM parameters (Eriksson et al., 2012) to generate 4,950 equally plausible unique models of human population growth and migration. We did this using Latin hypercube sampling (Stein, 1987).

We calculated the mean and standard deviation for population size in each grid cell at each 25-year timestep from 21 ka BP, then reprojected the values to the same Lambert Azimuthal Equal Area projection we used for climate and suitability. N_e values were scaled between zero and one using the 95th percentile as an upper threshold (Canteri et al., 2022). We linearly interpolated the outputs from a 25-year to a 10-year timestep to match the generational length of the bison. We then generated plausible reconstructions of human abundance by sampling within ± 1 SD of N_e from a log-normal distribution. The centre of the sampling window within ± 1 SD of mean N_e was a variable model parameter in our climate-human-European bison process-explicit model.

3. Process-explicit model

We used spatiotemporal estimates of habitat suitability and human abundance (from our ENMs and CISGeM, respectively) as inputs to a SEPM that simulated landscape-level population processes, including metapopulation and dispersal dynamics (Fordham et al., 2022; Pilowsky, Haythorne, Brown, et al., 2022c). Each grid cell was modelled with a scalar-type stochastic model that simulates the finite rate of population increase "R", its variance and the population carrying capacity (Dunham et al., 2006). The approach has been used to skilfully reconstruct inferences of past range dynamics of large-bodied mammals (Canteri et al., 2022), including a closely related species of bison (*Bison priscus*) (Pilowsky, Haythorne, Brown, et al., 2022c). The SEPM, which had 11 variable parameters (Table S1), was run at generational time steps (10 years; see below) from 21 ka BP to 100 BP (1850 CE).

We estimated demographic rates for the European bison using current and historic field data, and a study of the closely related steppe bison (Pilowsky, Haythorne, Brown, et al., 2022c). We estimated maximum annual growth rate and its variance using time series data (see Supplementary Methods for details), scaling these annual growth rates for European bison to a 10-year generation length (calculated as the difference between reproductive life span and age at first birth (Pacifici et al.,

2013)). Population growth was modelled with a Ricker logistic density dependence function (Ricker, 1954), with the carrying capacity dependent on the habitat suitability in a given grid cell (Pilowsky, Haythorne, Brown, et al., 2022c). At a habitat suitability of 1, the carrying capacity was equal to the maximum density (Table S1), reducing with lower habitat suitability. A negative Allee effect was simulated using an abundance threshold below which populations became locally extinct (Fordham et al., 2022).

We simulated natal dispersal based on European bison in Poland (Krasińska & Krasiński, 2013). Between 5 and 25% of the population were allowed to disperse per generation, with a maximum dispersal distance of 0 – 300 km (Table S1). A dispersal friction landscape (Adriaensen et al., 2003) based on ice sheet reconstructions (Peltier, 2004) and land use change (see section 1c above) was used to ensure that bison only dispersed through ice-free grid cells, and that their dispersal was hindered in urban, agricultural, or pastoral environments. Harvesting was modelled as a non-linear function of prey density, human density, hunting rate and prey availability (Canteri et al., 2022; Pilowsky, Haythorne, Brown, et al., 2022c). All demographic parameters are described in more detail in the Supplementary Methods.

Once we had established biologically plausible intervals for demographic processes (population growth rate, dispersal, Allee effect), ecological requirements (niche volume and climatic specialisation), and human harvesting (human abundance and hunting function), we sampled the parameter space of these intervals using Latin hypercube sampling (Stein, 1987). All sampling was done using uniform distributions. This resulted in 25,000 model parameterisations, each with a distinct set of values for demography, environmental preferences and exploitation by humans. Each model was run for a single replicate and validated using POM techniques (Fordham et al., 2022).

4. Model validation

We used POM to evaluate the accuracy of model simulations and optimise parameter distributions (Grimm et al., 2005). Specifically, we used Approximate Bayesian Computation (ABC) to evaluate model projections against a multivariate target (Csilléry et al., 2010) consisting of spatiotemporal

occurrence, persistence in the Caucasus and number of persisting populations in 1850 CE. Simulations of spatiotemporal abundance were evaluated using an occurrence target consisting of 55 different fossil sites with ^{14}C dates and two sites with historical occurrence records. A simulation was considered to have successfully reconstructed occurrence if it projected occurrence in the grid cell with the fossil site (and/or its eight nearest neighbors) within ±2 × the error (SD) of the calibrated date. For the two historical records from the 19th century, there was no temporal band of uncertainty. To assess the capacity of models to simulate persistence in the Caucasus, we calculated the time of extirpation in the Caucasus Mountain region and then applied an annual penalty for each year that extirpation occurred before 1850 CE. The historical record shows that the European bison had collapsed to two refugia by 1850 CE: Białowieża Forest and the Caucasus (Heptner, Nasimovich, & Bannikov, 1961; Krasińska & Krasiński, 2013). We compared the number of simulated populations extant at 1850 CE against this validation target.

POM was done first on 25,000 simulations. We chose the top 0.25% of models via the rejection algorithm in the abc package (Csillery et al., 2015). We then ran three further rounds of POM (each with 10,000 simulations) using informed prior distributions based on these top models (Pilowsky, Haythorne, Brown, et al., 2022c). We ceased POM after these three additional rounds, because Bayes factors indicated that the posterior distributions had converged.

We did posterior predictive checks on the best 25 (0.25%) of models from the final round of POM. To do this, we generated 1,000 simulations based on the posterior distributions of parameters in the best models and did a goodness-of-fit test. We used the gfit function from the abc package, which tests goodness of fit by comparing how the observed metrics fit in the posterior distributions against their fit in distributions of pseudo-observed data generated from the prior distributions (Lemaire, Jay, Lee, Csilléry, & Blum, 2016).

We did two additional independent tests of SEPMs using the 1000 simulations for posterior predictive checks. Inferences of change in population size (based on effective population size) were used to assess the capacity of the best SEPMs to reconstruct relative change in total population size (Canteri et al., 2022). Methods and data used to calculate effective population size are described in the Supplementary Methods. We also tested whether bison were extant in regions with historical

records not used in POM. These historical records were all within the study region during the time period 1000 to 1500 CE (Heptner et al., 1961). To do this, we checked for bison occupancy at the grid cell location of the historical record and its eight nearest neighbours at the time of the historical record. We then assessed how closely the SEPM can reconstruct historical occurrence records between 1000 CE and 1500 CE using a goodness-of-fit test (see above).

5. Statistical analysis

We used generalised additive models (GAMs) implemented in the mgcv R package (Wood, 2022) to investigate the drivers of bison abundance in the Pleistocene (21 – 11.7 ka BP), early-to-mid Holocene (11.7 – 4.25 ka BP) and Late Holocene (4.25 – 0.45 ka BP). For the best SEPMs we extracted total bison abundance at generational timesteps. We also calculated average annual temperature, human abundance, and deforestation from occupied grid cells. Abundances and the three covariates were then aggregated to 100-year time bins to remove the effect of short-term decadal variation.

We optimised our GAMs to evaluate the effects of the three predictors on bison abundance in each time period. The main effects and any interactions were modelled as penalised thin-plate regression splines implemented for each time period. Following Marra & Wood (Marra & Wood, 2011) models were built using a double penalty approach whereby coefficient estimates could be reduced to zero for non-informative covariates. All GAMs included model ID as a random effect, with models optimised by maximum likelihood. Model selection was based on a chi-square test performed on two times the difference in the minimised smoothing parameter (i.e., maximum likelihood) between models with and without interactions. This approach is preferred over selection using AIC for models that include random effects (Wood, 2017).

6. Model scenarios

We ran counterfactual scenarios using our best SEPMs (available in an online repository (Pilowsky, Brown, Llamas, et al., 2022a)) to disentangle the roles of climate change, human hunting and land use change in the range collapse of the European bison. Counterfactual scenarios provide opportunities to explore the outcome of alternatives to what historically occurred in an ecological

system (Pilowsky, Haythorne, Brown, et al., 2022c). We simulated three counterfactual scenarios: *no hunting*, in which the human hunting rate was set to zero throughout the simulations; *no land use change*, in which biomass of temperate and boreal trees and shrubs was not reduced by land use change; and *no human pressures*, which combined both of the former counterfactuals. Thus, in the *no hunting* scenario, the only drivers of bison population dynamics were climate and land use change, in the *no land use change* scenario, the only drivers of bison population dynamics were climate and hunting, and in the *no human pressures* scenario, the only driver of bison population dynamics was climate.

In addition to counterfactual scenarios, we also explored scenarios of increased hunting from 1500 to 1870 CE. Based on historical records and the establishment of royal hunting reserves (Heptner et al., 1961), hunting pressure on European bison increased greatly after 1500 CE, due to technological advancements in hunting and cultural shifts in land use (Benecke, 2005). To address this, we ran scenarios of increased hunting from 1500 CE with maximum harvest increased at 10% intervals from 10 to 100% of pre-1500 CE maximum hunting rate. We validated the final abundance in 1870 against a historical estimate of 3,560 European bison. It is thought that in 1870 there were 2000 bison in the Caucasus (Heptner et al., 1961) and 1,560 bison in Białowieża Forest, for a total of 3,560 European bison (Krasińska & Krasiński, 2013).

Results

Using 55,000 SEPMs, pattern-oriented validation and extensive palaeoecological and historical data, we found that the range collapse of the European bison from 21 ka BP to 1500 CE was caused by a combination of environmental change, human hunting and land use change, with their effects on bison abundance differing across space and time.

Pattern-oriented validation

Our 'best' 25 SEPMs (0.0005% of all models) were able to reconcile inferences of spatiotemporal occurrence and persistence (Figure S2). This required successive rounds of simulation and pattern-oriented validation, with posterior parameter distributions stabilising after four iterations (all Bayes factors < 1). Specifically, these models correctly reconstructed the timing and place of occurrence

at most fossil sites. They were also able to predict persistence in the Caucasus (and Białowieża Forest) at the end of the simulation. However, projecting only two populations of European bison in 1850 CE was more difficult (Figure S2). Regardless, goodness of fit tests show reasonable resemblance between simulated and observed summary metrics (p > 0.05).

Independent validation tests, using inferences of change in total population size from ancient DNA and historical occupancy records, confirmed the robustness of the best SEPMs. We found strong overlap in the confidence intervals around the trend in simulated bison abundance and the trend in effective population size, with good concordance in the rate of decline in population size during the Pleistocene-Holocene transition (Figure S3). The best models were able to correctly reconstruct historical records of occupancy at up to 4 of the 5 historical sites of bison occurrence (mean = 3.3, SD = 1.11). The goodness-of-fit test indicated a reasonable resemblance between simulated and observed occurrence (p > 0.05).

Reconciling inferences of population persistence and extirpation based on palaeontological and historical evidence required specific constraints on habitat requirements and demography of bison (Figure S4). Comparisons of prior and posterior distributions revealed that the European bison is likely to have had a realised niche that is much smaller than its fundamental niche. This is based on the best models having small-to-medium niche volumes (58 – 72% of the full multi-temporal niche volume) and medium-to-high specialisation (based on outlying mean index). These comparisons also showed that a small Allee effect threshold (9 bison per 87 km × 76 km grid cell) and a low maximum dispersal distance (110 km) were needed to reconstruct the population dynamics of European bison over the late Pleistocene and Holocene. In each generation, ~5% of bison permanently dispersed, moving at least 76 km from their site of birth.

Population and range dynamics

The ensemble average total population size for European bison based on the best SEPMs showed that they were abundant at the LGM (Figure 1). Population numbers remained relatively stable, increasing slightly, during the onset of deglacial warming, falling sharply at 14.7 ka BP, in response to rapid warming and a corresponding reduction in bison carrying capacity at the Bølling-Allerød

warming event. Following 14.7 ka BP, the region-wide carrying capacity of European bison recovered, but abundance did not, probably because of harvesting by humans. Hunting increased at 14.7 ka BP as a result of higher human abundances, remaining high throughout the Holocene (Figure 1).

Reconstructions of spatiotemporal abundance of the European bison show that by the mid Holocene it had contracted its range to central and eastern Europe and the Caucasus, going extinct in southern Europe at ~11 ka BP, and extinct in Western Europe and Siberia at ~7 ka BP (Figure 2). During the early deglaciation (21-18 ka BP), European bison were distributed in disjunct metapopulations in Siberia, the Caucasus, southern Europe, and western Europe. From 18 ka BP, metapopulations in western and southern Europe started to slowly move eastward and northward, merging together some 6 ka later (Movie S1). By 12 ka BP, the only remaining European bison in Western Asia were in the refugium in the Caucasus. The Siberian metapopulation declined in size from 13 ka BP, going regionally extinct at 8 ka BP. By 1500 CE, the European bison was restricted to north-eastern Europe and a small refugium in the Caucasus, with abundances highest in the Caucasus and what is now Poland and Ukraine.

Drivers of decline

Analysis of our continuous reconstructions of population size of European bison from our best SEPMs using GAMs showed that the effects of humans and climate are likely to have varied temporally. The GAM of abundance regressed against mean annual temperature, human abundance, and deforestation as fixed effects for each time period, without interactions, and model as a random effect explained 89% of the variance in total population size (adjusted R^2 = 0.83). This was a significant improvement over the model with interactions between variables (ML = -123.13, df = 12, p < 0.001). Plots of partial effects show that European bison abundance was most strongly correlated with human abundance, with strong negative responses during the Pleistocene, early-to-mid Holocene and late Holocene (Figure 3). A strong positive effect of temperature and abundance was detected during the Pleistocene, with a weakly positive effect in the early-mid Holocene. Deforestation had a slight negative effect on bison abundance throughout the Holocene (Table S2).

Removing human activities from the best SEPMs and rerunning these models as counterfactual scenarios revealed the spatiotemporal footprint of humans on the local persistence of European bison (Figure 4). In the absence of hunting and land conversion by humans, European bison are likely to have persisted much longer in Scandinavia, the Balkans, and present-day Germany and southwestern Russia (Figure S5). We show that climatic change during the Pleistocene is the primary determinant of range contractions in Western Europe, Anatolia, and Siberia (Figure 4). During the Holocene, hunting caused range loss in the north and east of the species distribution, and land use change was responsible for losses in the west and south.

In the *no hunting* scenario, the range of the European bison in 1500 CE extended farther east into Russia, and the Caucasus refugium (where European bison persisted until its extinction in the wild) extended farther north (Figure 4). In the *no land use change* scenario, the range of the European bison extended farther west in continental Europe, and the Caucasus refugium extended farther west (Figure 3). In the *no human pressure* scenario, all of the range expansions from the other two counterfactual scenarios were observed. There were also areas in southern Denmark and France where the removal of both hunting and land use change allowed European bison to persist to 1500 CE.

Our best SEPMs overestimated the population size of European bison in 1870 CE (n = 3,560). However, we show that a 30% increase in maximum harvest rate after 1500 CE (in response to cultural and technological changes in hunting, including guns (Kirby & Watkins, 2015)) is enough to have depleted the population size of European bison to levels estimated in 1870 (Figure 5).

Discussion

Using spatially explicit models (SEPMs), extensive palaeontological and historical data, and pattern-oriented modelling methods, we were able to disentangle the effects of environmental change, human hunting, and land use change on European bison abundance in space and time. We show that the effects of natural and human drivers varied from the edge to the core of the European bison's range. Humans had the most pronounced impact in the centre of its range, contributing heavily to the population decline and range collapse of the European bison. By

identifying areas where the European bison would have persisted to 1500 CE in the absence of human pressures, we were able to pinpoint locations that are potentially climatically suitable for reintroduction of European bison today. We also reveal areas that have been climatically unsuitable for European bison for millennia and should be excluded from translocation and reintroduction efforts.

Our detailed reconstruction of the range dynamics of the European bison shows that its persistence was affected by biotic and abiotic stressors that varied spatiotemporally. We show that deglacial warming in the Pleistocene caused the European bison's range to contract toward its core, where human abundances in Eurasia were generally highest (Eriksson et al., 2012). Here, European bison were hunted for food and skins (Kitagawa et al., 2018). Reconciling inferences of demographic change from the extensive fossil record of European bison required SEPMs to include medium levels of hunting by humans (5 – 21% max. harvest rate), which aligns with isotopic analysis of human fossils of from Europe during the late Pleistocene that indicate that 10% of protein intake came from bovines (aurochs and European bison) (Wißing et al., 2019). Increasing geographic overlap between areas of high bison abundance and high human abundance eventually led to the demise of the European bison in the wild, both directly through overexploitation by hunting, and indirectly through land use change.

The abundance of European bison today is trending upward due to nearly 100 years of conservation intervention (Krasińska & Krasiński, 2013). However, the species still faces many threats and obstacles to long-term persistence (Plumb et al., 2020). Contemporary threats include land use change imposing barriers to dispersing bison, and poaching reducing population numbers (Kajetan Perzanowski et al., 2022; Plumb et al., 2020). As our modelling has shown, these threats are the same as those that put the European bison on a pathway to extinction many millennia ago. While the contemporary range of the European bison is broad, encompassing much of north-eastern Europe, this distribution is highly fragmented, with only 23% of populations having any connectivity to other populations (Plumb et al., 2020). Of the 47 free-living European bison populations, only eight are large enough to be self-sustaining, and all of these are dependent on supplemental feeding (Plumb et al., 2020).

The European bison is considered a priority species for conservation by the European Union (Council of the European Union, 1992), in part because of its role in restoring grassland habitat (Directorate-General for Environment (European Commission), 2021). An expansion of the species' range is needed. However, reintroductions of European bison have been opportunistic, often based on the interest of private landowners in tourism income (Root-Bernstein, Gooden, & Boyes, 2018) and the eagerness of governments for their ecosystem services (Brandtberg & Dabelsteen, 2013), despite a lack of evidence of habitat suitability or previous bison occupancy.

To successfully rewild Europe with large herbivores such as European bison, managers need information that will allow them to maximise the probability of reintroduction success, including population establishment (e.g., the minimum number of animals that need to be released), local and regional population persistence (e.g., habitat conditions that contribute to persistence and potential connectivity) and ecosystem functioning (e.g., how the species interacts with other species at the reintroduction site) (D. P. Armstrong & Seddon, 2008; Taylor et al., 2017). Without this information, the consequences of improper management decisions can be severe. For example, attempted reintroductions of European bison have failed due to human-bison conflict (e.g., in Crimea (Parnikoza & Kaluzhna, 2009) and western Russia (Sipko, 2009)), and slow-growing populations in unsuitable areas succumbing to inbreeding depression (e.g., in Siberia (Sipko, 2009)).

Our spatial reconstructions of European bison abundance in 1500 CE, along with our maps of where the species would have been found in 1500 CE in the absence of human pressures, provides new information to guide European bison reintroductions. Pattern-oriented modelling techniques, palaeontological data and historical records allowed us to establish the ecological requirements of European bison and to identify the most likely estimate of upper abundance. Ukraine emerges as an area of high projected abundance, and the bordering areas of western Russia also show bison occupancy in the absence of human hunting. Unfortunately, this region of Europe is an active conflict zone where over 50% of all free-living European bison are currently at risk (Kajetan Perzanowski et al., 2022). We show, however, that there are other regions that had medium densities of European bison until at least 1500 CE. These include the Baltic countries,

Poland, Slovakia, Romania, and the Caucasus mountain region. Considering that land use change is likely to have contributed to the extirpation of European bison in Germany, Czechia, Bulgaria and Serbia during the late Holocene, these areas could also provide suitable reintroduction sites after habitat restoration.

Our validated reconstructions of the range and population dynamics of the European bison provide new and important biogeographical insights. In addition to showing that the geographic range of the European bison began to implode in the late Pleistocene, we show that there was a metapopulation of European bison in Siberia, isolated from the metapopulation in Europe, that became extinct 7 ka BP. This result is consistent with research on European bison ancient DNA that has found a more cold-adapted clade of European bison that became extinct during the most recent deglaciation (Soubrier et al., 2016). Our model results suggest that this clade could have persisted into the Holocene in low abundances. We also show that in Europe at 21 ka BP there were two main subpopulations of European bison, one in Western Europe and one in Southern Europe, and these subpopulations fused together in Central Europe at the termination of the Pleistocene. This prediction could be directly tested using ancient DNA from Pleistocene fossils from the more warm-adapted clade of European bison, providing a higher-resolution understanding of genetic structure for European bison following the last ice age.

Our validated simulation models show that human pressures alone were not enough to cause the collapse of the range of the European bison. Our findings also rule out the hypothesis that habitat loss due to deforestation was the primary cause of the range collapse of the European bison, as we found the effect of deforestation on bison abundance was minor compared to mean annual temperature and human abundance. Our results do not rule out the hypothesis that European bison are grazers that were forced by human pressures into suboptimal forest habitat; however, our results cannot confirm the hypothesis either, as our data on palaeovegetation in Europe did not have a fine enough spatial resolution to pinpoint European bison preferences for open or closed habitat.

While our SEPM approach was able to reconstruct many key features of the range dynamics of the European bison over the last 21,000 years, the approach overestimated its population size in 1870

CE. This is likely to reflect a technological and cultural shift in bison hunting after 1500 CE (Kirby & Watkins, 2015), which we investigated further by simulating scenarios of increased hunting efficiency after this date. We show that a 30% increase in harvest efficiency after 1500 CE was enough to reconstruct this population size. Firearms began to be banned by European governments in 1500 CE in order to preserve game populations due to overhunting with this new type of weaponry (Nicholson, 2010). We found that reconstructing our validation targets required a short maximum dispersal distance. Dispersal in our models represents permanent relocations to new breeding territory, rather than the temporary movements of individuals. While research on European bison dispersal in Białowieza Forest has found that cow groups (equivalent to what was modelled here) disperse much shorter distances than individual males (Krasińska & Krasiński, 2013), further tests of the dispersal estimates that emerged from our model are needed.

By reconstructing past abundances and harvest rates, as well as mapping the distribution of the European bison in the absence of human pressures, we provide new insights into the dynamics of range collapse in the European bison, enabling future reintroductions and translocations to be guided by these biogeographic understandings. These biogeographical insights were made possible because our pattern-oriented modelling approach allowed us to validate the European bison's realised niche, as well as its occupancy and abundance. Similar approaches could be used to reconstruct the causes of population declines and range collapses of other large herbivores being reintroduced to Eurasia (Canteri et al., 2022), improving awareness of past threats and enhancing current conservation measures.
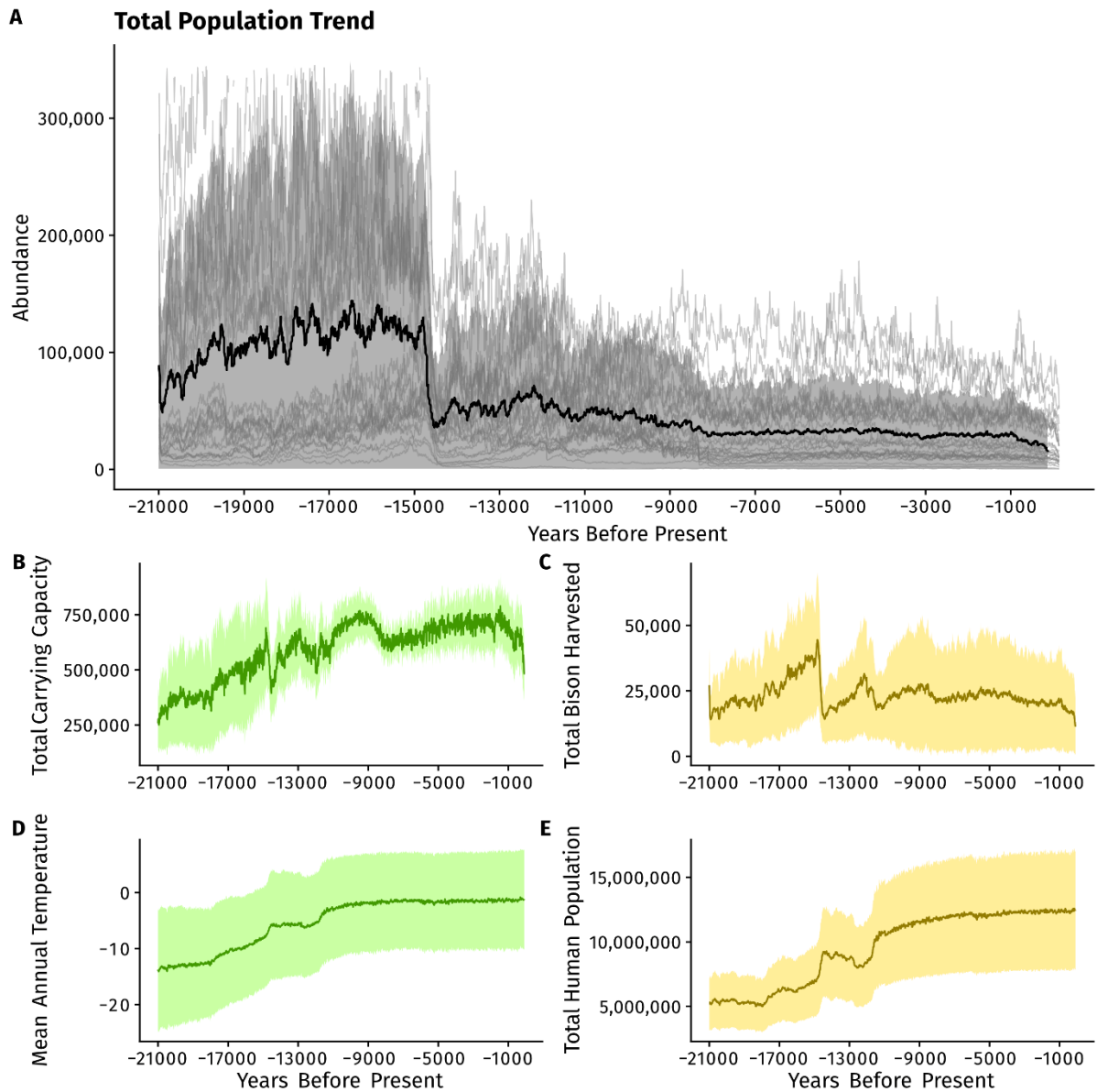
Acknowledgments

Figures

Figure 1: Bison abundance and its drivers. Total bison population size (A), carrying capacity (B) and harvested animals (C) projected from 21,000 BP to 450 BP (1500 CE). Mean annual temperature and total human population size for the study region (Figure 1) are shown in D and E, respectively. Shading shows +/- 1 SD. The population time series of the best 25 models are shown in light grey (A). Carrying capacity represents maximum potential bison population size in the absence of human impacts. Changes in other climate and environmental variables (including those used for the bison niche) are shown in Figure S1.
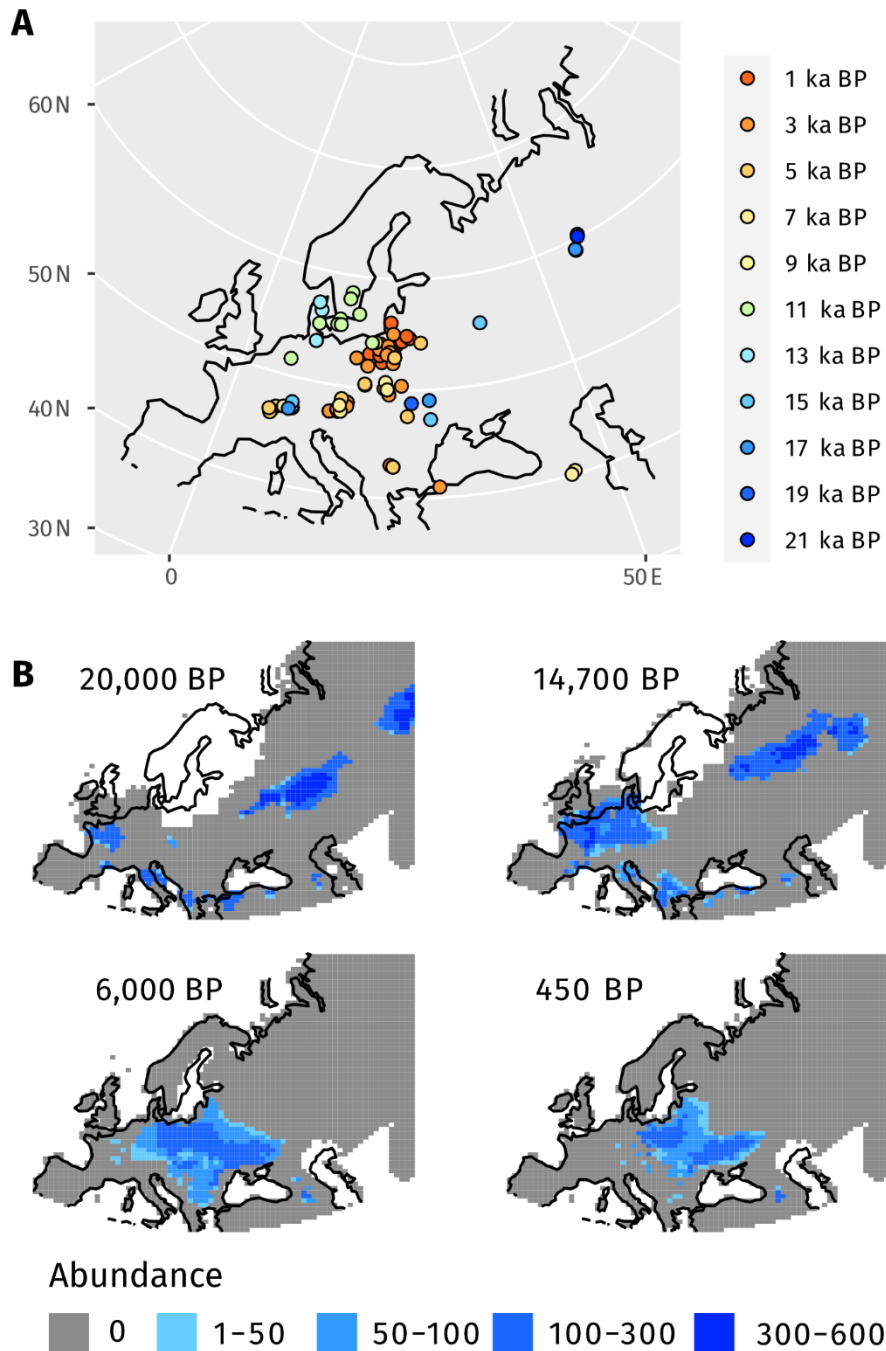
142

Figure 2: Range collapse of the European bison. Fossils and their radiocarbon dates for the European bison (A). Simulated bison abundance (B) for the end of the last glacial maximum stadial (20,000 BP), immediately prior to the Bølling-Allerød warming event (14,700 BP), the mid-Holocene (6,000 BP) and at the end of the simulation (450 BP or 1500 CE). Abundances are shown only for grid cells where at least 25% of the top models agreed that there was bison occupancy (see Figure S6 for abundance maps where cells with low model agreement are shown.)

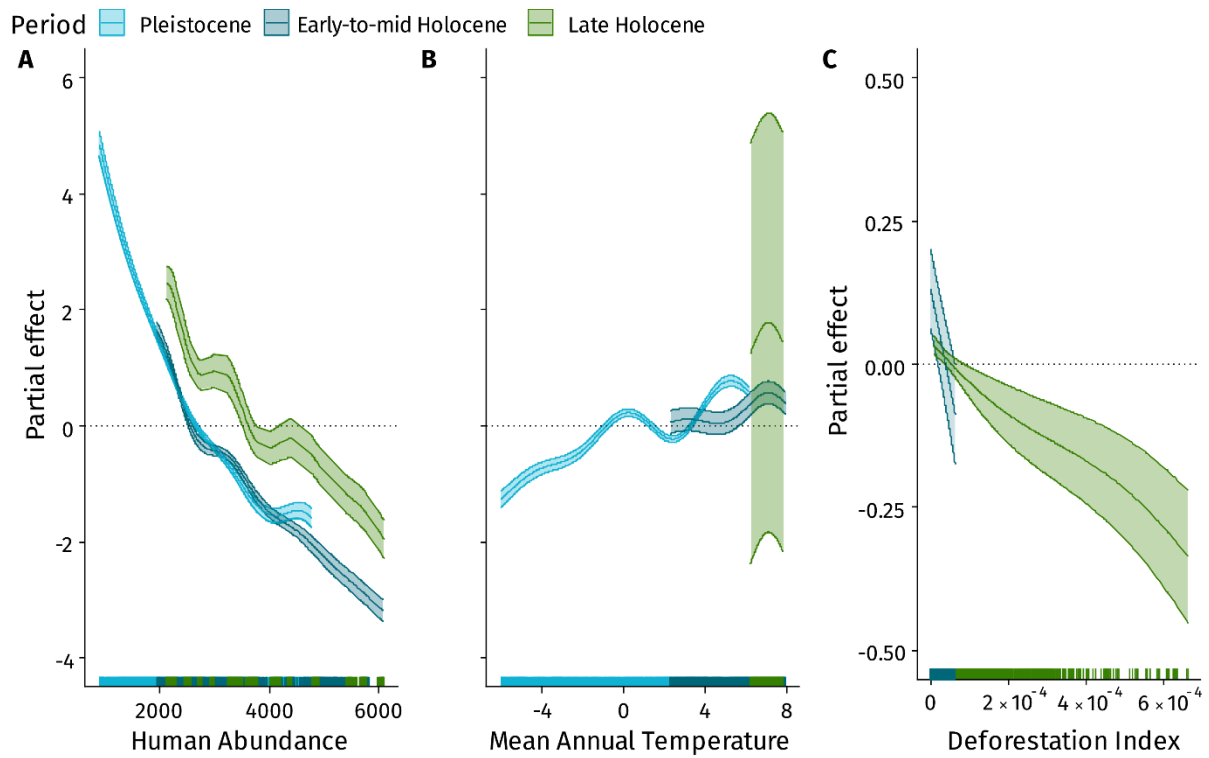**Figure 3: Predictors of population decline in European bison.** Partial effects plots for general additive models of drivers of bison abundance, including human abundance (A), mean annual temperature (B), and deforestation (C). Different colours show different time periods: Pleistocene (light blue), early-to-mid Holocene (dark blue), and late Holocene (green). Rug plots of sampling density are shown along the x-axis.
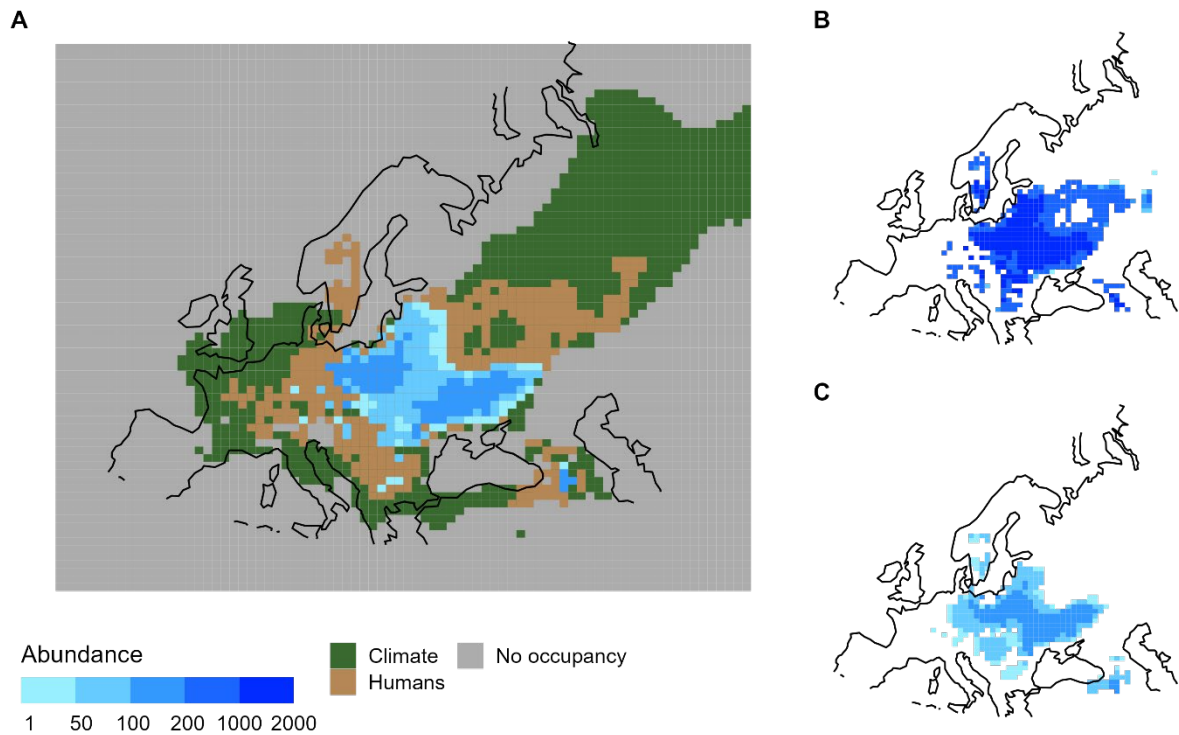
Figure 4: Drivers of range collapse for European bison. The effect of climate (green) and humans (brown) on the extirpation of European bison (Panel A). Population abundance for the projected extant range in 1500 CE is shown in blue. Maps of abundance of European bison without hunting (Panel B) and without land use change (Panel C). Abundances are shown only for grid cells where at least 25% of the models agreed that there was bison occupancy.
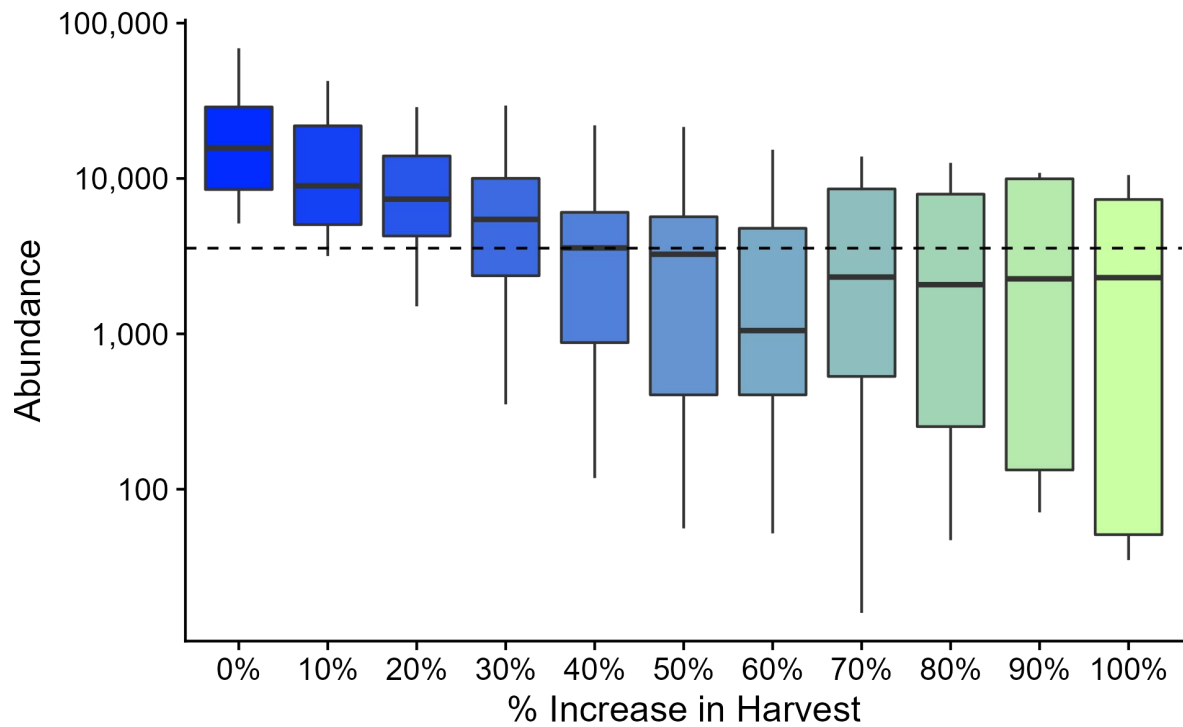
Figure 4: Harvest increase needed to simulate population size in 1870. Population size of European bison in 1870 in response to increased harvesting following 1500 CE. Dashed horizontal line shows estimated population size of European bison in 1870 (Heptner et al., 1961; Krasińska & Krasiński, 2013). Estimates are based on the output from individual runs of the best 0.25% of SEPMs.

Supplementary Material

1. Ecological niche

Land use-adjusted biomass

We used a global run of LPJ-GUESS coupled to HadCM3 palaeoclimate data (Allen et al., 2020), which had a native temporal resolution of 1000 years and a native spatial resolution of 0.5 × 0.5°. We converted the vegetation biomass data to an Albers equal area projection (resolution: 86.6 by 75.6 km) and temporally downscaled from a millennial to a decadal timestep by linear interpolation.

We determined which plant functional types co-occur with the European bison by intersecting the European bison fossil record with the LPJ-GUESS spatiotemporal simulations of vegetation types. Specifically, we matched each fossil in space and time to its corresponding plant functional types, using a window of +/- 2 SD around the radiocarbon date (Fordham et al., 2022). We assessed the biomass found within the spatiotemporal envelope of each European bison fossil and found that the four dominant plant functional types were boreal trees, boreal shrubs, temperate trees, and temperate shrubs. Based on this result, we generated spatiotemporal maps of plant biomass in European bison-suitable habitat using these plant functional types as a combined biomass raster.

We used the Hyde 3.2 dataset (Klein Goldewijk et al., 2017) to reconstruct land use through time at 10-year timesteps from 21 ka BP to present. Hyde 3.2 has a native spatial resolution of 5' × 5' and a native temporal resolution of 1000-year timesteps until 2000 BP, 100-year timesteps until 250 BP, and 10-year timesteps afterward. We identified the types of land use (urban, grazing, and agriculture) in Eurasia where European bison could not persist and binarised the land use data: zero = land use types where European bison cannot persist and 1 = land use types where they can persist. We transformed the spatial data for these land use types to a Lambert azimuthal equal area projection (resolution: 86.6 by 75.6 km), summed the hectares of transformed land across the types, and divided by the total area of the grid cell in hectares to obtain a proportion of each grid cell that had been transformed by human activity. We temporally downscaled the data to a decadal timestep by linear interpolation.

Because the estimates of plant biomass from LPJ-GUESS do not account for land use transformation, we added the land use transformation raster as a modifier to the combined biomass raster. We multiplied the biomass raster by the inverse of the land use raster, so that the biomass of trees and shrubs was reduced by the proportion of land that had been transformed to grazing, agricultural, or urban land. This produced our measure of land use-adjusted biomass.

Fundamental niche

We developed an ecological niche model (ENM) for the European bison based on three climate variables and one environmental variable. We used the hypervolume R package (Blonder & Harris,

2019) because it is suitable for presence-only data such as a fossil record. The climate variables were winter temperature, annual precipitation, and spring & summer evapotranspiration. These variables have been shown elsewhere to influence the range dynamics of the European bison (Kuemmerle et al., 2012) and closely related steppe bison (Pilowsky, Haythorne, Brown, et al., 2022c). Land use and vegetation cover are also important determinants of habitat suitability for the European bison (Bocherens et al., 2015; K. Perzanowski, Bleyhl, Olech, & Kuemmerle, 2020) which we characterised with a variable that combines vegetation and land use (see above.) In a preliminary analysis, we found that in +/- 2 SD spatiotemporal windows surrounding European bison fossil sites, there was higher vegetation cover and lower land use transformation than the mean for all of Eurasia in the same time windows.

We generated spatiotemporal suitability maps for the European bison in Eurasia from 21 kya to present using climate suitability hypervolumes (Blonder & Harris, 2019). First, we paired fossil occurrences with our three climate variables and one land use/habitat variable by sampling the data in a spatiotemporal bin around each fossil occurrence, the spatiotemporal bin being the spatial location of the fossil and its radiocarbon age ±2 SD around the calibrated radiocarbon date. We removed any duplicate data created by two fossil occurrences falling within identical or overlapping spatiotemporal bins (Fordham et al., 2022). We used this dataset to create a full Gaussian hypervolume, optimising for bandwidth that reduced the mean square error in cross-validation trials.

We validated the multi-temporal hypervolume using the present-day range of *B. bonasus* from the IUCN Red List as independent validation points against background probability from the hypervolume and found a continuous Boyce index of B = 0.62 and a weighted AUC of 0.65.

Realised niches

There is high uncertainty about the climatic niche of the European bison, given that its current range is largely an artefact of its recent reintroduction following its extinction in the wild. We account for the likelihood that the multi-temporal hypervolume overestimates the realised niche of the European bison by subsampling it into different volumes and marginalities (distance from the

centroid of the full hypervolume, measured by the outlying mean index). Following previous work on the closely related steppe bison (Pilowsky, Haythorne, Brown, et al., 2022c), we calculated niche samples using sampling windows of different widths, from 70% to 100% of the breadth of the full hypervolume. This results in many overlapping and some non-overlapping niches. We created a uniform distribution of volume and marginality for the hypervolumes and sampled evenly across the distribution, resulting in 783 realised niches once duplicates and edge cases with fewer than 20 data points were removed. After some preliminary modelling, we found that all simulations with a niche volume less than 2.7 resulted in extinction of all European bison in the first timestep, regardless of other model parameters, so we discarded all realised niches with a volume below this threshold, resulting in a set of 549 realised niches. All the hypervolumes were centred and scaled to the same scale as the full hypervolume.

We projected all of the hypervolumes back into dynamic spatiotemporal landscapes, creating maps of suitability scores in the equal-area projection detailed above. We tuned these projections over different functions of Gaussian decay from high-suitability zones to low-suitability zones, selecting the weighted function that produced a clear bimodal distribution of suitability, with one peak for less-suitable cells and another clearly differentiated peak for more-suitable cells. We scaled the suitability scores of each projection to a 0 – 1 interval based on the 95th percentile of habitat suitability from all projections.

2. Human density

The northward expansion of Palaeolithic humans during deglaciation was modelled using a process-explicit climate-informed spatial genetic model (CISGeM) that has been shown to accurately reconstruct the dispersal of humans after the LGM (Pilowsky, Manica, Brown, et al., 2022e). CISGeM simulates local effective population size (N_e) based on a cellular demographic model with carrying capacity modulated by net primary productivity (NPP). The cellular model is on a 100 km hexagonal grid, which allows for equidistant dispersal in all directions. The model has been validated using pattern-oriented procedures and shown to have the structure and parameterisation needed to reconstruct spatiotemporal genetic validation targets (Eriksson et al., 2012).

We parameterised the model using net primary productivity calculated from the HadCM3-based climate simulations generated by Eriksson et al. (2012) in the original CISGeM study, averaged at 30-year intervals on generational time steps for humans (25 years). More specifically, simulations of temperature and precipitation were converted to net primary productivity via the Miami vegetation model (Lieth, 1975). The relationship between carrying capacity and NPP, as well as demographic parameters (including colonisation rate, maximum growth rate, and NPP extinction threshold) were treated as variable parameters. We used 4,950 parameter combinations based on the posterior ranges of validated models (Eriksson et al., 2012).

We ran CISGeM from 120 ka BP to present to produce 4,950 continuous simulations of human migration out of Africa and growth and spread across the world. We converted estimates of N_e to a latitude-longitude grid, calculated the mean and variance of N_e for each grid cell at each time step (Fordham et al., 2022), and resampled the outputs to the 10-year timestep of the bison simulations. N_e was scaled between 0 and 1 using the 95th percentile as an upper threshold. We then generated plausible reconstructions of human abundance by sampling within ± 1 SD of N_e from a log-normal distribution. The centre of the sampling window within ± 1 SD of mean N_e was a dynamic model parameter systematically sampled through thousands of process-explicit simulations (Fordham et al., 2022).

3. Process-explicit model

The range dynamics of *Bison bonasus* were simulated at generational time steps from 21 ka BP to 100 BP using a scalar lattice-grid type spatially explicit population model configured in the R package paleopop v2.1.0 (Haythorne et al., 2021). Life-history traits from *B. bonasus* and its congener *B. bison* and posteriors from a previous process-explicit modelling study in the extinct congener *B. priscus* (Pilowsky, Haythorne, Brown, et al., 2022c) were used to set bounds for the priors of the demographic parameters in the model. These are described below and in the main paper.

Abundance threshold

We set the lower bound of the abundance threshold parameter at 0 (no Allee effect) and the upper bound at 469, based on the posterior distribution of abundance threshold from modelling the steppe bison (Pilowsky, Haythorne, Brown, et al., 2022c), scaled up to the larger grid cells used in this study. After some preliminary modelling, we found that all simulations with an abundance threshold greater than 250 resulted in extinction of the bison in the first timestep regardless of the other parameter values. Subsequently, we set a new maximum abundance threshold at 250.

Carrying capacity

The carrying capacity of each grid cell was based on the climate suitability (VanDerWal et al., 2009). We converted habitat suitability to carrying capacity by multiplying the habitat suitability score (on a 0 – 1 scale) by the maximum density, which was one of the varying demographic parameters in the model. We estimated plausible lower and upper bounds for maximum density by calculating the 50th and 99th percentiles of population density estimates from the reintroduced range of the European bison (Krasińska & Krasiński, 2013; Mysterud et al., 2007; Plumb et al., 2020; Radwan et al., 2010). Based on the assumption that a maximum of one-quarter of each grid cell could be suitable habitat for the steppe bison (Fordham et al., 2013), we scaled the maximum density values to one-quarter of each equal-area projection grid cell, resulting in a range of 851 to 4780 bison per grid cell. After some preliminary modelling, we found that this range was too high, resulting in unrealistic estimates of millions of bison in the present day in Europe alone (comparable to the number of plains bison in North America before European colonisation (Hedrick, 2009)). As a result, we adjusted the range of carrying capacity to 500 to 3000 bison per grid cell.

Generation length and population growth

Maximum annual growth rate and its variance were estimated using historical and modern time series data (Mysterud et al., 2007; Plumb et al., 2020; Samojlik et al., 2019). Maximum growth rate was calculated using time series data for founding populations growing exponentially (Fordham et al., 2022). This provided a mean estimate of 0.102 at an annual time scale. To measure the annual variation in growth rate, we used time series data for stable populations fluctuating around the

carrying capacity (Fordham et al., 2022). This provided a mean estimate of 0.022 at an annual time scale.

To convert estimates of maximum growth rate and variation in growth rate to generational rates, we exponentiated the lower and upper bounds of maximum annual growth rate to the generation length of the European bison, which is 10 years (Pacifici et al., 2013). We calculated the variance in population growth rate at the generational time step by running 1000 simulations of an annual model with the upper bound of annual growth rate and the upper bound of annual variance. We ran each simulation for 100 years, then calculated the mean standard deviation of the growth rate at the generational time step across all 1000 simulations (Fordham et al., 2022). The estimated standard deviation on the generational time scale was 0.244. Density dependence was modelled as a Ricker logistic density dependent response (Ricker, 1954), which has been shown to be an appropriate model for species with slow life histories like the European bison, especially when environmental variation is high (Koetke et al., 2020).

Dispersal

We used data on European bison in Poland to simulate natal dispersal (Krasińska & Krasiński, 2013). We modelled a mean dispersal rate of 15% of the population moving per generation at an average maximum distance of 300 km. We set upper and lower bounds on these estimates of 5 – 25% and 0 – 300 km, respectively. We did this by parameterising the following dispersal equation:

$$m_{ij} = \begin{cases} a^{\left(\frac{-D_{ij}}{b}\right)}, & D < D_{max} \\ 0, & D \geq D_{max} \end{cases}$$

where movement (m) between cells i and j is a function of D_{max} (the maximum dispersal distance), a, and b. The parameter a is half the total proportion of dispersers that leave a cell at each time step. The parameter b comes from fitting an exponential function of dispersal distance in which D_{max} is the 95th percentile of the distribution of distances. The lambda parameter of the fitted exponential function is the estimate of b.

The dispersal function was modulated by the dispersing fraction parameter, which set a ceiling on how many bison dispersed out of a grid cell. This approach prevents excessively large dispersal rates between closely neighbouring grid cells (Fordham et al., 2022).

Human hunting

We modelled the rate of human hunting in each grid cell as a function of relative abundance of humans (see above) and population density of European bison. The range of maximum harvest for the harvest function was 0 – 35% of the bison in a grid cell (Fordham et al., 2022). The proportion of bison harvested in a grid cell H is given by the following equation:

$$H \quad = \frac{\left(\frac{N \times F \times P^z}{G\ +\ P^z} \right)}{P}$$

where N is the relative abundance of humans scaled between 0 – 1, F is the maximum harvest, P is the prey density, G is a constant equal to the prey density at which harvest is half-maximal (Alroy, 2001; Brook & Bowman, 2004) and z shapes the harvest function from a type II to a type III functional response, where $z = 1$ corresponds to a type II response and $z = 2$ corresponds to a type III response. At $z = 1$, hunting is a function of prey density and predator satiation, resulting in higher hunting rates at low prey densities and lower hunting rates at high prey densities. At $z = 2$, hunting rates are lower at low densities and high densities, reaching their peak at an inflection point, due to prey adaptation and/or prey switching at low prey densities. We did not model any changes in the density of humans in response to predation, as the archaeological literature suggests that Eurasian hunter-gatherer populations changed largely in response to climate, and relied on a diverse array of food resources (Bevan et al., 2017).

At each time step, the simulator performs four basic steps: 1) the carrying capacity and human density landscapes update, 2) the population growth in each grid cell adjusts according to stochastic variation, carrying capacity and population density (if density dependence is switched on), 3) bison are harvested in each grid cell according to the bison density and human density (if humans are present in the cell), and 4) bison disperse between grid cells according to the carrying capacity of target cells, distance between origin cell and target cell, and dispersal barriers on the

landscape—that is, ice sheets and sea level as determined by the palaeoclimate data. (In the case of the Øresund strait between Denmark and Sweden, the spatial resolution of the land-sea-ice data was too coarse to include the opening of the strait, so we forced a dispersal barrier after the opening of the strait 8.5 ka (Andrén et al., 2011).

We used Latin hypercube sampling to thoroughly sample the 11 dynamic model parameters in an unbiased manner (Table 1). Latin hypercube sampling is stratified by subdividing probability distributions into areas of equal probability density (Stein, 1987). In the first round of models, we sampled model parameters using uniform distributions, generating 25,000 plausible combinations of parameter values. We ran 25,000 simulations of the European bison in Eurasia from 21 ka BP to 1850 CE. After pattern-oriented validation of the first round of models (see below), we fitted different distributions to the posteriors and chose the best fit by comparing AIC. For subsequent rounds of modelling, we sampled the informed prior distributions to generate 10,000 combinations of parameter values. The process continued until Bayes factors indicated that the posterior distributions had converged.

4. Model Validation

To validate the model, we used pattern-oriented validation, using spatiotemporal occurrence, persistence in the Caucasus, and number of persisting populations as validation targets.

Spatiotemporal occurrence

We used spatiotemporal occurrence within our study region and time period (n = 57) as a validation target. We created this dataset by combining fossil records with reliable historical records from the 19th century (Krasińska & Krasiński, 2013; Pucek, 1991). The fossil records (n = 120) were highly clustered in space and time, so we thinned them with a spatial thinning algorithm (Aiello-Lammens, Boria, Radosavljevic, Vilela, & Anderson, 2015). We divided the fossils into four temporal bins: the Pleistocene, lower Holocene, mid Holocene, and upper Holocene. We spatially thinned the fossils within each temporal bin with a thinning interval of 3,500 km.

We added a spatiotemporal envelope around each occurrence record in the thinned dataset corresponding to its 86.6 km by 75.6 km grid cell and its eight nearest neighbours, and ±2 × the

error of the calibrated date (except for the historical records, which did not have an error around the date.) Our target was for models to replicate occurrence at all 57 sites.

Persistence in the Caucasus

In our rounds of preliminary modelling before the main study, we found that it was significantly more difficult to model persistence in the European bison refugium in the Caucasus Mountains than the refugium in Białowieża Forest. Therefore, we included a validation target for persistence in the Caucasus. We defined the Caucasus by drawing a bounding box around a shapefile of the Caucasus Mountains. A penalty was applied for each timestep before 1850 that the bison became extinct in this area.

Number of persisting populations

As noted above, only two populations of European bison persisted in the year 1850. For this metric, we counted the number of European bison populations extant in the final time step of the simulation and compared against our target of two.

Statistical procedure

After each round of simulations (see above), we calculated the summary metrics and scaled them by their standard deviations. We used the Approximate Bayesian Computation rejection algorithm to choose the best 25 models and estimate posterior distributions for the model parameters. We then fitted prior distributions for the next round of simulations by fitting a variety of probability distributions and choosing the best-fitting distribution by Akaike Information Criterion.

Effective population size trend

We calculated a total population size trend for the European bison from 21 ka BP to present using a Bayesian skyride plot based on 131 ancient DNA samples from European bison fossils; the sequences are available on GenBank (K. Clark, Karsch-Mizrachi, Lipman, Ostell, & Sayers, 2016). Of the 131 fossils, 102 were directly radiocarbon-dated, and 22 were dated based on well-characterised archaeological contexts. We used the fossil dates and the uncertainty around them to characterise the prior distributions for the tip dates of the genealogy in BEAST v1.10.4 (Suchard et

al., 2018). We used the whole mtDNA sequences with the HKY substitution model and an uncorrelated relaxed molecular clock. We ran the Markov chain Monte Carlo algorithm with a chain length of 10^9, logging parameters every 10^4 simulations to avoid autocorrelation, then duplicated the analysis to ensure the chains had not reached a local maximum in the first run. We then analysed the output using Tracer v1.7.1 (Rambaut, Drummond, Xie, Baele, & Suchard, 2018) to generate a GMRF (Gaussian Markov Random Field) Bayesian skyride plot of effective population size from 21 ka BP to present.

We fitted a linear model to the GMRF Bayesian skyride plot (adjusted r^2 = 0.9247) and used the estimated slope as an additional validation of our model results. For each simulation, we fitted a linear model of total population size, and scored based on the congruence between the estimated slope and the slope fitted to the Bayesian skyride plot.

6. Model scenarios

We created a validated ensemble model, a weighted mean of the 25 selected models from the final round of simulation, which passed our checks for parameter stabilisation and goodness of fit to validation targets. We stopped the validated ensemble model at 1500 CE for the purposes of analysis (Canteri et al., 2022). This validated ensemble represents the *baseline scenario*, based on our standard model assumptions described above. We used the posterior distributions of the model parameters from the validated ensemble to simulate scenarios using different model settings to represent different possible scenarios for the European bison.

In the baseline scenario, the human hunting function is constant over time. The hunting rate differs based on the density of humans and bison in the grid cell, but the shape of the function does not change. However, based on historical records and the establishment of royal hunting reserves (Heptner et al., 1961), it is thought that hunting pressure on European bison increased greatly after 1500 CE, due to technological advancements in hunting and cultural shifts in land use (Benecke, 2005). The approximate population abundance of European bison in 1870 is known from historical records: there were 2000 bison in the Caucasus (Heptner et al., 1961) and 1,560 bison in Białowieża Forest, for a total of 3,560 European bison (Krasińska & Krasiński, 2013). In

the baseline scenario, the European bison range is realistic at 1500 CE but unrealistically large after 1500. To address this, we ran increased hunting scenarios: ten rounds of 25 simulations using the validated 'best' models from the baseline scenario from 1500 to 1870, increasing the maximum harvest rate by 10% each round, for a maximum 100% increase in maximum harvest rate. We validated the final abundance in 1870 against the estimated abundance from the historical record.

Parameter	Mean Prior	Mean Posterior
Ecological niche		
Niche volume	0.5 (0 – 1)	0.421 (0.308 – 0.559)
Niche outlier marginality index (OMI)	0.5 (0 – 1)	0.684 (0.263 – 0.924)
Human harvesting		
Maximum harvest (percent)	17.5 (0 – 35)	13.3 (5.4 – 20.8)
Harvest function (z)	1.5 (1 – 2)	1.383 (1.180 – 1.710)
Human density (p)	0.5 (0 – 1)	0.386 (0.190 – 0.600)
Dispersal		
Dispersing fraction	0.15 (0.05 – 0.25)	0.172 (0.136 – 0.211)
Maximum dispersal distance (km)	250 (0 – 500)	103.7 (94.0 – 124.0)
Population model		
Maximum growth rate (r)	0.5377 (0.0324 – 1.043)	0.637 (0.388 – 0.853)
Variance of growth rate	0.122 (0 – 0.244)	0.156 (0.086 – 0.214)
Allee effect (abundance threshold)	235 (0 – 469)	9 (3 – 18)
Maximum density (bison per grid cell)	2816 (851 – 4780)	2023 (1015 – 2655)

Table S2: Unscaled parameter distributions. The prior and posterior means, minima, and maxima are shown for parameters in the process-explicit model of European bison range and extinction dynamics. All priors are uniformly distributed. See section 3a of the Methods for details.

Model	▲ML	Adjusted R²	Deviance explained
Global model	123.1	0.85	88.5%
Global model without interactions	0	0.83	88.6%
Mean annual temperature only	988.2	0.76	82.3%
Human abundance only	690.6	0.80	85%
Deforestation only	2303.5	0.57	69.1%

Table S2: Comparison of general additive models explaining bison abundance. Metrics comparing the explanatory power of general additive models with different structures in explaining patterns in bison abundance over time. The optimal model was the global model without interactions based on a test of differences between the ML scores (Wood, 2017).

Movies

https://universityofadelaide.box.com/s/0ned4ig5yrvofmx251te8uqkq163at12

Movie S1: European bison abundance in Eurasia from 21 ka BP to 1500 CE. Abundance is shown as number of bison per 76 km by 87 km grid cell. Gray grid cells are areas where there is <25% model agreement on bison occupancy. Red points show radiocarbon-dated fossils of European bison.
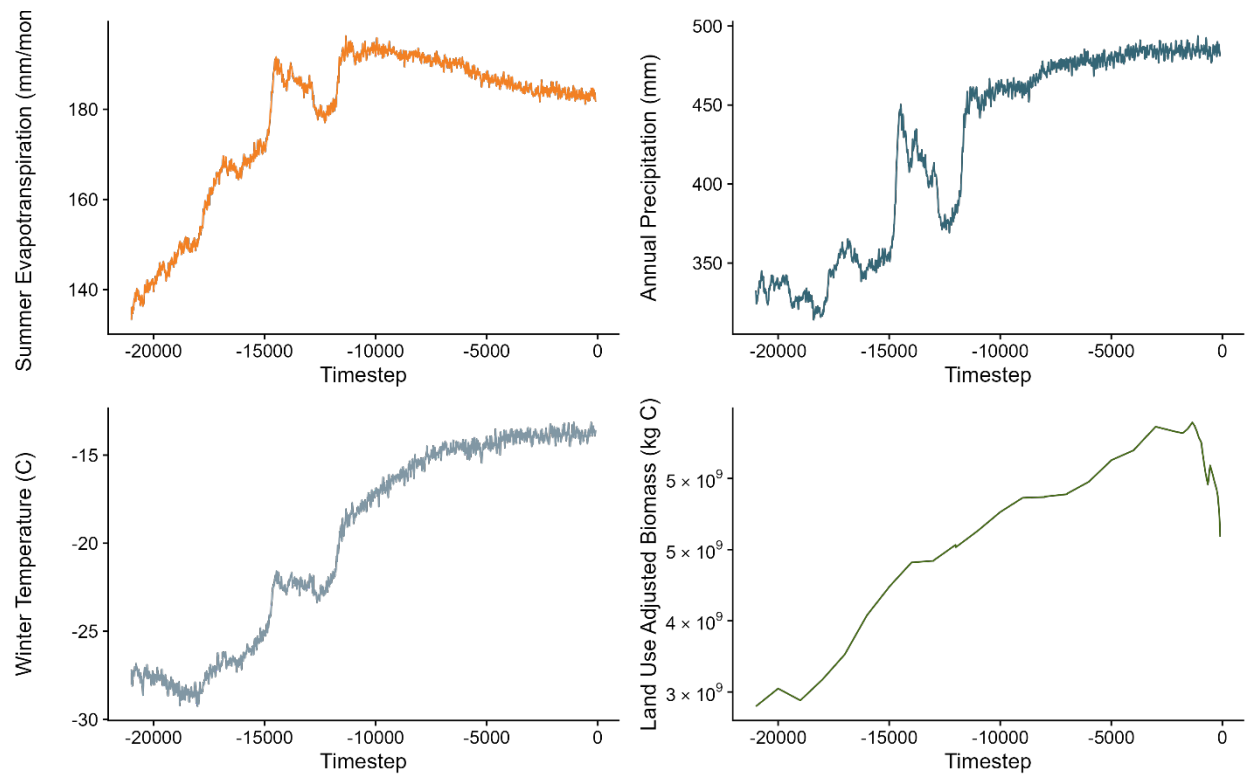
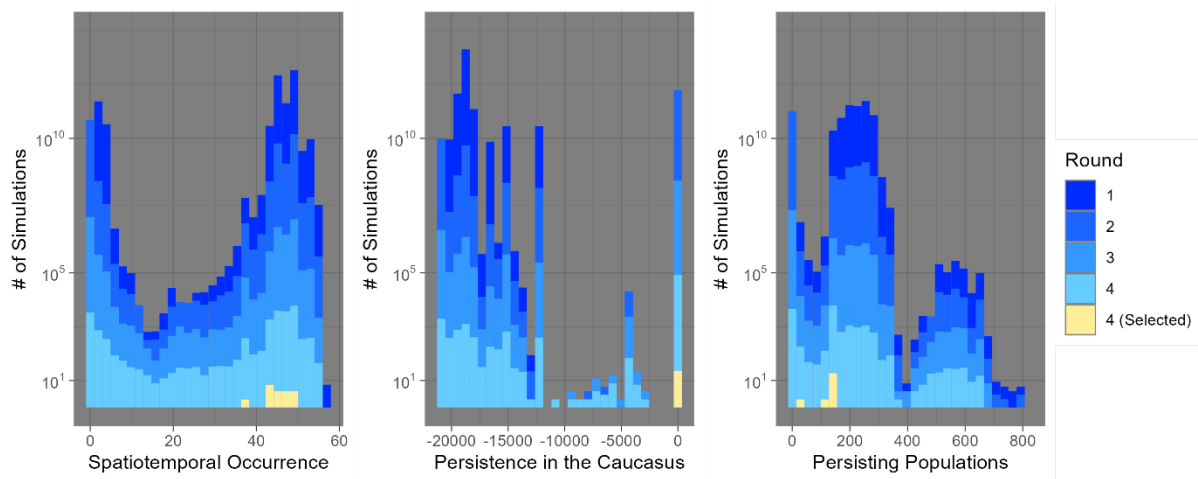Figure S1: Environmental variables used for the European bison niche.

Figure S2: Pattern-oriented model validation. Validation targets are A) spatiotemporal occurrence, showing the number of fossil and historical sites where spatiotemporal occurrence is simulated correctly, B) persistence in the Caucasus, showing timing of extirpation in the Caucasus region, and C) persisting populations, showing the number of persistent populations in 1850 CE. For A) the observed target was 57: the maximum number of sites with information on spatiotemporal occurrence. For B) the target was 0: no difference between simulated and target persistence time. For C) the target was 2: the number of bison populations in 1850 according to historical records. Different colours show four successive iterations of pattern-oriented modelling. See Methods for further details.
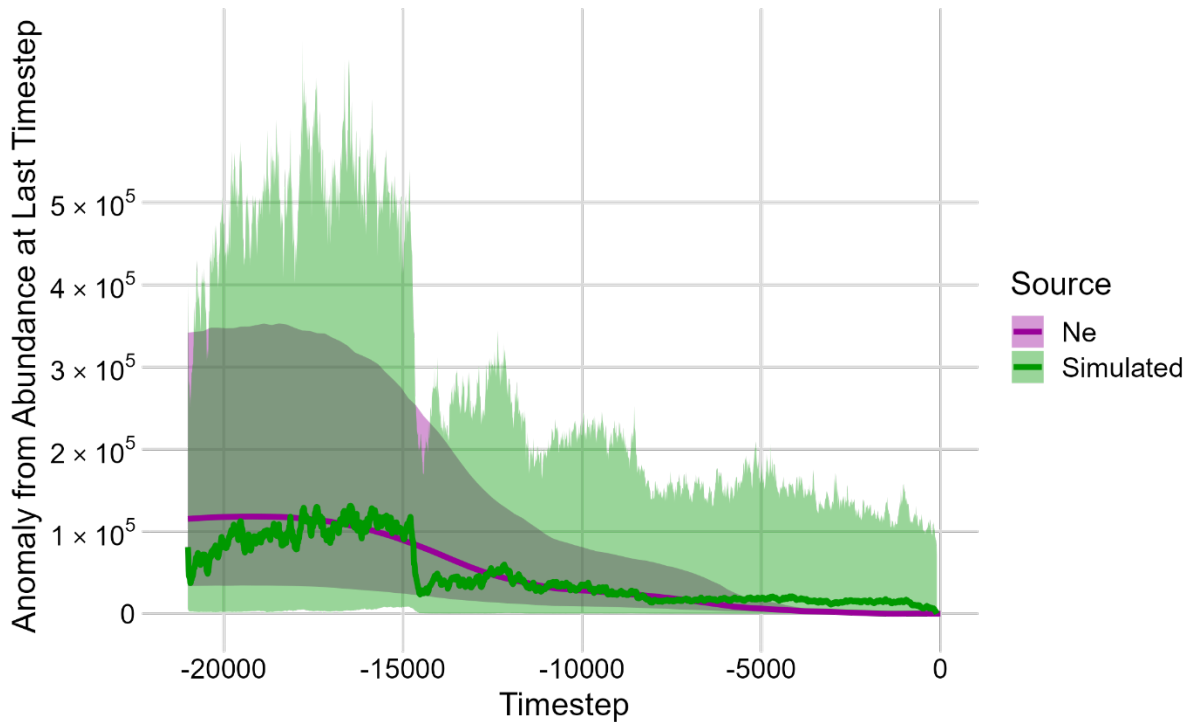
Figure S3: Effective population (N$_e$) and simulated population trends. Effective population size of the European bison (purple) was estimated from 21,000 ago to present using a Bayesian skyride plot (see Supplementary Methods for details.) The simulated population size (green) is from the validated ensemble of selected models. To facilitate comparison between census and effective population size, population trends are shown as anomalies from the abundance at the final timestep. The ribbons show 95% credible interval for the effective population size and 95% confidence interval for the simulated population size.
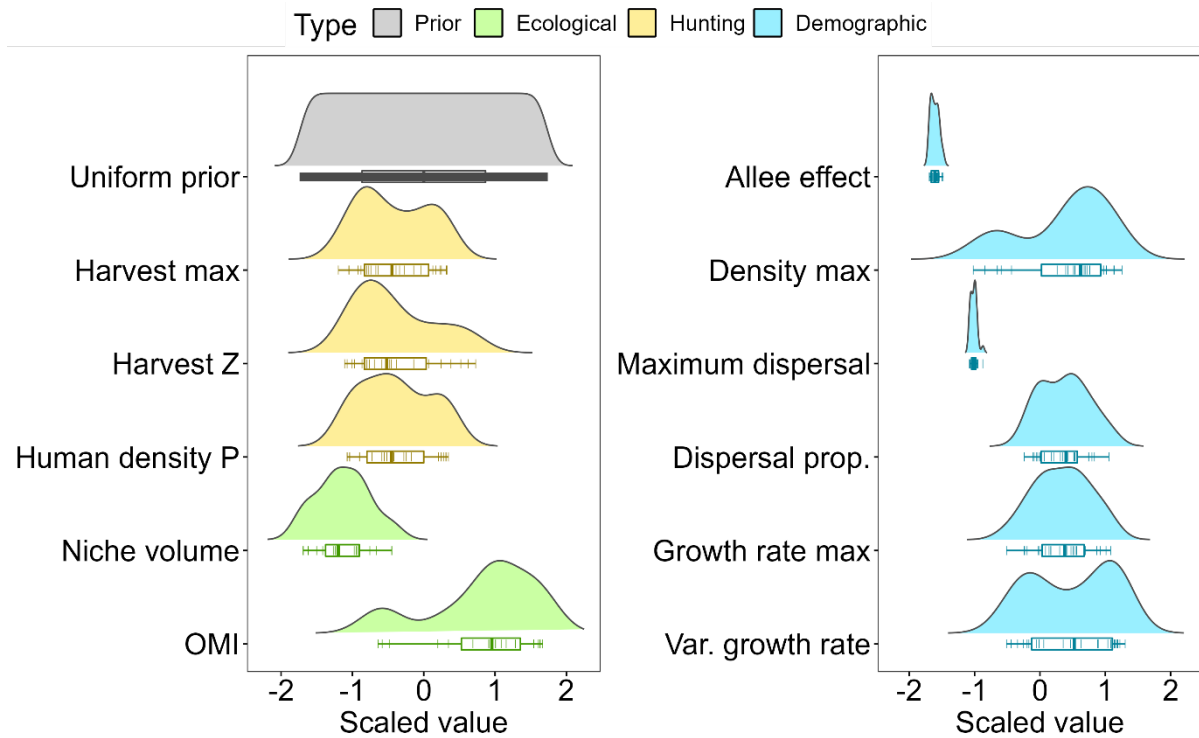
Figure S4: Posterior distributions for all variable model parameters. Shows the density of the posterior distribution for anthropogenic (yellow), environmental (green), and demographic (blue) parameters compared to a uniformly distributed prior (grey). Posterior distributions have all been scaled to a common axis. Variable human hunting parameters in the bison spatially explicit population model (SEPM) include the maximum percentage of the population hunted (Harvest max), the shape of the hunting function (Harvest Z), and the portion of the human abundance distribution sampled (Human density P). Variable parameters describing niche requirements include breadth of climatic conditions the species can occupy (Niche volume) and the marginality of the realised niche relative to the full niche (OMI). Variable demographic parameters include Allee effect, population density at maximum habitat suitability (Density max), maximum dispersal distance (Maximum dispersal), proportion of individuals dispersing at each timestep (Dispersal prop.), maximum population growth rate (Growth rate max), and its variance (Var. growth rate). Unscaled parameter values are provided in Table S1.
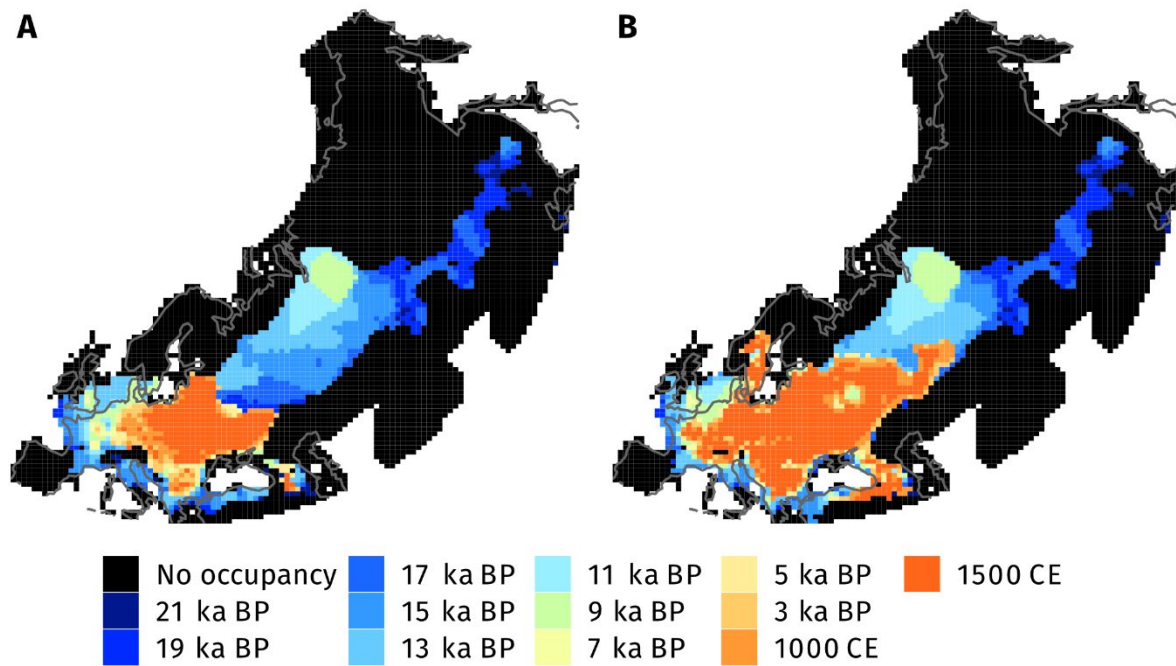
Figure S5: Extirpation times of European bison with and without human pressures.

Extirpation times of European bison in each grid cell of the study region are shown for the best 25 models (A) and a counterfactual scenario where human hunting and land use change did not affect the European bison (B).
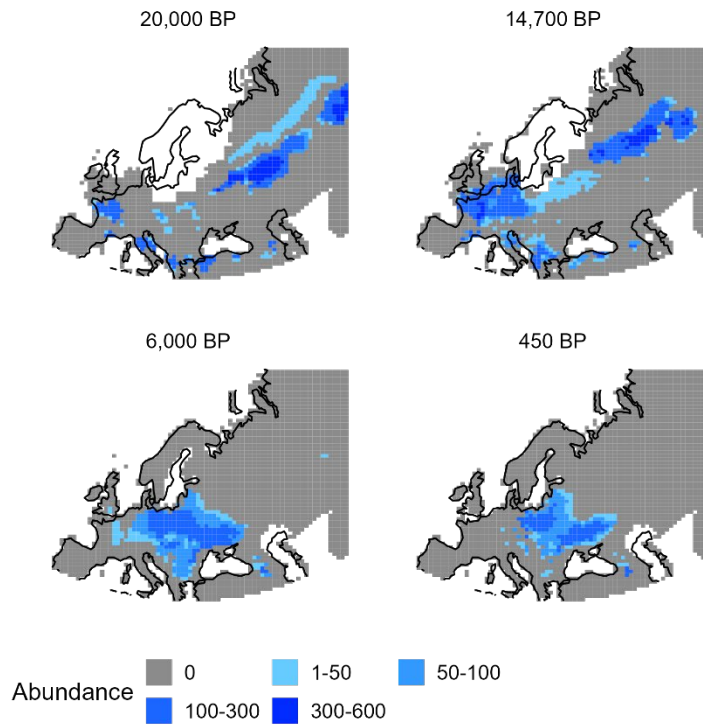
Figure S6: Extended maps of the range collapse of the European bison. Simulated bison abundance for the end of the last glacial maximum stadial (20,000 BP), immediately prior to the Bølling-Allerød warming event (14,700 BP), the mid-Holocene (6,000 BP), and at the end of the simulation (450 BP or 1500 CE).

DISCUSSION

In this thesis, I identified the crucial role that process-explicit models play in identifying causes of biodiversity loss and informing strategies to mitigate that loss. I found ways to improve the use of process-explicit models in the future. I used these models to find causes of extinction in the steppe bison and European bison. In doing so, I not only contributed to knowledge of these species and to the conservation of the European bison, but also demonstrated how process-explicit models can be used to investigate the causes of extinction in other species of concern.

In **Chapter I** of the thesis, I did a comprehensive review of the last fifty years of ecological research on using process-explicit models to study patterns of biodiversity. I identified emerging trends, which included the use of all five ecological and evolutionary processes to model community-level diversity, and gaps, which included a common failure to validate process-explicit models using high statistical rigor. Going forward, I made the case that as a field, macroecologists should ultimately aim for the system approach and rigor of process-explicit climate models, particularly as the next generation of biodiversity models is developed.

In **Chapter II**, I did the first ever sensitivity analysis of a process-explicit model of human expansion and found that key output metrics of the model were more sensitive to human demographic parameters than the choice of palaeoclimate model. This finding indicates that for this type of process-explicit model, more research on human demographic parameter values is needed to ensure accurate and precise model outputs. This is important because many downstream analyses (such as Chapters III and IV) rely on these outputs to parameterise human abundance in space and time.

The last two chapters of the thesis focused on reconstructing the range and population dynamics of two bison species over thousands of years using process-explicit ecological models. In **Chapter III**, I reconstructed the range and extinction dynamics of the steppe bison (*Bison priscus*) in Siberia from 50,000 to 5,000 years before present. Based on these models, I found that a combination of human hunting and rapid deglacial warming drove the steppe bison to extinction in Eurasia. In **Chapter IV**, I modeled the range collapse and extinction in the wild of the European bison (*Bison bonasus*), which is intensively targeted by conservation efforts such as rewilding its former range. I

166

found that a combination of warming climate, human hunting, and land use change drove the collapse of the European bison in the wild, and that these pressures varied in space and time. My findings pinpoint ideal areas for the reintroduction of European bison and reveal areas of Europe that are unsuitable because their extirpation there was driven by climate change.

Understanding biodiversity loss with process-explicit models

This thesis contributes to the field of process-explicit models of biodiversity by incorporating interactions between ecological processes and global change drivers while upholding statistical rigor and biological realism. Statistical validation against multivariate observed ecological patterns, is crucial for assessing the accuracy of these models. While this level of rigor is standard among genetic-level process-explicit models, it is lacking in most models of higher levels of biological organisation. I show that a promising avenue for improving the statistical rigor of process-explicit models is pattern-oriented validation, which assesses models by their ability to reconstruct multiple observed patterns simultaneously (Grimm et al., 2005).

While high resolution palaeoclimate models have become more widely available in recent years, further advances are needed to improve our ability to model biodiversity over long timescales (Fordham et al., 2020). First, most process-explicit models of biodiversity over palaeo timescales cover only the last ice age, due to a paucity of quality palaeoclimate simulations before the Last Glacial Maximum (Holden et al., 2019). However, I was able to go beyond this limitation in Chapters II and III, simulating human migration and bison range dynamics over periods of 100,000 and 60,000 years, respectively. This has opened the future possibility of continuously simulating biodiversity change since the last inter-glacial period.

In Chapter II, I demonstrated the importance of doing global sensitivity analyses of process-explicit models. I found that estimates of migration of *Homo sapiens* into North America are highly sensitive to demographic parameters (e.g., colonisation rate), and that there is a great deal of uncertainty around human palaeodemography. It is likely that these parameter estimates could be improved through research on the relationship between human population growth rate and net primary productivity, as well as rates of human dispersal into previously unoccupied regions

(French et al., 2021). In addition, increasing the spatiotemporal coverage of genetic validation targets would also improve the accuracy of these models.

My work in this thesis on modelling biodiversity dynamics and loss also shows a need to generate robust reconstructions of drivers of these patterns at high spatiotemporal resolutions. The process-explicit model of human migration that I ran and evaluated in Chapter II, CISGeM, provided crucial inputs to drive human hunting in my models of bison range collapse in Chapters III and IV. Further, the inclusion of land use change as a driver in Chapter IV was made possible by the recent publication of HYDE v3.2, a dataset of human-driven land use change from 12,000 years ago to present featuring high spatial and temporal resolution (Klein Goldewijk et al., 2017).

Drivers of range collapse and extinction

One of the core aims of my doctoral research was to investigate how global change drivers, ecological processes, and their interactions cause range collapse and ultimate extinction. In Chapters III and IV, I investigated drivers of population in the steppe bison and European bison. Despite the close phylogenetic relationship between the two species, and the negative impact of human hunting and deglacial warming on population abundance in both species, I found different patterns of range collapse for each.

Steppe bison faced multiple demographic limitations—a high Allee effect, high human abundance and hunting pressure—that combined with a relatively small realised niche to drive the species into marginal habitat in the Siberian highlands during the Pleistocene-Holocene transition. Isolated in this marginal habitat, the steppe bison became extinct. When I ran a counterfactual scenario that excluded hunting, I found that the bison were able to persist in refugia in northern Siberia. Meanwhile, European bison were limited by a small and specific set of ecological niche requirements, which combined with infrequent dispersal to trap the species in suboptimal habitat. Like the steppe bison, the range and abundance of European bison were strongly affected by climatic warming and human hunting during the Pleistocene-Holocene transition. In addition to these drivers, my research shows that human-driven land use change in the late Holocene excluded European bison from the southern and western edges of their potential range. This is the first

direct evidence of the effect of human land use change on megafauna abundance dating back thousands of years.

My research shows that drivers of range and extinction dynamics widely vary across space and time, even for highly related species. For example, I show that climatic warming made the northern coast of Siberia suitable for steppe bison and humans at the termination of the Pleistocene. This resulted in humans driving them out of these northern climatic refugia into more southerly highland regions that could not support steppe bison populations in the long term. For the European bison, environmental change caused the geographic range of the species to contract inwardly from all directions. In the inner part of the range, humans were the most important driver of extirpation. Hunting restricted the bison's range from the north and east, and land use change restricted the range from the south and west. These complex spatiotemporal interactions between ecological processes and natural and human drivers could not be disentangled correlatively, illustrating the importance of process-explicit models for understanding species' range dynamics and threats to biodiversity in space.

The findings of Chapters III and IV highlight the importance of modeling extinctions over long time scales, as pathways to extinction may start tens of thousands of years before the last individual dies. Most of the population decline of the steppe bison occurred more than 30,000 years ago, setting the time and location of extinction in Siberia some 21,000 years later. In the case of the European bison, I found that temperature had a significant effect on bison abundance in the Pleistocene and early to mid-Holocene, but had no effect on bison abundance in the late Holocene. Thus, investigating the European bison only in the last 4,000 years would miss a crucial component of the species' decline farther back in time.

Conservation applications

My research has both direct and indirect applications to conservation, such as conservation policy suggestions and development of software to model extinctions. In Chapter III, I introduced the R package 'paleopop', which I co-developed. 'paleopop' is an extension to the R package poems that enables spatially explicit, process-explicit simulation of populations over tens of thousands of years.

'paleopop' can be used to model long-term causes of extinction for a variety of organisms and has utility far beyond the modelling the bison range collapse that I have presented in this thesis. While it is too late to save the steppe bison from extinction, there is still time to use this process-explicit ecological modelling approach to conserve other species of concern. For the European bison, I show how 'paleopop' can be used to identify potential causes of extinction and intervene appropriately.

There is ongoing debate about where to reintroduce European bison to bolster their population sizes and range extent in the long term (Kerley et al., 2020). My research in Chapter IV contributes to this debate by providing a map of where the European bison became extinct due to environmental change, land use change, and/or human hunting. Attempts to reintroduce the European bison to Western Europe are failing (Plumb et al., 2020). My research indicates that this is because much of Western Europe has been climatically unsuitable for European bison for many millennia due to post-glacial environmental change. In contrast, areas that have become unsuitable because of land use change and/or hunting pressure represent prime regions for restoration efforts and protected nature reserves where bison will thrive if reintroduced.

Conclusions and future directions

My research in Chapters II, III, and IV made use of inferences from both modern and ancient DNA as validation targets for these process-explicit models. This genetic information was not used to parameterise the models, serving as crucial independent observations to evaluate model accuracy and refine parameter distributions. However, these data were coarse, and did not provide information on population changes on fine temporal scales. New genetic techniques are providing insight on genetic responses on human-relevant timescales (Roycroft et al., 2021) and will increase the utility of ancient DNA as a data source for model validation.

My doctoral research shows the utility of process-explicit models in reconstructing past biodiversity dynamics and, more specifically, their capacity to integrate disparate inferences of demographic change from a wide variety of palaeo-archives. The increasing availability of databases of radiocarbon-dated fossils, ancient DNA sequences, species occurrence records, and palaeoclimate reconstructions will continue to aid the development of ever more complex

biodiversity models that will reveal biodiversity dynamics at finer spatiotemporal resolution over longer timescales.

It is important to consider these longer timescales because they enable the study of biodiversity change under past climates that are analogous to future climates under likely emission scenarios (Fordham et al., 2020). In my thesis, I modelled biodiversity change in the Palearctic and Nearctic during the last deglaciation, a time of very rapid warming that is analogous to current Arctic warming (Rantanen et al., 2022). This research provides important insight into how species ranges shift in response to rapid warming, and how this warming can interact with other threats to biodiversity. One of the best past analogues to projected future warming scenarios is the Eemian interglacial stage that ended 115,000 years ago (Fordham et al., 2020). Modeling biodiversity on longer timescales back to the Eemian interglacial will contribute to knowledge about biodiversity patterns under future climates.

Process-explicit models allowed me to make inferences that it would not be possible to make with correlative models alone. I was able to project abundances of humans, steppe bison, and European bison at high spatiotemporal resolution over long timescales. I could disentangle the effects of human hunting, land use change, and environmental change on species range dynamics. This thesis demonstrates the importance of process-explicit models as a tool for conserving biodiversity into the future.

REFERENCES

Adriaensen, F., Chardon, J. P., De Blust, G., Swinnen, E., Villalba, S., Gulinck, H., & Matthysen, E. (2003). The application of 'least-cost' modelling as a functional landscape model. *Landscape and Urban Planning*, *64*(4), 233–247. https://doi.org/10.1016/S0169-2046(02)00242-6

Aiello-Lammens, M. E., Boria, R. A., Radosavljevic, A., Vilela, B., & Anderson, R. P. (2015). spThin: An R package for spatial thinning of species occurrence records for use in ecological niche models. *Ecography*, *38*(5), 541–545. https://doi.org/10.1111/ecog.01132

Allen, J. R. M., Forrest, M., Hickler, T., Singarayer, J. S., Valdes, P. J., & Huntley, B. (2020). Global vegetation patterns of the past 140,000 years. *Journal of Biogeography*, *47*(10), 2073–2090. https://doi.org/10.1111/jbi.13930

Alroy, J. (2001). A multispecies overkill simulation of the end-Pleistocene megafaunal mass extinction. *Science*, *292*(5523), 1893–1896. https://doi.org/10.1126/science.1059342

Alzate, A., Janzen, T., Bonte, D., Rosindell, J., & Etienne, R. S. (2019). A simple spatially explicit neutral model explains the range size distribution of reef fishes. *Global Ecology and Biogeography*, *28*(7), 875–890. https://doi.org/10.1111/geb.12899

Anderson, B. J., Akçakaya, H. R., Araújo, M. B., Fordham, D. A., Martinez-Meyer, E., Thuiller, W., & Brook, B. W. (2009). Dynamics of range margins for metapopulations under climate change. *Proceedings of the Royal Society B: Biological Sciences*, *276*(1661), 1415–1420. https://doi.org/10.1098/rspb.2008.1681

Anderson, E., & Hubricht, L. (1938). Hybridization in Tradescantia. III. The evidence for introgressive hybridization. *American Journal of Botany*, *25*(6), 396–402. https://doi.org/10.2307/2436413

Anderson, P. M., & Lozhkin, A. V. (2001). The Stage 3 interstadial complex (Karginskii/middle Wisconsinan interval) of Beringia: Variations in paleoenvironments and implications for paleoclimatic interpretations. *Quaternary Science Reviews*, *20*(1–3), 93–125. https://doi.org/10.1016/S0277-3791(00)00129-3

Andrén, T., Björck, S., Andrén, E., Conley, D., Zillén, L., & Anjar, J. (2011). The Development of the Baltic Sea Basin During the Last 130 ka. In J. Harff, S. Björck, & P. Hoth (Eds.), *The Baltic Sea Basin* (pp. 75–97). Berlin, Heidelberg: Springer. https://doi.org/10.1007/978-3-642-17220-5_4

Antoniadis, A., Lambert-Lacroix, S., & Poggi, J.-M. (2021). Random forests for global sensitivity analysis: A selective review. *Reliability Engineering & System Safety*, *206*, 107312. https://doi.org/10.1016/j.ress.2020.107312

Arenas, M., Ray, N., Currat, M., & Excoffier, L. (2012). Consequences of range contractions and range shifts on molecular diversity. *Molecular Biology and Evolution*, *29*(1), 207–218. https://doi.org/10.1093/molbev/msr187

Armstrong, D. P., & Seddon, P. J. (2008). Directions in reintroduction biology. *Trends in Ecology & Evolution*, *23*(1), 20–25. https://doi.org/10.1016/j.tree.2007.10.003

Armstrong, E., Hopcroft, P. O., & Valdes, P. J. (2019). A simulated Northern Hemisphere terrestrial climate dataset for the past 60,000 years. *Scientific Data*, *6*(1), 1–16. https://doi.org/10.1038/s41597-019-0277-1

Avise, J. C. (2000). *Phylogeography: The History and Formation of Species*. Harvard University Press.

Bakker, E. S., Gill, J. L., Johnson, C. N., Vera, F. W. M., Sandom, C. J., Asner, G. P., & Svenning, J.-C. (2016). Combining paleo-data and modern exclosure experiments to assess the impact of megafauna extinctions on woody vegetation. *Proceedings of the National Academy of Sciences*, *113*(4), 847–855. https://doi.org/10.1073/pnas.1502545112

Barnes, R., & Clark, A. T. (2017). Sixty-five million years of change in temperature and topography explain evolutionary history in eastern North American plethodontid salamanders. *The American Naturalist*, *190*(1), E1–E12. https://doi.org/10.1086/691796

Barnosky, A. D., & Lindsey, E. L. (2010). Timing of Quaternary megafaunal extinction in South America in relation to human arrival and climate change. *Quaternary International*, *217*(1), 10–29. https://doi.org/10.1016/j.quaint.2009.11.017

Bartlett, L. J., Newbold, T., Purves, D. W., Tittensor, D. P., & Harfoot, M. B. J. (2016). Synergistic impacts of habitat loss and fragmentation on model ecosystems. *Proceedings of the Royal Society B: Biological Sciences*, *283*(1839), 20161027. https://doi.org/10.1098/rspb.2016.1027

Beaumont, L. J., Pitman, A. J., Poulsen, M., & Hughes, L. (2007). Where will species go? Incorporating new advances in climate modelling into projections of species distributions. *Global Change Biology*, *13*(7), 1368–1385. https://doi.org/10.1111/j.1365-2486.2007.01357.x

Beaumont, M. A., Zhang, W., & Balding, D. J. (2002). Approximate Bayesian computation in population genetics. *Genetics*, *162*(4), 2025–2035. https://doi.org/10.1093/genetics/162.4.2025

Bemmels, J. B., Knowles, L. L., & Dick, C. W. (2019). Genomic evidence of survival near ice sheet margins for some, but not all, North American trees. *Proceedings of the National Academy of Sciences*, *116*(17), 8431–8436. https://doi.org/10.1073/pnas.1901656116

Benecke, N. (2005). The Holocene distribution of European bison—The archaeozoological record. *Munibe Antropologia - Arkeologia*, *57*, 421–428.

Benson, D. A., Cavanaugh, M., Clark, K., Karsch-Mizrachi, I., Lipman, D. J., Ostell, J., & Sayers, E. W. (2012). GenBank. *Nucleic Acids Research*, *41*(D1), D36–D42.

Bevan, A., Colledge, S., Fuller, D., Fyfe, R., Shennan, S., & Stevens, C. (2017). Holocene fluctuations in human population demonstrate repeated links to food production and climate. *Proceedings of the National Academy of Sciences*, *114*(49), E10524–E10531. https://doi.org/10.1073/pnas.1709190114

Beven, K. (2006). A manifesto for the equifinality thesis. *Journal of Hydrology*, *320*(1), 18–36. https://doi.org/10.1016/j.jhydrol.2005.07.007

Beyer, R., Krapp, M., & Manica, A. (2020). An empirical evaluation of bias correction methods for palaeoclimate simulations. *Climate of the Past*, *16*(4), 1493–1508. https://doi.org/10.5194/cp-16-1493-2020

Beyer, R. M., Krapp, M., Eriksson, A., & Manica, A. (2021). Climatic windows for human migration out of Africa in the past 300,000 years. *Nature Communications*, *12*(1), 4889. https://doi.org/10.1038/s41467-021-24779-1

Bi, K., Linderoth, T., Singhal, S., Vanderpool, D., Patton, J. L., Nielsen, R., … Good, J. M. (2019).
Temporal genomic contrasts reveal rapid evolutionary responses in an alpine mammal during recent climate change. *PLOS Genetics*, *15*(5), e1008119.
https://doi.org/10.1371/journal.pgen.1008119

Blaauw, M. (2010). Methods and code for 'classical' age-modelling of radiocarbon sequences.
Quaternary Geochronology, *5*(5), 512–518. https://doi.org/10.1016/j.quageo.2010.01.002

Blonder, B., & Harris, D. J. (2019). *hypervolume: High Dimensional Geometry and Set Operations Using Kernel Density Estimation, Support Vector Machines, and Convex Hulls*. Retrieved from https://CRAN.R-project.org/package=hypervolume

Blonder, B., Morrow, C. B., Maitner, B., Harris, D. J., Lamanna, C., Violle, C., … Kerkhoff, A. J. (2018). New approaches for delineating n-dimensional hypervolumes. *Methods in Ecology and Evolution*, *9*(2), 305–319. https://doi.org/10.1111/2041-210X.12865

Bocherens, H., Hofman-Kamińska, E., Drucker, D. G., Schmölcke, U., & Kowalczyk, R. (2015).
European Bison as a Refugee Species? Evidence from Isotopic Data on Early Holocene Bison and Other Large Herbivores in Northern Europe. *PLOS ONE*, *10*(2), e0115090.
https://doi.org/10.1371/journal.pone.0115090

Boeskorov, G. G., Potapova, O. R., Protopopov, A. V., Plotnikov, V. V., Agenbroad, L. D., Kirikov, K. S., … van der Plicht, J. (2016). The Yukagir Bison: The exterior morphology of a complete frozen mummy of the extinct steppe bison, Bison priscus from the early Holocene of northern Yakutia, Russia. *Quaternary International*, *406*, 94–110.
https://doi.org/10.1016/j.quaint.2015.11.084

Boit, A., Sakschewski, B., Boysen, L., Cano-Crespo, A., Clement, J., Garcia Alaniz, N., … Thonicke, K. (2019). Using dynamic global vegetation models (DGVMs) for projecting ecosystem services at regional scales. In M. Schröter, A. Bonn, S. Klotz, R. Seppelt, & C. Baessler (Eds.), *Atlas of Ecosystem Services: Drivers, Risks, and Societal Responses* (pp. 57–61). Cham: Springer International Publishing.

Bonan, G. B. (2008). Forests and climate change: Forcings, feedbacks, and the climate benefits of forests. *Science*, *320*(5882), 1444–1449. https://doi.org/10.1126/science.1155121

Bonan, G. B., Levis, S., Sitch, S., Vertenstein, M., & Oleson, K. W. (2003). A dynamic global vegetation model for use with climate models: Concepts and description of simulated vegetation dynamics. *Global Change Biology*, *9*(11), 1543–1566. https://doi.org/10.1046/j.1365-2486.2003.00681.x

Bondeau, A., Smith, P. C., Zaehle, S., Schaphoff, S., Lucht, W., Cramer, W., … Smith, B. (2007). Modelling the role of agriculture for the 20th century global terrestrial carbon balance. *Global Change Biology*, *13*(3), 679–706. https://doi.org/10.1111/j.1365-2486.2006.01305.x

Boyce, M. S. (1992). Population Viability Analysis. *Annual Review of Ecology and Systematics*, *23*, 481–506.

Bradshaw, C. J. A., Cooper, A., Turney, C. S. M., & Brook, B. W. (2012). Robust estimates of extinction time in the geological record. *Quaternary Science Reviews*, *33*, 14–19. https://doi.org/10.1016/j.quascirev.2011.11.021

Brandtberg, N. H., & Dabelsteen, T. (2013). Habitat selection of two European bison (Bison bonasus) on the Danish island Bornholm. *European Bison Conservation Newsletter*, *6*, 73–80.

Brenner, W. (1921). Växtgeografiska studier i Baräsunds skjärgård. *Acta Sociatatis pro Fauna et Flora Fennica*, *49*, 1–151.

Briscoe, N. J., Elith, J., Salguero-Gómez, R., Lahoz-Monfort, J. J., Camac, J. S., Giljohann, K. M., … McMahon, S. M. (2019). Forecasting species range dynamics with process-explicit models: Matching methods to applications. *Ecology Letters*, *22*(11), 1940–1956. https://doi.org/10.1111/ele.13348

Brook, B. W., & Bowman, D. M. J. S. (2002). Explaining the Pleistocene megafaunal extinctions: Models, chronologies, and assumptions. *Proceedings of the National Academy of Sciences*, *99*(23), 14624–14627. https://doi.org/10.1073/pnas.232126899

Brook, B. W., & Bowman, D. M. J. S. (2004). The uncertain blitzkrieg of Pleistocene megafauna. *Journal of Biogeography*, *31*(4), 517–523. https://doi.org/10.1046/j.1365-2699.2003.01028.x

Brook, B. W., Sodhi, N. S., & Bradshaw, C. J. A. (2008). Synergies among extinction drivers under global change. *Trends in Ecology & Evolution*, *23*(8), 453–460. https://doi.org/10.1016/j.tree.2008.03.011

Brown, J. H., Gupta, V. K., Li, B.-L., Milne, B. T., Restrepo, C., & West, G. B. (2002). The fractal nature of nature: Power laws, ecological complexity and biodiversity. *Philosophical Transactions of the Royal Society of London. Series B: Biological Sciences*, *357*(1421), 619–626.

Brown, J. H., & Maurer, B. A. (1989). Macroecology: The Division of Food and Space Among

Species on Continents. *Science*, *243*(4895), 1145–1150.

https://doi.org/10.1126/science.243.4895.1145

Brown, J. L., & Knowles, L. L. (2012). Spatially explicit models of dynamic histories: Examination

of the genetic consequences of Pleistocene glaciation and recent climate change on the

American Pika. *Molecular Ecology*, *21*(15), 3757–3775. https://doi.org/10.1111/j.1365-

294X.2012.05640.x

Brown, J. L., Weber, J. J., Alvarado-Serrano, D. F., Hickerson, M. J., Franks, S. J., & Carnaval, A.

C. (2016). Predicting the genetic consequences of future climate change: The power of

coupling spatial demography, the coalescent, and historical landscape changes. *American

Journal of Botany*, *103*(1), 153–163. https://doi.org/10.3732/ajb.1500117

Brown, S. C., Wigley, T. M. L., Otto-Bliesner, B. L., & Fordham, D. A. (2020). StableClim,

continuous projections of climate stability from 21000 BP to 2100 CE at multiple spatial

scales. *Scientific Data*, *7*(1), 335. https://doi.org/10.1038/s41597-020-00663-3

Brown, S. C., Wigley, T. M. L., Otto-Bliesner, B. L., Rahbek, C., & Fordham, D. A. (2020).

Persistent Quaternary climate refugia are hospices for biodiversity in the Anthropocene.

Nature Climate Change, *10*(3), 244–248. https://doi.org/10.1038/s41558-019-0682-7

Cabral, J. S., Valente, L., & Hartig, F. (2017). Mechanistic simulation models in macroecology and

biogeography: State-of-art and prospects. *Ecography*, *40*(2), 267–280.

https://doi.org/10.1111/ecog.02480

Canteri, E., Brown, S. C., Schmidt, N. M., Heller, R., Nogués-Bravo, D., & Fordham, D. A.

(2022). Spatiotemporal influences of climate and humans on muskox range dynamics over

multiple millennia. *Global Change Biology*, *28*(22), 6602–6617.

https://doi.org/10.1111/gcb.16375

Cardillo, M., & Bromham, L. (2001). Body size and risk of extinction in Australian mammals.

Conservation Biology, *15*(5), 1435–1440. https://doi.org/10.1111/j.1523-

1739.2001.00286.x

Caswell, H. (2001). *Matrix Population Models*. Sunderland, MA, USA: Sinauer.

Caughley, G. (1994). Directions in Conservation Biology. *Journal of Animal Ecology*, *63*(2), 215–

244. https://doi.org/10.2307/5542

Chang, W. (2019). *R6: Encapsulated Classes with Reference Semantics*. Retrieved from

https://CRAN.R-project.org/package=R6

Chase, J. M., & Leibold, M. A. (2003). *Ecological Niches: Linking Classical and Contemporary*

Approaches. University of Chicago Press.

Cheptou, P., & Massol, F. (2009). Pollination fluctuations drive evolutionary syndromes linking

dispersal and mating system. *The American Naturalist*, *174*(1), 46–55.

https://doi.org/10.1086/599303

Chuine, I., & Beaubien, E. G. (2001). Phenology is a major determinant of tree species range.

Ecology Letters, *4*(5), 500–510.

Clark, K., Karsch-Mizrachi, I., Lipman, D. J., Ostell, J., & Sayers, E. W. (2016). GenBank. *Nucleic*

Acids Research, *44*(D1), D67–D72. https://doi.org/10.1093/nar/gkv1276

Clark, P. U., Dyke, A. S., Shakun, J. D., Carlson, A. E., Clark, J., Wohlfarth, B., … McCabe, A. M.

(2009). The Last Glacial Maximum. *Science*, *325*(5941), 710–714.

https://doi.org/10.1126/science.1172873

Collie, J. S., Botsford, L. W., Hastings, A., Kaplan, I. C., Largier, J. L., Livingston, P. A., … Werner, F. E. (2016). Ecosystem models for fisheries management: Finding the sweet spot. *Fish and Fisheries*, *17*(1), 101–125. https://doi.org/10.1111/faf.12093

Collins, W. D., Bitz, C. M., Blackmon, M. L., Bonan, G. B., Bretherton, C. S., Carton, J. A., … Smith, R. D. (2006). The Community Climate System Model Version 3 (CCSM3). *Journal of Climate*, *19*(11), 2122–2143. https://doi.org/10.1175/JCLI3761.1

Colwell, R. K., & Rangel, T. F. (2010). A stochastic, evolutionary model for range shifts and richness on tropical elevational gradients under Quaternary glacial cycles. *Philosophical Transactions of the Royal Society B: Biological Sciences*, *365*(1558), 3695–3707. https://doi.org/10.1098/rstb.2010.0293

Connolly, S. R., Keith, S. A., Colwell, R. K., & Rahbek, C. (2017). Process, mechanism, and modeling in macroecology. *Trends in Ecology & Evolution*, *32*(11), 835–844. https://doi.org/10.1016/j.tree.2017.08.011

Connor, E. F., & McCoy, E. D. (1979). The statistics and biology of the species-area relationship. *The American Naturalist*, *113*(6), 791–833. https://doi.org/10.1086/283438

Contreras, D. A., Bondeau, A., Guiot, J., Kirman, A., Hiriart, E., Bernard, L., … Fader, M. (2019). From paleoclimate variables to prehistoric agriculture: Using a process-based agro-ecosystem model to simulate the impacts of Holocene climate change on potential agricultural productivity in Provence, France. *Quaternary International*, *501*, 303–316. https://doi.org/10.1016/j.quaint.2018.02.019

Cooper, A., Turney, C., Hughen, K. A., Brook, B. W., McDonald, H. G., & Bradshaw, C. J. (2015). Abrupt warming events drove Late Pleistocene Holarctic megafaunal turnover. *Science*, *349*(6248), 602–606. https://doi.org/10.1126/science.aac4315

Council of the European Union. Council Directive 92/43/EEC of 21 May 1992 on the conservation of natural habitats and of wild fauna and flora. , 206 OJ L § (1992).

Cramer, W., Bondeau, A., Woodward, F. I., Prentice, I. C., Betts, R. A., Brovkin, V., … Young-Molling, C. (2001). Global response of terrestrial ecosystem structure and function to CO2 and climate change: Results from six dynamic global vegetation models. *Global Change Biology*, *7*(4), 357–373. https://doi.org/10.1046/j.1365-2486.2001.00383.x

Crespi, C. M., & Boscardin, W. J. (2009). Bayesian model checking for multivariate outcome data. *Computational Statistics & Data Analysis*, *53*(11), 3765–3772. https://doi.org/10.1016/j.csda.2009.03.024

Cromsigt, J. P. G. M., Kemp, Y. J. M., Rodriguez, E., & Kivit, H. (2018). Rewilding Europe's large grazer community: How functionally diverse are the diets of European bison, cattle, and horses? *Restoration Ecology*, *26*(5), 891–899. https://doi.org/10.1111/rec.12661

Csilléry, K., Blum, M. G. B., Gaggiotti, O. E., & François, O. (2010). Approximate Bayesian Computation (ABC) in practice. *Trends in Ecology & Evolution*, *25*(7), 410–418. https://doi.org/10.1016/j.tree.2010.04.001

Csillery, K., Lemaire, L., Francois, O., & Blum, M. (2015). *abc: Tools for Approximate Bayesian Computation (ABC)*. Retrieved from https://CRAN.R-project.org/package=abc

Currat, M., Ruedi, M., Petit, R. J., & Excoffier, L. (2008). The hidden side of invasions: Massive introgression by local genes. *Evolution*, *62*(8), 1908–1920. https://doi.org/10.1111/j.1558-5646.2008.00413.x

Currie, D. J. (1991). Energy and large-scale patterns of animal and plant species richness. *The American Naturalist*, *137*(1), 27–49.

Davidson, A. D., Hamilton, M. J., Boyer, A. G., Brown, J. H., & Ceballos, G. (2009). Multiple ecological pathways to extinction in mammals. *Proceedings of the National Academy of Sciences*, *106*(26), 10702–10705. https://doi.org/10.1073/pnas.0901956106

DeAngelis, D. L., & Grimm, V. (2014). Individual-based models in ecology after four decades. *F1000Prime Reports*, *6*, 39. https://doi.org/10.12703/P6-39

DeAngelis, D. L., & Mooij, W. M. (2005). Individual-based modeling of ecological and evolutionary processes. *Annual Review of Ecology, Evolution, and Systematics*, *36*(1), 147–168. https://doi.org/10.1146/annurev.ecolsys.36.102003.152644

DelGiudice, G. D., Moen, R. A., Singer, F. J., & Riggs, M. R. (2001). Winter nutritional restriction and simulated body condition of Yellowstone elk and bison before and after the fires of 1988. *Wildlife Monographs*, (147), 1–60.

DelGiudice, G. D., Singer, F. J., Seal, U. S., & Bowser, G. (1994). Physiological responses of Yellowstone bison to winter nutritional deprivation. *The Journal of Wildlife Management*, *58*(1), 24–34. https://doi.org/10.2307/3809545

Descombes, P., Gaboriau, T., Albouy, C., Heine, C., Leprieur, F., & Pellissier, L. (2018). Linking species diversification to palaeo-environmental changes: A process-based modelling

approach. *Global Ecology and Biogeography*, *27*(2), 233–244.

https://doi.org/10.1111/geb.12683

Díaz, S., Zafra-Calvo, N., Purvis, A., Verburg, P. H., Obura, D., Leadley, P., … Zanne, A. E.

(2020). Set ambitious goals for biodiversity and sustainability. *Science*, *370*(6515), 411–

413. https://doi.org/10.1126/science.abe1530

Dietl, G. P., Kidwell, S. M., Brenner, M., Burney, D. A., Flessa, K. W., Jackson, S. T., & Koch, P.

L. (2015). Conservation paleobiology: Leveraging knowledge of the past to inform

conservation and restoration. *Annual Review of Earth and Planetary Sciences*, *43*(1), 79–

103. https://doi.org/10.1146/annurev-earth-040610-133349

Díez-del-Molino, D., Sánchez-Barreiro, F., Barnes, I., Gilbert, M. T. P., & Dalén, L. (2018).

Quantifying temporal genomic erosion in endangered species. *Trends in Ecology &

Evolution*, *33*(3), 176–185. https://doi.org/10.1016/j.tree.2017.12.002

Diniz-Filho, J. A. F., Souza, K. S., Bini, L. M., Loyola, R., Dobrovolski, R., Rodrigues, J. F. M., …

Gouveia, S. (2019). A macroecological approach to evolutionary rescue and adaptation to

climate change. *Ecography*, *42*(6), 1124–1141. https://doi.org/10.1111/ecog.04264

Directorate-General for Environment (European Commission). (2021). *EU biodiversity strategy

for 2030: Bringing nature back into our lives*. LU: Publications Office of the European

Union. Retrieved from https://data.europa.eu/doi/10.2779/677548

Doebeli, M., & Dieckmann, U. (2003). Speciation along environmental gradients. *Nature*,

421(6920), 259–264. https://doi.org/10.1038/nature01274

Dolédec, S., Chessel, D., & Gimaret-Carpentier, C. (2000). Niche separation in community analysis: A new method. *Ecology*, *81*(10), 2914–2927. https://doi.org/10.1890/0012-9658(2000)081[2914:NSICAA]2.0.CO;2

Dunham, A. E., Akçakaya, H. R., & Bridges, T. S. (2006). Using Scalar Models for Precautionary Assessments of Threatened Species. *Conservation Biology*, *20*(5), 1499–1506. https://doi.org/10.1111/j.1523-1739.2006.00474.x

Dunning, J. B., Stewart, D. J., Danielson, B. J., Noon, B. R., Root, T. L., Lamberson, R. H., & Stevens, E. E. (1995). Spatially explicit population models: Current forms and future uses. *Ecological Applications*, *5*(1), 3–11. https://doi.org/10.2307/1942045

Dytham, C. (2009). Evolved dispersal strategies at range margins. *Proceedings of the Royal Society B-Biological Sciences*, *276*(1661), 1407–1413. https://doi.org/10.1098/rspb.2008.1535

Ellis, E. C., Gauthier, N., Goldewijk, K. K., Bird, R. B., Boivin, N., Díaz, S., … Watson, J. E. M. (2021). People have shaped most of terrestrial nature for at least 12,000 years. *Proceedings of the National Academy of Sciences*, *118*(17), e2023483118. https://doi.org/10.1073/pnas.2023483118

Eriksson, A., Betti, L., Friend, A. D., Lycett, S. J., Singarayer, J. S., von Cramon-Taubadel, N., … Manica, A. (2012). Late Pleistocene climate change and the global expansion of anatomically modern humans. *Proceedings of the National Academy of Sciences of the United States of America*, *109*(40), 16089–16094. https://doi.org/10.1073/pnas.1209494109

Erm, P., & Phillips, B. L. (2019). Evolution transforms pushed waves into pulled waves. *The American Naturalist*, *195*(3), E87–E99. https://doi.org/10.1086/707324

Faurby, S., & Svenning, J.-C. (2015). Historic and prehistoric human-driven extinctions have reshaped global mammal diversity patterns. *Diversity and Distributions*, *21*(10), 1155–1166. https://doi.org/10.1111/ddi.12369

Fenner, J. N. (2005). Cross-cultural estimation of the human generation interval for use in genetics-based population divergence studies. *American Journal of Physical Anthropology*, *128*(2), 415–423. https://doi.org/10.1002/ajpa.20188

Ferrier, S., Ninan, K. N., Leadley, P., & Alkemade, R. (2016). *The Methodological Assessment Report on Scenarios and Models of Biodiversity and Ecosystem Services*. IPBES.

Foley, J. A., Prentice, I. C., Ramankutty, N., Levis, S., Pollard, D., Sitch, S., & Haxeltine, A. (1996). An integrated biosphere model of land surface processes, terrestrial carbon balance, and vegetation dynamics. *Global Biogeochemical Cycles*, *10*(4), 603–628. https://doi.org/10.1029/96GB02692

Fordham, D. A., Akçakaya, H. R., Alroy, J., Saltré, F., Wigley, T. M. L., & Brook, B. W. (2016). Predicting and mitigating future biodiversity loss using long-term ecological proxies. *Nature Climate Change*, *6*(10), 909–916. https://doi.org/10.1038/nclimate3086

Fordham, D. A., Bertelsmeier, C., Brook, B. W., Early, R., Neto, D., Brown, S. C., ... Araújo, M. B. (2018). How complex should models be? Comparing correlative and mechanistic range dynamics models. *Global Change Biology*, *24*(3), 1357–1370. https://doi.org/10.1111/gcb.13935

Fordham, D. A., Brook, B. W., Moritz, C., & Nogués-Bravo, D. (2014). Better forecasts of range dynamics using genetic data. *Trends in Ecology & Evolution*, *29*(8), 436–443. https://doi.org/10.1016/j.tree.2014.05.007

Fordham, D. A., Brown, S. C., Akçakaya, H. R., Brook, B. W., Haythorne, S., Manica, A., …

   Nogues-Bravo, D. (2022). Process-explicit models reveal pathway to extinction for woolly

   mammoth using pattern-oriented validation. *Ecology Letters*, *25*(1), 125–137.

   https://doi.org/10.1111/ele.13911

Fordham, D. A., Haythorne, S., Brown, S. C., Buettel, J. C., & Brook, B. W. (2021). poems: R

   package for simulating species' range dynamics using pattern-oriented validation. *Methods

   in Ecology and Evolution*, *12*(12), 2364–2371. https://doi.org/10.1111/2041-210X.13720

Fordham, D. A., Jackson, S. T., Brown, S. C., Huntley, B., Brook, B. W., Dahl-Jensen, D., …

   Nogues-Bravo, D. (2020). Using paleo-archives to safeguard biodiversity under climate

   change. *Science*, *369*(6507), eabc5654. https://doi.org/10.1126/science.abc5654

Fordham, D. A., Mellin, C., Russell, B. D., Akçakaya, R. H., Bradshaw, C. J. A., Aiello-Lammens,

   M. E., … Brook, B. W. (2013). Population dynamics can be more important than

   physiological limits for determining range shifts under climate change. *Global Change

   Biology*, *19*(10), 3224–3237. https://doi.org/10.1111/gcb.12289

Fordham, D. A., Saltré, F., Brown, S. C., Mellin, C., & Wigley, T. M. L. (2018). Why decadal to

   century timescale palaeoclimate data are needed to explain present-day patterns of

   biological diversity and change. *Global Change Biology*, *24*(3), 1371–1381.

   https://doi.org/10.1111/gcb.13932

Fordham, D. A., Saltré, F., Haythorne, S., Wigley, T. M., Otto-Bliesner, B. L., Chan, K. C., &

   Brook, B. W. (2017). PaleoView: A tool for generating continuous climate projections

   spanning the last 21 000 years at regional and global scales. *Ecography*, *40*(11), 1348–1358.

Frankham, R. (2010). Challenges and opportunities of genetic approaches to biological

    conservation. *Biological Conservation*, *143*(9), 1919–1927.

    https://doi.org/10.1016/j.biocon.2010.05.011

French, J. C., Riris, P., Fernandéz-López de Pablo, J., Lozano, S., & Silva, F. (2021). A manifesto

    for palaeodemography in the twenty-first century. *Philosophical Transactions of the Royal*

    Society B: Biological Sciences, *376*(1816), 20190707.

    https://doi.org/10.1098/rstb.2019.0707

Fuller, J. A., Garrott, R. A., & White, P. J. (2007). Emigration and density dependence in

    Yellowstone bison. *The Journal of Wildlife Management*, *71*(6), 1924–1933.

Fulton, E. A., Link, J. S., Kaplan, I. C., Savina-Rolland, M., Johnson, P., Ainsworth, C., … Smith,

    D. C. (2011). Lessons in modelling and management of marine ecosystems: The Atlantis

    experience: Lessons learnt with Atlantis. *Fish and Fisheries*, *12*(2), 171–188.

    https://doi.org/10.1111/j.1467-2979.2011.00412.x

Gallagher, C. A., Chudzinska, M., Larsen-Gray, A., Pollock, C. J., Sells, S. N., White, P. J. C., &

    Berger, U. (2021). From theory to practice in pattern-oriented modelling: Identifying and

    using empirical patterns in predictive models. *Biological Reviews*, *96*(5), 1868–1888.

    https://doi.org/10.1111/brv.12729

Gates, C. C., & Larter, N. C. (1990). Growth and dispersal of an erupting large herbivore

    population in northern Canada: The Mackenzie wood bison (Bison bison athabascae).

    Arctic, *43*(3), 231–238.

Gelman, A., Hwang, J., & Vehtari, A. (2014). Understanding predictive information criteria for Bayesian models. *Statistics and Computing*, *24*(6), 997–1016. https://doi.org/10.1007/s11222-013-9416-2

Giampoudakis, K., Marske, K. A., Borregaard, M. K., Ugan, A., Singarayer, J. S., Valdes, P. J., … Nogués-Bravo, D. (2017). Niche dynamics of Palaeolithic modern humans during the settlement of the Palaearctic. *Global Ecology and Biogeography*, *26*(3), 359–370. https://doi.org/10.1111/geb.12543

Goebel, T. (2002). The "microblade adaptation" and recolonization of Siberia during the Late Upper Pleistocene. *Archaeological Papers of the American Anthropological Association*, *12*(1), 117–131. https://doi.org/10.1525/ap3a.2002.12.1.117

Goebel, T., Waters, M. R., & O'Rourke, D. H. (2008). The late Pleistocene dispersal of modern humans in the Americas. *Science*, *319*(5869), 1497–1502. https://doi.org/10.1126/science.1153569

Gotelli, N. J., Anderson, M. J., Arita, H. T., Chao, A., Colwell, R. K., Connolly, S. R., … Willig, M. R. (2009). Patterns and causes of species richness: A general simulation model for macroecology. *Ecology Letters*, *12*(9), 873–886. https://doi.org/10.1111/j.1461-0248.2009.01353.x

Grimm, V., & Railsback, S. F. (2012). Pattern-oriented modelling: A 'multi-scope' for predictive systems ecology. *Philosophical Transactions of the Royal Society B: Biological Sciences*, *367*(1586), 298–310. https://doi.org/10.1098/rstb.2011.0180

Grimm, V., Revilla, E., Berger, U., Jeltsch, F., Mooij, W. M., Railsback, S. F., ... DeAngelis, D. L.

    (2005). Pattern-oriented modeling of agent-based complex systems: Lessons from ecology.

    Science, *310*(5750), 987–991. https://doi.org/10.1126/science.1116681

Gritti, E. S., Cassignat, C., Flores, O., Bonnefille, R., Chalie, F., Guiot, J., & Jolly, D. (2010).

    Simulated effects of a seasonal precipitation change on the vegetation in tropical Africa.

    Climate of the Past, *6*(2), 169–178. https://doi.org/10.5194/cp-6-169-2010

Groucutt, H. S., Petraglia, M. D., Bailey, G., Scerri, E. M. L., Parton, A., Clark-Balzan, L., ... Scally,

    A. (2015). Rethinking the dispersal of Homo sapiens out of Africa. *Evolutionary*

    Anthropology: Issues, News, and Reviews, *24*(4), 149–164.

    https://doi.org/10.1002/evan.21455

Guthrie, R. D. (2006). New carbon dates link climatic change with human colonization and

    Pleistocene extinctions. *Nature*, *441*(7090), 207–209.

    https://doi.org/10.1038/nature04604

Guthrie, R. Dale. (1989). *Frozen Fauna of the Mammoth Steppe: The Story of Blue Babe*. Chicago,

    USA: University of Chicago Press.

Hagen, O., Flück, B., Fopp, F., Cabral, J. S., Hartig, F., Pontarp, M., ... Pellissier, L. (2021).

    gen3sis: A general engine for eco-evolutionary simulations of the processes that shape

    Earth's biodiversity. *PLOS Biology*, *19*(7), e3001340.

    https://doi.org/10.1371/journal.pbio.3001340

Haile, J., Froese, D. G., MacPhee, R. D. E., Roberts, R. G., Arnold, L. J., Reyes, A. V., ...

    Willerslev, E. (2009). Ancient DNA reveals late survival of mammoth and horse in interior

Alaska. *Proceedings of the National Academy of Sciences*, *106*(52), 22352–22357. https://doi.org/10.1073/pnas.0912510106

Halley, J. M., & Iwasa, Y. (2011). Neutral theory as a predictor of avifaunal extinctions after habitat loss. *Proceedings of the National Academy of Sciences of the United States of America*, *108*(6), 2316–2321. https://doi.org/10.1073/pnas.1011217108

Halley, J. M., Sgardeli, V., & Triantis, K. A. (2014). Extinction debt and the species–area relationship: A neutral perspective. *Global Ecology and Biogeography*, *23*(1), 113–123.

Hamby, D. M. (1994). A review of techniques for parameter sensitivity analysis of environmental models. *Environmental Monitoring and Assessment*, *32*(2), 135–154. https://doi.org/10.1007/BF00547132

Hanski, I. (1989). Metapopulation dynamics: Does it help to have more of the same? *Trends in Ecology & Evolution*, *4*(4), 113–114. https://doi.org/10.1016/0169-5347(89)90061-X

Hanski, I. (1998). Metapopulation dynamics. *Nature*, *396*(6706), 41–49. https://doi.org/10.1038/23876

Hanski, I., Pakkala, T., Kuussaari, M., & Lei, G. (1995). Metapopulation persistence of an endangered butterfly in a fragmented landscape. *Oikos*, *72*(1), 21–28. https://doi.org/10.2307/3546033

Harfoot, M. B., Newbold, T., Tittensor, D. P., Emmott, S., Hutton, J., Lyutsarev, V., … Purves, D. W. (2014). Emergent global patterns of ecosystem structure and function from a mechanistic general ecosystem model. *PLOS Biology*, *12*(4), e1001841. https://doi.org/10.1371/journal.pbio.1001841

Haythorne, S., Pilowsky, J. A., Brown, S., & Fordham, D. (2021). *paleopop: Pattern-Oriented Modeling Framework for Coupled Niche-Population Paleo-Climatic Models*. Retrieved from https://CRAN.R-project.org/package=paleopop

Hedrick, P. W. (2009). Conservation Genetics and North American Bison (Bison bison). *Journal of Heredity*, *100*(4), 411–420. https://doi.org/10.1093/jhered/esp024

Heino, M., & Hanski, I. (2001). Evolution of migration rate in a spatially realistic metapopulation model. *The American Naturalist*, *157*(5), 495–511. https://doi.org/10.1086/319927

Heptner, V. G., Nasimovich, A. A., & Bannikov, A. G. (1961). *Mammals of the Soviet Union Volume I: Artiodactyla and Perissodactyla* (Vol. 1). Moscow, Russia: Vysshaya Shkola Publishers.

Hofman-Kamińska, E., Bocherens, H., Drucker, D. G., Fyfe, R. M., Gumiński, W., Makowiecki, D., ... Kowalczyk, R. (2019). Adapt or die—Response of large herbivores to environmental changes in Europe during the Holocene. *Global Change Biology*, *25*(9), 2915–2930. https://doi.org/10.1111/gcb.14733

Holden, P. B., Edwards, N. R., Rangel, T. F., Pereira, E. B., Tran, G. T., & Wilkinson, R. D. (2019). PALEO-PGEM v1.0: A statistical emulator of Pliocene–Pleistocene climate. *Geoscientific Model Development*, *12*(12), 5137–5155. https://doi.org/10.5194/gmd-12-5137-2019

Holt, R. D. (2003). On the evolutionary ecology of species' ranges. *Evolutionary Ecology Research*, *5*(2), 159–178.

Houghton, J. T., Ding, Y., Griggs, D. J., Noguer, M., Linden, P. J. van der, Dai, X., ... Johnson, C. A. (2001). *Climate Change 2001: The Scientific Basis: Contribution of Working Group I to*

the Third Assessment Report of the Intergovernmental Panel on Climate Change.

Cambridge University Press.

Hovestadt, T., & Poethke, H. J. (2005). Dispersal and establishment: Spatial patterns and species–

area relationships. *Diversity and Distributions*, *11*(4), 333–340.

https://doi.org/10.1111/j.1366-9516.2005.00161.x

Hubbell, S. P. (2001). *The unified neutral theory of biodiversity and biogeography*. Princeton, NJ,

USA: Princeton University Press.

Humboldt, A. von. (1877). *Personal Narrative of Travels to the Equinoctial Regions of the New*

Continent During the Years 1799-1804. G. Bell.

Hurtt, G. C., Chini, L., Sahajpal, R., Frolking, S., Bodirsky, B. L., Calvin, K., … Zhang, X. (2020).

Harmonization of global land use change and management for the period 850–2100

(LUH2) for CMIP6. *Geoscientific Model Development*, *13*(11), 5425–5464.

https://doi.org/10.5194/gmd-13-5425-2020

IUCN-CEM. (2016). *The IUCN Red List of Ecosystems* (No. Version 2016-1). Retrieved from

http://iucnrle.org/

Jones, P. W. (1999). First- and second-order conservative remapping schemes for grids in spherical

coordinates. *Monthly Weather Review*, *127*(9), 2204–2210.

https://doi.org/10.1175/1520-0493(1999)127<2204:FASOCR>2.0.CO;2

Julien, M.-A., Bocherens, H., Burke, A., Drucker, D. G., Patou-Mathis, M., Krotova, O., & Péan,

S. (2012). Were European steppe bison migratory? 18O, 13C and Sr intra-tooth isotopic

variations applied to a palaeoethological reconstruction. *Quaternary International*, *271*,

106–119. https://doi.org/10.1016/j.quaint.2012.06.011

Jung, T. S. (2017). Extralimital movements of reintroduced bison (Bison bison): Implications for potential range expansion and human-wildlife conflict. *European Journal of Wildlife Research*, *63*(2), 35. https://doi.org/10.1007/s10344-017-1094-5

Kaplan, J. O., Bigelow, N. H., Prentice, I. C., Harrison, S. P., Bartlein, P. J., Christensen, T. R., … Lozhkin, A. V. (2003). Climate change and Arctic ecosystems: 2. Modeling, paleodata-model comparisons, and future projections. *Journal of Geophysical Research: Atmospheres*, *108*(D19), 8171. https://doi.org/10.1029/2002JD002559

Kearney, M., & Porter, W. (2009). Mechanistic niche modelling: Combining physiological and spatial data to predict species' ranges. *Ecology Letters*, *12*(4), 334–350.

Keith, S. A., & Connolly, S. R. (2013). Effects of diversity-dependent colonization-extinction dynamics on the mid-domain effect. *Global Ecology and Biogeography*, *22*(7), 773–783. https://doi.org/10.1111/geb.12035

Kerley, G. I. H., Cromsigt, J. P. G. M., & Kowalczyk, R. (2020). European bison conservation cannot afford to ignore alternative hypotheses: A commentary on Perzanowski et al. (2019). *Animal Conservation*, *23*(5), 479–481. https://doi.org/10.1111/acv.12605

Kerley, G. I. H., Kowalczyk, R., & Cromsigt, J. P. G. M. (2012). Conservation implications of the refugee species concept and the European bison: King of the forest or refugee in a marginal habitat? *Ecography*, *35*(6), 519–529. https://doi.org/10.1111/j.1600-0587.2011.07146.x

Kim, H., Rosa, I. M. D., Alkemade, R., Leadley, P., Hurtt, G., Popp, A., … Pereira, H. M. (2018). A protocol for an intercomparison of biodiversity and ecosystem services models using harmonized land-use and climate scenarios. *Geoscientific Model Development*, *11*(11), 4537–4562. https://doi.org/10.5194/gmd-11-4537-2018

Kimura, M. (1979). The neutral theory of molecular evolution. *Scientific American*, *241*(5), 98–129.

Kingman, J. F. C. (1982). On the genealogy of large populations. *Journal of Applied Probability*, *19*, 27–43. https://doi.org/10.2307/3213548

Kirby, K., & Watkins, C. (2015). *Europe's Changing Woods and Forests: From Wildwood to Managed Landscapes*. CABI.

Kirkpatrick, M., & Barton, N. H. (1997). Evolution of a species' range. *The American Naturalist*, *150*(1), 1–23.

Kitagawa, K., Julien, M.-A., Krotova, O., Bessudnov, A. A., Sablin, M. V., Kiosak, D., … Patou-Mathis, M. (2018). Glacial and post-glacial adaptations of hunter-gatherers: Investigating the late Upper Paleolithic and Mesolithic subsistence strategies in the southern steppe of Eastern Europe. *Quaternary International*, *465*, 192–209. https://doi.org/10.1016/j.quaint.2017.01.005

Klein Goldewijk, K., Beusen, A., Doelman, J., & Stehfest, E. (2017). Anthropogenic land use estimates for the Holocene – HYDE 3.2. *Earth System Science Data*, *9*(2), 927–953. https://doi.org/10.5194/essd-9-927-2017

Klopfstein, S., Currat, M., & Excoffier, L. (2006). The fate of mutations surfing on the wave of a range expansion. *Molecular Biology and Evolution*, *23*(3), 482–490. https://doi.org/10.1093/molbev/msj057

Knowles, L. L. (2009). Statistical phylogeography. *Annual Review of Ecology, Evolution, and Systematics*, *40*(1), 593–612. https://doi.org/10.1146/annurev.ecolsys.38.091206.095702

Knowles, L. L., & Alvarado-Serrano, D. F. (2010). Exploring the population genetic consequences of the colonization process with spatio-temporally explicit models: Insights from coupled ecological, demographic and genetic models in montane grasshoppers. *Molecular Ecology*, *19*(17), 3727–3745. https://doi.org/10.1111/j.1365-294X.2010.04702.x

Koch, P. L., & Barnosky, A. D. (2006). Late Quaternary extinctions: State of the debate. *Annual Review of Ecology, Evolution, and Systematics*, *37*(1), 215–250. https://doi.org/10.1146/annurev.ecolsys.34.011802.132415

Koetke, L. J., Duarte, A., & Weckerly, F. W. (2020). Comparing the Ricker and θ-logistic models for estimating elk population growth. *Natural Resource Modeling*, *33*(4), e12270. https://doi.org/10.1111/nrm.12270

Koons, D. N., Terletzky, P., Adler, P. B., Wolfe, M. L., Ranglack, D., Howe, F. P., ... du Toit, J. T. (2012). Climate and density-dependent drivers of recruitment in plains bison. *Journal of Mammalogy*, *93*(2), 475–481. https://doi.org/10.1644/11-MAMM-A-281.1

Kramer, A. M., Dennis, B., Liebhold, A. M., & Drake, J. M. (2009). The evidence for Allee effects. *Population Ecology*, *51*(3), 341–354. https://doi.org/10.1007/s10144-009-0152-6

Krasińska, M., & Krasiński, Z. (2013). *European Bison: The Nature Monograph*. Springer Science & Business Media.

Kuemmerle, T., Hickler, T., Olofsson, J., Schurgers, G., & Radeloff, V. C. (2012). Reconstructing range dynamics and range fragmentation of European bison for the last 8000 years. *Diversity and Distributions*, *18*(1), 47–59. https://doi.org/10.1111/j.1472-4642.2011.00849.x

Kutzbach, J., Gallimore, R., Harrison, S., Behling, P., Selin, R., & Laarif, F. (1998). Climate and biome simulations for the past 21,000 years. *Quaternary Science Reviews*, *17*(6), 473–506. https://doi.org/10.1016/S0277-3791(98)00009-2

Laliberte, A. S., & Ripple, W. J. (2004). Range contractions of North American carnivores and ungulates. *BioScience*, *54*(2), 123–138. https://doi.org/10.1641/0006-3568(2004)054[0123:RCONAC]2.0.CO;2

Leadley, P. (2010). *Biodiversity Scenarios: Projections of 21st Century Change in Biodiversity, and Associated Ecosystem Services: a Technical Report for the Global Biodiversity Outlook 3*. UNEP/Earthprint.

Leibold, M. A., Holyoak, M., Mouquet, N., Amarasekare, P., Chase, J. M., Hoopes, M. F., … Gonzalez, A. (2004). The metacommunity concept: A framework for multi-scale community ecology. *Ecology Letters*, *7*(7), 601–613. https://doi.org/10.1111/j.1461-0248.2004.00608.x

Lemaire, L., Jay, F., Lee, I.-H., Csilléry, K., & Blum, M. G. B. (2016, January 15). *Goodness-of-fit statistics for approximate Bayesian computation*. arXiv. https://doi.org/10.48550/arXiv.1601.04096

Leprieur, F., Descombes, P., Gaboriau, T., Cowman, P. F., Parravicini, V., Kulbicki, M., … Pellissier, L. (2016). Plate tectonics drive tropical reef biodiversity dynamics. *Nature Communications*, *7*, 11461. https://doi.org/10.1038/ncomms11461

Levins, R. (1969). Some demographic and genetic consequences of environmental heterogeneity for biological control. *Bulletin of the Entomological Society of America*, *15*(3), 237–240. https://doi.org/10.1093/besa/15.3.237

Liaw, A., & Wiener, M. (2002). Classification and regression by randomForest. *R News*, *2*(3), 18–22.

Lieth, H. (1975). Modeling the Primary Productivity of the World. In H. Lieth & R. H. Whittaker (Eds.), *Primary Productivity of the Biosphere* (pp. 237–263). Berlin, Heidelberg: Springer. https://doi.org/10.1007/978-3-642-80913-2_12

Liu, H., Prugnolle, F., Manica, A., & Balloux, F. (2006). A geographically explicit genetic model of worldwide human-settlement history. *The American Journal of Human Genetics*, *79*(2), 230–237. https://doi.org/10.1086/505436

Liu, Z., Otto-Bliesner, B. L., He, F., Brady, E. C., Tomas, R., Clark, P. U., … Cheng, J. (2009). Transient simulation of last deglaciation with a new mechanism for Bølling–Allerød warming. *Science*, *325*(5938), 310–314. https://doi.org/10.1126/science.1171041

Loreau, M. (2010). Linking biodiversity and ecosystems: Towards a unifying ecological theory. *Philosophical Transactions of the Royal Society B: Biological Sciences*, *365*(1537), 49–60. https://doi.org/10.1098/rstb.2009.0155

Lorenzen, E. D., Nogués-Bravo, D., Orlando, L., Weinstock, J., Binladen, J., Marske, K. A., … Willerslev, E. (2011). Species-specific responses of Late Quaternary megafauna to climate and humans. *Nature*, *479*(7373), 359–364. https://doi.org/10.1038/nature10574

MacArthur, R. H., & Wilson, E. O. (1967). *The theory of island biogeography*. Princeton, NJ, USA: Princeton University Press.

Mace, G. M., Barrett, M., Burgess, N. D., Cornell, S. E., Freeman, R., Grooten, M., & Purvis, A. (2018). Aiming higher to bend the curve of biodiversity loss. *Nature Sustainability*, *1*(9), 448–451. https://doi.org/10.1038/s41893-018-0130-0

Macias-Fauria, M., Jepson, P., Zimov, N., & Malhi, Y. (2020). Pleistocene Arctic megafaunal

ecological engineering as a natural climate solution? *Philosophical Transactions of the Royal*

Society B: Biological Sciences, *375*(1794), 20190122.

https://doi.org/10.1098/rstb.2019.0122

Mangel, M. (2002). The important role of theory in conservation biology. *Conservation Biology*,

16(3), 843–844. https://doi.org/10.1046/j.1523-1739.2002.01638.x

Mann, D. H., Groves, P., Gaglioti, B. V., & Shapiro, B. A. (2019). Climate-driven ecological

stability as a globally shared cause of Late Quaternary megafaunal extinctions: The Plaids

and Stripes Hypothesis. *Biological Reviews*, *94*(1), 328–352.

https://doi.org/10.1111/brv.12456

Markova, A. K., Puzachenko, A. Yu., van Kolfschoten, T., Kosintsev, P. A., Kuznetsova, T. V.,

Tikhonov, A. N., … Kuitems, M. (2015). Changes in the Eurasian distribution of the musk

ox (Ovibos moschatus) and the extinct bison (Bison priscus) during the last 50 ka BP.

Quaternary International, *378*, 99–110. https://doi.org/10.1016/j.quaint.2015.01.020

Marra, G., & Wood, S. N. (2011). Practical variable selection for generalized additive models.

Computational Statistics & Data Analysis, *55*(7), 2372–2387.

https://doi.org/10.1016/j.csda.2011.02.004

Mathewson, P. D., Moyer-Horner, L., Beever, E. A., Briscoe, N. J., Kearney, M., Yahn, J. M., &

Porter, W. P. (2017). Mechanistic variables can enhance predictive models of endotherm

distributions: The American pika under current, past, and future climates. *Global Change*

Biology, *23*(3), 1048–1064. https://doi.org/10.1111/gcb.13454

May, F., Wiegand, T., Lehmann, S., & Huth, A. (2016). Do abundance distributions and species

aggregation correctly predict macroecological biodiversity patterns in tropical forests?

Global Ecology and Biogeography, *25*(5), 575–585. https://doi.org/10.1111/geb.12438

McClanahan, T. R. (1995). A coral reef ecosystem-fisheries model: Impacts of fishing intensity

and catch selection on reef structure and processes. *Ecological Modelling*, *80*(1), 1–19.

https://doi.org/10.1016/0304-3800(94)00042-G

Metcalf, J. L., Prost, S., Nogues-Bravo, D., DeChaine, E. G., Anderson, C., Batra, P., ... Guralnick,

R. P. (2014). Integrating multiple lines of evidence into historical biogeography hypothesis

testing: A Bison bison case study. *Proceedings of the Royal Society B-Biological Sciences*,

281(1777), 20132782. https://doi.org/10.1098/rspb.2013.2782

Mittermeier, R. A., Turner, W. R., Larsen, F. W., Brooks, T. M., & Gascon, C. (2011). Global

biodiversity conservation: The critical role of hotspots. In *Biodiversity hotspots* (pp. 3–22).

New York, NY, USA: Springer.

Mondal, P., & Southworth, J. (2010). Evaluation of conservation interventions using a cellular

automata-Markov model. *Forest Ecology and Management*, *260*(10), 1716–1725.

https://doi.org/10.1016/j.foreco.2010.08.017

Mumby, P. J. (2006). The impact of exploiting grazers (Scaridae) on the dynamics of Caribbean

coral reefs. *Ecological Applications*, *16*(2), 747–769. https://doi.org/10.1890/1051-

0761(2006)016[0747:TIOEGS]2.0.CO;2

Murton, J. B., Edwards, M. E., Lozhkin, A. V., Anderson, P. M., Savvinov, G. N., Bakulina, N., ...

Zanina, O. G. (2017). Preliminary paleoenvironmental analysis of permafrost deposits at

Batagaika megaslump, Yana Uplands, northeast Siberia. *Quaternary Research*, *87*(2), 314–330. https://doi.org/10.1017/qua.2016.15

Mysterud, A., Bartoń, K. A., Jędrzejewska, B., Krasiński, Z. A., Niedzialkowska, M., Kamler, J. F., … Stenseth, N. C. (2007). Population ecology and conservation of endangered megafauna: The case of European bison in Białowieża Primeval Forest, Poland. *Animal Conservation*, *10*(1), 77–87.

Naeem, S. (2002). Ecosystem consequences of biodiversity loss: The evolution of a paradigm. *Ecology*, *83*(6), 1537–1552. https://doi.org/10.1890/0012-9658(2002)083[1537:ECOBLT]2.0.CO;2

Neukom, R., & Gergis, J. (2012). Southern Hemisphere high-resolution palaeoclimate records of the last 2000 years. *The Holocene*, *22*(5), 501–524.

Nicholson, C. (2010). Between Menace and Utility: Handguns in Early Sixteenth-Century Bohemia. *Bad Behaviour*, *3*, 40–51. University of Kent, Canterbury, UK.

Nogués-Bravo, D. (2009). Predicting the past distribution of species climatic niches. *Global Ecology and Biogeography*, *18*(5), 521–531. https://doi.org/10.1111/j.1466-8238.2009.00476.x

Nogués-Bravo, D., Rodríguez-Sánchez, F., Orsini, L., de Boer, E., Jansson, R., Morlon, H., … Jackson, S. T. (2018). Cracking the code of biodiversity responses to past climate change. *Trends in Ecology & Evolution*, *33*(10), 765–776. https://doi.org/10.1016/j.tree.2018.07.005

Oliveira, S., Oehler, F., San-Miguel-Ayanz, J., Camia, A., & Pereira, J. M. C. (2012). Modeling spatial patterns of fire occurrence in Mediterranean Europe using multiple regression and

random forest. *Forest Ecology and Management*, *275*, 117–129.

https://doi.org/10.1016/j.foreco.2012.03.003

O'Neill, B. C., Tebaldi, C., Van Vuuren, D. P., Eyring, V., Friedlingstein, P., Hurtt, G., ... Lowe, J.

(2016). The scenario model intercomparison project (ScenarioMIP) for CMIP6.

Geoscientific Model Development, *9*(9), 3461–3482.

Owens, I. P. F., & Bennett, P. M. (2000). Ecological basis of extinction risk in birds: Habitat loss

versus human persecution and introduced predators. *Proceedings of the National Academy

of Sciences*, *97*(22), 12144–12148. https://doi.org/10.1073/pnas.200223397

Pacifici, M., Santini, L., Di Marco, M., Baisero, D., Francucci, L., Marasini, G. G., ... Rondinini,

C. (2013). Generation length for mammals. *Nature Conservation-Bulgaria*, *5*, 87–94.

https://doi.org/10.3897/natureconservation.5.5734

Parnikoza, I., & Kaluzhna, M. (2009). Primary search of woodlands suitable for free ranging Bison

bonasus populations in Ukraine. *European Bison Conservation Newsletter*, *2*, 47–53.

Pearson, R. G., Stanton, J. C., Shoemaker, K. T., Aiello-Lammens, M. E., Ersts, P. J., Horning, N.,

... Akçakaya, H. R. (2014). Life history and spatial traits predict extinction risk due to

climate change. *Nature Climate Change*, *4*(3), 217–221.

https://doi.org/10.1038/nclimate2113

Peltier, W. R. (2004). Global glacial isostasy and the surface of the ice-age earth: The ICE-5G

(VM2) Model and GRACE. *Annual Review of Earth and Planetary Sciences*, *32*(1), 111–

149. https://doi.org/10.1146/annurev.earth.32.082503.144359

Pereira, H. M., & Daily, G. C. (2006). Modeling biodiversity dynamics in countryside landscapes. *Ecology*, *87*(8), 1877–1885. https://doi.org/10.1890/0012-9658(2006)87[1877:MBDICL]2.0.CO;2

Pereira, H. M., Daily, G. C., & Roughgarden, J. (2004). A framework for assessing the relative vulnerability of species to land-use change. *Ecological Applications*, *14*(3), 730–742. https://doi.org/10.1890/02-5405

Perzanowski, K., Bleyhl, B., Olech, W., & Kuemmerle, T. (2020). Connectivity or isolation? Identifying reintroduction sites for multiple conservation objectives for wisents in Poland. *Animal Conservation*, *23*(2), 212–221. https://doi.org/10.1111/acv.12530

Perzanowski, Kajetan, Klich, D., & Olech, W. (2022). European Union needs urgent strategy for the European bison. *Conservation Letters*. https://doi.org/10.1111/conl.12923

Petzoldt, T. (2019). *growthrates: Estimate Growth Rates from Experimental Data*. Retrieved from https://CRAN.R-project.org/package=growthrates

Phillips, B. L. (2012). Range shift promotes the formation of stable range edges. *Journal of Biogeography*, *39*(1), 153–161. https://doi.org/10.1111/j.1365-2699.2011.02597.x

Pilowsky, J. A., Brown, S. C., & Fordham, D. A. (2022). *Model code for Causes of range collapse and extinction in the wild of European bison*. Zenodo. https://doi.org/10.5281/zenodo.7297867

Pilowsky, J. A., Brown, S. C., Llamas, B., van Loenen, A., Kowalczyk, R., Hofman-Kamińska, E., … Fordham, D. A. (2022a). *Process-explicit simulations of European bison abundance in Eurasia from 21,000 years ago to 1500 CE* [Data set]. figshare. https://doi.org/10.6084/M9.FIGSHARE.21624369

Pilowsky, J. A., Brown, S. C., Llamas, B., van Loenen, A., Kowalczyk, R., Hofman-Kamińska, E., … Fordham, D. A. (2022b). *Quality-controlled carbon-14 dates of European bison (Bison bonasus) fossils* [Data set]. figshare. https://doi.org/10.6084/M9.FIGSHARE.17059592.V2

Pilowsky, J. A., Colwell, R. K., Rahbek, C., & Fordham, D. A. (2022a). *Dichotomous key of process-explicit models of biodiversity*. figshare. Retrieved from https://doi.org/10.6084/m9.figshare.19441655

Pilowsky, J. A., Colwell, R. K., Rahbek, C., & Fordham, D. A. (2022b). Process-explicit models reveal the structure and dynamics of biodiversity patterns. *Science Advances*, *8*(31), eabj2271. https://doi.org/10.1126/sciadv.abj2271

Pilowsky, J. A., Haythorne, S., Brown, S. C., Krapp, M., Armstrong, E., Brook, B. W., … Fordham, D. A. (2021). *Quality-controlled carbon-14 dates of steppe bison (Bison priscus) fossils* [Data set]. figshare. https://doi.org/10.6084/M9.FIGSHARE.17059592.V2

Pilowsky, J. A., Haythorne, S., Brown, S. C., Krapp, M., Armstrong, E., Brook, B. W., … Fordham, D. A. (2022c). Range and extinction dynamics of the steppe bison in Siberia: A pattern-oriented modelling approach. *Global Ecology and Biogeography*, *31*(12), 2483–2497. https://doi.org/10.1111/geb.13601

Pilowsky, J. A., Manica, A., Brown, S. C., Rahbek, C., & Fordham, D. A. (2022d). *Process-explicit simulations of human migration in North America 19,000 years ago to present* [Data set]. figshare. https://doi.org/10.6084/M9.FIGSHARE.20078630

Pilowsky, J. A., Manica, A., Brown, S., Rahbek, C., & Fordham, D. A. (2022e). Simulations of human migration into North America are more sensitive to demography than choice of

palaeoclimate model. *Ecological Modelling*, *473*(2022), 110115.

https://doi.org/10.1016/j.ecolmodel.2022.110115

Plumb, G. E., Kowalczyk, R., & Hernandez-Blanco, J. A. (2020). IUCN Red List of Threatened

Species: Bison bonasus. *IUCN Red List of Threatened Species*. Retrieved from

https://www.iucnredlist.org/species/2814/45156279

Plumb, G. E., White, P. J., Coughenour, M. B., & Wallen, R. L. (2009). Carrying capacity,

migration, and dispersal in Yellowstone bison. *Biological Conservation*, *142*(11), 2377–

2387. https://doi.org/10.1016/j.biocon.2009.05.019

Pontarp, M., Bunnefeld, L., Cabral, J. S., Etienne, R. S., Fritz, S. A., Gillespie, R., … Hurlbert, A.

H. (2019). The latitudinal diversity gradient: Novel understanding through mechanistic

eco-evolutionary models. *Trends in Ecology & Evolution*, *34*(3), 211–223.

https://doi.org/10.1016/j.tree.2018.11.009

Porter, W. P., & Mitchell, J. W. (2006). *United States Patent No. US7155377B2*. Retrieved from

https://patents.google.com/patent/US7155377B2/en

Price, M. H., Capriles, J. M., Hoggarth, J. A., Bocinsky, K., Ebert, C. E., & Jones, J. H. (2020, July

4). *End-to-end Bayesian analysis of 14C dates reveals new insights into lowland Maya

demography*. bioRxiv. https://doi.org/10.1101/2020.07.02.185256

Prohaska, A., Racimo, F., Schork, A. J., Sikora, M., Stern, A. J., Ilardo, M., … Willerslev, E. (2019).

Human disease variation in the light of population genomics. *Cell*, *177*(1), 115–131.

https://doi.org/10.1016/j.cell.2019.01.052

Prowse, T. A. A., Bradshaw, C. J. A., Delean, S., Cassey, P., Lacy, R. C., Wells, K., … Brook, B. W. (2016). An efficient protocol for the global sensitivity analysis of stochastic ecological models. *Ecosphere*, *7*(3), e01238. https://doi.org/10.1002/ecs2.1238

Pucek, Z. (1991). History of the European bison and problems of its protection and management. *Global Trends in Wildlife Management Trans. 18th IUGB Congress, Krakow 1987*, 19–39.

Pucek, Z., Belousova, I. P., Krasinska, M., Krasinski, Z. A., & Olech, W. (2004). *European bison: Status survey and conservation action plan*. IUCN. Retrieved from https://portals.iucn.org/library/node/8501

Pushkina, D., & Raia, P. (2008). Human influence on distribution and extinctions of the late Pleistocene Eurasian megafauna. *Journal of Human Evolution*, *54*(6), 769–782. https://doi.org/10.1016/j.jhevol.2007.09.024

Radwan, J., Demiaszkiewicz, A. W., Kowalczyk, R., Lachowicz, J., Kawałko, A., Wójcik, J. M., … Babik, W. (2010). An evaluation of two potential risk factors, MHC diversity and host density, for infection by an invasive nematode Ashworthius sidemi in endangered European bison (Bison bonasus). *Biological Conservation*, *143*(9), 2049–2053. https://doi.org/10.1016/j.biocon.2010.05.012

Raghavan, M., Steinrücken, M., Harris, K., Schiffels, S., Rasmussen, S., DeGiorgio, M., … Willerslev, E. (2015). Genomic evidence for the Pleistocene and recent population history of Native Americans. *Science*, *349*(6250), aab3884. https://doi.org/10.1126/science.aab3884

Rambaut, A., Drummond, A. J., Xie, D., Baele, G., & Suchard, M. A. (2018). Posterior Summarization in Bayesian Phylogenetics Using Tracer 1.7. *Systematic Biology*, *67*(5), 901–904. https://doi.org/10.1093/sysbio/syy032

Ramos, A., Petit, O., Longour, P., Pasquaretta, C., & Sueur, C. (2016). Space Use and Movement Patterns in a Semi-Free-Ranging Herd of European Bison (Bison bonasus). *PLOS ONE*, *11*(2), e0147404. https://doi.org/10.1371/journal.pone.0147404

Ramsey, C. B. (2017). OxCal Program, Version 4.3. *Oxford Radiocarbon Accelerator Unit: University of Oxford*.

Rangel, T. F., Diniz-Filho, J. A. F., & Colwell, R. K. (2007). Species richness and evolutionary niche dynamics: A spatial pattern–oriented simulation experiment. *The American Naturalist*, *170*(4), 602–616. https://doi.org/10.1086/521315

Rangel, T. F., Edwards, N. R., Holden, P. B., Diniz-Filho, J. A. F., Gosling, W. D., Coelho, M. T. P., … Colwell, R. K. (2018). Modeling the ecology and evolution of biodiversity: Biogeographical cradles, museums, and graves. *Science*, *361*(6399), eaar5452. https://doi.org/10.1126/science.aar5452

Rantanen, M., Karpechko, A. Yu., Lipponen, A., Nordling, K., Hyvärinen, O., Ruosteenoja, K., … Laaksonen, A. (2022). The Arctic has warmed nearly four times faster than the globe since 1979. *Communications Earth & Environment*, *3*(1), 168. https://doi.org/10.1038/s43247-022-00498-3

Rasmussen, M., Guo, X., Wang, Y., Lohmueller, K. E., Rasmussen, S., Albrechtsen, A., … Willerslev, E. (2011). An Aboriginal Australian genome reveals separate human dispersals into Asia. *Science*, *334*(6052), 94–98. https://doi.org/10.1126/science.1211177

Ray, N., Currat, M., Berthier, P., & Excoffier, L. (2005). Recovering the geographic origin of early modern humans by realistic and spatially explicit simulations. *Genome Research*, *15*(8), 1161–1167. https://doi.org/10.1101/gr.3708505

Reimer, P. J., Austin, W. E. N., Bard, E., Bayliss, A., Blackwell, P. G., Bronk Ramsey, C., … Talamo, S. (2020). The IntCal20 Northern Hemisphere Radiocarbon Age Calibration Curve (0-55 cal kBP). *Radiocarbon*, *62*(4), 725–757. https://doi.org/10.1017/RDC.2020.41

Reimer, P. J., Bard, E., Bayliss, A., Beck, J. W., Blackwell, P. G., Ramsey, C. B., … Friedrich, M. (2013). IntCal13 and Marine13 radiocarbon age calibration curves 0–50,000 years cal BP. *Radiocarbon*, *55*(4), 1869–1887. https://doi.org/10.2458/azu_js_rc.55.16947

Rice, J. A., Miller, T. J., Rose, K. A., Crowder, L. B., Marschall, E. A., Trebitz, A. S., & DeAngelis, D. L. (2003). Growth rate variation and larval survival: Inferences from an individual-based size-dependent predation model. *Canadian Journal of Fisheries and Aquatic Sciences*, *50*(1), 133–142. (Ottawa, Canada). https://doi.org/10.1139/f93-015

Ricker, W. E. (1954). Stock and recruitment. *Journal of the Fisheries Research Board of Canada*, *11*(5), 559–623. https://doi.org/10.1139/f54-039

Rieb, J. T., Chaplin-Kramer, R., Daily, G. C., Armsworth, P. R., Böhning-Gaese, K., Bonn, A., … Bennett, E. M. (2017). When, where, and how nature matters for ecosystem services: Challenges for the next generation of ecosystem service models. *BioScience*, *67*(9), 820–833. https://doi.org/10.1093/biosci/bix075

Risch, A. C., Heiri, C., & Bugmann, H. (2005). Simulating structural forest patterns with a forest gap model: A model evaluation. *Ecological Modelling*, *181*(2–3), 161–172.

Root-Bernstein, M., Gooden, J., & Boyes, A. (2018). Rewilding in practice: Projects and policy. *Geoforum*, *97*, 292–304. https://doi.org/10.1016/j.geoforum.2018.09.017

Roycroft, E., MacDonald, A. J., Moritz, C., Moussalli, A., Miguez, R. P., & Rowe, K. C. (2021). Museum genomics reveals the rapid decline and extinction of Australian rodents since European settlement. *Proceedings of the National Academy of Sciences*, *118*(27), e2021390118. https://doi.org/10.1073/pnas.2021390118

Rutherford, S., Mann, M. E., Osborn, T. J., Briffa, K. R., Jones, P. D., Bradley, R. S., & Hughes, M. K. (2005). Proxy-based Northern Hemisphere surface temperature reconstructions: Sensitivity to method, predictor network, target season, and target domain. *Journal of Climate*, *18*(13), 2308–2329.

Rykiel, E. J. (1996). Testing ecological models: The meaning of validation. *Ecological Modelling*, *90*(3), 229–244. https://doi.org/10.1016/0304-3800(95)00152-2

Sakschewski, B., von Bloh, W., Boit, A., Poorter, L., Peña-Claros, M., Heinke, J., ... Thonicke, K. (2016). Resilience of Amazon forests emerges from plant trait diversity. *Nature Climate Change*, *6*(11), 1032–1036. https://doi.org/10.1038/nclimate3109

Sales, L. P., Galetti, M., Carnaval, A., Monsarrat, S., Svenning, J.-C., & Pires, M. M. (2022). The effect of past defaunation on ranges, niches, and future biodiversity forecasts. *Global Change Biology*, *28*(11), 3683–3693. https://doi.org/10.1111/gcb.16145

Samojlik, T., Fedotova, A., Borowik, T., & Kowalczyk, R. (2019). Historical data on European bison management in Białowieża Primeval Forest can contribute to a better contemporary conservation of the species. *Mammal Research*, *64*(4), 543–557.

Scheiter, S., Langan, L., & Higgins, S. I. (2013). Next-generation dynamic global vegetation models: Learning from community ecology. *New Phytologist*, *198*(3), 957–969. https://doi.org/10.1111/nph.12210

Semenov, M. A., & Barrow, E. M. (2002). *LARS-WG: A stochastic weather generator for use in climate impact studies*.

Shapiro, B., Drummond, A. J., Rambaut, A., Wilson, M. C., Matheus, P. E., Sher, A. V., … Cooper, A. (2004). Rise and fall of the Beringian steppe bison. *Science*, *306*(5701), 1561–1565. https://doi.org/10.1126/science.1101074

Signor, P. W., Lipps, J. H., Silver, L. T., & Schultz, P. H. (1982). Sampling bias, gradual extinction patterns, and catastrophes in the fossil record. *Geological Implications of Impacts of Large Asteroids and Comets on the Earth*, *190*, 291–296.

Singarayer, J. S., & Valdes, P. J. (2010). High-latitude climate sensitivity to ice-sheet forcing over the last 120kyr. *Quaternary Science Reviews*, *29*(1), 43–55. https://doi.org/10.1016/j.quascirev.2009.10.011

Sipko, T. P. (2009). European bison in Russia–past, present and future. *European Bison Conservation Newsletter*, *2*, 148–159.

Sisson, S. A., Fan, Y., & Beaumont, M. (2018). *Handbook of Approximate Bayesian Computation*. CRC Press.

Sitch, S., Huntingford, C., Gedney, N., Levy, P. E., Lomas, M., Piao, S. L., … Woodward, F. I. (2008). Evaluation of the terrestrial carbon cycle, future plant geography and climate-carbon cycle feedbacks using five Dynamic Global Vegetation Models (DGVMs). *Global Change Biology*, *14*(9), 2015–2039. https://doi.org/10.1111/j.1365-2486.2008.01626.x

Skeels, A., & Cardillo, M. (2019). Reconstructing the geography of speciation from contemporary biodiversity data. *The American Naturalist*, *193*(2), 240–255. https://doi.org/10.1086/701125

Snell, R. S. (2014). Simulating long-distance seed dispersal in a dynamic vegetation model. *Global Ecology and Biogeography*, *23*(1), 89–98. https://doi.org/10.1111/geb.12106

Soberón, J., & Nakamura, M. (2009). Niches and distributional areas: Concepts, methods, and assumptions. *Proceedings of the National Academy of Sciences*, *106*(Supplement 2), 19644–19650. https://doi.org/10.1073/pnas.0901637106

Solomon, S., Qin, D., Manning, M., Chen, Z., Marquis, M., Averyt, K. B., … Miller, H. L. (2007). *Climate Change 2007: The Physical Science Basis. Contribution of Working Group I to the Fourth Assessment Report of the Intergovernmental Panel on Climate Change.* Cambridge University Press. Retrieved from http://www.cabdirect.org/cabdirect/abstract/20083115509

Soubrier, J., Gower, G., Chen, K., Richards, S. M., Llamas, B., Mitchell, K. J., … Cooper, A. (2016). Early cave art and ancient DNA record the origin of European bison. *Nature Communications*, *7*(1), 13158. https://doi.org/10.1038/ncomms13158

Stanton, J. C., Shoemaker, K. T., Pearson, R. G., & Akçakaya, H. R. (2015). Warning times for species extinctions due to climate change. *Global Change Biology*, *21*(3), 1066–1077. https://doi.org/10.1111/gcb.12721

Steele, J., Adams, J., & Sluckin, T. (1998). Modelling Paleoindian dispersals. *World Archaeology*, *30*(2), 286–305. https://doi.org/10.1080/00438243.1998.9980411

Stegen, J. C., Lin, X., Fredrickson, J. K., & Konopka, A. E. (2015). Estimating and mapping

    ecological processes influencing microbial community assembly. *Frontiers in Microbiology*,

    6, 370. https://doi.org/10.3389/fmicb.2015.00370

Stein, M. (1987). Large sample properties of simulations using Latin hypercube sampling.

    Technometrics, *29*(2), 143–151. https://doi.org/10.1080/00401706.1987.10488205

Strobl, C., Boulesteix, A.-L., Zeileis, A., & Hothorn, T. (2007). Bias in random forest variable

    importance measures: Illustrations, sources and a solution. *BMC Bioinformatics*, *8*(1), 25.

    https://doi.org/10.1186/1471-2105-8-25

Stuart, A. J. (2015). Late Quaternary megafaunal extinctions on the continents: A short review.

    Geological Journal, *50*(3), 338–363. https://doi.org/10.1002/gj.2633

Suchard, M. A., Lemey, P., Baele, G., Ayres, D. L., Drummond, A. J., & Rambaut, A. (2018).

    Bayesian phylogenetic and phylodynamic data integration using BEAST 1.10. *Virus*

    Evolution, *4*(1), vey016. https://doi.org/10.1093/ve/vey016

Sukumaran, J., Economo, E. P., & Knowles, L. L. (2016). Machine learning biogeographic

    processes from biotic patterns: A new trait-dependent dispersal and diversification model

    with model choice by simulation-trained discriminant analysis. *Systematic Biology*, *65*(3),

    525–545. https://doi.org/10.1093/sysbio/syv121

Tallavaara, M., Eronen, J. T., & Luoto, M. (2018). Productivity, biodiversity, and pathogens

    influence the global hunter-gatherer population density. *Proceedings of the National*

    Academy of Sciences, *115*(6), 1232–1237.

Taylor, G., Canessa, S., Clarke, R. H., Ingwersen, D., Armstrong, D. P., Seddon, P. J., & Ewen, J. G. (2017). Is Reintroduction Biology an Effective Applied Science? *Trends in Ecology & Evolution*, *32*(11), 873–880. https://doi.org/10.1016/j.tree.2017.08.002

Theodoridis, S., Fordham, D. A., Brown, S. C., Li, S., Rahbek, C., & Nogues-Bravo, D. (2020). Evolutionary history and past climate change shape the distribution of genetic diversity in terrestrial mammals. *Nature Communications*, *11*(1), 2557. https://doi.org/10.1038/s41467-020-16449-5

Thulke, H.-H., Grimm, V., Müller, M. S., Staubach, C., Tischendorf, L., Wissel, C., & Jeltsch, F. (1999). From pattern to practice: A scaling-down strategy for spatially explicit modelling illustrated by the spread and control of rabies. *Ecological Modelling*, *117*(2), 179–202. https://doi.org/10.1016/S0304-3800(98)00198-7

Timmermann, A., & Friedrich, T. (2016). Late Pleistocene climate drivers of early human migration. *Nature*, *538*(7623), 92–95. https://doi.org/10.1038/nature19365

Tomlinson, S., Lomolino, M. V., Woinarski, J. C. Z., Murphy, B. P., Reed, E., Johnson, C. N., … Fordham, D. A. (2022). *Reconstructing mechanisms of extinctions to guide mammal conservation biogeography*. in review.

Tuck, G., Glendining, M. J., Smith, P., House, J. I., & Wattenbach, M. (2006). The potential distribution of bioenergy crops in Europe under present and future climate. *Biomass and Bioenergy*, *30*(3), 183–197. https://doi.org/10.1016/j.biombioe.2005.11.019

United Nations Conference on Environment and Development: Convention on Biological Diversity. (1992). *International Legal Materials*, *31*(4), 822–841.

Urban, M. C., Bocedi, G., Hendry, A. P., Mihoub, J.-B., Pe'er, G., Singer, A., … Travis, J. M. J. (2016). Improving the forecast for biodiversity under climate change. *Science*, *353*(6304), aad8466. https://doi.org/10.1126/science.aad8466

Urban, Mark C., & De Meester, L. (2009). Community monopolization: Local adaptation enhances priority effects in an evolving metacommunity. *Proceedings of the Royal Society B: Biological Sciences*, *276*(1676), 4129–4138. https://doi.org/10.1098/rspb.2009.1382

Urban, N. A., & Matter, S. F. (2018). Metapopulation mirages: Problems parsing process from pattern. *Ecological Modelling*, *375*, 20–29. https://doi.org/10.1016/j.ecolmodel.2018.02.012

Vahdati, A. R., Weissmann, J. D., Timmermann, A., Ponce de León, M. S., & Zollikofer, C. P. E. (2019). Drivers of Late Pleistocene human survival and dispersal: An agent-based modeling and machine learning approach. *Quaternary Science Reviews*, *221*, 105867. https://doi.org/10.1016/j.quascirev.2019.105867

Valdes, P. J., Armstrong, E., Badger, M. P. S., Bradshaw, C. D., Bragg, F., Crucifix, M., … Williams, J. H. T. (2017). The BRIDGE HadCM3 family of climate models: HadCM3@Bristol v1.0. *Geoscientific Model Development*, *10*(10), 3715–3743. https://doi.org/10.5194/gmd-10-3715-2017

van der Vaart, E., Beaumont, M. A., Johnston, A. S. A., & Sibly, R. M. (2015). Calibration and evaluation of individual-based models using Approximate Bayesian Computation. *Ecological Modelling*, *312*, 182–190. https://doi.org/10.1016/j.ecolmodel.2015.05.020

van der Valk, T., Pečnerová, P., Díez-del-Molino, D., Bergström, A., Oppenheimer, J., Hartmann, S., … Dalén, L. (2021). Million-year-old DNA sheds light on the genomic history of mammoths. *Nature*, *591*, 265–269. https://doi.org/10.1038/s41586-021-03224-9

VanDerWal, J., Shoo, L. P., Johnson, C. N., Williams, S. E., Mooij, A. E. W. M., & DeAngelis, E. D. L. (2009). Abundance and the Environmental Niche: Environmental Suitability Estimated from Niche Models Predicts the Upper Limit of Local Abundance. *The American Naturalist*, *174*(2), 282–291. https://doi.org/10.1086/600087

Vasil'ev, S. A. (2003). Faunal exploitation, subsistence practices and Pleistocene extinctions in Paleolithic Siberia. *Deinsea*, *9*(1), 513–556.

Wallace, A. R. (1863). On the physical geography of the Malay archipelago. *The Journal of the Royal Geographical Society of London*, *33*, 217–234. https://doi.org/10.2307/1798448

Wang, Yucheng, Pedersen, M. W., Alsos, I. G., De Sanctis, B., Racimo, F., Prohaska, A., … Willerslev, E. (2021). Late Quaternary dynamics of Arctic biota from ancient environmental genomics. *Nature*, *600*, 86–92. https://doi.org/10.1038/s41586-021-04016-x

Wang, Yue, Porter, W., Mathewson, P. D., Miller, P. A., Graham, R. W., & Williams, J. W. (2018). Mechanistic modeling of environmental drivers of woolly mammoth carrying capacity declines on St. Paul Island. *Ecology*, *306*, 70. https://doi.org/10.1002/ecy.2524

Waters, M. R., & Stafford, T. W. (2007). Redefining the age of Clovis: Implications for the peopling of the Americas. *Science*, *315*(5815), 1122–1126.

Watts, M. J., Fordham, D. A., Akçakaya, H. R., Aiello-Lammens, M. E., & Brook, B. W. (2013). Tracking shifting range margins using geographical centroids of metapopulations weighted

by population density. *Ecological Modelling*, *269*, 61–69.

https://doi.org/10.1016/j.ecolmodel.2013.08.010

Weaver, A. J., Saenko, O. A., Clark, P. U., & Mitrovica, J. X. (2003). Meltwater Pulse 1A from

Antarctica as a trigger of the Bølling-Allerød warm interval. *Science*, *299*(5613), 1709–

1713. https://doi.org/10.1126/science.1081002

Welch, M. C., Kwan, P. W., & Sajeev, A. S. M. (2014). Applying GIS and high performance agent-

based simulation for managing an Old World Screwworm fly invasion of Australia. *Acta

Tropica*, *138*, S82–S93. https://doi.org/10.1016/j.actatropica.2014.03.021

Welker, F. (2018). Palaeoproteomics for human evolution studies. *Quaternary Science Reviews*,

190, 137–147. https://doi.org/10.1016/j.quascirev.2018.04.033

White, A., Cannell, M. G. R., & Friend, A. D. (2000). The high-latitude terrestrial carbon sink: A

model analysis. *Global Change Biology*, *6*(2), 227–245. https://doi.org/10.1046/j.1365-

2486.2000.00302.x

White, T. A., Perkins, S. E., Heckel, G., & Searle, J. B. (2013). Adaptive evolution during an

ongoing range expansion: The invasive bank vole (Myodes glareolus) in Ireland. *Molecular

Ecology*, *22*(11), 2971–2985. https://doi.org/10.1111/mec.12343

Whittaker, R. J., Triantis, K. A., & Ladle, R. J. (2008). A general dynamic theory of oceanic island

biogeography. *Journal of Biogeography*, *35*(6), 977–994.

Wilson, D. (1992). Complex interactions in metacommunities, with implications for biodiversity

and higher levels of selection. *Ecology*, *73*(6), 1984–2000.

https://doi.org/10.2307/1941449

Wißing, C., Rougier, H., Baumann, C., Comeyne, A., Crevecoeur, I., Drucker, D. G., … Bocherens, H. (2019). Stable isotopes reveal patterns of diet and mobility in the last Neandertals and first modern humans in Europe. *Scientific Reports*, *9*(1), 4433. https://doi.org/10.1038/s41598-019-41033-3

Wood, S. N. (2017). *Generalized Additive Models: An Introduction with R, Second Edition* (2nd ed.). New York: Chapman and Hall/CRC. https://doi.org/10.1201/9781315370279

Wood, S. N. (2022). *mgcv: Mixed GAM Computation Vehicle with Automatic Smoothness Estimation* [R]. Retrieved from https://CRAN.R-project.org/package=mgcv

Yeager, S. G., Shields, C. A., Large, W. G., & Hack, J. J. (2006). The Low-Resolution CCSM3. *Journal of Climate*, *19*(11), 2545–2566. https://doi.org/10.1175/JCLI3744.1

Yoder, A. D., Poelstra, J. W., Tiley, G. P., & Williams, R. C. (2018). Neutral theory is the foundation of conservation genetics. *Molecular Biology and Evolution*, *35*(6), 1322–1326. https://doi.org/10.1093/molbev/msy076

Yoshida, T., Jones, L. E., Ellner, S. P., Fussmann, G. F., & Hairston, N. G. (2003). Rapid evolution drives ecological dynamics in a predator–prey system. *Nature*, *424*(6946), 303–306. https://doi.org/10.1038/nature01767

Young, J. C., Waylen, K. A., Sarkki, S., Albon, S., Bainbridge, I., Balian, E., … Watt, A. (2014). Improving the science-policy dialogue to meet the challenges of biodiversity conservation: Having conversations rather than talking at one-another. *Biodiversity and Conservation*, *23*(2), 387–404. https://doi.org/10.1007/s10531-013-0607-0

Zhu, D., Ciais, P., Chang, J., Krinner, G., Peng, S., Viovy, N., … Zimov, S. (2018). The large mean body size of mammalian herbivores explains the productivity paradox during the Last

Glacial Maximum. *Nature Ecology & Evolution*, *2*(4), 640–649.

https://doi.org/10.1038/s41559-018-0481-y

Zhu, D., Galbraith, E. D., Reyes-García, V., & Ciais, P. (2021). Global hunter-gatherer population

densities constrained by influence of seasonality on diet composition. *Nature Ecology &*

Evolution, *5*(11), 1536–1545. https://doi.org/10.1038/s41559-021-01548-3

Zimov, S. A., Chuprynin, V. I., Oreshko, A. P., Chapin, F. S., Reynolds, J. F., & Chapin, M. C.

(1995). Steppe-Tundra Transition: A Herbivore-Driven Biome Shift at the End of the

Pleistocene. *The American Naturalist*, *146*(5), 765–794. https://doi.org/10.1086/285824

APPENDIX: PUBLISHED EDITIONS OF CHAPTERS I, II, AND III

ECOLOGY

Process-explicit models reveal the structure and dynamics of biodiversity patterns

Julia A. Pilowsky[1,2]*, Robert K. Colwell[2,3,4,5], Carsten Rahbek[2,6,7,8], Damien A. Fordham[1,2,6]*

With ever-growing data availability and computational power at our disposal, we now have the capacity to use process-explicit models more widely to reveal the ecological and evolutionary mechanisms responsible for spatiotemporal patterns of biodiversity. Most research questions focused on the distribution of diversity cannot be answered experimentally, because many important environmental drivers and biological constraints operate at large spatiotemporal scales. However, we can encode proposed mechanisms into models, observe the patterns they produce in virtual environments, and validate these patterns against real-world data or theoretical expectations. This approach can advance understanding of generalizable mechanisms responsible for the distributions of organisms, communities, and ecosystems in space and time, advancing basic and applied science. We review recent developments in process-explicit models and how they have improved knowledge of the distribution and dynamics of life on Earth, enabling biodiversity to be better understood and managed through a deeper recognition of the processes that shape genetic, species, and ecosystem diversity.

INTRODUCTION

The patterns of biodiversity we observe at different temporal and spatial scales result from the key evolutionary and ecological processes of speciation, ecological interaction, adaptation, movement, and extinction, acting separately or in concert (*1*). These processes can be stochastic or forced by natural drivers of environmental change (e.g., plate tectonics and paleoclimate change) or by human drivers, such as invasive species, land use, pollution, and harvesting (*2*). However, the interplay among these processes and their drivers is complex (*3*), and different sets of circumstances can produce similar patterns. This ambiguity has made it difficult to discern which ecological and evolutionary processes and drivers have shaped current-day patterns of biodiversity based on empirical data alone (*4*). Fortunately, key advances in process-explicit models over the past 50 years are now enabling the processes and drivers responsible for contemporary patterns of biodiversity to be disentangled in space and time. Here, we show how these advances in biodiversity modeling are revealing the generalizable mechanisms responsible for the distributions, abundances, and diversity of life on Earth and how they are strengthening basic and applied science, resulting in improved guidelines for the management of nature.

Process-explicit models in ecology and evolution represent the dynamics of a biological system as explicit functions of the events that drive change in that system (*5*). By causally linking current patterns to the past events that produced them (Fig. 1), process-explicit models help achieve a deeper understanding of the chain of causality leading to current-day spatial patterns of biodiversity, including human diversity (*6*). These models allow contested ecological and evolutionary theories to be assessed, enabling biodiversity to be understood and managed more effectively through a deeper recognition of the processes of genetic-, species-, and ecosystem-level endangerment and collapse (*7*).

Models that are process-explicit provide platforms for directly integrating ecological and evolutionary theory into conservation and environmental science (*8*), enhancing knowledge of the effects of biodiversity and its drivers on the functioning of species and ecosystems (*9*), and strengthening projections of biodiversity in a changing world (*10*), resulting in improvements to conservation management and policy (*11*). For example, process-explicit models derived from the neutral theory of biodiversity (*12*) were some of the first models to show that rare species are less frequent in island communities than in adjacent mainland communities (*13*), providing important new information to conservation policy-makers regarding vulnerability to human-driven environmental change (*14*). Process-explicit models of the neutral theory of molecular evolution, which simulate rates of genetic drift as products of effective population size and generation length (*15*), enabled conservation geneticists to study the behavior of neutral alleles to better understand why extinction risk increases for species with small population sizes (*16*). A stronger integration of ecological and evolutionary theory in conservation science using process-explicit modeling promises to further link the evolution of species traits at the individual level to the dynamics of communities and the overall functioning of ecosystems (*17*). Together, these advances are improving knowledge of how climatic and environmental changes have shaped species assemblages in the past, strengthening confidence in projections of biodiversity's future (*7*).

Recent reviews have established important benefits of process-explicit modeling approaches in macroecology (*5*, *18*), ecosystem ecology (*17*), conservation science (*10*), and related disciplines. These studies highlight a need to use process-explicit models for managing ecosystems (*17*), improving theory (*5*, *18*), and predicting species' range shifts under ongoing and future climate change (*10*). However, there has been no synthesis of the broader uses of process-explicit models for unraveling the biological mechanisms responsible for shaping patterns of biodiversity in space and time in response to

[1]The Environment Institute, School of Biological Sciences, University of Adelaide, Adelaide, Australia. [2]Center for Macroecology, Evolution, and Climate, GLOBE Institute, University of Copenhagen, Copenhagen, Denmark. [3]University of Colorado Museum of Natural History, Boulder, CO, USA. [4]Department of Ecology and Evolutionary Biology, University of Connecticut, Storrs, CT, USA. [5]Departmento de Ecología, Universidade Federal de Goiás, Goiás, Brazil. [6]Center for Global Mountain Biodiversity, GLOBE Institute, University of Copenhagen, Copenhagen, Denmark. [7]Institute of Ecology, Peking University, Beijing, China. [8]Danish Institute for Advanced Study, University of Southern Denmark, Odense, Denmark.
*Corresponding author. Email: julia.pilowsky@adelaide.edu.au (J.A.P.); damien.fordham@adelaide.edu.au (D.A.F.)
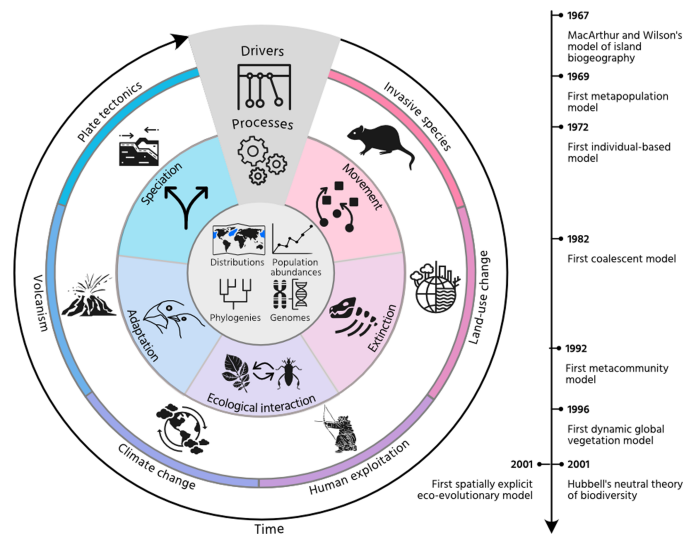
Fig. 1. Modeling the mechanisms that govern the structure and dynamics of biodiversity. Process-explicit models can simulate changes in species distributions, population abundance, phylogenies, and genomes based on evolutionary and ecological processes (movement, extinction, ecological interaction, adaptation, and speciation) and drivers of environmental change (invasive species, land-use change, human exploitation, climate change, volcanism, and plate tectonics). Processes and drivers are ordered clockwise according to the temporal scale at which they operate. The timeline shows breakthrough developments in process-explicit models of biodiversity up to 2001. Image of finches adapted from Charles Darwin.

Earth system drivers of environmental change. Here, we identify key properties of the structure and dynamics of biodiversity first uncovered by process-explicit models, many of which are now guiding the future management of biodiversity.

The application of process-explicit models of spatiotemporal diversity in ecology and evolution can be traced back to MacArthur and Wilson's model of island biogeography (Fig. 1), which linked patterns of biodiversity on islands to processes of movement (colonization) and local extinction (*19*). Early process-explicit models include metapopulation models (*20*), which are used frequently today for conservation planning (*21*) and for informing species' extinction risk (*22*). These models, which were initially limited to interactions and movements of subpopulations of a species, have now been expanded to include demographic and environmental stochasticity (*23*), species interactions, and community-level dynamics (*24*), allowing interlinked patches with different community compositions to be simulated and their dynamics understood. The first individual-based models followed shortly after the development of metapopulation models, permitting the inclusion of individual variation in dispersal behavior, genotype, competitive ability, and life history traits in simulations of population change (*25*). Today, individual-based models are used frequently not only for the management of specific populations, including fisheries stocks (*26*), but also to answer paradigmatic questions about community assembly, food web ecology, and zoonotic disease (*27*).

In the 1980s, development of coalescent models of simulated genealogies (*28*) enabled the diversification of lineages to be studied in space and time (*29*), giving rise to the field of phylogeography. These early models showed how lineages can diverge without geographic isolation, illustrating potential mechanisms of sympatric speciation. More recently, they have been used to show how pathogens

can rapidly evolve as they spread through a network of hosts (*30*), enriching fundamental understanding of past, current, and future disease dynamics (*31*). The latest generation of coalescent models can reconstruct genomic erosion in endangered species (*32*) and rapid directional selection (*33*) in response to subcentennial periods of environmental change.

The 1990s saw the advent of dynamic global vegetation models (DGVMs): process-explicit models that replicate global patterns of vegetation by simulating the growth and mortality of plant functional groups under different climatic conditions (*34*). This development enabled predictions of the capacity of the biosphere to store carbon (*35*) and produce crops (*36*) under current and future climate conditions. Today, DGVMs are being used to inform regional-to-global policies on food security, greenhouse gas emission scenarios, and the maintenance of ecosystem services (*37*). They can account for the effects of herbivory and fire regimes on vegetation structure (*38*), allowing the impacts of competing land management strategies to be compared (*11, 39*).

In the early 2000s, models that integrate the evolutionary processes of speciation and adaptation with the ecological processes of movement, extinction, and interaction began to be developed. By providing a mechanistic understanding of the physical and biological processes that shape Earth's biodiversity, these models have aimed to illuminate the origins of biodiversity through direct tests of competing scenarios (*40*). Many of these theories, established long ago by early naturalists (*41–43*), could not be directly tested with simpler process-explicit models or phenomenological approaches. Today, eco-evolutionary simulators provide opportunities to achieve new levels of realism in projections of assemblage dynamics under past and future global change (*44*).

The most recent developments in process-explicit modeling, which simulate multiple processes and patterns of biodiversity using complex mathematical components and logical algorithms, have resulted from a rapid rise in computational power following the turn of the 21st century (*44–46*). This advance, coupled with wider access to large ecological, genomics, and satellite-based remote sensing datasets, has enabled the generation and increasingly frequent application of a broad variety of process-explicit models in ecological and evolutionary studies, parameterized or validated with more data and based on more-realistic assumptions than previously possible. Despite this accelerated expansion, the development and application of process-explicit models have followed an opportunistic path, with little strategy or coordination (*47*).

To address this current shortfall, we provide here a much-needed review of recent developments in process-explicit models, outlining considerations for researchers who contemplate building process-explicit models to evaluate the mechanisms that govern the structure and dynamics of past, present, and future biodiversity. We scrutinize the processes of codifying theory into models, identify key scientific advances from simulation outputs, and illustrate with examples how process-explicit models can safeguard future biodiversity.

PROCESS VERSUS PATTERN

Narrative accounts (*42*), correlative studies (*48*), and experiments (*49*) lead to hypotheses about the underlying causes of biodiversity change, and theoretical models demonstrate possible mechanisms (*50*). In comparison, spatiotemporal process-explicit models can directly assess and disentangle competing theories for drivers of

biodiversity, helping to elucidate interactions among underlying ecological and evolutionary mechanisms and drivers (*5*). An example of competing theories for biodiversity dynamics and resultant patterns is the contrast between niche (*51*) and neutral theory (*12*). The former focuses on the role of environmental determinism, while the latter focuses on contingent and stochastic determinants of biodiversity dynamics.

Process-explicit models differ from pattern-based models by generating predictions based on explicit causal relationships between environmental drivers and ecological and evolutionary responses, rather than inferring implicit causal relationships based on correlations between observed and modeled patterns (*52*). A physiological model, for example, is process-explicit if it characterizes the occurrence of a tree species in a landscape based on where the tree can minimize water stress. In contrast, a model is phenomenological (or correlative) if it maps the tree's occurrence based on the statistical relationship between annual precipitation and observations of occurrence, because no processes linking precipitation and fitness are specified. The process-explicit model allows patterns (e.g., a contraction of the tree species' range) to be connected to processes that cause them (e.g., an increase in seedling mortality in a drought), while the phenomenological model cannot explicitly link a changing pattern to a causative agent (*53*). Similarly, a phenomenological model that hindcasts plant functional types on the landscape based on correlations between climate and pollen records cannot link pattern and process in the same way as a DGVM that hindcasts plant nutrient cycling and competition over the same period (*54*).

Phenomenological models and experimental observations sometimes find strong or unexpected correlations that can suggest the mechanisms that produce them. Proposed mechanisms can be used to build process-explicit models that can then be tested against observed patterns (*7*). Studies of the effect of biodiversity on ecosystem function offer an example of this ontology (Fig. 2). Effects of depauperate plant richness on ecosystem function were first observed empirically in experimental chambers and plots, which led to the proposed mechanism of niche complementarity, which, in turn, became the basis for mechanistic models of ecosystem function (*55*). In this way, phenomenological and experimental analysis can provide important insights into the workings of nature that can be tested using process-explicit models.

REVEALING STRUCTURE AND DYNAMICS

Process-explicit models can operate at diverse levels of biological organization, ranging from the gene to the ecosystem (Fig. 3). The level of biological organization that is simulated—genetic, species, or ecosystem diversity—has, to date, dictated the number and combination of possible biotic processes that are modeled (*7*). The five primary processes responsible for the origin, structure, and dynamics of biodiversity are speciation, ecological interaction, adaptation, movement, and extinction (including population extirpation). In this context, ecological interactions encompass both interspecific species interactions (competition, predation, herbivory, parasitism, and mutualism) and ecosystem processes (nutrient cycling, photosynthesis, stability, etc.).

Ecosystem- and population-level models were the earliest process-explicit models. They generally include ecological interaction and local- to range-wide extinction processes (Fig. 3), but not movement, speciation, or adaptation. In contrast, more recently developed
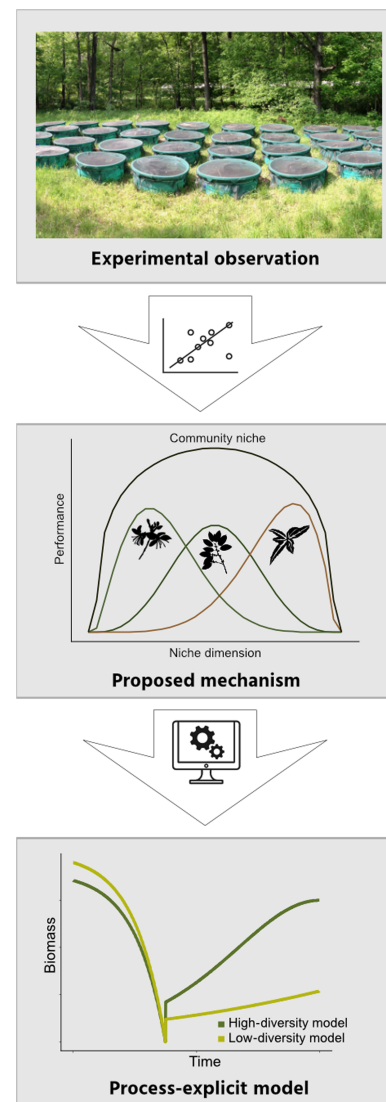

Fig. 2. Moving from empirical observations to process-explicit models. The relationship between biodiversity and ecosystem functioning can be observed experimentally in mesocosms. Statistical analysis of experimental data can lead to proposed mechanisms of biodiversity functioning, such as niche complementarity (*55*). This mechanism can be integrated into process-explicit models to simulate interactions between community structure and function. Image credits: photograph (top panel), Matthew Pintar; plant icons (middle panel), Andy Wilson.

community-level models simulate all five primary biotic processes (*46*). These and individual-based models are becoming more frequently used to unravel biological mechanisms that underpin spatiotemporal patterns of biodiversity (Fig. 3). These advances promise to lead to a greater awareness of the importance of eco-evolutionary processes in shaping biodiversity (*52*).

Genetic diversity

Although coalescent models have simulated genetic diversity—trait inheritance within species—for 40 years (*28*), early approaches did not model differences in DNA among individuals in space and time. This advance was not made until the beginning of the 21st century (Fig. 3) with the advent of a spatially explicit simulation framework
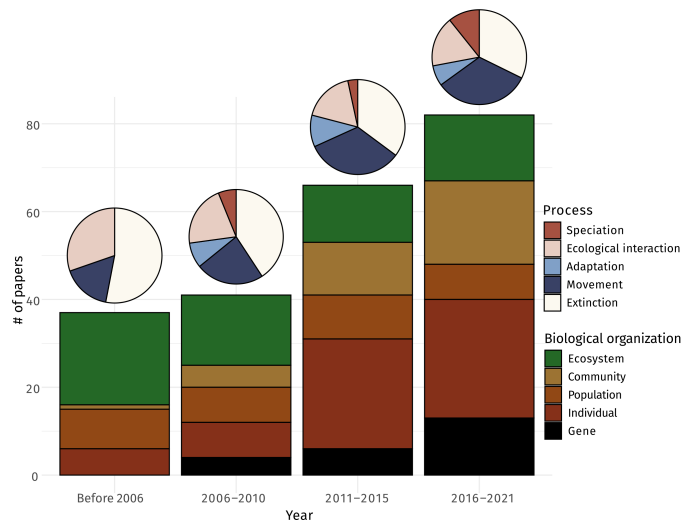
Fig. 3. Processes and levels of biological organization. Bars show the number of studies using process-explicit models published before 2006 and in the 5-year periods from 2006 to 2016 and from 2016 to 2021, color-coded to indicate the unit of biological organization simulated. Pie charts show the biotic processes (speciation, ecological interaction, adaptation, movement, and extinction) modeled as fractions of the total number of processes modeled across all studies for each time bin.

for population genetics: the serial-genetic simulator SPLATCHE (SPatial and Temporal Coalescent in a Heterogeneous Environment). The first studies to use SPLATCHE found that range expansions in heterogeneous environments produce genetic diversity patterns contingent on the geographical origin of the expansion, allowing spatially explicit genetic models to trace back the origin points of range expansions (56). Subsequently, coalescent-based process-explicit models have been frequently used to infer the effects of species' range expansions, contractions, and shifts on patterns of genetic diversity, using ancient and modern DNA. They have revealed that genetic diversity declines toward the leading edge of a species range more steeply than predicted by neutral theory (57) and that rapid range contractions conserve more genetic diversity in refugial populations than slow range contractions (58). These models have also shown that present-day isolation of a population is a poor indicator of the past diversity of the lineage and historical barriers to gene flow (59) and that rapid warming events can reconfigure species assemblages (60). Together, these reconstructions of past patterns of genetic diversity using process-explicit models are helping to improve projections of future patterns of genetic diversity by parameterizing known responses to environmental shifts (61).

Virtual genomes can be simulated to test and refine theories of genetic diversity. These genomes are simulated with mutation, migration, and divergence on computer-generated landscapes using a priori mutation rates and dispersal patterns. This approach has been used to simulate species' range expansions, revealing that introgression [transfer of genetic information from one species to another as a result of hybridization (62)] is likely to occur from the resident population to the invading population, regardless of the relative densities of the resident and invader populations (63). Simulations of virtual genomes have also shown that new mutations near the leading edge of an expanding range have a higher frequency and wider spatial distribution than in a stationary population (64). This result suggests that spatially expanding populations have an

increased rate of evolution at their frontier (64), with important implications for the management of invasive populations and range-shifting native species.

Species diversity

Process-explicit models can be used to decipher patterns of species diversity at the level of the individual, species, or community, and findings underpinning the operation of biological processes at these different levels of species diversity can reinforce or amplify one another. For example, an individual-level model can elucidate the evolution of optimal dispersal strategies within a single habitat island (65), a population-level model can reveal species diversity patterns across a chain of islands shaped by different dispersal strategies (66), and a community-level model can infer dispersal strategies in different functional groups, based on diversity across an entire region (67). In this way, process-explicit models at these three levels of organization allow us to investigate and potentially to integrate the impact of movement on species diversity patterns at multiple biological scales.

Processes can be modeled at the level of the individual organism with agent-based models (68) and physiological approaches (69). The former can potentially capture any of the five fundamental biotic processes responsible for biodiversity and can generate complex population- and community-level phenomena that arise from ecological interactions among individuals (70). For example, individual-based models of initial colonization in a range expansion or shift have shown that the interaction of local adaptation with timing (71) and speed (72) of colonization can alter the expected distribution of a species along an environmental gradient.

However, models built at the individual level can be computationally intensive, particularly if they simulate complex eco-evolutionary processes for many populations of individuals. Moreover, they can be difficult to parameterize and validate (Fig. 4), because data on biotic processes like movement and other attributes are often unavailable at the level of the individual. The computational demands of these models have led some researchers to use machine learning techniques (as emulators) to generalize process-explicit model behavior post hoc at small scales and apply those generalizations to larger scales (73). Others have used virtual landscapes to simulate and explore the population-level effects of different movement strategies, requiring neither biotic nor environmental data for parameterization (71). This approach, which allows for the simulation of data-poor processes at the individual level, has shown that range shifts can be accelerated by the evolution of greater dispersal ability in marginal habitats (65).

Physiological models, such as NicheMapper (74), and forest gap models, such as ForClim (75) and PHENOFIT (76), simulate only local- to range-wide extinction in animals and trees, respectively, making them computationally less intensive than individual-level models at large spatial scales. These approaches assume that if environmental conditions are suitable given an organism's physiological traits, it will persist; otherwise, it will die. These models are built on physiology and thermal tolerances, which are used to predict where individuals can survive. Physiological models can refine projections from phenomenological models of species distribution by identifying locales where heat stress will cause local extinction, informing conservation management (53, 77).

Individual-level models are, nevertheless, often constrained to ecological and evolutionary processes at local extents, often failing to account for potentially important coarser-scale processes that
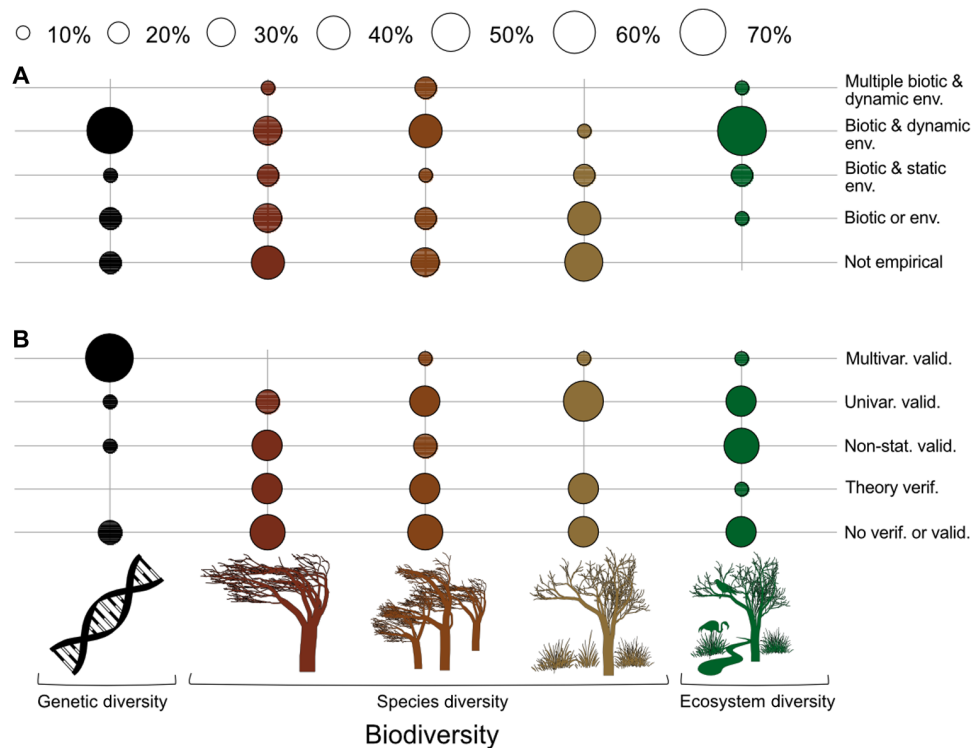
Fig. 4. Model structure and assessment. (**A**) shows model structure (parameterization) and (**B**) shows model assessment (verification and validation) for five levels of biological organization (left to right): gene, individual, population, community, and ecosystem. Model structure categories (A) include (top to bottom) multiple biotic processes and dynamic environment, single biotic process and dynamic environment, single biotic process and static environment, either a biotic process or environmental data, and no empirical data. Model assessment categories (B) include (top to bottom): multivariate validation (Multivar. valid.), univariate (Univar.) validation, nonstatistical (Non-stat.) validation, verification (verif.) using theory, and no verification or validation. For additional detail, see the "Relationship to data and theory" section and Supplementary Methods. Size of circles indicates the relative number of studies reviewed (total = 225).

can affect species diversity. Population models, which find their roots in simple logistic growth equations or matrix population models (*78*), can simulate movement and mortality in a network of populations extending across a species range (*79*, *80*). They can simulate trait values and genes, thus incorporating adaptation or speciation among populations over time, uncovering interactive effects of adaptation and dispersal on distributions of phenotypes (*81*). Although these models usually feature one or a few focal species, they can be used to simulate many populations of interacting species, capturing ecological interactions and community dynamics (*66*). For example, a model of competing and evolving populations has shown that certain syndromes of life history traits (mating system and dispersal ability) outcompete others—a mechanistic prediction that fits with empirical observations in plants (*81*).

Pathways to extinction are difficult to detect and disentangle phenomenologically (*82*) because they are complex, often starting long before the extinction event, resulting from biological responses to natural and human-induced factors that operate at multiple spatiotemporal scales (*80*). Linking population models to correlative species distribution models to address well-recognized limitations of pattern-based approaches (*83*) is allowing the processes of movement, extinction, and—most recently—adaptation to be simulated over multiple millennia (*84*). This approach is revealing how ecological strategies, and demographic and evolutionary traits, interact dynamically with past environmental change and human-driven factors to cause the decline and eventual extinction of species (*80*).

Biodiversity loss can be modeled for groups of interacting species using community-level models. Process-explicit models at the community level simulate biogeographical dynamics with species as functional units within the simulation (*52*). Unlike population models, which typically have species or population distributions as their outputs, or ecosystem models, which generally produce maps of ecosystem function or plant functional guilds (see below), these community-level biogeographical models usually generate species richness maps and range size frequencies (*46*).

Most community-level process-explicit models encompass all of the five biotic processes that drive biodiversity, making them aptly suited for testing differing hypotheses about the underlying causes of patterns of biodiversity, including how lineages diversify over space and time. For example, community-level process-explicit models have been used to determine whether neutral theory can explain empirical patterns of reef community dynamics, finding support for the theoretical expectation that range size should increase with dispersal ability (*85*). However, models of community-level processes not only are used to answer theoretical questions about biodiversity but also can be applied directly to real-world ecological systems to understand patterns of species richness (*86*), community assembly (*87*), and diversity loss (*88*) in a changing world. Diversification models with simple parameterization have applications in conservation biology, including identifying the effects of environmental change on biodiversity hotspots (*89*) and predicting the loss of species in a community after habitat destruction (*88*). Despite

their complexity, these process-explicit models of biogeographical dynamics can be validated (Fig. 4) using targets of current-day range size frequency distributions (*45*).

Ecosystem diversity

Ecosystem diversity models simulate the structure of functional groups of terrestrial and marine organisms. The coexistence and interactions of these groups are used to map the distribution of ecosystems (*90*). Interactions among terrestrial autotrophs and the abiotic environment are modeled with DGVMs (*34*), while fisheries management models (*91*) and general ecosystem models (*92*) also include primary and secondary consumer dynamics, enabling simulation of energy transfer through food webs. These ecosystem diversity models are being used to forecast and manage ecosystem services, including carbon storage (*93*), clean water supply (*94*), and food security (*95*) in a changing world. They have shown that freshwater supply will be reduced under future warming to the detriment of terrestrial ecosystem functioning (*96*), that increased hurricane frequency threatens the structure and productivity of reef-fish communities (*97*), and that habitat fragmentation affects the trophic structure of ecosystems (*98*). Furthermore, process-explicit ecosystem models have shown that forest function is more resilient to warming events in high- than in low-diversity forests (*99*), illustrating causative mechanisms for experimental observations (*55*).

DGVMs simulate the distribution of plant functional types as well as their fluxes of carbon, water, and nutrients through the environment (*34*), enabling them to simulate dynamic feedbacks between the biosphere and the climate when coupled to climate models (*100*). This coupling of models has uncovered important interactions between climate, CO_2, and ecosystem function, including evidence that a positive interaction between plant productivity and elevated levels of CO_2 can potentially offset the negative effects that climate change and, more specifically, increased aridification can have on productivity (*101*). Moreover, by hindcasting ecosystem diversity dynamics over glacial-interglacial cycles, DGVMs have disentangled many of the effects of climate on ecosystem structure (*102*). For example, modeling the interaction between deglacial warming and megaherbivore die-off following the last glacial maximum reveals how high-latitude mammoth steppe—Earth's most extensive biome at the time—was converted to a taiga-tundra ecotone (*38*).

While more complex general ecosystem models can simulate the entire ecosphere, from phyto- and zooplankton to apex carnivores, capturing complex food web dynamics, they do not as yet include two-way interactions with climate (*92*, *98*). Consequently, they are frequently used to test theories regarding ecosystem structure, including relationships between heterotroph biomass and net primary productivity (*92*), and to determine the impact of recent land-use change on ecosystem function (*98*). The application of these ecosystem-level models in fisheries management has uncovered crucial ecosystem services provided by coral reefs, including calcium carbonate deposition and coastal protection, showing how overfishing disrupts these services to nature and people (*103*).

RELATIONSHIP TO DATA AND THEORY

Process-explicit models have a variety of relationships with data and theory (fig. S1). Some process-explicit models are theory driven: Their purpose is to explore the implications or applications of an ecological theory, such as the neutral theory of biodiversity (*12*), the

species-area relationship (*104*), or the general dynamic theory of island biogeography (*105*). Others are theory scaffolded: Their purpose is to understand an ecological system empirically and to use theory as a scaffold by which to structure the model and interpret its outputs (*101*).

While process-explicit models are diverse in structure (*60*, *84*), they exist on two distinct continua, based on (i) their use of empirical data for parameterization and (ii) how they are verified and/or validated (Fig. 4). Empirical data are not necessary to build and run a process-explicit model. Indeed, many theory-driven models use arbitrary values for parameters and explore the interactions and patterns that result from the model (*87*). These models are at one end of a parameterization continuum. Further along the continuum are models that use either biotic data (such as genetic sequences or species occurrence) or environmental data (such as spatiotemporal climatic fluctuations or bathymetry change) to parameterize models, but not both (*46*). The next category of models includes those that use biotic and static environmental data (*106*), followed by models that use biotic and dynamic environmental data (*34*). In the last two cases, biotic data represent a single level of biological organization: gene, individual, population, community, or ecosystem (*7*). At the most extreme end of the parameterization continuum lie models that use dynamic environmental data and biotic data to simulate processes across multiple levels of biological organization: for example, simulating individual-level movement (based on seed dispersal by wind) and population-level mortality (based on survival across individuals) (*107*).

A second distinct gradient specifies how data are used for verification and validation in process-explicit models (Fig. 4). Verification is a check to ensure that the implemented model meets the primary theoretical assumptions it has been built to represent. In contrast, validation evaluates the level of correspondence between the implemented model and the study system (*108*). At one end of the verification and validation continuum, model outputs are not verified or validated at all. Moving up the continuum, output patterns can be verified for congruence with theory by comparing model outputs with well-established theoretical relationships, such as the mid-domain effect (*109*). Models can be validated through visual inspection of patterns based on observational data, using nonstatistical procedures (*110*). Statistical validation allows model outputs to be evaluated with patterns of empirical data, by means of measures such as coefficient of determination (r^2), root mean square error, or true skill statistic (*102*). At the most data-heavy end of the verification and validation continuum lies multivariate statistical validation (*59*), in which models are evaluated on the basis of their ability to simultaneously demonstrate goodness of fit to multiple empirical patterns. This demanding level of validation is now being applied to pattern-oriented modeling (an emerging and powerful technique in data science), in which mechanisms governing the structure and dynamics of biodiversity are identified by converging model simulations to independent multivariate validation targets (*45*, *80*).

Figure 4 shows how process-explicit models with diverse relationships to data can be used to decipher the mechanisms underlying the structure of biodiversity. Models that use little or no empirical data can be used to test ecological and evolutionary theories, such as modes of speciation (*111*). These primarily theory-driven models are useful even when biological data are not available for validation; for example, data-free process-explicit models can test the sensitivity of model outputs to underlying processes (*111*), distinguishing

metapopulation dynamics from neutral dynamics or random community assemblage (*112*). Theory-scaffolded models with complex parameterization often have greater explanatory power, particularly if they use more than one level of biotic data for parameterization and validation, and if they simulate dynamic drivers of global change affecting the spatial structure of biodiversity. These additional data inputs can allow otherwise necessary model assumptions to be relaxed, such as an assumption of unlimited movement (*107*) or static human land use (*39*), while multivariate validation targets (despite being, so far, rarely used) provide more stringent tests of model simulations.

SAFEGUARDING BIODIVERSITY

Sustainable management of biodiversity has been recognized as a policy goal for 30 years (*113*); however, progress in halting the decline and degradation of biodiversity has been limited (*114*). Reasons for failing to reduce biodiversity loss are complex, reflecting long-lasting knowledge gaps on biodiversity dynamics (*47*), as well as insufficient integration of biodiversity science in policy making (*115*) and lack of motivation to deliver the required biodiversity changes (*116*). An incomplete understanding of the mechanisms that govern the structure and dynamics of biodiversity and a tendency to use correlative rather than process-explicit approaches to forecast the future of biodiversity in a changing world (*10*) have constrained capabilities to set productive biodiversity targets, develop cross-cutting solutions for restoring nature, and obtain national commitments to biodiversity conservation.

Process-explicit models have a diverse range of applications, including formulating and assessing potential solutions for mitigating future genetic-, species-, and ecosystem-level collapse. Currently, for example, the paleorecord is being used to identify biological mechanisms that mediate responses to climate- and human-driven change using process-explicit models (*117*). These paleo-models can disentangle past determinants of genetic diversity, range shifts, species richness, and ecosystem structure and function. By specifying the causal processes that underpin biodiversity change, they can provide the context needed to improve confidence in predictions of biodiversity's future (*7*), leading to improved computational platforms for setting biodiversity targets and better solutions for mitigating adverse changes to biodiversity (*8*).

The genetic signatures of demographic responses of species to environmental changes can be decoded using genetic simulation models (*6*) to better manage future biodiversity (*118*). For example, process-explicit models of gene fixation, which allow demographic trends and gene flow to be reconstructed (*16*), are establishing the importance of intraspecific genetic diversity for resilience to accelerated climatic change (*119*). There is now a push to use this technique more widely to improve knowledge of how rapid climatic change affects patterns of genetic diversity (*61*). In the absence of ample genetic samples, process-explicit models can still be used to test theories central to conservation genetics using virtual genetic sequences and landscapes (*120*) to deliver valuable information for conserving future genetic diversity (*121*).

Historical context is crucial for understanding the threat of future declines in species distributions. Process-explicit models constructed at the individual and population level can be used to identify demographic processes that cause range shifts for a species or suites of species in response to climatic and environmental drivers, improving

species threat assessments (*77*). Because individual-based models often operate at a level of detail that is not necessary for simulating range dynamics across large extents, process-explicit population-level models are more commonly used to project past and future range dynamics. These population-level models can be used to identify ecological traits that cause species to be differentially prone to regional and range-wide extinction (*122*) and to evaluate the efficacy of current methods for identifying threatened species (*123*). Population-level models that incorporate adaptation as a process have been influential and instructive in revealing the role of gene flow along ecological selection gradients, and its inhibiting effect on local adaptation to environmental change (*124*).

Hotspots of biodiversity are of particular conservation concern because they support high concentrations of species, particularly endemics (*125*). Process-explicit models built and validated at the community level to simulate geographical patterns of species richness and endemism can identify mechanisms central to the maintenance of past and contemporary hotspots of species richness (*126*), providing a framework for assessing vulnerability to future climate and environmental change (Fig. 5). If simulations can capture community-level responses to realistic tempos and magnitudes of future global change, these new predictive approaches will benefit 21st century environmental management and conservation (*7*).

To illustrate the state of the art in broad-scale modeling of biodiversity and its potential application for biodiversity conservation, we offer an example of a community-level, process-explicit model that incorporates all five biological processes that govern the structure and dynamics of biodiversity in a temporally dynamic environment (*46*). The model was designed to simulate the geographic
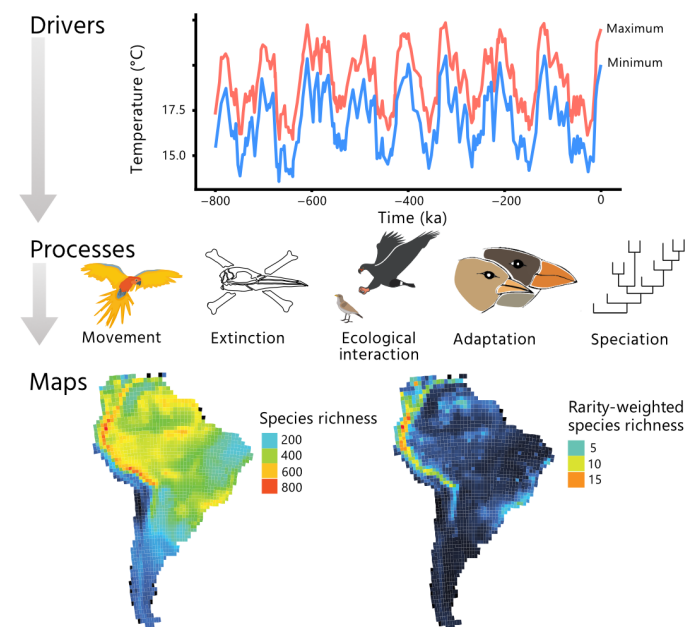

Fig. 5. Models for predicting continental species richness. Community-level biogeographical models (*46*), driven by interactions between climate and biological processes, can incorporate all five biological processes that govern biodiversity: movement, extinction, ecological interaction, adaptation, and speciation. Model outputs can simulate maps of current-day and future species richness and endemism (rarity-weighted species richness). Top plot shows temperature across thousands of years (ka). Image of finches adapted from Charles Darwin.

distributions and patterns of overlap of species ranges in response to the past 800,000 years of climate change in South America (Fig. 5). In this model, evolutionary niche dynamics drive range expansion and fragmentation (leading to speciation), adaptation to climatic conditions, and extinction. Combinations of parameter settings (dispersal distance, evolutionary rate, time for speciation, and intensity of competition) for virtual species were chosen a priori, producing many different potentially plausible range maps. Although not directed by any empirical validation targets, the emerging maps closely resembled contemporary species richness of major South American taxa. Combinations of parameters that closely reproduced the current-day biodiversity of South American avifauna (including hotspots of species richness and endemism) showed that low rates of adaptation to past climatic change were required to reconstruct observed patterns of species richness. In the future, such community-level simulation models (built to simulate the past and validated in the present; Fig. 5) could be parameterized with climate forecasts to predict strongholds of species richness under future climates. The subsequent results could be used to guide the protection and future management of biodiversity.

By identifying the biological mechanisms, drivers, and their interactions that mediate changes in ecosystem structure and function, process-explicit models can help safeguard the services ecosystems provide to nature and people. Early ecosystem models were used to investigate the effects of increased atmospheric carbon on vegetation communities (96). More recent models have incorporated complex interactions between multiple drivers of global change and ecosystem-level processes, including the effects of agriculture and land-use change (93). This research has strengthened knowledge of the drivers and responses that underpin change in ecosystem structure and function (36, 93), improving projections (127) and informing protocols for assessing ecosystem threat status (128). For example, DGVMs have shown mechanistically how 20th century agriculture caused a 24% reduction in global vegetation and a 10% reduction in global soil carbon (93). A better understanding of processes of ecosystem change enables the simulation of the effects of current and future climatic and environmental change (including altered fire regimes) on important ecosystem services, such as agricultural productivity, freshwater availability, and timber production (36, 39).

Climate projections are currently made using models characterized by complex system dynamics, including interactions and feedbacks between the atmosphere, ocean, land, and society (129). While analogous models for projecting biodiversity change have typically been simpler than approaches used in climate science, general ecosystem models (92) and process-based community assemblage models (44) offer new and more robust methods for projecting the future distribution of life on Earth. These next-generation biodiversity models, which explicitly capture the structure and dynamics of biodiversity, will strengthen our capacity to set achievable biodiversity targets that promote engagement and investment where change is needed.

LOOKING FORWARD

Although phenomenological models are a crucial first step toward understanding the potential determinants of current and past spatial patterns of biodiversity, process-explicit models are needed to identify causal processes that govern the structure and dynamics of biodiversity, and to exclude those that do not. Increased open access to curated georeferenced occurrence records, dated fossils, libraries

of genetic sequences, and climate simulations will continue to provide innovative opportunities to apply process-explicit models, especially to connect inferences of past responses of biodiversity to different rates and magnitudes of contemporary climate and environmental change (117). These opportunities include testing key assumptions of existing biodiversity models—such as the common assumption that processes driving changes in biodiversity are scale invariant (130)—and competing theories for large-scale biodiversity patterns, including geographical gradients in species richness (44).

Continuous simulations of the transient late Quaternary climate are needed, ideally at fine spatial resolutions, to determine population-, species-, community-, and ecosystem-level responses to abrupt (as well as gradual) climatic change using process-explicit models (131). The TRaCE21ka experiment based on the Community Climate System Model version 3 (132) has bridged this gap, but it spans only the past 21,000 years. Higher spatiotemporal resolution paleoclimate simulations from Earth systems models before 21,000 years ago that include solar flux, ice sheet extent, and sea level changes will provide a more thorough understanding of the mechanisms responsible for spatiotemporal patterns of biodiversity at evolutionary time scales (7). Statistical emulators of climatic change will be useful in filling this data and knowledge gap (133), particularly in the Southern Hemisphere, for which there is a paucity of high-resolution simulated data before the last glacial maximum (134). Including better reconstructions of solar variability, volcanic eruptions, and land use during the Holocene in transient simulations of Earth's climate will provide a more complete picture of more recent temporal change in regional climates and the biodiversity they support.

Integrating paleoecological and neoecological perspectives into process-explicit models is key to contextualizing the present and anticipating and visualizing ecological responses to future global change (117). Emerging genomic techniques are allowing genetic diversity and effective population size to be estimated over short periods (<100 years) of environmental change, providing inferences of eco-evolutionary change to recent and/or punctuated disturbance events (32, 33, 135) that can feed directly into process-explicit models of range collapse and population declines. Importantly, projections of recent climate, vegetation, and land-use change have been harmonized with ancient projections, allowing their effects on biodiversity to be characterized continuously in process-explicit models that run from as far back as 21,000 years ago to the present day (136) and, in some cases, into the future (137).

Adaptation was first incorporated into spatial process-explicit models in the early 2000s (138) and has since become more common in ecological and evolutionary models. However, it still remains the most infrequently modeled biological process. A more regular integration of adaptation into process-explicit models of climate change responses will benefit from taxonomically diverse datasets of historic DNA that are readily available today (139) and from technological advances that allow ancient DNA to be used to reconstruct shifts in genetic diversity and adaptations to large-magnitude and abrupt climatic change (140). Adding community dynamics to population models and demography to community models will also strengthen projections of biodiversity change. Metacommunity models with simplified food webs can bridge this gap by modeling demographic interactions between populations of multiple species in a spatiotemporally explicit manner (141). Community-level models can integrate a higher level of biological organization by combining

ecosystem-level drivers such as fire with processes of plant community assembly (*142*).

Achieving more detailed mechanistic understandings of patterns of biodiversity—from the gene to the ecosystem level—will require a greater focus on rigorous statistical validation of process-explicit models using independent multivariate data that are spatiotemporally explicit. In systems where theory is not yet well developed, empirical data for model parameterization are needed to simulate realistic outputs. However, as the mechanisms underpinning a system's biodiversity become better understood, model outputs will be simulated using theory alone. Realistic predictions generated from a strong theoretical framework are the pinnacle that ecologists and evolutionary biologists should be aiming for when wielding process-explicit models.

Process-explicit models have been instrumental in improving knowledge of the distribution of life on Earth, revealing complex causal processes for contemporary patterns of biodiversity that could not be discerned from experimental approaches or phenomenological models. A deeper recognition of the structure and dynamics of organisms, communities, and ecosystems in process-explicit models is helping to protect and restore biodiversity by formulating remedies to existing problems and countering undesirable future changes.

SUPPLEMENTARY MATERIALS
Supplementary material for this article is available at https://science.org/doi/10.1126/sciadv.abj2271

REFERENCES AND NOTES

1. R. D. Holt, On the evolutionary ecology of species' ranges. *Evol. Ecol. Res.* **5**, 159–178 (2003).
2. B. W. Brook, N. S. Sodhi, C. J. A. Bradshaw, Synergies among extinction drivers under global change. *Trends Ecol. Evol.* **23**, 453–460 (2008).
3. A. D. Davidson, M. J. Hamilton, A. G. Boyer, J. H. Brown, G. Ceballos, Multiple ecological pathways to extinction in mammals. *Proc. Natl. Acad. Sci. U.S.A.* **106**, 10702–10705 (2009).
4. K. Beven, A manifesto for the equifinality thesis. *J. Hydrol.* **320**, 18–36 (2006).
5. S. R. Connolly, S. A. Keith, R. K. Colwell, C. Rahbek, Process, mechanism, and modeling in macroecology. *Trends Ecol. Evol.* **32**, 835–844 (2017).
6. A. Eriksson, L. Betti, A. D. Friend, S. J. Lycett, J. S. Singarayer, N. von Cramon-Taubadel, P. J. Valdes, F. Balloux, A. Manica, Late Pleistocene climate change and the global expansion of anatomically modern humans. *Proc. Natl. Acad. Sci. U.S.A.* **109**, 16089–16094 (2012).
7. D. A. Fordham, S. T. Jackson, S. C. Brown, B. Huntley, B. W. Brook, D. Dahl-Jensen, M. T. P. Gilbert, B. L. Otto-Bliesner, A. Svensson, S. Theodoridis, J. M. Wilmshurst, J. C. Buettel, E. Canteri, M. McDowell, L. Orlando, J. Pilowsky, C. Rahbek, D. Nogues-Bravo, Using paleo-archives to safeguard biodiversity under climate change. *Science* **369**, eabc5654 (2020).
8. D. A. Fordham, H. R. Akçakaya, J. Alroy, F. Saltré, T. M. L. Wigley, B. W. Brook, Predicting and mitigating future biodiversity loss using long-term ecological proxies. *Nat. Clim. Change* **6**, 909–916 (2016).
9. G. B. Bonan, Forests and climate change: Forcings, feedbacks, and the climate benefits of forests. *Science* **320**, 1444–1449 (2008).
10. N. J. Briscoe, J. Elith, R. Salguero-Gómez, J. J. Lahoz-Monfort, J. S. Camac, K. M. Giljohann, M. H. Holden, B. A. Hradsky, M. R. Kearney, S. M. McMahon, Forecasting species range dynamics with process-explicit models: Matching methods to applications. *Ecol. Lett.* **22**, 1940–1956 (2019).
11. S. Ferrier, K. N. Ninan, P. Leadley, R. Alkemade, "The methodological assessment report on scenarios and models of biodiversity and ecosystem services" (IPBES, 2016), p. 348.
12. S. P. Hubbell, *The Unified Neutral Theory of Biodiversity and Biogeography* (Princeton Univ. Press, 2001), vol. 32 of *Monographs in Population Biology*.
13. M. Mangel, The important role of theory in conservation biology. *Conserv. Biol.* **16**, 843–844 (2002).
14. J. M. Halley, Y. Iwasa, Neutral theory as a predictor of avifaunal extinctions after habitat loss. *Proc. Natl. Acad. Sci. U.S.A.* **108**, 2316–2321 (2011).
15. M. Kimura, The neutral theory of molecular evolution. *Sci. Am.* **241**, 98–126 (1979).
16. A. D. Yoder, J. W. Poelstra, G. P. Tiley, R. C. Williams, Neutral theory is the foundation of conservation genetics. *Mol. Biol. Evol.* **35**, 1322–1326 (2018).
17. M. Loreau, Linking biodiversity and ecosystems: Towards a unifying ecological theory. *Philos. Trans. R. Soc. B Biol. Sci.* **365**, 49–60 (2010).
18. J. S. Cabral, L. Valente, F. Hartig, Mechanistic simulation models in macroecology and biogeography: State-of-art and prospects. *Ecography* **40**, 267–280 (2017).
19. R. H. MacArthur, E. O. Wilson, *The Theory of Island Biogeography* (Princeton Univ. Press, 1967), *Monographs in Population Biology*.
20. R. Levins, Some demographic and genetic consequences of environmental heterogeneity for biological control. *Bull. Entomol. Soc. Am.* **15**, 237–240 (1969).
21. I. Hanski, T. Pakkala, M. Kuussaari, G. Lei, Metapopulation persistence of an endangered butterfly in a fragmented landscape. *Oikos* **72**, 21–28 (1995).
22. R. G. Pearson, J. C. Stanton, K. T. Shoemaker, M. E. Aiello-Lammens, P. J. Ersts, N. Horning, D. A. Fordham, C. J. Raxworthy, H. Y. Ryu, J. McNees, H. R. Akçakaya, Life history and spatial traits predict extinction risk due to climate change. *Nat. Clim. Change* **4**, 217–221 (2014).
23. I. Hanski, Metapopulation dynamics: Does it help to have more of the same? *Trends Ecol. Evol.* **4**, 113–114 (1989).
24. D. Wilson, Complex interactions in metacommunities, with implications for biodiversity and higher levels of selection. *Ecology* **73**, 1984–2000 (1992).
25. D. L. DeAngelis, W. M. Mooij, Individual-based modeling of ecological and evolutionary processes. *Annu. Rev. Ecol. Evol. Syst.* **36**, 147–168 (2005).
26. J. A. Rice, T. J. Miller, K. A. Rose, L. B. Crowder, E. A. Marschall, A. S. Trebitz, D. L. DeAngelis, Growth rate variation and larval survival: Inferences from an individual-based size-dependent predation model. *Can. J. Fish. Aquat. Sci.* **50**, 133–142 (2003).
27. D. L. DeAngelis, V. Grimm, Individual-based models in ecology after four decades. *F1000Prime Rep.* **6**, 39 (2014).
28. J. F. C. Kingman, On the genealogy of large populations. *J. Appl. Probab.* **19**, 27–43 (1982).
29. J. C. Avise, *Phylogeography: The History and Formation of Species* (Harvard Univ. Press, 2000).
30. L. L. Knowles, Statistical phylogeography. *Annu. Rev. Ecol. Evol. Syst.* **40**, 593–612 (2009).
31. A. Prohaska, F. Racimo, A. J. Schork, M. Sikora, A. J. Stern, M. Ilardo, M. E. Allentoft, L. Folkersen, A. Buil, J. V. Moreno-Mayar, T. Korneliussen, D. Geschwind, A. Ingason, T. Werge, R. Nielsen, E. Willerslev, Human disease variation in the light of population genomics. *Cell* **177**, 115–131 (2019).
32. D. Díez-del-Molino, F. Sánchez-Barreiro, I. Barnes, M. T. P. Gilbert, L. Dalén, Quantifying temporal genomic erosion in endangered species. *Trends Ecol. Evol.* **33**, 176–185 (2018).
33. K. Bi, T. Linderoth, S. Singhal, D. Vanderpool, J. L. Patton, R. Nielsen, C. Moritz, J. M. Good, Temporal genomic contrasts reveal rapid evolutionary responses in an alpine mammal during recent climate change. *PLOS Genet.* **15**, e1008119 (2019).
34. J. A. Foley, I. C. Prentice, N. Ramankutty, S. Levis, D. Pollard, S. Sitch, A. Haxeltine, An integrated biosphere model of land surface processes, terrestrial carbon balance, and vegetation dynamics. *Global Biogeochem. Cycles* **10**, 603–628 (1996).
35. A. White, M. G. R. Cannell, A. D. Friend, The high-latitude terrestrial carbon sink: A model analysis. *Glob. Change Biol.* **6**, 227–245 (2000).
36. A. Boit, B. Sakschewski, L. Boysen, A. Cano-Crespo, J. Clement, N. Garcia Alaniz, K. Kok, M. Kolb, F. Langerwisch, A. Rammig, R. Sachse, M. van Eupen, W. von Bloh, D. C. Zemp, K. Thonicke, Using dynamic global vegetation models (DGVMs) for projecting ecosystem services at regional scales, in *Atlas of Ecosystem Services: Drivers, Risks, and Societal Responses*, M. Schröter, A. Bonn, S. Klotz, R. Seppelt, C. Baessler, Eds. (Springer International Publishing, 2019), pp. 57–61.
37. H. Kim, I. M. D. Rosa, R. Alkemade, P. Leadley, G. Hurtt, A. Popp, D. P. van Vuuren, P. Anthoni, A. Arneth, D. Baisero, E. Caton, R. Chaplin-Kramer, L. Chini, A. De Palma, F. Di Fulvio, M. Di Marco, F. Espinoza, S. Ferrier, S. Fujimori, R. E. Gonzalez, M. Gueguen, C. Guerra, M. Harfoot, T. D. Harwood, T. Hasegawa, V. Haverd, P. Havlík, S. Hellweg, S. L. L. Hill, A. Hirata, A. J. Hoskins, J. H. Janse, W. Jetz, J. A. Johnson, A. Krause, D. Leclère, I. S. Martins, T. Matsui, C. Merow, M. Obersteiner, H. Ohashi, B. Poulter, A. Purvis, B. Quesada, C. Rondinini, A. M. Schipper, R. Sharp, K. Takahashi, W. Thuiller, N. Titeux, P. Visconti, C. Ware, F. Wolf, H. M. Pereira, A protocol for an intercomparison of biodiversity and ecosystem services models using harmonized land-use and climate scenarios. *Geosci. Model Dev.* **11**, 4537–4562 (2018).
38. D. Zhu, P. Ciais, J. Chang, G. Krinner, S. Peng, N. Viovy, J. Peñuelas, S. Zimov, The large mean body size of mammalian herbivores explains the productivity paradox during the last glacial maximum. *Nat. Ecol. Evol.* **2**, 640–649 (2018).
39. D. A. Contreras, A. Bondeau, J. Guiot, A. Kirman, E. Hiriart, L. Bernard, R. Suarez, M. Fader, From paleoclimate variables to prehistoric agriculture: Using a process-based agro-ecosystem model to simulate the impacts of Holocene climate change on potential agricultural productivity in Provence, France. *Quat. Int.* **501**, 303–316 (2019).
40. F. May, T. Wiegand, S. Lehmann, A. Huth, Do abundance distributions and species aggregation correctly predict macroecological biodiversity patterns in tropical forests? *Glob. Ecol. Biogeogr.* **25**, 575–585 (2016).
41. W. Brenner, Växtgeografiska studier i Baräsunds skjärgård. *Acta Sociatatis Fauna Flora Fenn.* **49**, 1–151 (1921).

42. A. R. Wallace, On the physical geography of the Malay archipelago. *J. R. Geogr. Soc. Lond.* **33**, 217–234 (1863).

43. A. von Humboldt, *Personal Narrative of Travels to the Equinoctial Regions of the New Continent During the Years 1799–1804* (G. Bell, 1877).

44. O. Hagen, B. Flück, F. Fopp, J. S. Cabral, F. Hartig, M. Pontarp, T. F. Rangel, L. Pellissier, gen3sis: A general engine for eco-evolutionary simulations of the processes that shape Earth's biodiversity. *PLOS Biol.* **19**, e3001340 (2021).

45. T. F. Rangel, J. A. F. Diniz-Filho, R. K. Colwell, Species richness and evolutionary niche dynamics: A spatial pattern–oriented simulation experiment. *Am. Nat.* **170**, 602–616 (2007).

46. T. F. Rangel, N. R. Edwards, P. B. Holden, J. A. F. Diniz-Filho, W. D. Gosling, M. T. P. Coelho, F. A. S. Cassemiro, C. Rahbek, R. K. Colwell, Modeling the ecology and evolution of biodiversity: Biogeographical cradles, museums, and graves. *Science* **361**, eaar5452 (2018).

47. M. C. Urban, G. Bocedi, A. P. Hendry, J.-B. Mihoub, G. Pe'er, A. Singer, J. R. Bridle, L. G. Crozier, L. D. Meester, W. Godsoe, A. Gonzalez, J. J. Hellmann, R. D. Holt, A. Huth, K. Johst, C. B. Krug, P. W. Leadley, S. C. F. Palmer, J. H. Pantel, A. Schmitz, P. A. Zollner, J. M. J. Travis, Improving the forecast for biodiversity under climate change. *Science* **353**, aad8466 (2016).

48. R. Dale Guthrie, New carbon dates link climatic change with human colonization and Pleistocene extinctions. *Nature* **441**, 207–209 (2006).

49. T. Yoshida, L. E. Jones, S. P. Ellner, G. F. Fussmann, N. G. Hairston, Rapid evolution drives ecological dynamics in a predator–prey system. *Nature* **424**, 303–306 (2003).

50. M. Doebeli, U. Dieckmann, Speciation along environmental gradients. *Nature* **421**, 259–264 (2003).

51. J. M. Chase, M. A. Leibold, *Ecological Niches: Linking Classical and Contemporary Approaches* (University of Chicago Press, 2003).

52. N. J. Gotelli, M. J. Anderson, H. T. Arita, A. Chao, R. K. Colwell, S. R. Connolly, D. J. Currie, R. R. Dunn, G. R. Graves, J. L. Green, J.-A. Grytnes, Y.-H. Jiang, W. Jetz, S. K. Lyons, C. M. McCain, A. E. Magurran, C. Rahbek, T. F. Rangel, J. Soberón, C. O. Webb, M. R. Willig, Patterns and causes of species richness: A general simulation model for macroecology. *Ecol. Lett.* **12**, 873–886 (2009).

53. M. Kearney, W. Porter, Mechanistic niche modelling: Combining physiological and spatial data to predict species' ranges. *Ecol. Lett.* **12**, 334–350 (2009).

54. E. S. Gritti, C. Cassignat, O. Flores, R. Bonnefille, F. Chalie, J. Guiot, D. Jolly, Simulated effects of a seasonal precipitation change on the vegetation in tropical Africa. *Clim. Past* **6**, 169–178 (2010).

55. S. Naeem, Ecosystem consequences of biodiversity loss: The evolution of a paradigm. *Ecology* **83**, 1537–1552 (2002).

56. N. Ray, M. Currat, P. Berthier, L. Excoffier, Recovering the geographic origin of early modern humans by realistic and spatially explicit simulations. *Genome Res.* **15**, 1161–1167 (2005).

57. T. A. White, S. E. Perkins, G. Heckel, J. B. Searle, Adaptive evolution during an ongoing range expansion: The invasive bank vole (Myodes glareolus) in Ireland. *Mol. Ecol.* **22**, 2971–2985 (2013).

58. M. Arenas, N. Ray, M. Currat, L. Excoffier, Consequences of range contractions and range shifts on molecular diversity. *Mol. Biol. Evol.* **29**, 207–218 (2012).

59. J. L. Brown, L. L. Knowles, Spatially explicit models of dynamic histories: Examination of the genetic consequences of Pleistocene glaciation and recent climate change on the American pika. *Mol. Ecol.* **21**, 3757–3775 (2012).

60. J. B. Bemmels, L. L. Knowles, C. W. Dick, Genomic evidence of survival near ice sheet margins for some, but not all, North American trees. *Proc. Natl. Acad. Sci. U.S.A.* **116**, 8431–8436 (2019).

61. J. L. Brown, J. J. Weber, D. F. Alvarado-Serrano, M. J. Hickerson, S. J. Franks, A. C. Carnaval, Predicting the genetic consequences of future climate change: The power of coupling spatial demography, the coalescent, and historical landscape changes. *Am. J. Bot.* **103**, 153–163 (2016).

62. E. Anderson, L. Hubricht, Hybridization in Tradescantia. III. The evidence for introgressive hybridization. *Am. J. Bot.* **25**, 396–402 (1938).

63. M. Currat, M. Ruedi, R. J. Petit, L. Excoffier, The hidden side of invasions: Massive introgression by local genes. *Evolution* **62**, 1908–1920 (2008).

64. S. Klopfstein, M. Currat, L. Excoffier, The fate of mutations surfing on the wave of a range expansion. *Mol. Biol. Evol.* **23**, 482–490 (2006).

65. C. Dytham, Evolved dispersal strategies at range margins. *Proc. R. Soc. B Biol. Sci.* **276**, 1407–1413 (2009).

66. T. Hovestadt, H. J. Poethke, Dispersal and establishment: Spatial patterns and species–area relationships. *Divers. Distrib.* **11**, 333–340 (2005).

67. J. Sukumaran, E. P. Economo, L. L. Knowles, Machine learning biogeographic processes from biotic patterns: A new trait-dependent dispersal and diversification model with model choice by simulation-trained discriminant analysis. *Syst. Biol.* **65**, 525–545 (2016).

68. M. C. Welch, P. W. Kwan, A. S. M. Sajeev, Applying GIS and high performance agent-based simulation for managing an Old World screwworm fly invasion of Australia. *Acta Trop.* **138**, S82–S93 (2014).

69. Y. Wang, W. Porter, P. D. Mathewson, P. A. Miller, R. W. Graham, J. W. Williams, Mechanistic modeling of environmental drivers of woolly mammoth carrying capacity declines on St. Paul Island. *Ecology* **306**, 70 (2018).

70. V. Grimm, E. Revilla, U. Berger, F. Jeltsch, W. M. Mooij, S. F. Railsback, H.-H. Thulke, J. Weiner, T. Wiegand, D. L. DeAngelis, Pattern-oriented modeling of agent-based complex systems: Lessons from ecology. *Science* **310**, 987–991 (2005).

71. M. C. Urban, L. De Meester, Community monopolization: Local adaptation enhances priority effects in an evolving metacommunity. *Proc. R. Soc. B Biol. Sci.* **276**, 4129–4138 (2009).

72. B. L. Phillips, Range shift promotes the formation of stable range edges. *J. Biogeogr.* **39**, 153–161 (2012).

73. A. R. Vahdati, J. D. Weissmann, A. Timmermann, M. S. Ponce de León, C. P. E. Zollikofer, Drivers of Late Pleistocene human survival and dispersal: An agent-based modeling and machine learning approach. *Quat. Sci. Rev.* **221**, 105867 (2019).

74. W. P. Porter, J. W. Mitchell, Method and system for calculating the spatial-temporal effects of climate and other environmental conditions on animals. U.S. Patent 7,155,377 (2006).

75. A. C. Risch, C. Heiri, H. Bugmann, Simulating structural forest patterns with a forest gap model: A model evaluation. *Ecol. Model.* **181**, 161–172 (2005).

76. I. Chuine, E. G. Beaubien, Phenology is a major determinant of tree species range. *Ecol. Lett.* **4**, 500–510 (2001).

77. P. D. Mathewson, L. Moyer-Horner, E. A. Beever, N. J. Briscoe, M. Kearney, J. M. Yahn, W. P. Porter, Mechanistic variables can enhance predictive models of endotherm distributions: The American pika under current, past, and future climates. *Glob. Change Biol.* **23**, 1048–1064 (2017).

78. H. Caswell, *Matrix Population Models* (Sinauer, 2001).

79. D. A. Fordham, C. Mellin, B. D. Russell, R. H. Akçakaya, C. J. A. Bradshaw, M. E. Aiello-Lammens, J. M. Caley, S. D. Connell, S. Mayfield, S. A. Shepherd, B. W. Brook, Population dynamics can be more important than physiological limits for determining range shifts under climate change. *Glob. Change Biol.* **19**, 3224–3237 (2013).

80. D. A. Fordham, S. C. Brown, H. R. Akçakaya, B. W. Brook, S. Haythorne, A. Manica, K. T. Shoemaker, J. J. Austin, B. Blonder, J. Pilowsky, C. Rahbek, D. Nogues-Bravo, Process-explicit models reveal pathway to extinction for woolly mammoth using pattern-oriented validation. *Ecol. Lett.* **25**, 125–137 (2022).

81. P. Cheptou, F. Massol, Pollination fluctuations drive evolutionary syndromes linking dispersal and mating system. *Am. Nat.* **174**, 46–55 (2009).

82. M. Cardillo, L. Bromham, Body size and risk of extinction in Australian mammals. *Conserv. Biol.* **15**, 1435–1440 (2001).

83. D. A. Fordham, C. Bertelsmeier, B. W. Brook, R. Early, D. Neto, S. C. Brown, S. Ollier, M. B. Araújo, How complex should models be? Comparing correlative and mechanistic range dynamics models. *Glob. Change Biol.* **24**, 1357–1370 (2018).

84. J. A. F. Diniz-Filho, K. S. Souza, L. M. Bini, R. Loyola, R. Dobrovolski, J. F. M. Rodrigues, S. Lima-Ribeiro, L. C. Terribile, T. F. Rangel, I. Bione, R. Freitas, I. F. Machado, T. Rocha, M. L. Lorini, M. M. Vale, C. A. Navas, N. M. Maciel, F. Villalobos, M. A. Olalla-Tarraga, S. Gouveia, A macroecological approach to evolutionary rescue and adaptation to climate change. *Ecography* **42**, 1124–1141 (2019).

85. A. Alzate, T. Janzen, D. Bonte, J. Rosindell, R. S. Etienne, A simple spatially explicit neutral model explains the range size distribution of reef fishes. *Glob. Ecol. Biogeogr.* **28**, 875–890 (2019).

86. F. Leprieur, P. Descombes, T. Gaboriau, P. F. Cowman, V. Parravicini, M. Kulbicki, C. J. Melian, C. N. de Santana, C. Heine, D. Mouillot, D. R. Bellwood, L. Pellissier, Plate tectonics drive tropical reef biodiversity dynamics. *Nat. Commun.* **7**, 11461 (2016).

87. J. C. Stegen, X. Lin, J. K. Fredrickson, A. E. Konopka, Estimating and mapping ecological processes influencing microbial community assembly. *Front. Microbiol.* **6**, 370 (2015).

88. J. M. Halley, V. Sgardeli, K. A. Triantis, Extinction debt and the species–area relationship: A neutral perspective. *Glob. Ecol. Biogeogr.* **23**, 113–123 (2014).

89. P. Descombes, T. Gaboriau, C. Albouy, C. Heine, F. Leprieur, L. Pellissier, Linking species diversification to palaeo-environmental changes: A process-based modelling approach. *Glob. Ecol. Biogeogr.* **27**, 233–244 (2018).

90. J. Kutzbach, R. Gallimore, S. Harrison, P. Behling, R. Selin, F. Laarif, Climate and biome simulations for the past 21,000 years. *Quat. Sci. Rev.* **17**, 473–506 (1998).

91. J. S. Collie, L. W. Botsford, A. Hastings, I. C. Kaplan, J. L. Largier, P. A. Livingston, É. Plagányi, K. A. Rose, B. K. Wells, F. E. Werner, Ecosystem models for fisheries management: Finding the sweet spot. *Fish Fish.* **17**, 101–125 (2016).

92. M. B. Harfoot, T. Newbold, D. P. Tittensor, S. Emmott, J. Hutton, V. Lyutsarev, M. J. Smith, J. P. Scharlemann, D. W. Purves, Emergent global patterns of ecosystem structure and function from a mechanistic general ecosystem model. *PLOS Biol.* **12**, e1001841 (2014).

93. A. Bondeau, P. C. Smith, S. Zaehle, S. Schaphoff, W. Lucht, W. Cramer, D. Gerten, H. Lotze-Campen, C. Müller, M. Reichstein, B. Smith, Modelling the role of agriculture for the 20th century global terrestrial carbon balance. *Glob. Change Biol.* **13**, 679–706 (2007).

94. J. T. Rieb, R. Chaplin-Kramer, G. C. Daily, P. R. Armsworth, K. Böhning-Gaese, A. Bonn, G. S. Cumming, F. Eigenbrod, V. Grimm, B. M. Jackson, A. Marques, S. K. Pattanayak, H. M. Pereira, G. D. Peterson, T. H. Ricketts, B. E. Robinson, M. Schröter, L. A. Schulte, R. Seppelt, M. G. Turner, E. M. Bennett, When, where, and how nature matters for ecosystem services: Challenges for the next generation of ecosystem service models. *Bioscience* **67**, 820–833 (2017).

95. E. A. Fulton, J. S. Link, I. C. Kaplan, M. Savina-Rolland, P. Johnson, C. Ainsworth, P. Horne, R. Gorton, R. J. Gamble, A. D. M. Smith, D. C. Smith, Lessons in modelling and management of marine ecosystems: The Atlantis experience: Lessons learnt with Atlantis. *Fish Fish.* **12**, 171–188 (2011).

96. W. Cramer, A. Bondeau, F. I. Woodward, I. C. Prentice, R. A. Betts, V. Brovkin, P. M. Cox, V. Fisher, J. A. Foley, A. D. Friend, C. Kucharik, M. R. Lomas, N. Ramankutty, S. Sitch, B. Smith, A. White, C. Young-Molling, Global response of terrestrial ecosystem structure and function to CO_2 and climate change: Results from six dynamic global vegetation models. *Glob. Change Biol.* **7**, 357–373 (2001).

97. P. J. Mumby, The impact of exploiting grazers (Scaridae) on the dynamics of Caribbean coral reefs. *Ecol. Appl.* **16**, 747–769 (2006).

98. L. J. Bartlett, T. Newbold, D. W. Purves, D. P. Tittensor, M. B. J. Harfoot, Synergistic impacts of habitat loss and fragmentation on model ecosystems. *Proc. R. Soc. B Biol. Sci.* **283**, 20161027 (2016).

99. B. Sakschewski, W. von Bloh, A. Boit, L. Poorter, M. Peña-Claros, J. Heinke, J. Joshi, K. Thonicke, Resilience of Amazon forests emerges from plant trait diversity. *Nat. Clim. Change* **6**, 1032–1036 (2016).

100. J. T. Houghton, Y. Ding, D. J. Griggs, M. Noguer, P. J. van der Linden, X. Dai, K. Maskell, C. A. Johnson, *Climate Change 2001: The Scientific Basis: Contribution of Working Group I to the Third Assessment Report of the Intergovernmental Panel on Climate Change* (Cambridge Univ. Press, 2001).

101. S. Sitch, C. Huntingford, N. Gedney, P. E. Levy, M. Lomas, S. L. Piao, R. Betts, P. Ciais, P. Cox, P. Friedlingstein, C. D. Jones, I. C. Prentice, F. I. Woodward, Evaluation of the terrestrial carbon cycle, future plant geography and climate-carbon cycle feedbacks using five dynamic global vegetation models (DGVMs). *Glob. Change Biol.* **14**, 2015–2039 (2008).

102. J. O. Kaplan, N. H. Bigelow, I. C. Prentice, S. P. Harrison, P. J. Bartlein, T. R. Christensen, W. Cramer, N. V. Matveyeva, A. D. McGuire, D. F. Murray, V. Y. Razzhivin, B. Smith, D. A. Walker, P. M. Anderson, A. A. Andreev, L. B. Brubaker, M. E. Edwards, A. V. Lozhkin, Climate change and Arctic ecosystems: 2. Modeling, paleodata-model comparisons, and future projections. *J. Geophys. Res. Atmos.* **108**, 8171 (2003).

103. T. R. McClanahan, A coral reef ecosystem-fisheries model: Impacts of fishing intensity and catch selection on reef structure and processes. *Ecol. Model.* **80**, 1–19 (1995).

104. E. F. Connor, E. D. McCoy, The statistics and biology of the species-area relationship. *Am. Nat.* **113**, 791–833 (1979).

105. R. J. Whittaker, K. A. Triantis, R. J. Ladle, A general dynamic theory of oceanic island biogeography. *J. Biogeogr.* **35**, 977–994 (2008).

106. J. Alroy, A multispecies overkill simulation of the end-Pleistocene megafaunal mass extinction. *Science* **292**, 1893–1896 (2001).

107. R. S. Snell, Simulating long-distance seed dispersal in a dynamic vegetation model. *Glob. Ecol. Biogeogr.* **23**, 89–98 (2014).

108. E. J. Rykiel, Testing ecological models: The meaning of validation. *Ecol. Model.* **90**, 229–244 (1996).

109. S. A. Keith, S. R. Connolly, Effects of diversity-dependent colonization-extinction dynamics on the mid-domain effect. *Glob. Ecol. Biogeogr.* **22**, 773–783 (2013).

110. G. B. Bonan, S. Levis, S. Sitch, M. Vertenstein, K. W. Oleson, A dynamic global vegetation model for use with climate models: Concepts and description of simulated vegetation dynamics. *Glob. Change Biol.* **9**, 1543–1566 (2003).

111. A. Skeels, M. Cardillo, Reconstructing the geography of speciation from contemporary biodiversity data. *Am. Nat.* **193**, 240–255 (2019).

112. N. A. Urban, S. F. Matter, Metapopulation mirages: Problems parsing process from pattern. *Ecol. Model.* **375**, 20–29 (2018).

113. United Nations Conference on Environment and Development: Convention on Biological Diversity. *Int. Leg. Mater.* **31**, 822–841 (1992).

114. G. M. Mace, M. Barrett, N. D. Burgess, S. E. Cornell, R. Freeman, M. Grooten, A. Purvis, Aiming higher to bend the curve of biodiversity loss. *Nat. Sustain.* **1**, 448–451 (2018).

115. J. C. Young, K. A. Waylen, S. Sarkki, S. Albon, I. Bainbridge, E. Balian, J. Davidson, D. Edwards, R. Fairley, C. Margerison, D. McCracken, R. Owen, C. P. Quine, C. Stewart-Roper, D. Thompson, R. Tinch, S. Van den Hove, A. Watt, Improving the science-policy dialogue to meet the challenges of biodiversity conservation: Having conversations rather than talking at one-another. *Biodivers. Conserv.* **23**, 387–404 (2014).

116. S. Díaz, N. Zafra-Calvo, A. Purvis, P. H. Verburg, D. Obura, P. Leadley, R. Chaplin-Kramer, L. De Meester, E. Dulloo, B. Martín-López, M. R. Shaw, P. Visconti, W. Broadgate, M. W. Bruford, N. D. Burgess, J. Cavender-Bares, F. DeClerck, J. M. Fernández-Palacios, L. A. Garibaldi, S. L. L. Hill, F. Isbell, C. K. Khoury, C. B. Krug, J. Liu, M. Maron, P. J. K. McGowan, H. M. Pereira, V. Reyes-García, J. Rocha, C. Rondinini, L. Shannon, Y.-J. Shin, P. V. R. Snelgrove, E. M. Spehn, B. Strassburg, S. M. Subramanian, J. J. Tewksbury, J. E. M. Watson, A. E. Zanne, Set ambitious goals for biodiversity and sustainability. *Science* **370**, 411–413 (2020).

117. D. Nogués-Bravo, F. Rodríguez-Sánchez, L. Orsini, E. de Boer, R. Jansson, H. Morlon, D. A. Fordham, S. T. Jackson, Cracking the code of biodiversity responses to past climate change. *Trends Ecol. Evol.* **33**, 765–776 (2018).

118. D. A. Fordham, B. W. Brook, C. Moritz, D. Nogués-Bravo, Better forecasts of range dynamics using genetic data. *Trends Ecol. Evol.* **29**, 436–443 (2014).

119. R. Frankham, Challenges and opportunities of genetic approaches to biological conservation. *Biol. Conserv.* **143**, 1919–1927 (2010).

120. P. Erm, B. L. Phillips, Evolution transforms pushed waves into pulled waves. *Am. Nat.* **195**, E87–E99 (2019).

121. S. Theodoridis, D. A. Fordham, S. C. Brown, S. Li, C. Rahbek, D. Nogues-Bravo, Evolutionary history and past climate change shape the distribution of genetic diversity in terrestrial mammals. *Nat. Commun.* **11**, 2557 (2020).

122. H. M. Pereira, G. C. Daily, J. Roughgarden, A framework for assessing the relative vulnerability of species to land-use change. *Ecol. Appl.* **14**, 730–742 (2004).

123. J. C. Stanton, K. T. Shoemaker, R. G. Pearson, H. R. Akçakaya, Warning times for species extinctions due to climate change. *Glob. Change Biol.* **21**, 1066–1077 (2015).

124. M. Kirkpatrick, N. H. Barton, Evolution of a species' range. *Am. Nat.* **150**, 1–23 (1997).

125. R. A. Mittermeier, W. R. Turner, F. W. Larsen, T. M. Brooks, C. Gascon, in *Biodiversity Hotspots* (Springer, 2011), pp. 3–22.

126. S. C. Brown, T. M. L. Wigley, B. L. Otto-Bliesner, C. Rahbek, D. A. Fordham, Persistent Quaternary climate refugia are hospices for biodiversity in the Anthropocene. *Nat. Clim. Change* **10**, 244–248 (2020).

127. P. Leadley, *Biodiversity Scenarios: Projections of 21st Century Change in Biodiversity, and Associated Ecosystem Services: A Technical Report for the Global Biodiversity Outlook 3* (UNEP/Earthprint, 2010).

128. IUCN-CEM 2016, "The IUCN Red List of Ecosystems" (Version 2016-1); http://iucnrle.org/.

129. B. C. O'Neill, C. Tebaldi, D. P. Van Vuuren, V. Eyring, P. Friedlingstein, G. Hurtt, R. Knutti, E. Kriegler, J.-F. Lamarque, J. Lowe, The scenario model intercomparison project (ScenarioMIP) for CMIP6. *Geosci. Model Dev.* **9**, 3461–3482 (2016).

130. J. H. Brown, V. K. Gupta, B.-L. Li, B. T. Milne, C. Restrepo, G. B. West, The fractal nature of nature: Power laws, ecological complexity and biodiversity. *Philos. Trans. R. Soc. Lond. B Biol. Sci.* **357**, 619–626 (2002).

131. D. A. Fordham, F. Saltré, S. C. Brown, C. Mellin, T. M. L. Wigley, Why decadal to century timescale palaeoclimate data are needed to explain present-day patterns of biological diversity and change. *Glob. Change Biol.* **24**, 1371–1381 (2018).

132. Z. Liu, B. L. Otto-Bliesner, F. He, E. C. Brady, R. Tomas, P. U. Clark, A. E. Carlson, J. Lynch-Stieglitz, W. Curry, E. Brook, D. Erickson, R. Jacob, J. Kutzbach, J. Cheng, Transient simulation of last deglaciation with a new mechanism for Bølling–Allerød warming. *Science* **325**, 310–314 (2009).

133. P. B. Holden, N. R. Edwards, T. F. Rangel, E. B. Pereira, G. T. Tran, R. D. Wilkinson, PALEO-PGEM v1.0: A statistical emulator of Pliocene–Pleistocene climate. *Geosci. Model Dev.* **12**, 5137–5155 (2019).

134. R. Neukom, J. Gergis, Southern Hemisphere high-resolution palaeoclimate records of the last 2000 years. *Holocene* **22**, 501–524 (2012).

135. E. Roycroft, A. J. MacDonald, C. Moritz, A. Moussalli, R. P. Miguez, K. C. Rowe, Museum genomics reveals the rapid decline and extinction of Australian rodents since European settlement. *Proc. Natl. Acad. Sci. U.S.A.* **118**, e2021390118 (2021).

136. G. C. Hurtt, L. Chini, R. Sahajpal, S. Frolking, B. L. Bodirsky, K. Calvin, J. C. Doelman, J. Fisk, S. Fujimori, K. K. Goldewijk, T. Hasegawa, P. Havlik, A. Heinimann, F. Humpenöder, J. Jungclaus, J. O. Kaplan, J. Kennedy, T. Krisztin, D. Lawrence, P. Lawrence, L. Ma, O. Mertz, J. Pongratz, A. Popp, B. Poulter, K. Riahi, E. Shevliakova, E. Stehfest, P. Thornton, F. N. Tubiello, D. P. van Vuuren, X. Zhang, Harmonization of global land use change and management for the period 850–2100 (LUH2) for CMIP6. *Geosci. Model Dev.* **13**, 5425–5464 (2020).

137. S. C. Brown, T. M. L. Wigley, B. L. Otto-Bliesner, D. A. Fordham, StableClim, continuous projections of climate stability from 21000 BP to 2100 CE at multiple spatial scales. *Sci. Data* **7**, 335 (2020).

138. M. Heino, I. Hanski, Evolution of migration rate in a spatially realistic metapopulation model. *Am. Nat.* **157**, 495–511 (2001).

139. D. A. Benson, M. Cavanaugh, K. Clark, I. Karsch-Mizrachi, D. J. Lipman, J. Ostell, E. W. Sayers, GenBank. *Nucleic Acids Res.* **41**, D36–D42 (2012).

140. T. van der Valk, P. Pečnerová, D. Díez-del-Molino, A. Bergström, J. Oppenheimer, S. Hartmann, G. Xenikoudakis, J. A. Thomas, M. Dehasque, E. Sağlıcan, F. R. Fidan,

I. Barnes, S. Liu, M. Somel, P. D. Heintzman, P. Nikolskiy, B. Shapiro, P. Skoglund, M. Hofreiter, A. M. Lister, A. Götherström, L. Dalén, Million-year-old DNA sheds light on the genomic history of mammoths. *Nature* **591**, 265–269 (2021).

141. M. A. Leibold, M. Holyoak, N. Mouquet, P. Amarasekare, J. M. Chase, M. F. Hoopes, R. D. Holt, J. B. Shurin, R. Law, D. Tilman, M. Loreau, A. Gonzalez, The metacommunity concept: A framework for multi-scale community ecology. *Ecol. Lett.* **7**, 601–613 (2004).

142. S. Scheiter, L. Langan, S. I. Higgins, Next-generation dynamic global vegetation models: Learning from community ecology. *New Phytol.* **198**, 957–969 (2013).

143. J. Pilowsky, R. K. Colwell, C. Rahbek, D. A. Fordham, Dichotomous key of process-explicit models of biodiversity (2022); https://doi.org/10.6084/m9.figshare.19441655.

144. H. M. Pereira, G. C. Daily, Modeling biodiversity dynamics in countryside landscapes. *Ecology* **87**, 1877–1885 (2006).

Short communication

Simulations of human migration into North America are more sensitive to demography than choice of palaeoclimate model

Julia A. Pilowsky [a,b,*], Andrea Manica [c], Stuart Brown [a,d], Carsten Rahbek [b,e,f], Damien A. Fordham [a,g]

[a] The Environment Institute and School of Biological Sciences, University of Adelaide, SA 5005, Australia
[b] Center for Macroecology, Evolution, and Climate, GLOBE Institute, University of Copenhagen, Copenhagen Ø 2100, Denmark
[c] Department of Zoology, University of Cambridge, Cambridge, England United Kingdom
[d] Section for Evolutionary Genomics, GLOBE Institute, University of Copenhagen, Copenhagen K 1350, Denmark
[e] Danish Institute for Advanced Study, University of Southern Denmark, Odense 5230, Denmark
[f] Department of Ecology, Peking University, Beijing 100871, China
[g] Center for Global Mountain Biodiversity, GLOBE Institute, University of Copenhagen, Copenhagen Ø 2100, Denmark

ARTICLE INFO

ABSTRACT

Reconstructions of the spatiotemporal dynamics of human dispersal away from evolutionary origins in Africa are important for determining the ecological consequences of the arrival of anatomically modern humans in naïve landscapes and interpreting inferences from ancient genomes on indigenous population history. While efforts have been made to independently validate these projections against the archaeological record and contemporary measures of genetic diversity, there has been no comprehensive assessment of how parameter values and choice of palaeoclimate model affect projections of early human migration. We simulated human migration into North America with a process-explicit migration model using simulated palaeoclimate data from two different atmosphere-ocean general circulation models and did a sensitivity analysis on the outputs using a machine learning algorithm. We found that simulated human migration into North America was more sensitive to uncertainty in demographic parameters than choice of atmosphere-ocean general circulation model used for simulating climate-human interactions. Our findings indicate that the accuracy of process-explicit human migration models will be improved with further research on the population dynamics of ancient humans, and that uncertainties in model parameters must be considered in estimates of the timing and rate of human colonisation and their consequence on biodiversity.

1. Introduction

Early human migration has been reconstructed indirectly (Beyer et al., 2021), correlatively (Giampoudakis et al., 2017) and process-explicitly (Timmermann and Friedrich, 2016), allowing pathways for the expansion of modern humans to be identified by inferring or modelling relationships between climatic conditions, occupancy and population growth (Eriksson et al., 2012; Steele et al., 1998). Process-explicit models have advantages over correlative reconstructions and inferences based on climate metrics because they explicitly capture demographic responses to changing climatic and environmental conditions in model simulations (Pilowsky et al., 2022). However, they are generally data intensive, with complex model structures, often resulting in high variability amongst simulations of early human migration owing to large uncertainties in underlying demographic parameters (Timmermann and Friedrich, 2016). Furthermore, most models are fitted to a single set of simulated climatic reconstructions. It is unclear how different assumptions and biases in paleoclimate simulations (Solomon et al., 2007) affect model projections of human migration, and how important these effects are relative to uncertainties in demographic parameters. Sensitivity analyses can help improve projections of human expansion from process-explicit macroecology models by identifying parameters that contribute the most to model output, those that are insignificant and can be potentially omitted from the model, and those that need refining to improve model accuracy (Hamby, 1994).

The Climate-Informed Spatial Genetic Model (CISGeM) is one example of a process-explicit model of human dispersal out of Africa, which has been validated using genetic distances between contemporary human populations (Eriksson et al., 2012). Its outputs include human arrival times on non-African continents and islands, as well as spatial maps of effective population size (a proxy for relative abundance (Fordham et al., 2014)) from 120 kg-years before present (ka BP). The simulated outputs of CISGeM have been used to parametrise and inform other models of phenomena including megafaunal extinctions (Fordham et al., 2022) and species range dynamics (Canteri et al., 2022). However, CISGeM has never been subjected to a sensitivity analysis, meaning there is no knowledge of the importance of demographic parameters and climatic conditions on model projections. Here we simulate human migration into North America in the Pleistocene using CISGeM parametrised with two widely used atmosphere-ocean general circulation models (AOGCMs): the Hadley Centre Coupled Model, version 3 (HadCM3) (Singarayer and Valdes, 2010) and the Community Climate System Model version 3 (CCSM3) (Yeager et al., 2006) Transient Climate Evolution (TraCE-21ka) simulation (Z. Liu et al., 2009). We do a sensitivity analysis to determine whether well-established structural and projection differences in these two palaeoclimate models (; Burke et al., 2018; Kageyama et al., 2018) strongly influence CISGeM simulations of human colonisation of North America when uncertainties in key demographic parameters are also considered.

2. Material and methods

2.1. Human expansion model

We modelled the peopling of North America using CISGeM (Climate-Informed Spatial Genetic Model), which is a process- and spatially-explicit population model of global human migration during the late Pleistocene and Holocene (Eriksson et al., 2012). The model is driven by demographic processes responding to glacial-interglacial ice-land-sea dynamics, and spatiotemporal variation in net primary productivity that affects carrying capacities. The latter has been shown to be an important driver of population density for hunter-gatherers (Tallavaara et al., 2018; but see Zhu et al., 2021). Previous model testing has shown that CISGeM accurately reconstructs global genetic diversity and human arrival times on the non-African continents (Eriksson et al., 2012; Raghavan et al., 2015). See Supplementary Information for more details on the model structure of CISGeM.

Model parameters in CISGeM have been optimised using pattern-orientated modelling methods (Grimm et al., 2005) and Approximate Bayesian Computation (Csilléry et al., 2010). In this study, we used the posterior ranges of optimised model parameters to generate 4950 plausible CISGeM models, each with different parameter values (Table S1). These posterior ranges have been used elsewhere to reconstruct human migration rates in North America and Eurasia using CISGeM (Canteri et al., 2022; Fordham et al., 2022). We used Latin hypercube sampling to generate a stratified random subset of parameter input values for simulations by specifying the posterior range for each parameter and sampling all portions of the distributions (Stein, 1987). We then ran each of these models using palaeoclimate data from two AOGCMs, and did a global sensitivity analysis (Antoniadis et al., 2021) to determine the influence of demographic parameters and climate model parametrisation on CISGeM projections of human colonisation of North America (Figure S2).

2.2. Climate data

Plausible models ($n = 4950$) were simulated using palaeoclimate AOGCM data from HadCM3 (Singarayer and Valdes, 2010) and the CCSM3 TraCE-21ka simulation (Z. Liu et al., 2009). These two palaeoclimate models were chosen because their climatic outputs are most frequently used in macroecological models (Blois et al., 2013;

Theodoridis et al., 2020), including approaches that simulate colonisation and extinction processes (Canteri et al., 2022; Fordham et al., 2022; He et al., 2013). Their high usage in ecological models reflects their temporal coverage, which tends to be more continuous than many other widely accessible paleoclimate datasets (Armstrong et al., 2019; S. C. Brown et al., 2020; Fordham et al., 2017), many of which are limited to widely spaced snapshots of key climatic periods (J. L. Brown et al., 2018; Lima-Ribeiro et al., 2015). While projections from the HadCM3 have been shown to be congruent with those from the CCSM3 TraCE-21ka simulation for some climatic parameters in some regions and time points (Armstrong et al., 2019), there are important local-to-regional differences between projections from these AOGCMs (Burke et al., 2018; Kageyama et al., 2018), including in North America (Fig. 1).

Unlike the TraCE-21ka simulation, the HadCM3 is not a fully transient climate model, meaning that outputs from HadCM3 are climate snapshots rather than continuous projections. Climate snapshots from the HadCM3 outputs (separated by ≥ 1 ka) were temporally downscaled to 25 year timesteps to match the timestep of CISGeM simulations using a stochastic weather generator, which draws random values from empirical distributions adjusted to fit the temperature and precipitation intervals found in the climate data (Semenov and Barrow, 2002). The grid cell resolution of HadCM3 data is 3.75° longitude × 2.5° latitude. Forcings include orbitally forced insolation changes, changes in long-lived greenhouse gases, and meltwater from evolving ice sheets. These are the same forcings used in TraCE-21ka, with a key difference that HadCM3 does not account for vegetation-air-ocean interactions (Collins et al., 2006).

The TraCE-21ka simulation (Z. Liu et al., 2009) uses the CCSM3 (Yeager et al., 2006) to reconstruct daily global climate conditions at a spatial resolution of 3.75° longitude × 3.75 latitude (over land and sea) for the last 21,000 years. It accurately reproduces major climatic features associated with the most recent deglaciation event (Z. Liu et al., 2009), and predicts present-day climate patterns with verified hindcast skill (Fordham et al., 2017). Importantly, both HadCM3 and TRaCE-21ka model ice sheet dynamics using the ICE-5 G reconstruction (Peltier, 2004), meaning that ice sheet barriers to human dispersal in CISGeM models were identical in simulations regardless of palaeoclimate model (Movie S1). We spatially downscaled data from both models to the equal-area resolution of CISGeM (100 km width). See Supplementary Information for details.

2.3. Simulations

We ran a single replicate of CISGeM for each combination of plausible parameters and recorded the simulated effective population size at each hex cell and time point. Previously, it has been shown that running a single simulation iteration per parameter sample is optimal for sensitivity analysis if the parameter space is extensively sampled (Prowse et al., 2016). All simulations were global, began at the same starting location in East Africa at 120 ka BP, and proceeded until present (0 BP, 1950 C.E.) at 25-year time steps (Eriksson et al., 2012).

We identified, *a priori*, time of movement out of Alaska and rate of expansion through North America as two important metrics of regional human migration that are likely to be sensitive to changes in demographic parameters and variation in climate model projections. This is because climatic change facilitated the initial movement of people into North America (Becerra-Valdivia and Higham, 2020), and the speed of this movement was constrained by demographic processes and their interaction with climate and environmental conditions (Timmermann and Friedrich, 2016). We calculated time of movement out of Alaska (after 19 ka BP) and rate of expansion through North America (14.7 to 11 ka BP) for each projection. Movement out of Alaska was calculated as the time when the population-weighted centroid of the leading edge of the human range (Watts et al., 2013) crossed 130°W or 51°N. Rate of expansion through North America was calculated as the rate of movement, in kilometres per year, of the population-weighted centroid of the
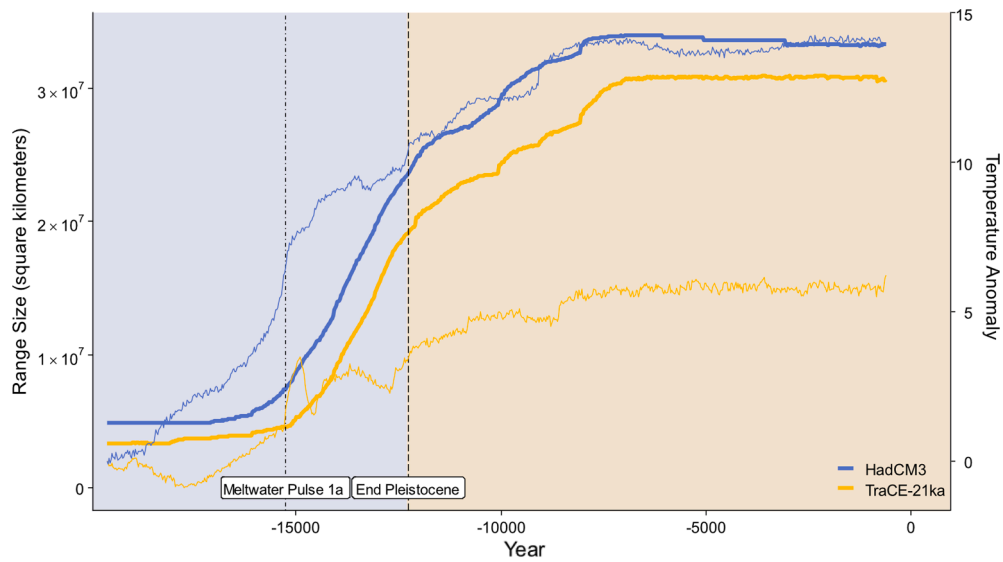
Fig. 1. Human range expansion in North America. Range size for humans in North America from 19,000 years ago to present according to simulations with the HadCM3 (blue) and CCSM3 TraCE-21ka (yellow) AOGCMs (thick lines). Thin lines show mean annual temperature anomaly for the two AOGCMs. .

leading edge of the human range. See Supplementary Information for more details on how these variables were calculated. CISGeM projections of time of movement out of Alaska were independently validated using inferences of the timing of arrival of Clovis culture in North America (13,250 to 12,800 years BP; Waters and Stafford 2007).

2.4. Sensitivity analysis

To determine which parameters contribute most to model projections of human expansion in North America, we did a global sensitivity analysis using our summary metrics of time of movement out of Alaska and rate of expansion through North America (Antoniadis et al.,

2021). Sensitivity analyses were done in two ways: (i) using only CIS-GeM models simulated using HadCM3 climate data (*demographic-only sensitivity analysis*); (ii) using models simulated with climate and precipitation data from HadCM3 and CCSM3 TRaCE-21ka palaeoclimate models (*demographic + climate sensitivity analysis*). This two-step approach was done because CISGeM were originally optimised using HadCM3 climate data (Eriksson et al., 2012). The sensitivity analysis did not account for potentially important structural uncertainties in CIS-GeM, including human generation length and the simulated sequence of modelled demographic processes.

We determined the sensitivity of timing of movement out of Alaska and expansion rate using random forest learning methods (Antoniadis
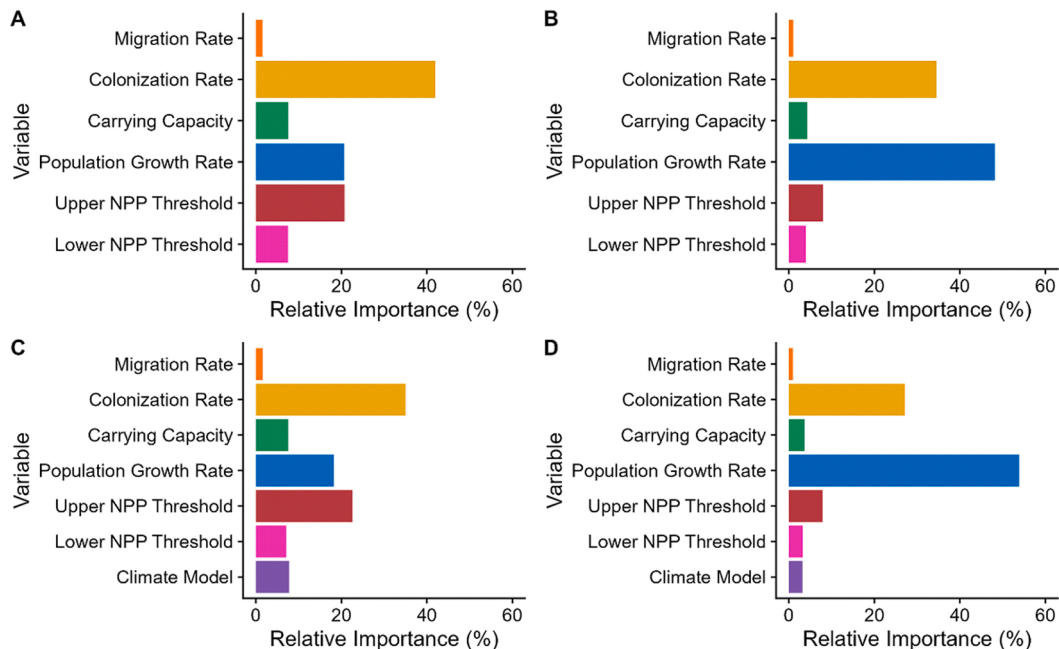

Fig. 2. Sensitivity analysis of human migration model parameters. Sensitivity of simulations of timing of human migration out of Alaska (A, C) and rate of southward expansion through North America (B, D). A and B are only for simulations run on HadCM3 climate data (demographic-only sensitivity analysis), while C and D are for both HadCM3- and TraCE-21ka-based simulations (demographic + climate sensitivity analysis). Relative importance scores from random forest models in B and C are shown for demographic parameters: migration rate, colonisation rate, carrying capacity, population growth rate, upper and lower net primary productivity (NPP) thresholds for occupancy. For C and D, relative importance scores also have choice of climate model simulation (HadCM3 or TraCE-21ka).

et al., 2021) following techniques established for process-explicit macroecology models (Pearson et al., 2014). We tuned the hyperparameters using k-fold cross-validation, choosing number of variables sampled per split and minimum node size by minimizing RMSE (RMSE = 478 ± 13.6 for exit from Alaska and RMSE = 479 ± 15.3 for expansion rate). We assessed variable importance using unscaled permutation importance (Strobl et al., 2007). See Supplementary Information for details.

3. Results

While range size of humans in North America varied according to AOGCM (Fig. 1), time of movement out of Alaska and rate of human migration were most sensitive to uncertainty in key demographic parameters (Fig. 2). The demographic-only sensitivity analysis, done using HadCM3 model-based simulations only, revealed: i) time of movement out of Alaska was most sensitive to colonisation rate, upper net primary productivity threshold for carrying capacity and population growth rate; while ii) population-weighted rate of expansion was most sensitive to population growth rate and colonisation rate (Fig. 2). This order of relative importance remained unchanged when the sensitivity analysis was done on simulations with varying temperature and precipitation inputs from the two AOGCMs (demographic + climate sensitivity analysis) (Fig. 2). This indicates a relatively low sensitivity of CISGeM projections to pronounced differences in palaeoclimate conditions in North America according to AOGCM (Fig. 1) when compared to uncertainties in demographic model parameters.

Independent tests of CISGeM projections of time of movement out from Alaska showed that simulations of land migration from CISGeM parametrised with TraCE21-ka climate data gave a median exit date from Alaska that was closer to the estimated Clovis arrival (median: 14,375 years BP, MAD: 482) compared to simulations parametrised with HadCM3 data (median: 15,000 years BP, MAD: 111). The difference for TraCE-21ka and HadCM3 was 1144 years (95% confidence interval [CI] = 1138–1150 years) and 1682 years (CI = 1663–1700 years), respectively. Model projections of migration patterns into North America and relative N_e for both models can be accessed on Figshare (Pilowsky et al., 2022).

4. Conclusions

While projections of the peopling of North America from process-explicit models vary in response to two choices of AOGCM, uncertainties in key demographic parameters have a disproportionately larger influence on simulations of time of movement out of Alaska and rate of expansion through North America. This shows the likely importance of considering uncertainties in the demographic parameters of process-explicit model projections of timing, rate and mechanisms of initial human expansion across continents (Raghavan et al., 2015), and the broader ecological consequences of human colonisation on biodiversity (Canteri et al., 2022; Fordham et al., 2022).

While arrival times of humans in different regions have been established archaeologically with reasonable certainty (Goebel et al., 2008; Groucutt et al., 2015), and dispersal rates have been inferred from genomic analysis of aDNA (Rasmussen et al., 2011), the pattern of human growth and expansion has been more difficult to reconstruct at fine spatiotemporal scales. Consequently, projections of early human migration across continents are still uncertain (H. Liu et al., 2006). This is partly because of overly simplistic parametrisation of the relationship between net primary productivity and population growth (Zhu et al., 2021) and large uncertainties in other demographic parameters, including dispersal (French et al., 2021)

Resolving these issues should be a priority, given how sensitive the rate of human movement in North America is to rates of population growth and colonisation. Promising avenues of research that could reduce uncertainty in early human demography include Bayesian analysis of spatiotemporal distributions of radiocarbon dates (Price

et al., 2020); phylogenetic analysis of the human palaeoproteome, which is more resistant to degradation over long timescales compared to the palaeogenome (Welker, 2018); and sampling of environmental DNA, which can detect arrival and movement of small populations better than the archaeological or fossil record (Wang et al., 2021).

Our finding that uncertainty in projections of human migration from process-explicit models is only weakly sensitive to the choice of underlying palaeoclimate model is in stark contrast to findings for correlative models of species distributions (Beaumont et al., 2007; Tuck et al., 2006), which model demographic processes implicitly, not explicitly (Pilowsky et al., 2022). When interpreting the generality of this result, it is important to recognise that CISGeM simulates pathways for the global expansion of modern humans. Therefore, in other regions and time periods, the parametrisation of palaeoclimate could have a larger effect on human migration, especially since migration occurred at different rates in different regions. While we tested the sensitivity of CISGeM to palaeoclimate uncertainty using two AOGCMs with very different climate sensitivities (Masson-Delmotte et al., 2013), spatiotemporal uncertainty could potentially be greater in North America if more models were considered. Nevertheless, our results highlight the importance of realistically capturing demographic mechanisms in process-explicit human migration models.

CRediT authorship contribution statement

Julia A. Pilowsky: Conceptualization, Validation, Formal analysis, Writing – original draft, Visualization. **Andrea Manica:** Methodology, Software, Writing – review & editing. **Stuart Brown:** Formal analysis, Writing – review & editing. **Carsten Rahbek:** Conceptualization, Supervision. **Damien A. Fordham:** Funding acquisition, Conceptualization, Supervision, Methodology, Writing – review & editing.

Declaration of Competing Interest

The authors declare that they have no known competing financial interests or personal relationships that could have appeared to influence the work reported in this paper.

Data Availability

Data are available on Figshare and have been cited in the text.

Supplementary materials

Supplementary material associated with this article can be found, in the online version, at doi:10.1016/j.ecolmodel.2022.110115.

References

Antoniadis, A., Lambert-Lacroix, S., Poggi, J.-.M., 2021. Random forests for global sensitivity analysis: a selective review. Reliab. Eng. Syst. Saf. 206, 107312 https://doi.org/10.1016/j.ress.2020.107312.

Armstrong, E., Hopcroft, P.O., Valdes, P.J., 2019. A simulated Northern Hemisphere terrestrial climate dataset for the past 60,000 years. Sci. Data 6 (1), 1–16. https://doi.org/10.1038/s41597-019-0277-1.

Beaumont, L.J., Pitman, A.J., Poulsen, M., Hughes, L., 2007. Where will species go? Incorporating new advances in climate modelling into projections of species distributions. Glob. Chang. Biol. 13 (7), 1368–1385. https://doi.org/10.1111/j.1365-2486.2007.01357.x.

Becerra-Valdivia, L., Higham, T., 2020. The timing and effect of the earliest human arrivals in North America. Nature 584, 1–5. https://doi.org/10.1038/s41586-020-2491-6.

Beyer, R.M., Krapp, M., Eriksson, A., Manica, A., 2021. Climatic windows for human migration out of Africa in the past 300,000 years. Nat. Commun. 12 (1), 4889. https://doi.org/10.1038/s41467-021-24779-1.

Blois, J.L., Williams, J.W., Fitzpatrick, M.C., Jackson, S.T., Ferrier, S., 2013. Space can substitute for time in predicting climate-change effects on biodiversity. Proc. Natl. Acad. Sci. 110 (23), 9374–9379. https://doi.org/10.1073/pnas.1220228110.

Brown, J.L., Hill, D.J., Dolan, A.M., Carnaval, A.C., Haywood, A.M., 2018. PaleoClim, high spatial resolution paleoclimate surfaces for global land areas. Sci. Data 5 (1), 180254. https://doi.org/10.1038/sdata.2018.254.

Brown, S.C., Wigley, T.M.L., Otto-Bliesner, B.L., Fordham, D.A., 2020. StableClim, continuous projections of climate stability from 21000 BP to 2100 CE at multiple spatial scales. Sci. Data 7 (1), 335. https://doi.org/10.1038/s41597-020-00663-3.

Burke, K.D., Williams, J.W., Chandler, M.A., Haywood, A.M., Lunt, D.J., Otto-Bliesner, B. L., 2018. Pliocene and Eocene provide best analogs for near-future climates. Proceedings of the National Academy of Sciences 115 (52), 13288–13293. https://doi.org/10.1073/pnas.1809600115.

Canteri, E., Brown, S.C., Schmidt, N.M., Heller, R., Nogues-Bravo, D., Fordham, D.A., 2022. Spatiotemporal influences of climate and humans on muskox range dynamics over multiple millennia. Glob. Chang. Biol. https://doi.org/10.1111/gcb.16375.

Collins, W.D., Bitz, C.M., Blackmon, M.L., Bonan, G.B., Bretherton, C.S., Carton, J.A., Chang, P., Doney, S.C., Hack, J.J., Henderson, T.B., Kiehl, J.T., Large, W.G., McKenna, D.S., Santer, B.D., Smith, R.D., 2006. The Community Climate System Model Version 3 (CCSM3). J. Clim. 19 (11), 2122–2143. https://doi.org/10.1175/JCLI3761.1.

Csilléry, K., Blum, M.G.B., Gaggiotti, O.E., François, O., 2010. Approximate Bayesian Computation (ABC) in practice. Trends Ecol. Evol. (Amst.) 25 (7), 410–418. https://doi.org/10.1016/j.tree.2010.04.001.

Eriksson, A., Betti, L., Friend, A.D., Lycett, S.J., Singarayer, J.S., von Cramon-Taubadel, N., Valdes, P.J., Balloux, F., Manica, A., 2012. Late Pleistocene climate change and the global expansion of anatomically modern humans. Proc. Natl. Acad. Sci. U.S.A. 109 (40), 16089–16094. https://doi.org/10.1073/pnas.1209494109.

Fordham, D.A., Brook, B.W., Moritz, C., Nogués-Bravo, D., 2014. Better forecasts of range dynamics using genetic data. Trends Ecol. Evol. (Amst.) 29 (8), 436–443. https://doi.org/10.1016/j.tree.2014.05.007.

Fordham, D.A., Brown, S.C., Akçakaya, H.R., Brook, B.W., Haythorne, S., Manica, A., Shoemaker, K.T., Austin, J.J., Blonder, B., Pilowsky, J., Rahbek, C., Nogues-Bravo, D., 2022. Process-explicit models reveal pathway to extinction for woolly mammoth using pattern-oriented validation. Ecol. Lett. 25 (1), 125–137. https://doi.org/10.1111/ele.13911.

Fordham, D.A., Saltré, F., Haythorne, S., Wigley, T.M., Otto-Bliesner, B.L., Chan, K.C., Brook, B.W., 2017. PaleoView: a tool for generating continuous climate projections spanning the last 21 000 years at regional and global scales. Ecography 40 (11), 1348–1358.

French, J.C., Riris, P., Fernandéz-López de Pablo, J., Lozano, S., Silva, F., 2021. A manifesto for palaeodemography in the twenty-first century. Philos. Trans. Royal Soc. B Biol. Sci.s 376 (1816), 20190707. https://doi.org/10.1098/rstb.2019.0707.

Giampoudakis, K., Marske, K.A., Borregaard, M.K., Ugan, A., Singarayer, J.S., Valdes, P. J., Rahbek, C., Nogués-Bravo, D., 2017. Niche dynamics of Palaeolithic modern humans during the settlement of the Palaearctic. Global Ecol. Biogeogr. 26 (3), 359–370. https://doi.org/10.1111/geb.12543.

Goebel, T., Waters, M.R., O'Rourke, D.H, 2008. The late Pleistocene dispersal of modern humans in the Americas. Science 319 (5869), 1497–1502. https://doi.org/10.1126/science.1153569.

Grimm, V., Revilla, E., Berger, U., Jeltsch, F., Mooij, W.M., Railsback, S.F., Thulke, H.-H., Weiner, J., Wiegand, T., DeAngelis, D.L., 2005. Pattern-oriented modeling of agent-based complex systems: lessons from ecology. Science 310 (5750), 987–991. https://doi.org/10.1126/science.1116681.

Groucutt, H.S., Petraglia, M.D., Bailey, G., Scerri, E.M.L., Parton, A., Clark-Balzan, L., Jennings, R.P., Lewis, L., Blinkhorn, J., Drake, N.A., Breeze, P.S., Inglis, R.H., Devès, M.H., Meredith-Williams, M., Boivin, N., Thomas, M.G., Scally, A., 2015. Rethinking the dispersal of Homo sapiens out of Africa. Evolution. Anthropol. Issues News Rev. 24 (4), 149–164. https://doi.org/10.1002/evan.21455.

Hamby, D.M., 1994. A review of techniques for parameter sensitivity analysis of environmental models. Environ. Monit. Assess. 32 (2), 135–154. https://doi.org/10.1007/BF00547132.

He, Q., Edwards, D.L., Knowles, L.L., 2013. Integrative testing of how environments from the past to the present shape genetic structure across landscapes. Evolution (N Y) 67 (12), 3386–3402. https://doi.org/10.1111/evo.12159.

Kageyama, M., Braconnot, P., Harrison, S.P., Haywood, A.M., Jungclaus, J., Otto-Bliesner, B.L., Peterschmitt, J.-.Y., Abe-Ouchi, A., Albani, S., Bartlein, P.J., 2018. PMIP4-CMIP6: the contribution of the Paleoclimate Modelling Intercomparison Project to CMIP6. Geosci. Model Develop. Discuss. 11 (3), 1033–1057.

Lima-Ribeiro, M.S., Varela, S., González-Hernández, J., de Oliveira, G., Diniz-Filho, J.A. F., Terribile, L.C., 2015. EcoClimate: a database of climate data from multiple models for past, present, and future for macroecologists and biogeographers. Biodiver. Inform. 10.

Liu, H., Prugnolle, F., Manica, A., Balloux, F., 2006. A geographically explicit genetic model of worldwide human-settlement history. American J. Human Genet. 79 (2), 230–237. https://doi.org/10.1086/505436.

Liu, Z., Otto-Bliesner, B.L., He, F., Brady, E.C., Tomas, R., Clark, P.U., Carlson, A.E., Lynch-Stieglitz, J., Curry, W., Brook, E., Erickson, D., Jacob, R., Kutzbach, J., Cheng, J., 2009. Transient simulation of last deglaciation with a new mechanism for

Bølling–Allerød warming. Science 325 (5938), 310–314. https://doi.org/10.1126/science.1171041.

Masson-Delmotte, V., Schulz, M., Abe-Ouchi, A., Beer, J., Ganopolski, A., González Rouco, J.F., Jansen, E., Lambeck, K., Luterbacher, J., Naish, T., Osborn, T., Otto-Bliesner, B., Quinn, T., Ramesh, R., Rojas, M., Shao, X., Timmermann, A., 2013. Information from Paleoclimate Archives. *Climate Change 2013: The Physical Science Basis. Contribution of Working Group I to the Fifth Assessment Report of the Intergovernmental Panel on Climate Change* [Stocker, T.F., D. Qin, G.-K. Plattner, M. Tignor, S.K. Allen, J. Boschung, A. Nauels, Y. Xia, V. Bex and P.M. Midgley (eds.)]. Cambridge University Press, Cambridge, UK and New York, NY, USA.

Pearson, R.G., Stanton, J.C., Shoemaker, K.T., Aiello-Lammens, M.E., Ersts, P.J., Horning, N., Fordham, D.A., Raxworthy, C.J., Ryu, H.Y., McNees, J., Akçakaya, H.R., 2014. Life history and spatial traits predict extinction risk due to climate change. Nat. Clim. Chang. 4 (3), 217–221. https://doi.org/10.1038/nclimate2113.

Peltier, W.R., 2004. Global glacial isostasy and the surface of the ice-age earth: the ICE-5G (VM2) Model and GRACE. Annu. Rev. Earth Planet Sci. 32 (1), 111–149. https://doi.org/10.1146/annurev.earth.32.082503.144359.

Pilowsky, J.A., Colwell, R.K., Rahbek, C., Fordham, D.A., 2022a. Process-explicit models reveal the structure and dynamics of biodiversity patterns. Sci. Adv. 8 (31), eabj2271. https://doi.org/10.1126/sciadv.abj2271.

Pilowsky, J.A., Manica, A., Brown, S.C., Rahbek, C., & Fordham, D.A. (2022). *Process-explicit simulations of human migration in North America 19,000 years ago to present* [Data set]. figshare. https://doi.org/10.6084/M9.FIGSHARE.20078630.

Price, M.H., Capriles, J.M., Hoggarth, J.A., Bocinsky, K., Ebert, C.E., & Jones, J.H. (2020). *End-to-end Bayesian analysis of 14C dates reveals new insights into lowland Maya demography* (10.1101/2020.07.02.185256). bioRxiv. https://doi.org/10.1101/2020.07.02.185256.

Prowse, T.A.A., Bradshaw, C.J.A., Delean, S., Cassey, P., Lacy, R.C., Wells, K., Aiello-Lammens, M.E., Akçakaya, H.R., Brook, B.W., 2016. An efficient protocol for the global sensitivity analysis of stochastic ecological models. Ecosphere 7 (3), e01238. https://doi.org/10.1002/ecs2.1238.

Raghavan, M., Steinrücken, M., Harris, K., Schiffels, S., Rasmussen, S., DeGiorgio, M., Albrechtsen, A., Valdiosera, C., Ávila-Arcos, M.C., Malaspinas, A.-.S., Eriksson, A., Moltke, I., Metspalu, M., Homburger, J.R., Wall, J., Cornejo, O.E., Moreno-Mayar, J. V., Korneliussen, T.S., Pierre, T., Willerslev, E., 2015. Genomic evidence for the Pleistocene and recent population history of Native Americans. Science 349 (6250), aab3884. https://doi.org/10.1126/science.aab3884.

Rasmussen, M., Guo, X., Wang, Y., Lohmueller, K.E., Rasmussen, S., Albrechtsen, A., Skotte, L., Lindgreen, S., Metspalu, M., Jombart, T., Kivisild, T., Zhai, W., Eriksson, A., Manica, A., Orlando, L., De La Vega, F.M., Tridico, S., Metspalu, E., Nielsen, K., Willerslev, E., 2011. An Aboriginal Australian genome reveals separate human dispersals into Asia. Science 334 (6052), 94–98. https://doi.org/10.1126/science.1211177.

Semenov, M.A., & Barrow, E.M. (2002). *LARS-WG: a stochastic weather generator for use in climate impact studies* (3.0).

Singarayer, J.S., Valdes, P.J., 2010. High-latitude climate sensitivity to ice-sheet forcing over the last 120kyr. Quat. Sci. Rev. 29 (1), 43–55. https://doi.org/10.1016/j.quascirev.2009.10.011.

Solomon, S., Qin, D., Manning, M., Chen, Z., Marquis, M., Averyt, K.B., Tignor, M., Miller, H.L., 2007. Climate Change 2007: The Physical Science Basis. Contribution of Working Group I to the Fourth Assessment Report of the Intergovernmental Panel On Climate Change. Cambridge University Press. http://www.cabdirect.org/cabdirect/abstract/20083115509.

Steele, J., Adams, J., Sluckin, T., 1998. Modelling Paleoindian dispersals. World Archaeol. 30 (2), 286–305. https://doi.org/10.1080/00438243.1998.9980411.

Stein, M., 1987. Large sample properties of simulations using Latin hypercube sampling. Technometrics 29 (2), 143–151. https://doi.org/10.1080/00401706.1987.10488205.

Strobl, C., Boulesteix, A.-.L., Zeileis, A., Hothorn, T., 2007. Bias in random forest variable importance measures: illustrations, sources and a solution. BMC Bioinformatics 8 (1), 25. https://doi.org/10.1186/1471-2105-8-25.

Tallavaara, M., Eronen, J.T., Luoto, M., 2018. Productivity, biodiversity, and pathogens influence the global hunter-gatherer population density. Proc. Natl. Acad. Sci. 115 (6), 1232–1237.

Theodoridis, S., Fordham, D.A., Brown, S.C., Li, S., Rahbek, C., Nogues-Bravo, D., 2020. Evolutionary history and past climate change shape the distribution of genetic diversity in terrestrial mammals. Nat. Commun. 11 (1), 2557. https://doi.org/10.1038/s41467-020-16449-5.

Timmermann, A., Friedrich, T., 2016. Late Pleistocene climate drivers of early human migration. Nature 538 (7623), 92–95. https://doi.org/10.1038/nature19365.

Tuck, G., Glendining, M.J., Smith, P., House, J.I., Wattenbach, M., 2006. The potential distribution of bioenergy crops in Europe under present and future climate. Biomass Bioenergy 30 (3), 183–197. https://doi.org/10.1016/j.biombioe.2005.11.019.

Wang, Y., Pedersen, M.W., Alsos, I.G., De Sanctis, B., Racimo, F., Prohaska, A., Coissac, E., Owens, H.L., Merkel, M.K.F., Fernandez-Guerra, A., Rouillard, A., Lammers, Y., Alberti, A., Denoeud, F., Money, D., Ruter, A.H., McColl, H., Larsen, N. K., Cherezova, A.A., Willerslev, E., 2021. Late Quaternary dynamics of Arctic biota from ancient environmental genomics. Nature 600, 86–92. https://doi.org/10.1038/s41586-021-04016-x.

Waters, M.R., Stafford, T.W., 2007. Redefining the age of Clovis: implications for the peopling of the Americas. Science 315 (5815), 1122–1126.

Watts, M.J., Fordham, D.A., Akçakaya, H.R., Aiello-Lammens, M.E., Brook, B.W., 2013. Tracking shifting range margins using geographical centroids of metapopulations weighted by population density. Ecol. Modell. 269, 61–69. https://doi.org/10.1016/j.ecolmodel.2013.08.010.

Welker, F., 2018. Palaeoproteomics for human evolution studies. Quat. Sci. Rev 190, 137–147. https://doi.org/10.1016/j.quascirev.2018.04.033.

Yeager, S.G., Shields, C.A., Large, W.G., Hack, J.J., 2006. The Low-Resolution CCSM3. J. Clim. 19 (11), 2545–2566. https://doi.org/10.1175/JCLI3744.1.

Zhu, D., Galbraith, E.D., Reyes-García, V., Ciais, P., 2021. Global hunter-gatherer population densities constrained by influence of seasonality on diet composition. Nat. Ecol. Evol. 5 (11), 1536–1545. https://doi.org/10.1038/s41559-021-01548-3.

RESEARCH ARTICLE

Range and extinction dynamics of the steppe bison in Siberia: A pattern-oriented modelling approach

Julia A. Pilowsky[1,2] | Sean Haythorne[1,3] | Stuart C. Brown[1,4] | Mario Krapp[5,6] | Edward Armstrong[7] | Barry W. Brook[8] | Carsten Rahbek[2,9,10,11] | Damien A. Fordham[1,2,11]

[1]The Environment Institute and School of Biological Sciences, University of Adelaide, Adelaide, South Australia, Australia

[2]Center for Macroecology, Evolution and Climate, Globe Institute, University of Copenhagen, Copenhagen Ø, Denmark

[3]School of BioSciences, University of Melbourne, Melbourne, Victoria, Australia

[4]Section for Evolutionary Genomics, Globe Institute, University of Copenhagen, Copenhagen K, Denmark

[5]Antarctic Research Centre, Victoria University of Wellington, Wellington, New Zealand

[6]GNS Science, Lower Hutt, New Zealand

[7]Department of Geosciences and Geography, University of Helsinki, Helsinki, Finland

[8]School of Biological Sciences and Australian Research Council Centre of Excellence for Australian Biodiversity and Heritage, University of Tasmania, Hobart, Tasmania, Australia

[9]Danish Institute for Advanced Study, University of Southern Denmark, Odense, Denmark

[10]Institute of Ecology, Peking University, Beijing, China

[11]Center for Mountain Biodiversity, Globe Institute, University of Copenhagen, Copenhagen Ø, Denmark

Correspondence
Julia A. Pilowsky and Damien A. Fordham, The Environment Institute and School of Biological Sciences, University of Adelaide, Adelaide, SA 5005, Australia.
Email: julia.pilowsky@adelaide.edu.au (J.A.P.) and damien.fordham@adelaide.edu.au (D.A.F.)

Abstract

Aim: To determine the ecological processes and drivers of range collapse, population decline and eventual extinction of the steppe bison in Eurasia.

Location: Siberia.

Time period: Pleistocene and Holocene.

Major taxa studied: Steppe bison (*Bison priscus*).

Methods: We configured 110,000 spatially explicit population models (SEPMs) of climate–human–steppe bison interactions in Siberia, which we ran at generational time steps from 50,000 years before present. We used pattern-oriented modelling (POM) and fossil-based inferences of distribution and demographic change of steppe bison to identify which SEPMs adequately simulated important interactions between ecological processes and biological threats. These "best models" were then used to disentangle the mechanisms that were integral in the population decline and later extinction of the steppe bison in its last stronghold in Eurasia.

Results: Our continuous reconstructions of the range and extinction dynamics of steppe bison were able to reconcile inferences of spatio-temporal occurrence and the timing and location of extinction in Siberia based on hundreds of radiocarbon-dated steppe bison fossils. We showed that simulating the ecological pathway to extinction

for steppe bison in Siberia in the early Holocene required very specific ecological niche constraints, demographic processes and a constrained synergy of climate and human hunting dynamics during the Pleistocene–Holocene transition.

Main conclusions: Ecological processes and drivers that caused ancient population declines of species can be reconstructed at high spatio-temporal resolutions using SEPMs and POM. Using this approach, we found that climatic change and hunting by humans are likely to have interacted with key ecological processes to cause the extinction of the steppe bison in its last refuge in Eurasia.

KEYWORDS

climate change, distribution, extinction dynamics, mechanistic model, metapopulation, palaeoclimate, range shift, spatially explicit population model, steppe bison, synergistic threats

1 | INTRODUCTION

Several hypotheses have been proposed for how extinctions manifest in space and time (Davidson et al., 2009; Owens & Bennett, 2000), but generalities across landscapes and time periods have been difficult to formulate (Laliberte & Ripple, 2004). Theories of range shifts, population declines and extinctions are now being tested directly using historical and palaeo-reconstructions (Fordham et al., 2021, 2022), permitting inferences of how biodiversity is likely to respond to future environmental change (Fordham et al., 2020). However, reconstructing past demographic changes at landscape scales poses unique modelling challenges, including the reliance on indirect proxies to draw inferences about range collapses and the timing and location of extinction (Dietl et al., 2015); uncertainty in reconstructions of past climates (Rutherford et al., 2005) and human-driven environmental threats (Ellis et al., 2021; Pilowsky, Manica, et al., 2022); and a lack of information on the ecological lifestyles and traits of many species (Fordham et al., 2016).

Some of these issues can be addressed, at least in part, using process-explicit models, particularly if they are combined with pattern-oriented modelling (POM) techniques (Box 1). Process-explicit models simulate ecological and evolutionary mechanisms responsible for spatio-temporal patterns of biodiversity (Pilowsky, Colwell, et al., 2022). These mechanisms include extirpation, movement, ecological interactions, adaptation and speciation. Unlike correlative approaches, such as species distribution models, process-explicit models establish causal links between process and pattern (Urban et al., 2016). However, high data demand and model complexity have meant that, to date, they have been used less frequently in studies of the structure and dynamics of patterns of biodiversity. This is steadily changing, owing to increased data availability, computational power (Pilowsky, Colwell, et al., 2022) and a growing need for stronger inferences about the causes of contemporary and ancient changes in biodiversity (Fordham et al., 2020; Pontarp et al., 2019; Rangel et al., 2018).

POM methods (Grimm & Railsback, 2012) can directly address some of the problems of data availability and subsequent parameter uncertainty in process-explicit models of species distributions

---

BOX 1 Biodiversity modelling terms

Approximate Bayesian computation (ABC): A statistical technique that uses Bayesian statistics to estimate the distributions of model parameters by comparing simulated probability distributions of summary statistics against their observed distributions (Beaumont et al., 2002).

Correlative models: Models that statistically relate environmental variables to observation data in order to infer biological patterns (Pilowsky, Colwell, et al., 2022).

Pattern-oriented modelling (POM): An approach for optimizing model parameters using independent validation targets (Grimm et al., 2005).

Process-explicit models: Models that represent the dynamics of an ecological system as explicit functions of the processes that drive change in that system. Also known as process-based and mechanistic models (Connolly et al., 2017).

Spatially explicit population models (SEPMs): Process-explicit models that simulate mortality, reproduction and movement in a network of populations on a landscape map (Dunning Jr et al., 1995).

---

and community dynamics (Canteri et al., 2022; Fordham et al., 2022; Rangel et al., 2018). Although POM was first used in ecology and evolution to optimize uncertain parameters in individual- and agent-based models (Thulke et al., 1999), it has since been used to simulate demographic change using spatially explicit population models (Canteri et al., 2022; Fordham et al., 2022), genetic diversification in lineages of species (Knowles & Alvarado-Serrano, 2010), changes in community structure (Colwell & Rangel, 2010) and evolutionary shifts in populations (Barnes & Clark, 2017). It uses optimization routines to determine model parameter values based on observed (or inferred, if operating across palaeo time frames) empirical patterns (Grimm & Railsback, 2012), increasing the likelihood of capturing

key biological processes in model simulations. This strategy assumes that observed patterns are fingerprints of underlying ecological and evolutionary processes, enabling models to be parameterized initially using uncertain but plausible information on these processes (Gallagher et al., 2021).

Despite offering new opportunities to gain a better understanding of the mechanisms that regulate biodiversity under past climate and environmental change, POM methods are only now being used in conjunction with spatially explicit population models (SEPMs) to reconstruct species' range and extinction dynamics over palaeo time-scales (but see Canteri et al., 2022; Fordham et al., 2022). SEPMs simulate movement, mortality and reproduction in networks of populations over time (Anderson et al., 2009; Hanski, 1998), allowing the identification of ecological mechanisms and threats that caused ancient extinctions and range collapses (Canteri et al., 2022). POM optimization is done using patterns inferred from the fossil record and ancient DNA (Fordham et al., 2022). Here, we show the utility of combining POM methods with SEPMs to reconstruct and disentangle the extinction dynamics of the steppe bison (*Bison priscus*) in Eurasia. The approach uses multiple rounds of SEPM optimization to reconstruct continuously the interactions between the ecological lifestyle and demography of steppe bison and drivers of global change (climatic change and human activities) over a period going back 50,000 years. We do this using the R package PALEOPOP v2.1.0 (Haythorne et al., 2021) that we developed as an extension to POEMS (Fordham et al., 2021), adding important new functionality for modelling species range dynamics over multi-millennial time-scales.

The steppe bison was one of the many large herbivores that dominated the "mammoth steppe" biome of the Ice Age (Guthrie, 1989), all of which declined in range size as the mammoth steppe was replaced by a taiga–tundra ecotone during the Pleistocene–Holocene transition (Lorenzen et al., 2011; Markova et al., 2015). The relative abundance of steppe bison (based on reconstructions of effective population size) peaked during the late Pleistocene (Shapiro et al., 2004), when the mammoth steppe was maximally distributed (Anderson & Lozhkin, 2001), with regional extinction in Eurasia at *c.* 8.7 kilo-years before present (kyr BP) (Boeskorov et al., 2016) and global extinction in North America some 6–8 kyr later (Shapiro et al., 2004). In Eurasia, isotopic analysis of late Pleistocene fossils shows that the steppe bison was a strict grazer that did not migrate seasonally (Julien et al., 2012). Here, they competed with the European bison (*Bison bonasus*) for ecological dominance until climate-induced vegetation change following the Last Glacial Maximum [LGM; a period from 26.5 to 19 kyr BP (Clark et al., 2009)] restricted the less ecologically flexible steppe bison to Siberia (Soubrier et al., 2016).

The processes leading to the megafaunal extinctions of the mammoth steppe during the late Pleistocene and early Holocene are uncertain, with intense debate regarding the timing, location and the roles of human hunting and climatic change (Mann et al., 2019; Stuart, 2015; Wang et al., 2021). Here, we configure 110,000 SEPMs of climate–human–steppe bison interactions in Siberia, which we test against inferences of demographic change and range collapse

inferred from fossils using POM methods. Our continuous reconstructions of the range and extinction dynamics of steppe bison from 50 kyr BP reveal the ecological processes and threats that led to the demise of the steppe bison in its last stronghold in Eurasia at *c.* 9 kyr BP.

2 | MATERIALS AND METHODS

The steppe bison is an extinct species of bison that was once widespread in the steppe of the Northern Hemisphere (Markova et al., 2015). Its relative abundance (based on reconstructions of effective population size) peaked during the late Pleistocene (Shapiro et al., 2004), when the mammoth steppe biome was maximally distributed (Anderson & Lozhkin, 2001), and it became regionally extinct in Eurasia *c.* 8.7 kyr BP (Boeskorov et al., 2016). We simulated the ecological pathway to extinction for the steppe bison in Siberia.

2.1 | PALEOPOP

PALEOPOP is an object-oriented R package (Haythorne et al., 2021) that we developed to simulate range and extinction dynamics of species over multiple millennia, enabling causal insights into likely past driver–state relationships. PALEOPOP uses a lattice-grid population model to simulate ecological processes (demography and ecological requirements) and their interactions over long temporal scales. PALEOPOP is an extension to the R package POEMS v.1.0.1 (Fordham et al., 2021), which implements SEPMs and POM methods to identify ecological processes of range shifts and extinctions (Figure 1). PALEOPOP adds three major features to POEMS: (1) the capacity to simulate long-term processes of landscape change (sea level rise; movement of glacial ice sheets) occurring over glacial–interglacial cycles; (2) a palaeo-population simulator optimized for simulating demographic change resulting from metapopulation and dispersal dynamics over multiple millennia; and (3) a palaeo-results object suitable for storing the data-heavy output from the palaeo-population simulator.

2.2 | Steppe bison niche

2.2.1 | Fossil data

We gathered radiocarbon-dated data on steppe bison fossils from the palaeontological literature (for details, see Supporting Information Appendix S1). We regularized inconsistent and outdated species names, discarding any records where the species was ambiguous (e.g., "bison" without clear indicators of whether it was the steppe bison or another bison species). In cases where a site name was available but latitude and longitude were not, we compared maps from the source literature against OpenStreetMap and Google Earth to geocode locations
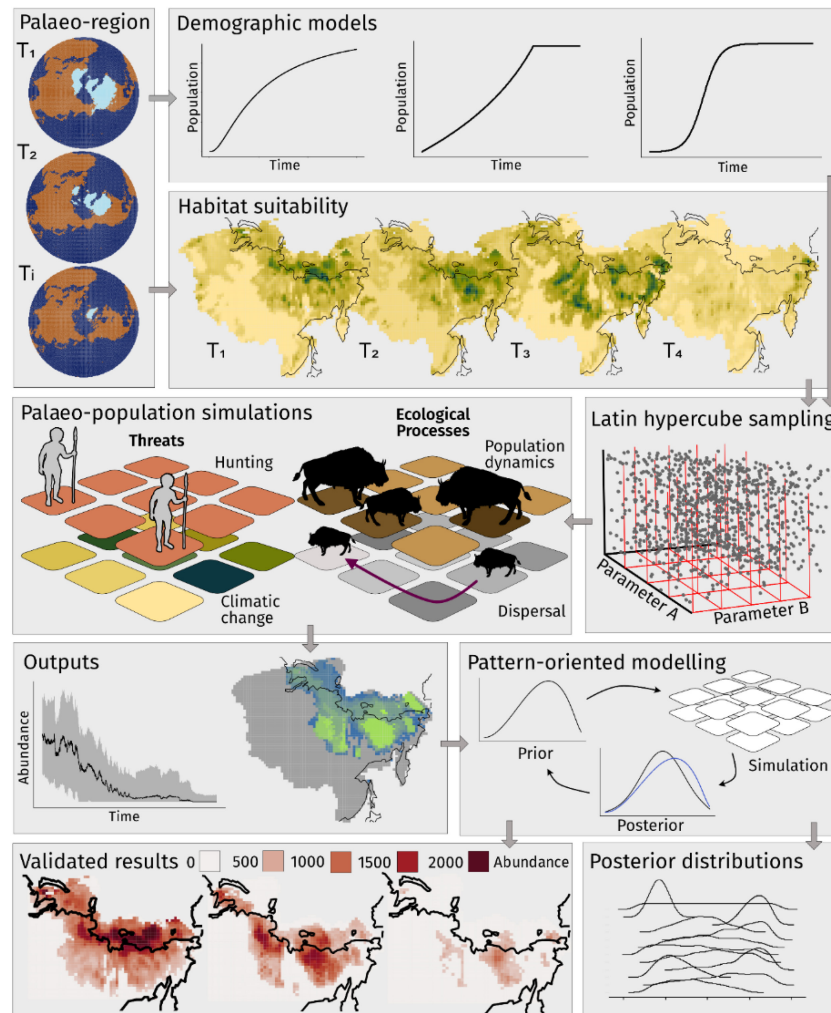
FIGURE 1 Modelling species range dynamics over palaeo time-scales. The modelled dynamic palaeo-region changes temporally owing to climatic change and associated rising sea levels and melting ice sheets. Spatially explicit population models (SEPMs) are built by coupling a demographic model with a grid-lattice-type spatial structure of habitat suitability. Latin hypercube sampling is used to sample SEPM parameter space exhaustively, resulting in tens of thousands of parameter combinations, each of which is used to parameterize an SEPM. The palaeo-population simulations include ecological processes (including dispersal and extinction) responding to key threats of human hunting and climatic change. These simulations reconstruct outputs of past population size and abundance maps. Pattern-oriented modelling (POM) is used to identify models that reconcile patterns of demographic change inferred from palaeo-archives. This involves optimizing values of SEPM parameters by comparing the distributions of posterior and prior parameter ranges (posterior distributions) for successive iterations of model building and testing. Models that do best at simulating inferred patterns of range and extinction dynamics are used to generate validated projections.

manually. The quality of all radiocarbon dates was assessed based on stratigraphy, association and the material dated. We retained 378 records rated as "reliable" (Barnosky & Lindsey, 2010). We calibrated these radiocarbon dates using the OxCal v.4.4 tool (Ramsey, 2017) and the IntCal13 curve (Reimer et al., 2013), which returned calibrated age and standard deviation estimates. The fossil record can be accessed from Figshare (Pilowsky et al., 2021).

2.2.2 | Climate data

Palaeoclimate simulations of precipitation, temperature and latent heat flux used to model the ecological niche of the steppe bison

(see below) are from the HadCM3B coupled ocean–ice–atmosphere model (Valdes et al., 2017). These palaeoclimate simulations incorporate monthly and interannual climate variability (directly from model output) and millennial-scale variability (by assimilating model and Greenland ice core data) and have been downscaled to $0.5° \times 0.5°$ spatial resolution (Armstrong et al., 2019). We extracted monthly data for the study region of Siberia (Supporting Information Appendix S1, Figure S1.1) from 50 to 5 kyr BP and generated 30-year averages at a 12-year (generational; see description of the process-explicit model below) time step for: (1) total annual precipitation; (2) mean boreal winter (DJF) temperature; and (3) total evapotranspiration during boreal spring and summer (MAMJJA). Evapotranspiration (ET) was calculated by dividing the average monthly latent heat

flux by the latent heat of vaporization based on average monthly temperatures:

$$ET \,(mm\,/\,month) = \left(\frac{\text{heat flux}}{(2.501 - 0.00237 \times \text{temperature}) \times 1 \times 10^6} \right) \times 86,400 \times 30$$

(1)

where heat flux and temperature are the modelled monthly heat flux (in watts per square metre) and temperature (in degrees Celsius) for each month.

The mean temperature of the coldest month, mean temperature of the warmest month and annual precipitation have been used previously to model the ecological niche and distribution of high-latitude herbivores, including the steppe bison (Lorenzen et al., 2011) and the American bison (*Bison bison*) (Metcalf et al., 2014). This is because the temperature variables are likely to capture the upper and lower thermal limits of the species, and precipitation drives demographic rates in extant bison species (Koons et al., 2012). Given that spring and summer evapotranspiration was moderately correlated with the temperature of the warmest month (Kendall's τ = .548), we chose to model only spring and summer evapotranspiration because it captures better the structure of vegetation available as forage in the warmer months (Guthrie, 2006). We used average temperature across all boreal winter months (DJF) instead of only the coldest month, because it captures better the stressors and limitations created by winter conditions (DelGiudice et al., 1994, 2001). None of the three variables were correlated with each other by more than Kendall's τ = .5.

2.2.3 | Niche model

We generated continuous habitat suitability maps (based on probability of occurrence) for the steppe bison in Siberia from 50 to 5 kyr BP using ecological niche models (Nogués-Bravo, 2009). To do this, we paired fossil occurrences with our three selected climate variables, accounting for dating uncertainty (Fordham et al., 2022). Climate data were paired spatially, as determined by the grid cell where the fossil occurred, and temporally, as determined by the band of uncertainty [±2SD, which is commonly used for calibrated radiocarbon date distributions (Blaauw, 2010)] around the calibrated radiocarbon date. We removed any duplicate climate data created by two fossil occurrences falling within identical or overlapping spatio-temporal bins (Canteri et al., 2022). We used this climate dataset to create a full (multi-temporal) Gaussian hypervolume, optimized for appropriate bandwidth (Blonder et al., 2018), which provided an estimate of the fundamental niche of steppe bison (Nogués-Bravo, 2009).

Given that the realized climatic niche of steppe bison is likely to be a subset of its fundamental niche (Soberón & Nakamura, 2009), we thoroughly subsampled the full hypervolume of potentially livable climatic conditions (Supporting Information Appendix S1, Figure S1.2) and determined the realized niche using SEPMs and POM (see section 2.4 below). We did this by cutting the full hypervolume into

smaller hypervolumes (n = 1000) of different volumes and marginalities (climatic specialization) using outlying mean index analysis (Dolédec et al., 2000). We projected the hypervolumes back into geographical space, creating time series of maps of habitat suitability based on the probability density of the climate hypervolume at the set of environmental conditions in each grid cell (77.8 km × 71.0 km grid cell resolution) from 50 to 5 kyr BP. We scaled the suitability scores of each projection to a zero to one interval, based on the 95th percentile of maximum habitat suitability values in grid cells across time and space.

2.3 | Palaeolithic humans

The expansion of Palaeolithic humans into northern Eurasia was modelled using a process-explicit climate-informed spatial genetic model (CISGEM) that has been shown accurately to reconstruct the dispersal of *Homo sapiens* out of Africa (Eriksson et al., 2012). CISGEM simulates local effective population size (N_e) based on a cellular demographic model, with carrying capacity modulated by net primary productivity. We ran CISGEM from 120 kyr BP to the present using the HadCM3B ocean–ice–atmosphere model (Valdes et al., 2017) and 4950 parameter combinations that had previously been shown to reconstruct patterns of human migration and growth robustly (Eriksson et al., 2012). We calculated the mean and variance of the 4950 simulation results (Supporting Information Appendix S1, Figure S1.3) and scaled the projections of N_e between zero and one (taking an approach identical to the scaling of steppe bison habitat suitability projections). We then resampled the outputs from the time step of CISGEM (25 years) to the time step of the bison simulations (12 years). To parameterize human hunting in our demographic models, we generated 50,000 potential trajectories of relative human density (using relative N_e as a proxy) in Siberia by sampling a lognormal distribution of relative effective population size (based on the mean and variance of the 4950 simulations), accounting for spatially autocorrelated stochasticity (see Supporting Information Appendix S1 for an extended description of the methods used to reconstruct human densities in Siberia).

2.4 | Process-explicit model

We generated an SEPM in PALEOPOP that simulated the ecological processes of movement and demographic change (extinction), responding to shifting climates, sea levels, ice sheets and human hunting. Key ecological processes we modelled for the steppe bison included density-dependent population growth, dispersal and source–sink dynamics. These processes were simulated at generational time steps (12 years) using scalar-type SEPMs (Fordham et al. 2018). Habitat suitabilities from the potential realized niche models were used to structure the metapopulation by providing estimates of relative upper abundance in space and time (Fordham et al., 2022), assuming no adaptation to climatic or environmental change over the

course of the simulation. Simulations were run at 12-year time steps from 50 to 5 kyr BP. To ensure stable metapopulation dynamics at the beginning of the simulation (Fordham et al., 2018), all simulations were preceded by a burn-in period of 100 generations, whereby grid cell upper abundance values were held at 50 kyr BP values for the burn-in period.

2.4.1 | Demography

Demographic rates for congeneric species (*B. bison* and *B. bonasus*) were used as surrogates for the steppe bison (Fordham et al., 2016). We estimated the maximum annual growth rate and its variance using time series data for *B. bison* and *B. bonasus* (for details, see Supporting Information Appendix S1). We scaled these growth rates to a generational time step based on the 12-year generation length of *B. bison* (Pacifici et al., 2013). After testing the stability of population dynamics with different density dependence functions, we modelled population growth with Ricker logistic density dependence (Ricker, 1954), with the carrying capacity dependent on the habitat suitability in a given grid cell. At a habitat suitability of one, the carrying capacity was equal to the maximum density (Table 1), reducing with lower suitability scores. We modelled a negative Allee effect, using a quasi-extinction threshold below which populations immediately dropped to zero (Fordham et al., 2018).

We simulated natal dispersal based on empirical estimates for *B. bison* (Jung, 2017). Between 5 and 25% of the population dispersed per generation, with a maximum dispersal distance of 100–500 km (Table 1). A dispersal friction landscape (Adriaensen et al., 2003) based on ice sheet reconstructions was used to ensure that bison dispersed only through ice-free grid cells. Human hunting was simulated based on relative abundance (see above). The harvest

z parameter shaped the hunting function from a type II ($z = 1$) to type III ($z = 2$) functional response (Brook & Bowman, 2002), with the maximum harvest set from 0 to 35% (Fordham et al., 2022). All demographic parameters are described in more detail in the Supporting Information (Appendix S1).

2.4.2 | Model simulations

To address parameter uncertainty, which is inevitably high for extinct species (Brook & Bowman, 2004), we created 50,000 unique SEPM parameterizations using Latin hypercube sampling (Stein, 1987), drawing samples from uniform prior distributions for 11 model parameters (Table 1). This stratified sampling of the priors allowed us to generate a large suite of SEPMs, covering the parameter space of demographic processes, ecological requirements (based on realized niche breadth and specialty) and hunting pressure. We selected realized niches to generate the carrying capacity landscapes in each simulation. Each sampled combination of parameters, including niche estimates, was integrated into an SEPM and simulated for a single replicate (Fordham et al., 2022). Fifty thousand simulations took 214 h in parallel on an eight-core Windows machine with a 3.6 GHz processor.

2.5 | Pattern-oriented modelling

2.5.1 | Validation targets

POM (Grimm et al., 2005) was used to evaluate different SEPM parameterizations. Simulations were validated using POM methods by comparing simulated estimates of spatio-temporal occurrences in Siberia, and the timing and location of extinction, with

Parameter	Mean prior	Mean posterior
Ecological niche		
Niche volume	0.5 (0–1)	0.438 (0.332–0.775)
Niche outlier marginality index (OMI)	0.5 (0–1)	0.197 (0.166–0.237)
Human harvesting		
Maximum harvest (%)	17.5 (0–35)	25.3 (9.5–34.1)
Harvest function (z)	1.5 (1–2)	1.46 (1.04–1.89)
Human density (p)	0.5 (0–1)	0.782 (0.585–0.984)
Movement		
Dispersing fraction	0.15 (0.05–0.25)	0.212 (0.121–0.249)
Maximum dispersal distance (km)	300 (100–500)	419 (285–495)
Population model		
Maximum growth rate (r)	2.07 (1.31–2.84)	2.066 (1.566–2.816)
Variance of growth rate	0.123 (0–0.245)	0.172 (0.095–0.228)
Allee effect (abundance threshold)	250 (0–500)	212 (126–298)
Maximum density (bison per grid cell)	1875 (500–3250)	2542 (1840–3203)

TABLE 1 Parameter distributions: The prior and posterior means, minima and maxima are shown for parameters in the process-explicit model of steppe bison range and extinction dynamics

Note: All priors are uniformly distributed. For details, see Materials and Methods.

fossil-based inferences (Supporting Information Appendix S1). We estimated the timing of extinction in Siberia from the fossil record to be 8734 yr BP (95% confidence interval: 8810–8657 yr BP) using a Gaussian-resampled, inverse-weighted method (Bradshaw et al., 2012) that accounts for the Signor–Lipps effect (Signor et al., 1982). We estimated the extinction location to be in the Lena River basin, based on the youngest fossil (Pilowsky et al., 2021). To calculate spatio-temporal occurrence, we set a spatio-temporal window of uncertainty around each steppe bison fossil in our study region ($n = 31$), then quantified the agreement between simulated and inferred occurrence. The spatial window was based on the grid cell and its eight nearest neighbours, and the temporal band of uncertainty was based on ±2SD of the calibrated date. The same temporal band of uncertainty was used to quantify climatic conditions for the multi-temporal niche. A simulated presence of bison within the inferred window of occurrence was treated as a correctly simulated occurrence.

2.5.2 | Statistical procedure

POM was done in the R package ABC v.2.1 (Csilléry et al., 2012) using approximate Bayesian computation with the rejection algorithm to select the 100 best models. All summary metrics for analysis were scaled based on their standard deviations (van der Vaart et al., 2015). The POM procedure was repeated using informed priors from previous model runs. This was done until Bayes factors indicated that the posteriors had converged (Supporting Information Appendix S2, S2.1). The procedure involved running four additional rounds of 10,000 simulations each, selecting the best 100 models each time and using the posterior distributions as the priors for the subsequent round. Posterior predictive checks were done to determine whether the posterior distributions resulted in a good resemblance between simulated and observed data (Gelman et al., 2014).

2.6 | Counterfactual scenarios

Counterfactual scenarios create possible alternatives to what occurred historically (Mondal & Southworth, 2010). We used counterfactual analysis to determine the consequences of rates of past climatic change and hunting by humans on the decline and extinction of steppe bison in Siberia (Fordham et al., 2022). We created an optimized ensemble based on the 100 best models selected from the final round of simulations, which served as a "baseline scenario" (non-counterfactual) of what is historically likely to have occurred in Siberia based on our POM approach. We used this optimized ensemble of models to simulate two counterfactual scenarios: no harvest, which modelled no hunting of steppe bison by humans from 50 kyr BP (i.e., steppe bison responding only to climate change); and constant climate, which held climatic suitability for steppe bison in Siberia at LGM values from 21 kyr BP to the end of the simulation. For the constant climate scenario, the density of humans remained dynamic. Demographic and ecological parameters for the counterfactual

scenarios were generated using random draws from the posterior distributions of the optimized ensemble model, using the Latin hypercube sampling approach described above. The counterfactual and baseline scenarios were compared using 10,000 simulations per scenario.

3 | RESULTS

Our validated simulations showed that the range of the steppe bison in Siberia contracted in a north-easterly direction until 33 kyr BP, when the range fragmented into smaller populations (Figure 2). This fragmentation continued through the Pleistocene–Holocene transition, resulting in only refugial populations in north-eastern Siberia from 11 kyr BP (Supporting Information Movie S1). The time of extinction in Siberia was simulated to occur at 7.4 kyr BP (±1.5 kyr BP), based on the ABC-weighted average of the best 100 process-explicit models. The oldest end of the window of uncertainty in our simulated estimate of time of extinction overlapped with the time of extinction based on the fossil record (8.81–8.66 kyr BP; see Materials and Methods). The youngest end overlapped with independent environmental DNA evidence of prolonged persistence of steppe bison in north-eastern Siberia, with the youngest inference of occurrence being at 6.4 ± 0.6 kyr BP (Wang et al., 2021). This ensemble of "best models" projected the last surviving population to be in the east Siberian highlands, occurring *c.* 500 km from the last known fossil, located at Batagaika in the Lena River valley (Murton et al., 2017).

The capacity of SEPMs to simulate fossil-based inferences of timing and location of extinction was high after five iterations of POM (Figure 3). Bayes factors showed convergence in prior and posterior distributions after these five iterations of POM (all Bayes factors were less than one; Supporting Information Appendix S2, Figure S2.1). Posterior predictive checks showed that these posterior parameter distributions resulted in reasonable resemblance between simulated and observed data for extinction location and extinction time ($p > .01$; Supporting Information Appendix S2, Table S2.1). However, there was a poorer fit between the simulated spatio-temporal occurrence of bison at fossil sites and the observed fossil-based inference of spatio-temporal occurrence ($p < .01$).

3.1 | Posterior distributions of model parameters

Comparison of posterior and prior parameters showed that accurately reconstructing inferences of range contraction and the timing and location of extinction from the fossil record required specific demographic and niche constraints and hunting pressure (Figure 4). Posterior distributions showed that specific niche requirements were needed to reconstruct the range and extinction dynamics of steppe bison. The posterior distributions for niche volume and outlying mean index (Table 1) indicated that steppe bison in Siberia fulfilled a subset of core climatic conditions available to the species across its entire multi-temporal range. This was shown by a small-to-medium
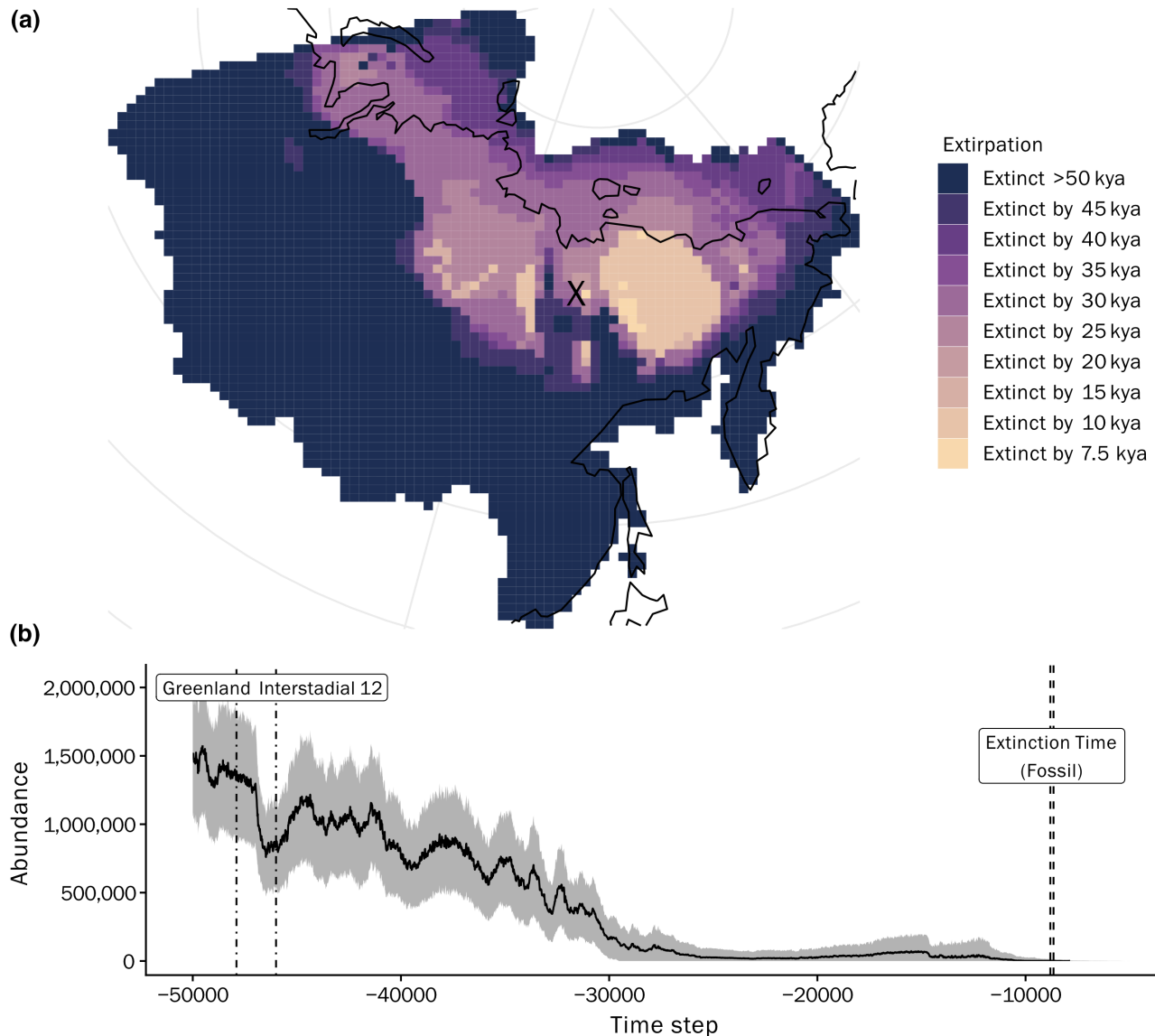
(a)

(b)

FIGURE 2 Validated reconstruction of the extinction of the steppe bison in Siberia. (a) The map shows the multi-model average estimate of the time of extirpation for the best models according to pattern-oriented modelling. The location of the site of extinction based on fossil data is marked with a cross. (b) The time series shows simulated total population size for steppe bison in Siberia. Vertical lines show extinction time as estimated from the fossil record and Greenland interstadial 12. The latter is a period of climatic warming between 47.9 and 46.0 kyr BP.

niche volume (60% of the full multi-temporal niche volume) and small outlying mean index. Among demographic processes, the posterior distributions showed that a high variance in growth rate, a medium-sized Allee effect, high maximum density and high dispersal (in terms of both maximum dispersal distance and dispersing fraction) were important for reconstructing range and extinction dynamics of the steppe bison in Siberia (Table 1). Furthermore, hitting validation targets required high human densities and high rates of harvest (Table 1).

3.2 | Counterfactual scenarios

In a no hunting scenario, the total population size of steppe bison in Siberia was higher throughout the simulation compared with the baseline (with hunting), and they did not go extinct before the end of the

simulation at 5 kyr BP (Figure 5). Before 30 kyr BP in the no hunting scenario, the range of the steppe bison extended further south and west, fragmenting into smaller subpopulations only in the final 5000 years of the simulation (Supporting Information Movie S1). In a constant climate scenario, in which the climate was unvarying from 21 kyr BP, total population size stabilized at 19 kyr BP (Figure 5), while the range contracted to two large subpopulations that were linked by dispersal, both of which persisted to the end of the simulation (Supporting Information Movie S1).

Neither of the counterfactual scenarios did as well as the baseline model at predicting the timing and location of extinction (Supporting Information Appendix S2, Figure S2.2). Models without human hunting (no hunting scenario) were generally better able to simulate spatio-temporal occurrence than the constant climate and baseline scenarios. This was because the absence of hunting
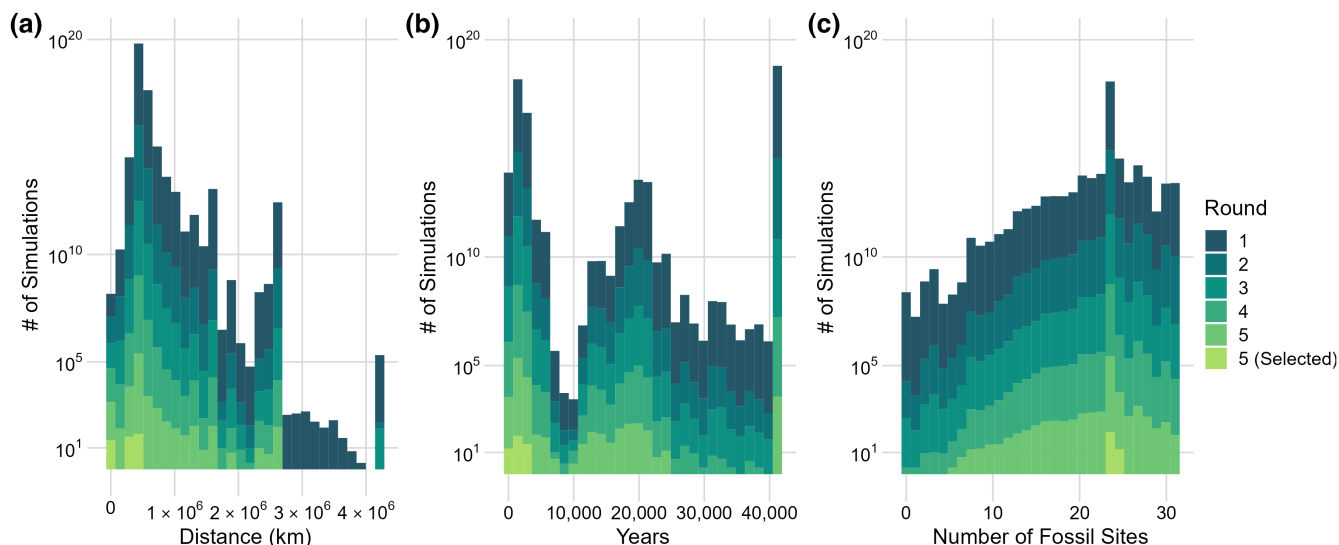
FIGURE 3 Reconstructions of validation targets using pattern-oriented modelling (POM). Validation targets for POM are: (a) extinction location, evaluated by difference (in kilometres) between simulated extinction location and the location based on the youngest fossil; (b) extinction time, evaluated by difference (in years) between simulated and inferred time of extinction based on the fossil record; and (c) fossil-based occurrence, evaluated by the number of sites where spatio-temporal occurrence is simulated correctly. For (a) and (b), the target for POM was zero (no difference between simulated and target value). For (c), the target was 31, which is equal to the total number of fossil occurrence sites. Different colours show five successive iterations of POM. For further details, see the Materials and Methods.
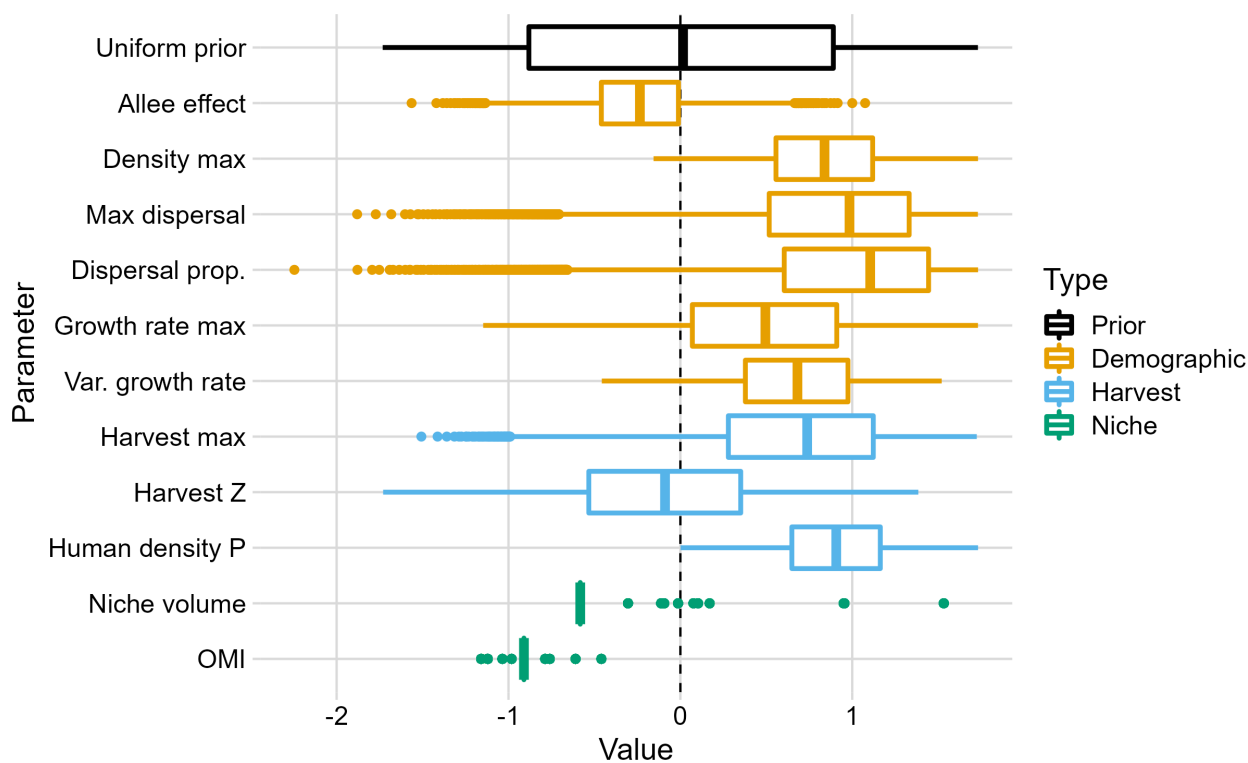

FIGURE 4 Regression-adjusted posterior distributions for parameters. Maximum (max) dispersal distance and the fraction of bison that dispersed in each generation (dispersing fraction) combine to simulate dispersal. Maximum density of bison in each grid cell, Allee effect, variance (var.) and maximum growth rate all interact to simulate population growth. Human density (relative human density), harvest z (shape of the harvest function) and maximum harvest (maximum proportion of bison hunted) determine the hunting rate. Volume and outlying mean index (OMI) are measures of climatic niche space (the size of the climatic niche and the marginality of climatic preferences, respectively). All prior distributions were uniform. Parameters are described in more detail in the Materials and Methods. Unscaled parameter ranges are provided in Table 1.
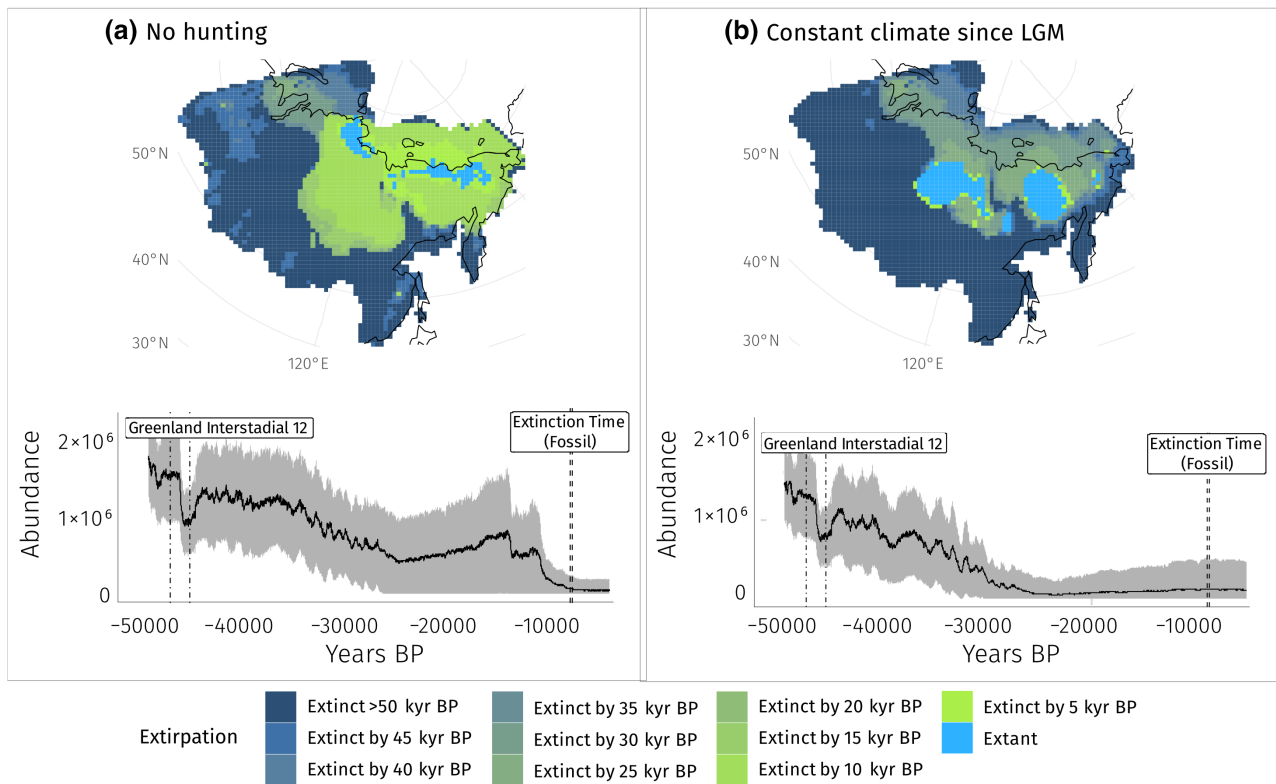
FIGURE 5 Alternative scenarios of extirpation and population decline. Counterfactual scenarios simulate: (a) climate change but no human harvesting of bison (no hunting); and (b) no climate change from 21 kyr BP, but harvesting of bison before and after that time [constant climate since Last Glacial Maximum (LGM)]. Maps show when populations in each grid cell went extinct locally. Populations that survived to the end of the simulation are shown in bright blue (extant). Line graphs show the simulated trajectories of total abundance in Siberia (±1SD). They include timing of Greenland interstadial 12 and timing of extinction in Siberia inferred from fossils. For details, see Figure 2.

by humans resulted in larger areas of occupied habitat in Siberia through time (Supporting Information Movie S1).

4 | DISCUSSION

We were able to reconcile inferences of spatio-temporal occurrence and the timing and location of extinction for steppe bison in Siberia based on hundreds of radiocarbon-dated fossils. Our ensemble of "best models" projected extinction to have occurred in the east Siberian highlands at 7.4 kyr BP, occurring on average 1300 years after the fossil estimate. This is consistent with fossil-based estimates of extinction often being hundreds to thousands of years earlier than the likely timing of the extinction event (Haile et al., 2009; Wang et al., 2021), because they represent the last time that a species was abundant (Mann et al., 2019). We show that simulating the ecological pathway to extinction for steppe bison in its last refuge in Eurasia required very specific ecological niche constraints, demographic processes and hunting dynamics. It also required these processes to respond to climatic change, human abundance and their interaction during the Pleistocene–Holocene transition. Counterfactual scenarios confirmed that human hunting and climatic change were both pivotal long-term drivers of regional extinction for the steppe bison in Siberia and, most probably,

Eurasia more generally. These results demonstrate how SEPMs and POM methods can be used in macroecology and palaeoecology to disentangle the mechanisms that were integral in the decline and later extinction of species.

The processes leading to the megafauna extinctions of the late Pleistocene and early Holocene are uncertain, with intense debate on the roles of human hunting and climatic change (Mann et al., 2019; Stuart, 2015). The steppe bison was an iconic herbivore that dominated the "mammoth steppe" of the Ice Age Arctic (Guthrie, 1989). Although the timing, location and causes of megafaunal extinctions in this biome are contested (Cooper et al., 2015; Koch & Barnosky, 2006; Stuart, 2015), our process-explicit models show that a synergy of climatic change and exploitation by humans most probably drove the steppe bison, and perhaps other herbivores of the mammoth steppe, to extinction during the late Pleistocene and early Holocene.

POM revealed the ecological processes that regulated the extinction dynamics of steppe bison. Reconstructing fossil-based evidence of spatio-temporal occurrence and extinction in the northern Lena River valley requires steppe bison to have an ecological niche volume of 59–74% of the size of the full multi-temporal niche (Nogués-Bravo, 2009). This reduced niche volume has low marginality (Dolédec et al., 2000), meaning that the ecological niche for steppe bison in Siberia represented the core climatic preferences of steppe bison more generally. Among demographic processes,

dispersal and the effect of small population size on extirpation are likely to have influenced the range and extinction dynamics of steppe bison. Hitting our multivariate validation target required a pronounced Allee effect and the capacity for high dispersal, among other demographic constraints. Evidence for an Allee effect at low population densities has been found in natural populations of other temperate and polar ungulates: bighorn sheep (*Ovis canadensis*), chamois (*Rupicapra rupicapra*), elk (*Cervus elaphus*), pronghorn (*Antilocapra americana*) and woodland caribou (*Rangifer tarandus*) (Kramer et al., 2009). This has been attributed largely to cooperative defence and predator satiation reducing mortality at high densities, although mate selection at low density could also be a factor (Kramer et al., 2009). A high capacity for movement, including long-distance dispersal, was also needed to reconstruct inferences of demographic change from the fossil record. Research on American bison has shown that they migrate seasonally in response to forage availability in winter (Gates & Larter, 1990). They will also disperse towards unoccupied habitat when population densities become high (Plumb et al., 2009).

Reconciling inferences of range collapse and extinction from the palaeo-record required hunting by humans. More specifically, humans needed to be found in medium to high regional densities (based on projections for Siberia), with high harvest offtake. Holding the hunting of bison constant to zero exploitation and analysing the effect of this constraint on dynamic processes and emergent patterns revealed that human hunting was a crucial and chronic driver of extinction of steppe bison in Siberia. Without hunting by humans, steppe bison maintained a wider distribution and larger population size and did not go extinct by 5 kyr BP (the end of the simulation). Instead, bison persisted in two small subpopulations in the far north of Siberia with suitable climatic conditions. This finding aligns with archaeological evidence showing that human hunters in Siberia relied heavily on bison prey during the Pleistocene–Holocene transition (Vasil'ev, 2003) and that bison were disproportionately selected by hunters (Pushkina & Raia, 2008).

Keeping climatic conditions constant for steppe bison (but not humans) since the LGM in the constant climate counterfactual scenario showed that hunting alone could not have driven the steppe bison to extinction. Without deglacial warming negatively affecting range and abundance, steppe bison were projected to be at large abundances at 5 kyr BP despite hunting by humans. Taken together, our counterfactual hypotheses of the drivers of range collapse and extinction of steppe bison show that human hunting and climatic change were important determinants of the ecological pathway to extinction for steppe bison in Siberia. This association is likely to have been synergistic, with humans accelerating the range collapse of steppe bison during the Pleistocene–Holocene transition, hastening the extirpation of populations that had become fragmented owing to deglacial warming and associated shifts in vegetation. A similar mechanistic explanation has been proposed for the extinction of the woolly mammoth (Fordham et al., 2022).

Although we have shown that the application of POM methods to process-explicit modelling provides a powerful approach

for continuously reconstructing range dynamics over thousands of years, the approach is only as accurate as the validation targets being used. Our validation targets were independent from the data used to parameterize the model. They captured a hierarchy of demographic responses (Gallagher et al., 2021), and they were estimated robustly using statistical techniques applied to fossil data (Bradshaw et al., 2012). Therefore, we have confidence in our POM and results, including the posterior distributions for model parameters and their multi-model averaged projections of range and extinction dynamics (Grimm & Railsback, 2012). However, for many other species, an abundant and spatially representative fossil record will not be available to optimize SEPMs of species range dynamics using POM. Here, other types of palaeo-validation data could be considered, including ancient DNA estimates of past population change (Fordham et al., 2014) and inferences of spatio-temporal occurrence from environmental DNA in sediments and ice cores (Wang et al., 2021). For threatened species or for species that went extinct recently (such as the thylacine in Australia), historical sightings can provide important sources of validation data (Fordham et al., 2021).

Posterior predictive checks of our process-explicit model showed that the posterior ranges of model parameters reconstruct extinction time and location reasonably well (Gelman et al., 2014). However, it was more difficult to reconcile fossil evidence of spatio-temporal occurrence. Indeed, this target was easier to reconstruct in simulations without human hunting, because in the no hunting scenario, steppe bison maintained larger ranges through time. Larger ranges resulted in occurrence being higher not only at fossil sites, but also in areas that were unlikely to have been habitable by steppe bison during periods in the past. It is possible that the difficulty with correctly simulating spatio-temporal occurrence at fossil sites could stem from the hunting dynamics in our process-explicit model. These dynamics were relatively simple, not accounting for technological developments that are likely to have occurred during the time frame of the simulation (Goebel, 2002). The wide posterior range for the functional response of human hunting of steppe bison extends from the selected best models having a diverse range of hunting strategies, suggesting that a variety of parameter values can give a close fit to inferences of extinction dynamics from the fossil record. Also, the model we used to simulate the peopling of Siberia (and Eurasia more generally in CISGEM) does not account for topography, which could have caused barriers to movement, particularly in the Siberian highlands (Eriksson et al., 2012), affecting spatio-temporal harvest rates.

Our process-explicit modelling shows that climatic change and hunting by humans in Siberia during the late Pleistocene and early Holocene is likely to have interacted with key ecological requirements and demographic processes of steppe bison to cause their extinction in Eurasia during the early Holocene. Moreover, it shows that process-explicit models validated with POM methods can continuously simulate the ecological processes and drivers that cause the population declines of species over many millennia, in addition to the final extinction event. Although synthesis of long- and short-term causes of population decline (Caughley, 1994) remains rare, the

integrated computational framework used here provides new opportunities to establish ecological pathways to extinction over long time periods. If applied to a diverse range of species, generalities in ecological processes of extinction could be identified.

DATA AVAILABILITY STATEMENT

The data used for the analysis is available on Figshare (DOI: 10.6084/m9.figshare.17059592.v2) and an example of the R code is available on Zenodo (DOI: 10.5281/zenodo.7098687).

ORCID

Julia A. Pilowsky 🔟 https://orcid.org/0000-0002-6376-2585
Stuart C. Brown 🔟 https://orcid.org/0000-0002-0669-1418
Mario Krapp 🔟 https://orcid.org/0000-0002-2599-0683
Edward Armstrong 🔟 https://orcid.org/0000-0001-9561-0159
Barry W. Brook 🔟 https://orcid.org/0000-0002-2491-1517
Carsten Rahbek 🔟 https://orcid.org/0000-0003-4585-0300
Damien A. Fordham 🔟 https://orcid.org/0000-0003-2137-5592

REFERENCES

Adriaensen, F., Chardon, J. P., De Blust, G., Swinnen, E., Villalba, S., Gulinck, H., & Matthysen, E. (2003). The application of 'least-cost' modelling as a functional landscape model. *Landscape and Urban Planning*, *64*(4), 233–247. https://doi.org/10.1016/S0169-2046(02)00242-6

Anderson, B. J., Akçakaya, H. R., Araújo, M. B., Fordham, D. A., Martinez-Meyer, E., Thuiller, W., & Brook, B. W. (2009). Dynamics of range margins for metapopulations under climate change. *Proceedings of the Royal Society B: Biological Sciences*, *276*(1661), 1415–1420. https://doi.org/10.1098/rspb.2008.1681

Anderson, P. M., & Lozhkin, A. V. (2001). The stage 3 interstadial complex (Karginskii/middle Wisconsinan interval) of Beringia: Variations in paleoenvironments and implications for paleoclimatic interpretations. *Quaternary Science Reviews*, *20*(1–3), 93–125. https://doi.org/10.1016/S0277-3791(00)00129-3

Armstrong, E., Hopcroft, P. O., & Valdes, P. J. (2019). A simulated northern hemisphere terrestrial climate dataset for the past 60,000 years. *Scientific Data*, *6*(1), 1–16. https://doi.org/10.1038/s41597-019-0277-1

Barnes, R., & Clark, A. T. (2017). Sixty-five million years of change in temperature and topography explain evolutionary history in eastern north American plethodontid salamanders. *The American Naturalist*, *190*(1), E1–E12. https://doi.org/10.1086/691796

Barnosky, A. D., & Lindsey, E. L. (2010). Timing of Quaternary megafaunal extinction in South America in relation to human arrival and climate change. *Quaternary International*, *217*(1), 10–29. https://doi.org/10.1016/j.quaint.2009.11.017

Beaumont, M. A., Zhang, W., & Balding, D. J. (2002). Approximate Bayesian computation in population genetics. *Genetics*, *162*(4), 2025–2035. https://doi.org/10.1093/genetics/162.4.2025

Blaauw, M. (2010). Methods and code for "classical" age-modelling of radiocarbon sequences. *Quaternary Geochronology*, *5*(5), 512–518. https://doi.org/10.1016/j.quageo.2010.01.002

Blonder, B., Morrow, C. B., Maitner, B., Harris, D. J., Lamanna, C., Violle, C., Enquist, B. J., & Kerkhoff, A. J. (2018). New approaches for delineating n-dimensional hypervolumes. *Methods in Ecology and Evolution*, *9*(2), 305–319. https://doi.org/10.1111/2041-210X.12865

Boeskorov, G. G., Potapova, O. R., Protopopov, A. V., Plotnikov, V. V., Agenbroad, L. D., Kirikov, K. S., Pavlov, I. S., Shchelchkova, M. V., Belolyubskii, I. N., Tomshin, M. D., Kowalczyk, R., Davydov, S. P., Kolesov, S. D., Tikhonov, A. N., & van der Plicht, J. (2016). The Yukagir Bison: The exterior morphology of a complete frozen mummy of the extinct steppe bison, Bison priscus from the early Holocene of northern Yakutia, Russia. *Quaternary International*, *406*, 94–110. https://doi.org/10.1016/j.quaint.2015.11.084

Bradshaw, C. J. A., Cooper, A., Turney, C. S. M., & Brook, B. W. (2012). Robust estimates of extinction time in the geological record. *Quaternary Science Reviews*, *33*, 14–19. https://doi.org/10.1016/j.quascirev.2011.11.021

Brook, B. W., & Bowman, D. M. J. S. (2002). Explaining the Pleistocene megafaunal extinctions: Models, chronologies, and assumptions. *Proceedings of the National Academy of Sciences*, *99*(23), 14624–14627. https://doi.org/10.1073/pnas.232126899

Brook, B. W., & Bowman, D. M. J. S. (2004). The uncertain blitzkrieg of Pleistocene megafauna. *Journal of Biogeography*, *31*(4), 517–523. https://doi.org/10.1046/j.1365-2699.2003.01028.x

Canteri, E., Brown, S. C., Schmidt, N. M., Heller, R., Nogues-Bravo, D., & Fordham, D. A. (2022). Spatiotemporal influences of climate and humans on muskox range dynamics over multiple millennia. *Global Change Biology*. https://doi.org/10.1111/gcb.16375

Caughley, G. (1994). Directions in conservation biology. *Journal of Animal Ecology*, *63*(2), 215–244. https://doi.org/10.2307/5542

Clark, P. U., Dyke, A. S., Shakun, J. D., Carlson, A. E., Clark, J., Wohlfarth, B., Mitrovica, J. X., Hostetler, S. W., & McCabe, A. M. (2009). The last glacial maximum. *Science*, *325*(5941), 710–714. https://doi.org/10.1126/science.1172873

Colwell, R. K., & Rangel, T. F. (2010). A stochastic, evolutionary model for range shifts and richness on tropical elevational gradients under Quaternary glacial cycles. *Philosophical Transactions of the Royal Society B: Biological Sciences*, *365*(1558), 3695–3707. https://doi.org/10.1098/rstb.2010.0293

Connolly, S. R., Keith, S. A., Colwell, R. K., & Rahbek, C. (2017). Process, mechanism, and modeling in macroecology. *Trends in Ecology & Evolution*, *32*(11), 835–844. https://doi.org/10.1016/j.tree.2017.08.011

Cooper, A., Turney, C., Hughen, K. A., Brook, B. W., McDonald, H. G., & Bradshaw, C. J. (2015). Abrupt warming events drove late Pleistocene Holarctic megafaunal turnover. *Science*, *349*(6248), 602–606. https://doi.org/10.1126/science.aac4315

Csilléry, K., François, O., & Blum, M. G. B. (2012). abc: An R package for approximate Bayesian computation (ABC). *Methods in Ecology and Evolution*, *3*(3), 475–479. https://doi.org/10.1111/j.2041-210X.2011.00179.x

Davidson, A. D., Hamilton, M. J., Boyer, A. G., Brown, J. H., & Ceballos, G. (2009). Multiple ecological pathways to extinction in mammals. *Proceedings of the National Academy of Sciences*, *106*(26), 10702–10705. https://doi.org/10.1073/pnas.0901956106

DelGiudice, G. D., Moen, R. A., Singer, F. J., & Riggs, M. R. (2001). Winter nutritional restriction and simulated body condition of Yellowstone elk and bison before and after the fires of 1988. *Wildlife Monographs*, *147*, 1–60.

DelGiudice, G. D., Singer, F. J., Seal, U. S., & Bowser, G. (1994). Physiological responses of Yellowstone bison to winter nutritional deprivation. *The Journal of Wildlife Management*, *58*(1), 24–34. https://doi.org/10.2307/3809545

Dietl, G. P., Kidwell, S. M., Brenner, M., Burney, D. A., Flessa, K. W., Jackson, S. T., & Koch, P. L. (2015). Conservation paleobiology: Leveraging knowledge of the past to inform conservation and restoration. *Annual Review of Earth and Planetary Sciences*, *43*(1), 79–103. https://doi.org/10.1146/annurev-earth-040610-133349

Dolédec, S., Chessel, D., & Gimaret-Carpentier, C. (2000). Niche separation in community analysis: A new method. *Ecology*, *81*(10), 2914–2927. https://doi.org/10.1890/0012-9658(2000)081[2914:NSICAA]2.0.CO;2

Dunning, J. B., Jr., Stewart, D. J., Danielson, B. J., Noon, B. R., Root, T. L., Lamberson, R. H., & Stevens, E. E. (1995). Spatially explicit population models: Current forms and future uses. *Ecological Applications*, *5*(1), 3–11. https://doi.org/10.2307/1942045

Ellis, E. C., Gauthier, N., Goldewijk, K. K., Bird, R. B., Boivin, N., Díaz, S., Fuller, D. Q., Gill, J. L., Kaplan, J. O., Kingston, N., Locke, H., McMichael, C. N. H., Ranco, D., Rick, T. C., Shaw, M. R., Stephens, L., Svenning, J.-C., & Watson, J. E. M. (2021). People have shaped most of terrestrial nature for at least 12,000 years. *Proceedings of the National Academy of Sciences of the United States of America*, *118*(17), e2023483118. https://doi.org/10.1073/pnas.2023483118

Eriksson, A., Betti, L., Friend, A. D., Lycett, S. J., Singarayer, J. S., von Cramon-Taubadel, N., Valdes, P. J., Balloux, F., & Manica, A. (2012). Late Pleistocene climate change and the global expansion of anatomically modern humans. *Proceedings of the National Academy of Sciences of the United States of America*, *109*(40), 16089–16094. https://doi.org/10.1073/pnas.1209494109

Fordham, D. A., Akçakaya, H. R., Alroy, J., Saltré, F., Wigley, T. M. L., & Brook, B. W. (2016). Predicting and mitigating future biodiversity loss using long-term ecological proxies. *Nature Climate Change*, *6*(10), 909–916. https://doi.org/10.1038/nclimate3086

Fordham, D. A., Bertelsmeier, C., Brook, B. W., Early, R., Neto, D., Brown, S. C., Ollier, S., & Araújo, M. B. (2018). How complex should models be? Comparing correlative and mechanistic range dynamics models. *Global Change Biology*, *24*(3), 1357–1370. https://doi.org/10.1111/gcb.13935

Fordham, D. A., Brook, B. W., Moritz, C., & Nogués-Bravo, D. (2014). Better forecasts of range dynamics using genetic data. *Trends in Ecology & Evolution*, *29*(8), 436–443. https://doi.org/10.1016/j.tree.2014.05.007

Fordham, D. A., Brown, S. C., Akçakaya, H. R., Brook, B. W., Haythorne, S., Manica, A., Shoemaker, K. T., Austin, J. J., Blonder, B., Pilowsky, J., Rahbek, C., & Nogues-Bravo, D. (2022). Process-explicit models reveal pathway to extinction for woolly mammoth using pattern-oriented validation. *Ecology Letters*, *25*(1), 125–137. https://doi.org/10.1111/ele.13911

Fordham, D. A., Haythorne, S., Brown, S. C., Buettel, J. C., & Brook, B. W. (2021). Poems: R package for simulating species' range dynamics using pattern-oriented validation. *Methods in Ecology and Evolution*, *12*(12), 2364–2371. https://doi.org/10.1111/2041-210X.13720

Fordham, D. A., Jackson, S. T., Brown, S. C., Huntley, B., Brook, B. W., Dahl-Jensen, D., Gilbert, M. T. P., Otto-Bliesner, B. L., Svensson, A., Theodoridis, S., Wilmshurst, J. M., Buettel, J. C., Canteri, E., McDowell, M., Orlando, L., Pilowsky, J., Rahbek, C., & Nogues-Bravo, D. (2020). Using paleo-archives to safeguard biodiversity under climate change. *Science*, *369*(6507), eabc5654. https://doi.org/10.1126/science.abc5654

Gallagher, C. A., Chudzinska, M., Larsen-Gray, A., Pollock, C. J., Sells, S. N., White, P. J. C., & Berger, U. (2021). From theory to practice in pattern-oriented modelling: Identifying and using empirical patterns in predictive models. *Biological Reviews*, *96*(5), 1868–1888. https://doi.org/10.1111/brv.12729

Gates, C. C., & Larter, N. C. (1990). Growth and dispersal of an erupting large herbivore population in northern Canada: The Mackenzie wood bison (Bison bison athabascae). *Arctic*, *43*(3), 231–238.

Gelman, A., Hwang, J., & Vehtari, A. (2014). Understanding predictive information criteria for Bayesian models. *Statistics and Computing*, *24*(6), 997–1016. https://doi.org/10.1007/s11222-013-9416-2

Goebel, T. (2002). The "microblade adaptation" and recolonization of Siberia during the late upper Pleistocene. *Archaeological Papers of the American Anthropological Association*, *12*(1), 117–131. https://doi.org/10.1525/ap3a.2002.12.1.117

Grimm, V., & Railsback, S. F. (2012). Pattern-oriented modelling: A "multiscope" for predictive systems ecology. *Philosophical Transactions of the Royal Society B: Biological Sciences*, *367*(1586), 298–310. https://doi.org/10.1098/rstb.2011.0180

Grimm, V., Revilla, E., Berger, U., Jeltsch, F., Mooij, W. M., Railsback, S. F., Thulke, H.-H., Weiner, J., Wiegand, T., & DeAngelis, D. L. (2005). Pattern-oriented modeling of agent-based complex systems: Lessons from ecology. *Science*, *310*(5750), 987–991. https://doi.org/10.1126/science.1116681

Guthrie, R. D. (1989). *Frozen Fauna of the mammoth steppe: The story of blue babe*. University of Chicago Press.

Guthrie, R. D. (2006). New carbon dates link climatic change with human colonization and Pleistocene extinctions. *Nature*, *441*(7090), 207–209. https://doi.org/10.1038/nature04604

Haile, J., Froese, D. G., MacPhee, R. D. E., Roberts, R. G., Arnold, L. J., Reyes, A. V., Rasmussen, M., Nielsen, R., Brook, B. W., Robinson, S., Demuro, M., Gilbert, M. T. P., Munch, K., Austin, J. J., Cooper, A., Barnes, I., Möller, P., & Willerslev, E. (2009). Ancient DNA reveals late survival of mammoth and horse in interior Alaska. *Proceedings of the National Academy of Sciences*, *106*(52), 22352–22357. https://doi.org/10.1073/pnas.0912510106

Hanski, I. (1998). Metapopulation dynamics. *Nature*, *396*(6706), 41–49. https://doi.org/10.1038/23876

Haythorne, S., Pilowsky, J. A., Brown, S., & Fordham, D. (2021). Paleopop: Pattern-oriented modeling framework for coupled niche-population paleo-climatic models (v.2.1.2) [Computer software]. https://CRAN.R-project.org/package=paleopop

Julien, M.-A., Bocherens, H., Burke, A., Drucker, D. G., Patou-Mathis, M., Krotova, O., & Péan, S. (2012). Were European steppe bison migratory? 18O, 13C and Sr intra-tooth isotopic variations applied to a palaeoethological reconstruction. *Quaternary International*, *271*, 106–119. https://doi.org/10.1016/j.quaint.2012.06.011

Jung, T. S. (2017). Extralimital movements of reintroduced bison (Bison bison): Implications for potential range expansion and human-wildlife conflict. *European Journal of Wildlife Research*, *63*(2), 35. https://doi.org/10.1007/s10344-017-1094-5

Knowles, L. L., & Alvarado-Serrano, D. F. (2010). Exploring the population genetic consequences of the colonization process with spatio-temporally explicit models: Insights from coupled ecological, demographic and genetic models in montane grasshoppers. *Molecular Ecology*, *19*(17), 3727–3745. https://doi.org/10.1111/j.1365-294X.2010.04702.x

Koch, P. L., & Barnosky, A. D. (2006). Late Quaternary extinctions: State of the debate. *Annual Review of Ecology, Evolution, and Systematics*, *37*(1), 215–250. https://doi.org/10.1146/annurev.ecolsys.34.011802.132415

Koons, D. N., Terletzky, P., Adler, P. B., Wolfe, M. L., Ranglack, D., Howe, F. P., Hersey, K., Paskett, W., & du Toit, J. T. (2012). Climate and density-dependent drivers of recruitment in plains bison. *Journal of Mammalogy*, *93*(2), 475–481. https://doi.org/10.1644/11-MAMM-A-281.1

Kramer, A. M., Dennis, B., Liebhold, A. M., & Drake, J. M. (2009). The evidence for Allee effects. *Population Ecology*, *51*(3), 341–354. https://doi.org/10.1007/s10144-009-0152-6

Laliberte, A. S., & Ripple, W. J. (2004). Range contractions of north American carnivores and ungulates. *Bioscience*, *54*(2), 123–138. https://doi.org/10.1641/0006-3568(2004)054[0123:RCONAC]2.0.CO;2

Lorenzen, E. D., Nogués-Bravo, D., Orlando, L., Weinstock, J., Binladen, J., Marske, K. A., Ugan, A., Borregaard, M. K., Gilbert, M. T. P., Nielsen, R., Ho, S. Y. W., Goebel, T., Graf, K. E., Byers, D., Stenderup, J. T., Rasmussen, M., Campos, P. F., Leonard, J. A., Koepfli, K.-P., … Willerslev, E. (2011). Species-specific responses of late Quaternary megafauna to climate and humans. *Nature*, *479*(7373), 359–364. https://doi.org/10.1038/nature10574

Mann, D. H., Groves, P., Gaglioti, B. V., & Shapiro, B. A. (2019). Climate-driven ecological stability as a globally shared cause of late Quaternary megafaunal extinctions: The plaids and stripes hypothesis. *Biological Reviews*, *94*(1), 328–352. https://doi.org/10.1111/brv.12456

Markova, A. K., Puzachenko, A. Y., van Kolfschoten, T., Kosintsev, P. A., Kuznetsova, T. V., Tikhonov, A. N., Bachura, O. P., Ponomarev, D. V., van der Plicht, J., & Kuitems, M. (2015). Changes in the Eurasian distribution of the musk ox (*Ovibos moschatus*) and the extinct bison (*Bison priscus*) during the last 50 ka BP. *Quaternary International*, *378*, 99–110. https://doi.org/10.1016/j.quaint.2015.01.020

Metcalf, J. L., Prost, S., Nogues-Bravo, D., DeChaine, E. G., Anderson, C., Batra, P., Araujo, M. B., Cooper, A., & Guralnick, R. P. (2014). Integrating multiple lines of evidence into historical biogeography hypothesis testing: A Bison bison case study. *Proceedings of the Royal Society B-Biological Sciences*, *281*(1777), 20132782. https://doi.org/10.1098/rspb.2013.2782

Mondal, P., & Southworth, J. (2010). Evaluation of conservation interventions using a cellular automata-Markov model. *Forest Ecology and Management*, *260*(10), 1716–1725. https://doi.org/10.1016/j.foreco.2010.08.017

Murton, J. B., Edwards, M. E., Lozhkin, A. V., Anderson, P. M., Savvinov, G. N., Bakulina, N., Bondarenko, O. V., Cherepanova, M. V., Danilov, P. P., Boeskorov, V., Goslar, T., Grigoriev, S., Gubin, S. V., Korzun, J. A., Lupachev, A. V., Tikhonov, A., Tsygankova, V. I., Vasilieva, G. V., & Zanina, O. G. (2017). Preliminary paleoenvironmental analysis of permafrost deposits at Batagaika megaslump, Yana uplands, Northeast Siberia. *Quaternary Research*, *87*(2), 314–330. https://doi.org/10.1017/qua.2016.15

Nogués-Bravo, D. (2009). Predicting the past distribution of species climatic niches. *Global Ecology and Biogeography*, *18*(5), 521–531. https://doi.org/10.1111/j.1466-8238.2009.00476.x

Owens, I. P. F., & Bennett, P. M. (2000). Ecological basis of extinction risk in birds: Habitat loss versus human persecution and introduced predators. *Proceedings of the National Academy of Sciences*, *97*(22), 12144–12148. https://doi.org/10.1073/pnas.200223397

Pacifici, M., Santini, L., Di Marco, M., Baisero, D., Francucci, L., Marasini, G. G., Visconti, P., & Rondinini, C. (2013). Generation length for mammals. *Nature Conservation-Bulgaria*, *5*, 87–94. https://doi.org/10.3897/natureconservation.5.5734

Pilowsky, J. A., Colwell, R. K., Rahbek, C., & Fordham, D. A. (2022). Process-explicit models reveal the structure and dynamics of biodiversity patterns. *Science Advances*, *8*(31), eabj2271. https://doi.org/10.1126/sciadv.abj2271

Pilowsky, J. A., Haythorne, S., Brown, S. C., Krapp, M., Armstrong, E., Brook, B. W., Rahbek, C., & Fordham, D. A. (2021). *Quality-controlled carbon-14 dates of steppe bison (Bison priscus) fossils* [Data set]. figshare. https://doi.org/10.6084/M9.FIGSHARE.17059592.V2

Pilowsky, J. A., Manica, A., Brown, S. C., Rahbek, C., & Fordham, D. A. (2022). Simulations of human migration into North America are more sensitive to demography than choice of palaeoclimate model. *Ecological Modelling*, *473*, 110115. https://doi.org/10.1016/j.ecolmodel.2022.110115

Plumb, G. E., White, P. J., Coughenour, M. B., & Wallen, R. L. (2009). Carrying capacity, migration, and dispersal in Yellowstone bison. *Biological Conservation*, *142*(11), 2377–2387. https://doi.org/10.1016/j.biocon.2009.05.019

Pontarp, M., Bunnefeld, L., Cabral, J. S., Etienne, R. S., Fritz, S. A., Gillespie, R., Graham, C. H., Hagen, O., Hartig, F., Huang, S., Jansson, R., Maliet, O., Münkemüller, T., Pellissier, L., Rangel, T. F., Storch, D., Wiegand, T., & Hurlbert, A. H. (2019). The latitudinal diversity gradient: Novel understanding through mechanistic eco-evolutionary models. *Trends in Ecology & Evolution*, *34*(3), 211–223. https://doi.org/10.1016/j.tree.2018.11.009

Pushkina, D., & Raia, P. (2008). Human influence on distribution and extinctions of the late Pleistocene Eurasian megafauna. *Journal of Human Evolution*, *54*(6), 769–782. https://doi.org/10.1016/j.jhevol.2007.09.024

Ramsey, C. B. (2017). *OxCal program, version 4.3. Oxford radiocarbon accelerator unit*. University of Oxford.

Rangel, T. F., Edwards, N. R., Holden, P. B., Diniz-Filho, J. A. F., Gosling, W. D., Coelho, M. T. P., Cassemiro, F. A. S., Rahbek, C., & Colwell, R. K. (2018). Modeling the ecology and evolution of biodiversity: Biogeographical cradles, museums, and graves. *Science*, *361*(6399), eaar5452. https://doi.org/10.1126/science.aar5452

Reimer, P. J., Bard, E., Bayliss, A., Beck, J. W., Blackwell, P. G., Ramsey, C. B., Buck, C. E., Cheng, H., Edwards, R. L., & Friedrich, M. (2013). IntCal13 and Marine13 radiocarbon age calibration curves 0–50,000 years cal BP. *Radiocarbon*, *55*(4), 1869–1887. https://doi.org/10.2458/azu_js_rc.55.16947

Ricker, W. E. (1954). Stock and recruitment. *Journal of the Fisheries Research Board of Canada*, *11*(5), 559–623. https://doi.org/10.1139/f54-039

Rutherford, S., Mann, M. E., Osborn, T. J., Briffa, K. R., Jones, P. D., Bradley, R. S., & Hughes, M. K. (2005). Proxy-based northern hemisphere surface temperature reconstructions: Sensitivity to method, predictor network, target season, and target domain. *Journal of Climate*, *18*(13), 2308–2329.

Shapiro, B., Drummond, A. J., Rambaut, A., Wilson, M. C., Matheus, P. E., Sher, A. V., Pybus, O. G., Gilbert, M. T. P., Barnes, I., Binladen, J., Willerslev, E., Hansen, A. J., Baryshnikov, G. F., Burns, J. A., Davydov, S., Driver, J. C., Froese, D. G., Harington, C. R., Keddie, G., … Cooper, A. (2004). Rise and fall of the Beringian steppe bison. *Science*, *306*(5701), 1561–1565. https://doi.org/10.1126/science.1101074

Signor, P. W., Lipps, J. H., Silver, L. T., & Schultz, P. H. (1982). Sampling bias, gradual extinction patterns, and catastrophes in the fossil record. *Geological Implications of Impacts of Large Asteroids and Comets on the Earth*, *190*, 291–296.

Soberón, J., & Nakamura, M. (2009). Niches and distributional areas: Concepts, methods, and assumptions. *Proceedings of the National Academy of Sciences*, *106*(Supplement 2), 19644–19650. https://doi.org/10.1073/pnas.0901637106

Soubrier, J., Gower, G., Chen, K., Richards, S. M., Llamas, B., Mitchell, K. J., Ho, S. Y. W., Kosintsev, P., Lee, M. S. Y., Baryshnikov, G., Bollongino, R., Bover, P., Burger, J., Chivall, D., Crégut-Bonnoure, E., Decker, J. E., Doronichev, V. B., Douka, K., Fordham, D. A., … Cooper, A. (2016). Early cave art and ancient DNA record the origin of European bison. *Nature Communications*, *7*(1), 13158. https://doi.org/10.1038/ncomms13158

Stein, M. (1987). Large sample properties of simulations using Latin hypercube sampling. *Technometrics*, *29*(2), 143–151. https://doi.org/10.1080/00401706.1987.10488205

Stuart, A. J. (2015). Late quaternary megafaunal extinctions on the continents: A short review. *Geological Journal*, *50*(3), 338–363. https://doi.org/10.1002/gj.2633

Thulke, H.-H., Grimm, V., Müller, M. S., Staubach, C., Tischendorf, L., Wissel, C., & Jeltsch, F. (1999). From pattern to practice: A scaling-down strategy for spatially explicit modelling illustrated by the spread and control of rabies. *Ecological Modelling*, *117*(2), 179–202. https://doi.org/10.1016/S0304-3800(98)00198-7

Urban, M. C., Bocedi, G., Hendry, A. P., Mihoub, J.-B., Pe'er, G., Singer, A., Bridle, J. R., Crozier, L. G., Meester, L. D., Godsoe, W., Gonzalez, A., Hellmann, J. J., Holt, R. D., Huth, A., Johst, K., Krug, C. B., Leadley, P. W., Palmer, S. C. F., Pantel, J. H., ... Travis, J. M. J. (2016). Improving the forecast for biodiversity under climate change. *Science*, *353*(6304), aad8466. https://doi.org/10.1126/science.aad8466

Valdes, P. J., Armstrong, E., Badger, M. P. S., Bradshaw, C. D., Bragg, F., Crucifix, M., Davies-Barnard, T., Day, J. J., Farnsworth, A., Gordon, C., Hopcroft, P. O., Kennedy, A. T., Lord, N. S., Lunt, D. J., Marzocchi, A., Parry, L. M., Pope, V., Roberts, W. H. G., Stone, E. J., ... Williams, J. H. T. (2017). The BRIDGE HadCM3 family of climate models: HadCM3@Bristol v1.0. *Geoscientific Model Development*, *10*(10), 3715–3743. https://doi.org/10.5194/gmd-10-3715-2017

van der Vaart, E., Beaumont, M. A., Johnston, A. S. A., & Sibly, R. M. (2015). Calibration and evaluation of individual-based models using approximate Bayesian computation. *Ecological Modelling*, *312*, 182–190. https://doi.org/10.1016/j.ecolmodel.2015.05.020

Vasil'ev, S. A. (2003). Faunal exploitation, subsistence practices and Pleistocene extinctions in Paleolithic Siberia. *Deinsea*, *9*(1), 513–556.

Wang, Y., Pedersen, M. W., Alsos, I. G., De Sanctis, B., Racimo, F., Prohaska, A., Coissac, E., Owens, H. L., Merkel, M. K. F., Fernandez-Guerra, A., Rouillard, A., Lammers, Y., Alberti, A., Denoeud, F., Money, D., Ruter, A. H., McColl, H., Larsen, N. K., Cherezova, A. A., ... Willerslev, E. (2021). Late quaternary dynamics of Arctic biota from ancient environmental genomics. *Nature*, *600*, 86–92. https://doi.org/10.1038/s41586-021-04016-x

BIOSKETCH

We are an interdisciplinary team of macroecologists, ecological modellers, evolutionary biologists and climate scientists interested in developing process-explicit models to improve our understanding of the mechanisms responsible for the distributions of organisms, communities and ecosystems in space and time.

SUPPORTING INFORMATION

Additional supporting information can be found online in the Supporting Information section at the end of this article.